Chapter 7
Supramolecular Chemistry of Polymer Metal Chelates

Abstract In this chapter the basic concepts and synthetic strategies leading to the different types of metallosupramolecular polymers containing metal chelate units including linear, branched, cross-linked as well as heterometallic polymers are summarized and discussed. Included are metallosupramolecular polyelectrolytes, polymer gels, self-assembled metallosupramolecular monolayers, and supramolecular metal chelate dendrimers. Special attention is paid to such new synthetic approaches to the supramolecular polymers as hierarchical and orthogonal self-assembling based on combination of metal–ligand coordination with hydrogen-bonding and host-guest interactions. The stimuli-responsive, self-healing and shape-memory metallosupramolecular polymers containing metal chelate units are considered.

Within relatively short time interval, with respect to historical scale, supramolecular chemistry has turned into very rapidly developed and interdisciplinary science, which includes chemical, physical, and biological aspects of studying more complicated than molecules chemical systems assembled into integral whole through intermolecular (non-covalent) interactions [1–8]. Today it is absolutely clear that supramolecular systems have a special niche, a level in hierarchy of matter, in which such principles of organizing and functioning matter as molecular recognition, selective bonding, receptor-substrate interaction, trans-membrane transfer, and supramolecular catalysis are realized. Nature has maximally used these principles for creation of biological objects. Likely to self-assembling most complicated spatial structures in living systems, objects of supramolecular chemistry, supramolecular assemblies, are built spontaneously from complementary, i.e. having geometrical and chemical similarity, fragments. In nanometer world, which is ascribed to 1 to 100-nm scaling elements, supramolecular systems, usually having 1 to 10-nm scale, are the smallest elements of this world. Therefore, it is possible to state that supramolecular chemistry eliminates a gap between molecular world and nanotechnologies, and also provides designing new classes of materials and devices for future nanotechnologies [9]. One of the fundamental problems of contemporary chemistry is oriented structuring such systems, development of highly ordered supramolecular assemblies made

G. I. Dzhardimalieva and I. E. Uflyand, *Chemistry of Polymeric Metal Chelates*, Springer Series in Materials Science 257,
https://doi.org/10.1007/978-3-319-56024-3_7

of molecular building blocks, having a given structure and properties. Supramolecular formations are characterized by spatial disposition of their components, their architecture, «suprastructure», and also types of intermolecular interactions, which keep components together.

Two main principles, molecular recognition and supramolecular function, lie in the center of understanding supramolecular chemistry concept [10]. While bonding does not necessary means recognition, molecular recognition is, as a rule, considered as a patterned process with participation of structurally well-defined set of intermolecular interactions, i.e. purported bonding [1]. Based on chemical recognition (which is chemical informatics) self-organizing, programmed self-assembling supramolecular systems are performed. Molecular recognition is a process, in which some molecules («host» or receptor) choose and bound molecules («guest» or substrate) due to intermolecular forces into structurally-organized system. In supramolecular chemistry non-covalent interactions are realized between molecular structural blocks, which form supramolecular fragments using molecular recognition and self-assembling. In these systems each additional block contains exact information on creation via self-assembling (each step of self-organization process) regular final structure inside all possible structures [11]. General structure of purported assembly is controlled using symmetry features of some building blocks. Finally, assemblies can have special properties or supramolecular functions, which can only be found in assembly, but which are not contributing to molecules [12].

Idea of self-assembling is determinative for supramolecular chemistry. This term is referred to spontaneous assembling two or more components under equilibrium conditions bringing to creation of stable, structurally clearly defined discrete oligomer supramolecules or extended supramolecular assemblies, which is realized due to non-covalent interactions [1, 13]. As a rule, non-covalent interactions are weaker than covalent, therefore supramolecular assemblies are less stable thermodynamically, more labile kinetically, and more flexible dynamically than molecules. Even under weak external influence on a supramolecular system it can reversibly change its structure due to change in geometry of mutual positions of atoms comprising the supramolecular system and, respectively, can change characteristics of the whole system.

A special feature of supramolecular systems is their capacity to form different architectures without change in chemical composition of a system. In other words, polymorphism of supramolecular systems should be regarded. Because a structure of a supramolecular system changes under external influence there is a possibility of control over structure of produced supramolecular assemblies and their properties.

Self-organizing is ordered association under given conditions of individual structural components into supramolecular structures [1], which are characterized by definite spatial disposition of components (architecture) and intermolecular interactions keeping them together. Supramolecular structures have definite conformation, thermodynamic, kinetic, and dynamic properties. Self-organization is selective and spontaneous formation of one or more ordered structures in a complex mixture, which in the opposite case could have formed greater variety of structures [14].

Together terms «self-assembly» and «self-organization» involve processes, which give an opportunity for programmed molecular components or tectons (from Greek «tekton»—a builder) to assemble spontaneously, exactly in a definite way forming assemblies, whose organization proceeds in one, two or three dimensions and, probably, though not necessary, in time [15, 16]. Molecules, which form assemblies with typical architectural and functional features, are accepted as tectons [17, 18]. In fact, supramolecular tectons are supramolecular building blocks capable of self-assembling into ordered assemblies. It should be especially noted that supramolecular assemblies should be related, together with other complicated systems, to higher level of tectons, «nanoarchitectonics» for designing and preparation of dynamic functional materials [19, 20]. In the nanoarchitectonics concept these materials are projected through controlled harmonized interactions, which provide development of unexpected functions.

An idea of supramolecular synthons is introduced [21] for designation of structural elements distinguished on the basis of analysis of intermolecular contacts with account for some additional geometric characteristics. The term «supramolecular synthon» is well studied and accepted tool in crystal engineering for designing of desired supramolecular structures [21–23]. Advantage of the terms «supramolecular tectonics» and «supramolecular synthon» is in more comprehensive information on structure as compared with traditional terms («complex», «associate», etc.). Supramolecular synthon plays the same key role in supramolecular polymerization as a synthon plays in covalent synthesis. Supramolecular synthons are spatial positions of intermolecular non-covalent interactions, which are often met in supramolecular assemblies. Numerous examples of supramolecular structures, in which supramolecular synthons were used, point to strength of supramolecular synthons [24–31].

Supramolecular chemistry operates with various intermolecular interactions (supramolecular synthons), which differ in their character, energy and directionality. They include ion-ionic (100–350 kJ mol^{-1}), ion-dipole (50–200 kJ mol^{-1}), dipole-dipole (5–50 kJ mol^{-1}), cation-π-system (50–80 kJ mol^{-1}), π-π-stacking (0–50 kJ mol^{-1}), metallophilic (<10 kJ mol^{-1}), Van der Waals (<5 kJ mol^{-1}) interactions, coordination (40–400 kJ mol^{-1}) and hydrogen (4–120 kJ mol^{-1}) bonds [32]. Therefore there are a great number of possibilities for building supramolecular assemblies using only one type of non-covalent interaction or combination of two or more types, which can additively contribute to common energy and/or integrate a great number of factors for structural control.

7.1 Supramolecular Polymers

Supramolecular chemistry can be divided into two broad, partly superimposed areas, in which supramolecules and supramolecular polymers, respectively, are considered. Supramolecules are represented by well-defined, discrete, oligomolecular formations created due to intermolecular association of several components (receptor and

substrate) according to some «program» operating by principles of molecular recognition. Supramolecular polymers are polymolecular assemblies generated due to spontaneous self-assembling a great number of components in specific phase characterized by more or less definite organization at microscopic level and having macroscopic properties depending on a character of a phase (film, layer, membrane, vesicle, mesomorphic phase, crystal, etc.) [33–40]. In order to overcome a gap between these two abovementioned species, a new class of organized assemblies, suprasupermolecules is proposed [41, 42]. Therefore, «supramolecular chemistry» is a wide term, which relates to chemistry of all types of supramolecular assemblies, including well-defined supramolecules, extended, more or less organized polymolecular assemblies, and their respective combinations.

Supramolecular polymers can be divided in three categories depending on their formation mechanism: isodesmic, cooperative, and ring-chain polymerization processes. Without going in details of these well studied mechanisms of supramolecular polymerization and their thermodynamic aspects [34, 43–45], we shall notice only that isodesmic process can be compared with step-growth polymerization, and all stages of self-assembling are characterized by the same constant values of association, independently on aggregate sizes [43–45]. Cooperative mechanism (or nucleation-growth) includes two states of the process, in which formation of thermodynamically adverse types consisting of limited number of monomer units (nucleation) is followed by more favorable stage of elongation, which is characterized by higher values of association constants (Fig. 7.1a). The result of cooperative polymerization is formation of self-assembled assemblies with high degree of internal order as compared with isodesmic analogues, which bring to random-coil supramolecular polymers without internal ordering.

To separate these two self-assembling mechanisms, it is necessary to choose thoroughly experimental and calculative methods of studying [46–48]. Ideally, there should be a possibility of monitoring of complete transformation from monomer types to completely aggregated types during temperature- or concentration-dependent studies. This happens in the case when α_{agg} parameter (a fraction of aggregated types) can be determined exactly. It changes from 0 (all monomer units are in molecular solved state) to 1 (all monomer units are in aggregated state). The dependence α_{agg} on concentration or temperature will be a curve, which has a shape determined by self-assembling mechanism (Fig. 7.1b).

Ring-chain supramolecular polymerization is typical of ditopic monomer units, in which there is equilibrium between linear and cyclic analogues [43].

Supramolecular polymers are dynamic in nature; therefore, their components are linked via reversible bonds and are subjected to spontaneous and continuous processes of assembling/dissembling under certain conditions [49]. Due to dynamic and reversible character of non-covalent interactions, supramolecular polymers have ability to adapt to environment and have wide spectrum of intriguing properties, such as a tendency to degradation, shape memory, and self-healing, which makes them unique candidates for supramolecular materials [50–65].

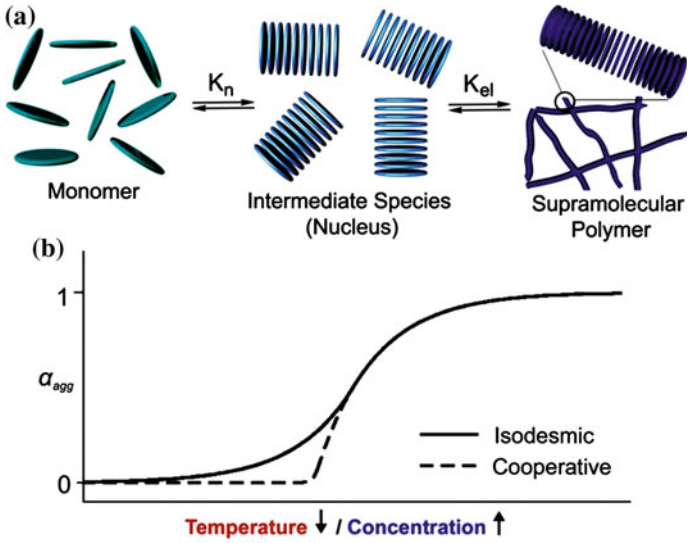

Fig. 7.1 **a** Schematic representation of the supramolecular cooperative growth following the nucleation-elongation pathway. **b** Plot of α_{agg} against increasing temperature and decreasing concentration, respectively, giving rise to characteristic curves corresponding to an isodesmic or cooperative growth [46]

There are different approaches to synthesis of supramolecular polymers, including using hydrogen bonds (H-bonds) [43, 66–74], metal–ligand (M–L) [35, 43, 50, 72, 76–87], ionic [88–90], π-π [38, 43, 70, 72, 91, 92], and Van der Waals interactions [43, 70, 72, 92].

The main difference between covalently bound polymers and supramolecular polymers is dependence of average DP on interaction strength of terminal groups, and, respectively, solvent, temperature and concentration. To estimate DP of reversible supramolecular polymers, (7.1) is used [43, 70, 75, 93–95]:

$$\mathrm{DP} \sim (\mathrm{K_a}[\mathrm{M}])^{1/2}, \tag{7.1}$$

where K_a is general association constant, M is concentration of monomer.

Graphical dependence DP on K for different concentrations is presented in Fig. 7.2. To obtain polymers with high DP, high association constant between repeated units is needed. By analogy with covalent polymers, chain length of supramolecular polymers can be changed by addition of monofunctional chain stoppers. The main advantage of supramolecular polymers as compared with their classical analogues is a possibility to produce tailor-made materials using knowledge on association constants.

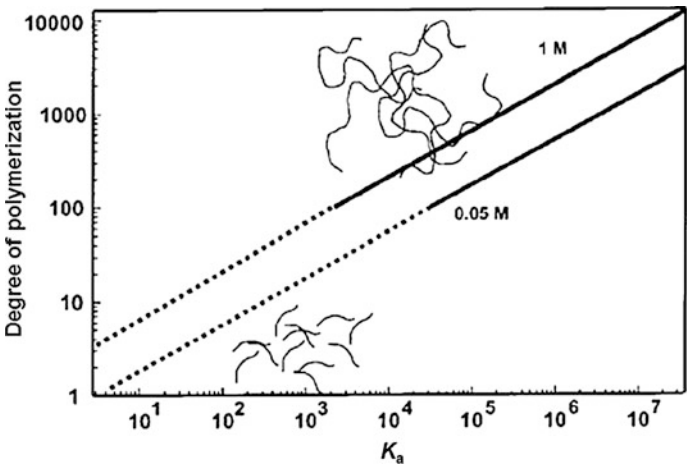

Fig. 7.2 Theoretical relationship between the association constant K_a and DP, using a simple isodesmic association function, or «multistage open association» model [70]

7.2 Metallosupramolecular Polymerization

Metallosupramolecular polymerization is a process of spontaneous self-assembling polytopic organic ligands and metal ions with formation of metallosupramolecular polymers (MSPs) (Fig. 7.3) [96]. Taking into account orientation of this book, hereafter only those MSPs will be considered which include metal chelate units as a basic supramolecular motif. Concept of metallosupramolecular polymerization requires that a chelating monomer would be a telechelic system capable of continuous elongation of a chain in presence of a metal ion via well-known consecutive polycondensation mechanism.

The MSP is a special class of supramolecular polymers obtained from polytopic monomers containing two or more chelating groups (ligands) at each end, where a bond between monomers is provided by M–L coordination [70, 75, 93, 97, 98]. MSP can be considered as a subset of metal-containing polymers, in which M–L interaction is dynamic by its character and, therefore, acts as supramolecular motif. These organic/inorganic hybrid systems potentially offer attractive combination of functionality of metal ions, mechanical properties and workability of polymers, as well as characteristics of self-assembling and dynamic character of supramolecular chemistry.

Self-assembling discrete structures using as a main driving force M–L coordination, is already known for more than two decades, and during this time MSP chemistry is steadily developed [75, 87, 99–113]. It is especially noted that M–L bond of donor centers of organic molecule with a metal ion is one of the strongest types of intermolecular interactions in supramolecular polymers [12, 50, 75, 96, 114–119].

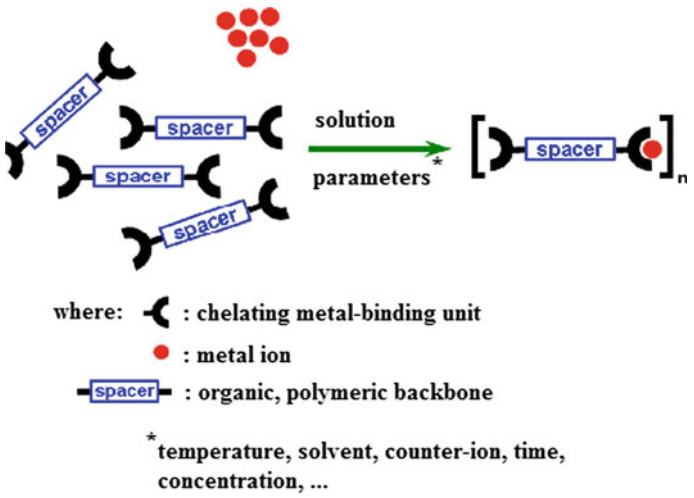

Fig. 7.3 Schematic representation of the metallosupramolecular polymerization process [96]

In MSP metal ions function as bridges for linking organic ligands, thus forming a polymer chain. An advantage of the concept of metallosupramolecular polymerization is a possibility to choose respective M–L combination so as to take control over bond strength (thermodynamic characteristic) and exchange rate (kinetic characteristic). The process of metallosupramolecular polymerization is mainly controlled by strength of M–L bond between a metal and chelating block of a polytopic ligand. Nature of this interaction is predominantly donation of lone-pair of ligand (Lewis base) to a metal ion (Lewis acid) in combination with electrostatic interaction between a positively charged metal ion and negatively polarized/charged donor atom of ligand [120]. When developing MSP, a special attention should be paid to some important factors, which can be used to influence a polymer not only during, but also after building metallosupramolecular assemblies. A possibility of changing a polymer structure of MSP after its preparation has a significant advantage as compared with covalent polymers.

The most important features of coordination-driven self-assembling is narrow directionality of M–L bonds [110], diversity of supramolecular assemblies, stipulated by variety of building blocks (polydentate ligands and different metals), combination of strong and weak bonds, a possibility of control over a reaction mechanism, i.e. its proceeding under conditions of thermodynamic or kinetic control [75, 95]. The principle of molecular recognition in coordination-driven self-assembling is based on the stoichiometric model [121, 122]. The most varied factors, for example, metal cation properties (electronic configuration and size, which define coordination geometry of a metal chelate node), softness or hardness of cations and ligands, chelate effect, etc. should be taken into account in the coordination-driven self-assembling. Contemporary coordination chemistry suggests a vast variety of supramolecular motifs based on metal chelates with different

geometry, appropriate electronic and magnetic properties, which can be included in MSP [123]. If a ligand contains several chelating groups, divergently positioned in a molecule, it can participate in binding of several metal ions in one MSP. Bonds of metal ions with polymers can change almost continuously from strong, actually covalent bonds, which bring to irreversible or «static» binding of a metal, to weak and unstable non-covalent M–L interactions, which provide reversible, «dynamic» or «metallosupramolecular» binding. Since binding energy between a metal and a ligand is relatively high, the obtained structures can be linked with relatively small number of these bonds. This is a main difference of methodology based on M–L interaction from other types of discrete self-assembling, for example, such as self-assembling through H-bonds. Other advantages of M–L interactions, in particular, are in large database of available ligands in line with applied metal ions, containing almost half of the periodical system, which means that there is a broad range of easily available M–L chelates [76]. For intermolecular interactions detailed study of thermodynamics and kinetics of chelation is necessary for choice of appropriate M–L combination for respective application. Thermodynamic properties determined by binding constants, give a possibility to predict whether a complex will be stable or unstable, while kinetic properties are expressed by conditions of inertness or lability, and can be expressed, in particular, in terms of half-life period of respective M–L bond [75, 84, 124–126].

Properties of MSP will depend on such factors as DP, architecture (for example, linear or branched) and dynamics/life-time of assembly, which can be driven with the binding force, stoichiometry, and kinetics of supramolecular motif. To obtain polymers with high molecular weight, the necessary condition is high binding constant and high concentration of initial components [92]. Excess of metal ions should bring to larger assemblies than in the case when there is excess of a monomer, if there is some cooperation, i.e. binding a second ligand is more advantageous, than of the first [76, 127].

Ideal combination is a system, which provides a complex of high thermodynamic stability in connection with high kinetic lability [128]. Thermodynamic stability of M–L interactions will determine size (or DP) of assembly, while their kinetic lability should bring to «dynamic» polymers responsive to environmental factors. This combination provides building MSP, which has advantages of reversible supramolecular systems, i.e. external stimulus can be applied to them, which allows switching from monomer to polymer state or switching between different self-assembling architectures, such as macrocycles and polymers. Some of these systems can be multiply included, oppositely to classic covalent polymers, which are formed irreversibly [43, 50, 77, 129, 130].

It should be noted that metal ions provide geometry and CNs, which are absent or hardly available in covalent chemistry. By choosing chelating ligands, metal ions, counter-ions, and boundary conditions of self-assembling (M:L ratio, concentration, solvent, ionic strength, pH, etc.), it is easy to obtain vast MSP database with resources of kinetic, thermodynamic, and functional properties [73, 131]. Since for most applications, high PD are preferable, and in many cases increase in

concentration is impossible due to practical limitations or low solubility, control over binding force is most important. Increase in K_a can be reached by combination of several interacting binding sites, the simplest of which is using chelating ligands and polyvalent metal ions. Character of M–L interaction has a strong effect on properties of obtained MSP, and the binding constant is the main parameter, which should be taken into account. If M–L interaction is very weak, polymer assemblies are not formed, and if it is too strong, a polymer may be deposited. Intermediate binding constants imply easy exchange with ligands, i.e. soluble MSP are, as a rule, dynamically equilibrium systems. However, dynamic character is a serious problem for establishment of characteristics, because structure and properties of MSP depend on external conditions.

Architecture of synthesized MSP depends on localization of metal chelates [132]. In «main chain» MSP polymer matrix is self-assembled from non-covalently bound low molecular weight monomers through M–L bonds [96, 122]. Other polymer MSP architectures, which are formed, include side chain [34, 95, 133–139], branched [130], cross-linked [140–142], macrocyclic [143–151], helical [152, 153], dendritic [154] or star-like MSP [155, 156].

The aim of MSP synthesis is design of new materials, which can show specific and multifunctional properties. On one hand, presence of metal ions makes it possible to obtain coordination supramolecules with special optical, electric, magnetic and catalytic properties [11, 35, 81, 85, 130, 157–167]. On the other hand, properties of projected materials can be driven not only by thorough choice of metal ions, but also by main polymer chain. At the same time, including metal chelate nodes in supramolecular polymer system makes it possible to obtain hybrid supramolecular materials with synergetic combination of typical features of M–L chelates (special electrochemical, optical, magnetic properties) and properties of polymer (workability, mechanical properties, solubility, etc.) [168–172].

It should be noted that recently coordination-driven self-assembling becomes a powerful tool of synthesis of polymer supramolecules of nanoscale size. Moreover, dynamic character of M–L bonds provides switching capacity of a system imitating behavior of natural supramolecular structures [173, 174]. Building blocks of MSPs should be thoroughly chosen to design new materials with tunable and defined properties, which suggest a convenient platform for development of intelligent materials. Presently M–L coordination is often used as fascinating reversible non-covalent interaction, which simplifies building stimulus-responsive, memory shape, and self-healing MSP [53, 159, 175, 176]. During recent decades associated with flourishing studies on synthesis and properties of MSP solutions [81, 130, 157, 159–161], considerable efforts are taken in building molecular devices using these supramolecular assemblies. These devices include self-assembled nanostructures of MSP, as well as co-assembled objects with other modulus, which are hierarchic assemblies of self-assembled coordination supramolecules.

7.3 Linear Metallosupramolecular Polymers

The simplest way to access linear MSPs is coordination of bis-ligand functionalized ditopic monomers (sometimes called macromonomers if a spacer is oligomer or polymer) to metal ions in the ratio 1:1 bringing to MSP with multiple M–L complexes in a main chain (Fig. 7.4). These polymers usually show dynamic behavior to a greater extent than covalent polymers, because reversibility of M–L coordination provides polymerization/depolymerization and ring-chain equilibrium.

To build dynamic constitutional metallosupramolecular systems, it is possible to apply principles of dynamic constitutional chemistry advancing self-evolution of supramolecular systems to choice of discrete systems made of mixtures of objects, reversibly and continuously changing at nano- and macroscopic scales [177]. This makes it possible to obtain single or double levels of dynamic supramolecular databases using M–L and reversible ligand exchanges. The process of metal ion coordination can put ligands in immediate closeness to each other. This closeness potentially simplifies reversible supramolecular non-covalent interactions bringing to restructuring coordinating ligands within the limits of confined interactional space determined by coordination geometry around metal centers. This made it possible, for example, to automate the process of parallel coordination-driven polymerization of tpy-bis-functionalized PEO using different metal salts [178].

From the beginning MSP studies, the keenest attention of researchers was attracted to chelating polytopic monomers, in particular, polypyridyl ligands, including bpy, phen, and tpy fragments [84, 179–182].

Thus, in one of the first examples variety of constitutionally clearly defined kinetically labile MSP is obtained using phen-based bidentate ligands (Scheme 7.1) [183–186]. Ligand exchange went instantly in coordinating solvents, such as acetonitrile, while in the non-coordinated solvent 1,1,2,2-tetrachloroethane no signs of ligand exchange were observed even during several hours.

Coordination of 5,5′-bound bis-phen ligands with Cu(II), Ni(II), Ag(I), and Zn (II) ions in stoichiometric ratio 1:1 brings to formation of MSP with high molecular weights, more than 100,000 [187]. It is important that properties of MSP are characterized by reversibility depending of external factors, such as electrochemical action or addition of competitive complexing ligands.

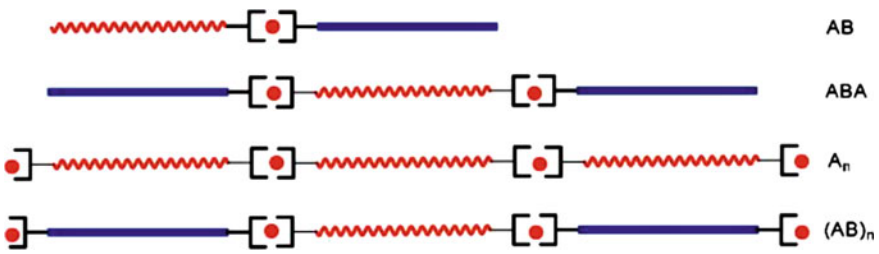

Fig. 7.4 Various accessible architectures of linear MSPs

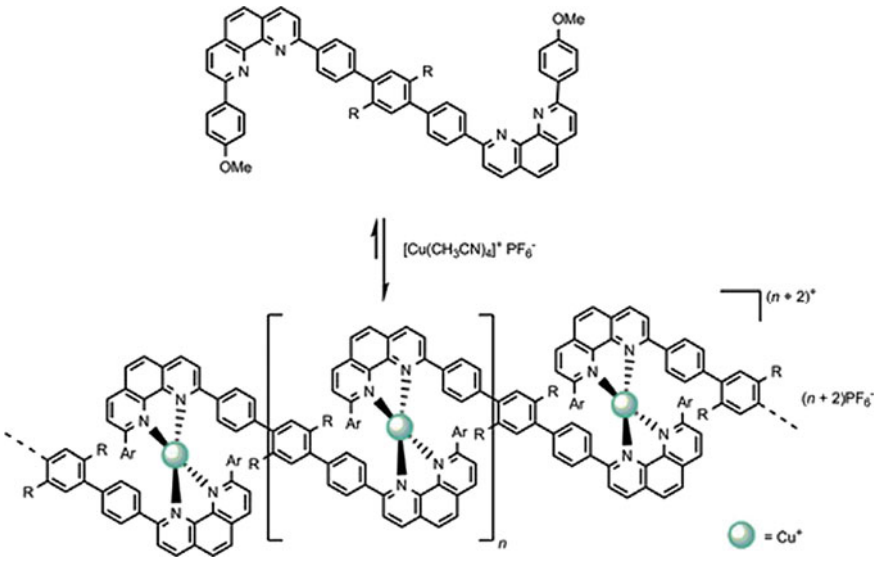

Scheme 7.1 Reversible MSP formed from bifunctional phen-based ligand monomers and Cu(I) ions

MSPs obtained by 1:1 chelation of metal ions with organic ditopic bis-phen ligands have shown unique electro- and photochemical properties based on M–L interactions. Thus, we shall notice green Cu-based MSP, for which there is typical excellent electrochromic color change from green to colorless at electrochemical reduction from Cu(II) to Cu(I) [188].

In the case of Ni(II)-based MSP with bis-phen ligands having different spacers and/or substituents, ionic conductivity of polymer films increases considerably with increase in relative moisture, and a polymer without hydrophobic spacer has shown conductivity 0.75×10^{-3} S cm^{-1} at 98% of relative moisture, which is by about 500 times higher than ionic conductivity of a polymer with a spacer [189].

Fe(II)-, Ru(II)-, and Cu(II)-based MSP films showed reversible electrochromic behavior, which was used in fabrication of devices of electrochromic display (Fig. 7.5). It is interesting that a polymer containing both Fe(II) and Ru(II) ions exhibited multicolor electrochromic properties, and for Eu(III)-based polymer vapoluminascence is typical. Besides, reversible switching emission is reached in the polymer with Fe(II) and Eu(III) ions integrated alternately [99].

A series of functional MSPs based on polyhedral oligomer silsesquioxane and phen ligand was obtained using two-staged approach [190, 191]. At the first stage phen-based ligand is used for synthesis of amino-functionalized complex of a transition metal using Sn(II) chloride, and at the second stage this metal complex is subjected to interaction with octakis(3-chloropropyl) octasilsesquioxane, bringing to MSP carrying a structure of polyhedral oligomer silsesquioxane. The obtained

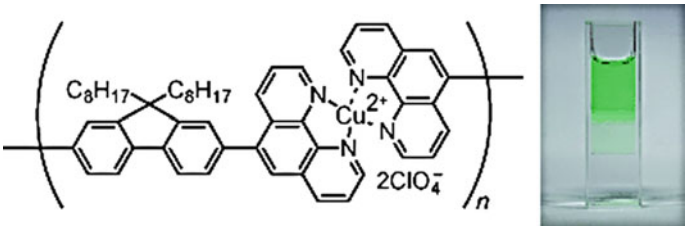

Fig. 7.5 Cu(II)-based MSP obtained by the 1:1 chelation of metal ions and bis(phen)s with reversible electrochromic behavior [99]

MSP has shown electro- and chemo-responsive properties and is a good candidate for smart stimulus-responsive materials.

Polytopic ligands with tpy and structurally related fragments have a considerable place in MSP design. Using similar ligands is interesting for building a vast variety of different architectures including both linear MSPs, and AB block-copolymers, graft-copolymers, and metal supramolecular micelles. In particular, rigid linear building blocks with tpy fragments bring to rod-like MSP, and building blocks with flexible spacer blocks or rigid spacer units, which give well-defined angle between chelating fragments, bring to cyclic structures [125, 192–194]. It has been shown, for example, upon synthesis of MSP such as [bis(tpy-4′-yl)-$FeCl_2$-di(ethylene glycol)]$_n$, [bis(tpy-4′-yl)-Ru$(BF_4)_2$-di(ethylene glycol)]$_n$, [bis(tpy-4′-yl)-$FeCl_2$-PEG_{180}]$_n$ and [bis(tpy-4′-yl)-Ru$(BF_4)_2$-PEG_{180}]$_n$ [195].

A rich variety of new ditopic bis-tpy [160] obtained by symmetric and non-symmetric introduction of functional groups in pyridine rings, and also by tuning spacers for linking of two tpy-fragments is described. These bis-tpy are convenient ligands for development of new MSP with different functions, and for studying structure-property relationship. In particular, it occurs that such structural factors of bis-tpy-based MSP as functional group nature in peripheral ring of ligands and spacers between two chelating tpy fragments have a significant effect on charge transfer and electrochemical properties of different types of Co(II) bis-tpy MSP.

Linear MSPs are usually formed between molecules of ditopic ligand (bis-ligand), which have two chelating heads and metal ions, as is shown in Fig. 7.6a [132]. Chelating heads of these ditopic molecules of a ligand often contain di- or tpy-, and sometimes carbonyl groups. Figure 7.6b–d shows some examples of linear MSPs [81, 130, 157, 160, 196, 197]. DP of linear MSPs has a strong dependence on concentration and ratio of components of a mixture [127, 197]. Long chains can only be formed for 1:1 M–L ratio at high concentrations, and deviation from 1:1 mixing brings to such a chain ends formation that the chain growth is stopped. Concentrated 1:1 mixed system of bis-ligands and metal ions can be very viscous and elastic, while diluted system is water-like with small ring oligomers present [197].

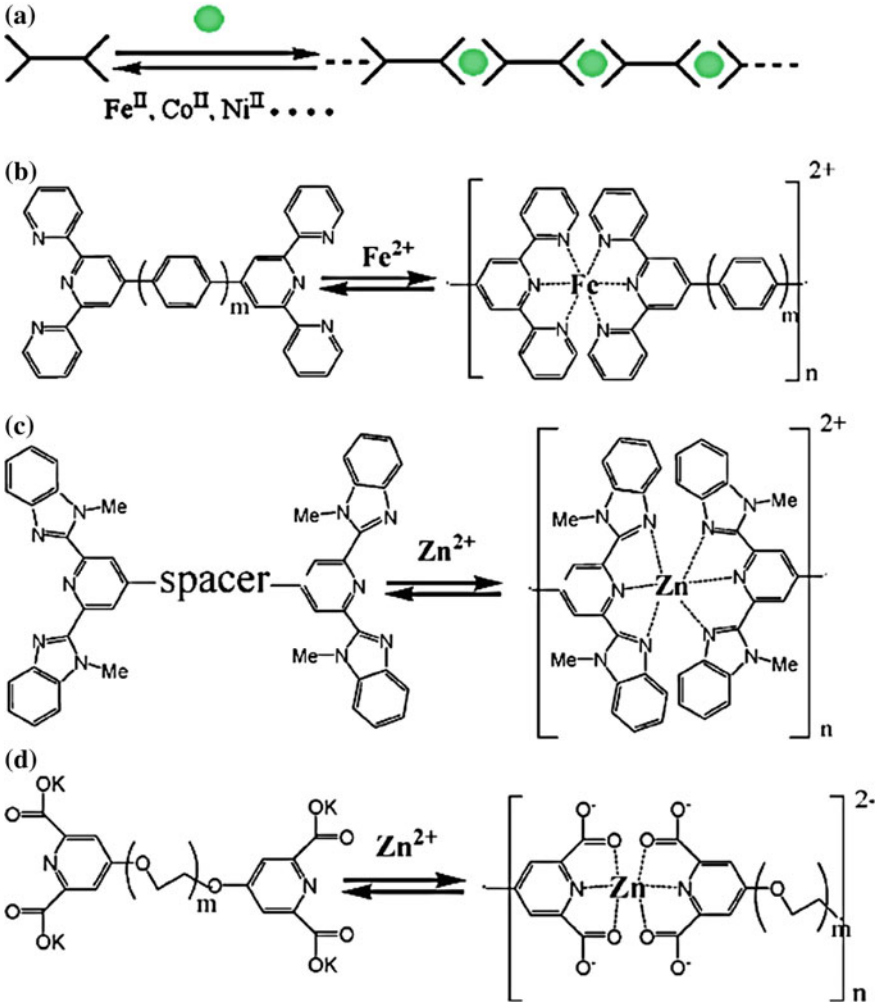

Fig. 7.6 **a** Schematic representation of formation of linear MSP and **b–d** are appropriate examples [132]

We shall notice the concept of thiol-*para*-fluorine click chemistry used for fast and efficient formation of Ru(II) bis-tpy MSP. Oppositely to widespread methods of MSP assembling, demanding high temperatures and longtime of reaction, using penta-fluorine-phenyl-substituted homoleptic Ru(II) bis-tpy complex as a monomer, thiol-functionalized organic spacer blocks can be easily integrated at low temperatures and for very short reaction time [198].

Soluble MSP based on Ru(II)tpy_2 chelate is obtained through two different ways of synthesis: (1) coordination of telechelic tpy ligand with activated Ru(II) species,

(2) Pd-catalyzed polycondensation of Ru(II) bis-tpy chelate carrying functionality of a halogen with diboronic acid (Scheme 7.2) [96]. Comparison of the final products of the reaction has shown that the 1st method has brought to more macromolecular species as compared to the 2nd method, which has given only oligomer structures.

Random Zn(II)-based and alternating Ru(II)-based MSPs containing bis-tpy ligands with different central donor (fluorene or Cz) and acceptor (benzothiadiazole) fragments are synthesized (Scheme 7.3) [199]. It occurs that due to strong donor-acceptor interactions with participation of Zn(II) and Ru(II) ions absorption spectra of obtained MSPs cover a wide range 260–750 nm with a gap width 1.57–1.77 eV.

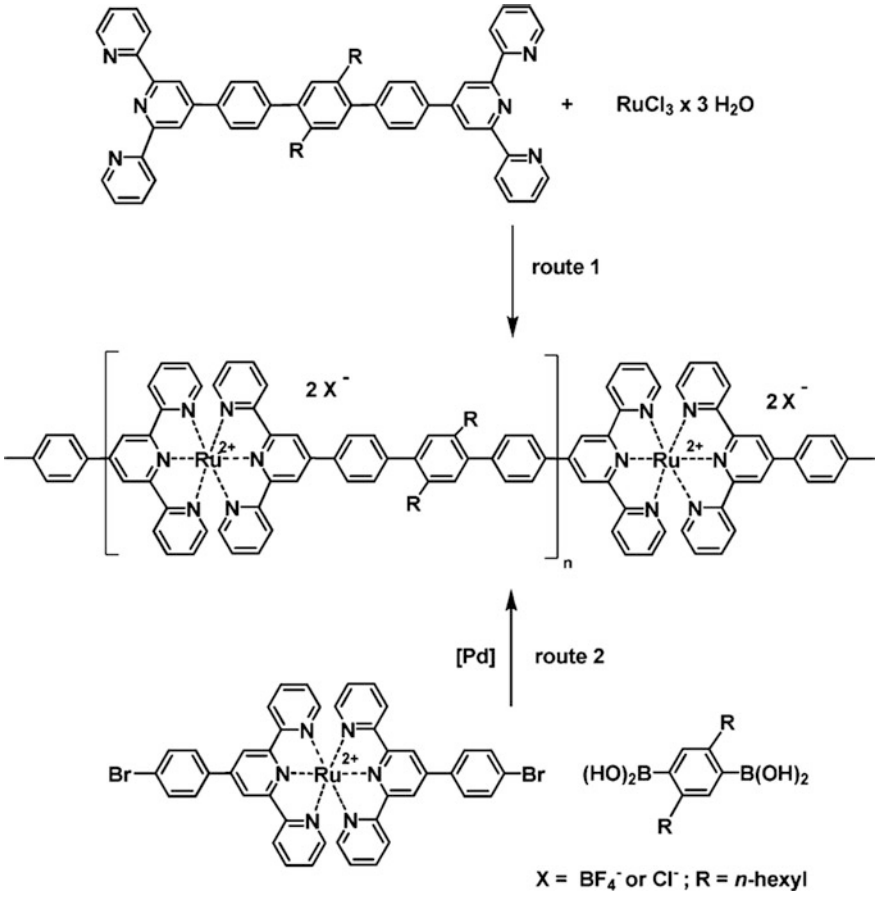

Scheme 7.2 Two different routes of synthesis of Ru(II) chain-extended polymers [96]

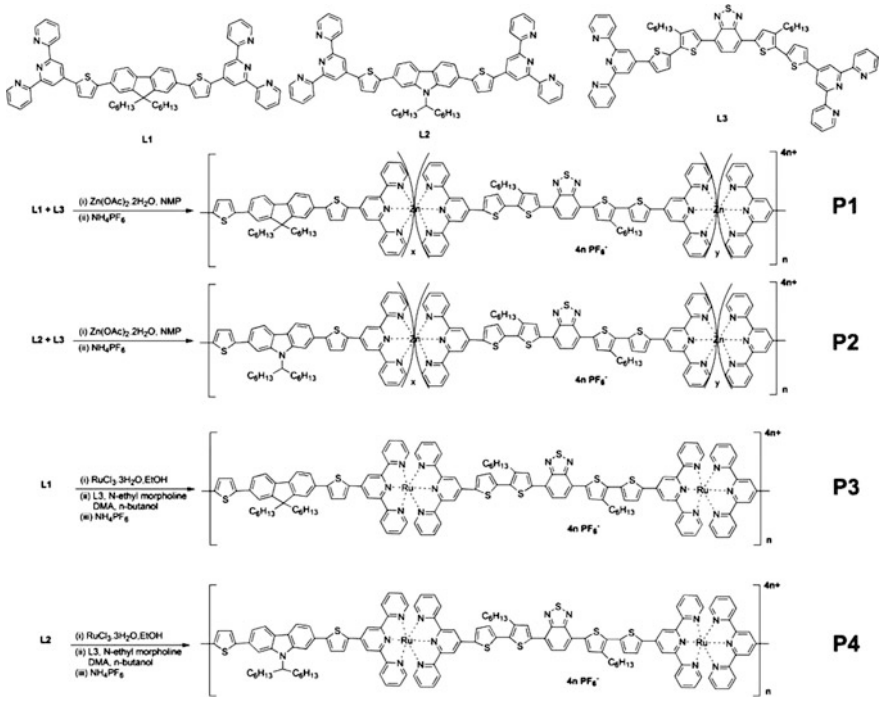

Scheme 7.3 Two random Zn(II)-based and two alternating Ru(II)-based metallo-copolymers containing bis-tpy ligands with various central donor (i.e., fluorene or Cz) and acceptor (i.e., benzothiadiazole) moieties [199]

Similar results were obtained in the studies of Zn(II)-based MSP produced by 1:1 complexation of $Zn(ClO_4)_2$ and bis-tpy ligands with electron-donor (alkoxy) and electron-acceptor (cyano) groups in 6-position of peripheral pyridine fragment [200]. In particular, Zn(II)-based MSPs have shown relatively high quantum yields (Φ_{PL} = 0.68–0.76) in solution at room temperature, and different luminescent colors: blue, light blue, and green in film state due to considerable Stokes shift caused by the effect of a ligand substituents.

Thermodynamics of chelation between tpy ligands and Zn(II) ions is studied in detail [201]. The results of the studies provide conclusions that Zn(II) ions offer interesting balance between reversibility of chelation process and stability of projected structures due to high affinity constants. Besides, telechelic tpy ligands are obtained carrying organic fluorophore spacer.

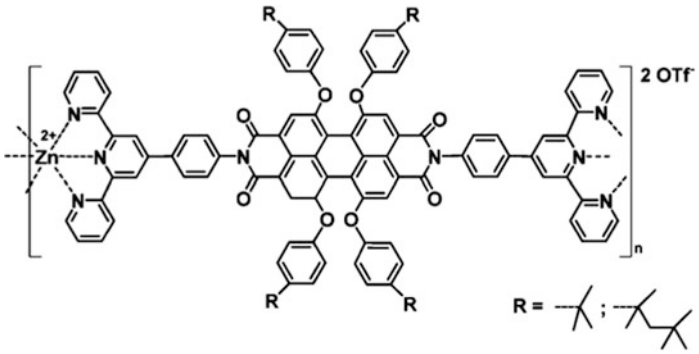

For Zn(II) MSP based on bis-tpy ligands considerable effect of a metal ion on EL properties of synthesized MSP is typical [158, 202]. Zn(II) MSP has shown very good luminescent properties (very strong red-light-emitting) with high potential for integration in layered polyelectrolyte devices. Also incorporation of Zn(II) ions in MSP through polycondensation of bis-tpy ligands carrying different π-conjugated architectures of a spacer is studied (Scheme 7.4) [203]. The obtained chain-extended Zn(II) MSP has shown emission from violet to yellow.

Two routes of incorporation of bis-tpy ligands carrying chromophores or π-conjugated spacer into polymer structures via Zn(II) suprapolymerization have been developed (Scheme 7.5) [204, 205]. For these polymers blue emission of photoluminescence (about 420 nm) with quantum yield from 11 to 23% (in DMF) is typical, and in this case formation of excimers is suppressed by integration of Cz side groups. Besides, obtained MSP have shown green emission of EL (about 550 nm).

A vast variety of labile tpy MSP is obtained [193, 206–208]. In particular, by studying MSP formation based on bis-tpy PEG (M_n = 8000) with different transition metal ions the effect of metal ions such as Cd(II), Cu(II), Co(II), Ni(II), Fe(II) on DP and resulting molecular weights is considered.

We shall also notice [209] MSP production by chelation of dimethyl-substituted bis-tpy ditopic ligand with Ru(II), Fe(II), Co(II) ions in respective solvent. In this case stoichiometry 1:1 of chelation of a ligand with a metal ion in MSP is confirmed, affinity constants (log K) are very high (>9) showing that spatial hindering of the ligand methyl groups has no effect on formation of MSP.

Formation of metal-bis-tpy MSP is influenced by two main factors of chelation. The first is the formation of a mono-tpy-chelate by coordination of one tpy ligand to one metal ion. At the second step the bis-tpy-chelate is formed by addition of another ligand in the system. Possible exchange in the solution between ligand, metal ion, mono-chelate and bis-chelate comprehensively described for tpy MSP [73, 76].

Extremely interesting is production of thin filmed databases of Zn(II) bis-tpy MSP produced by jet-printing for studying structure-property relationship and their possible using for organic photoelectric or PLED applications [210]. During using

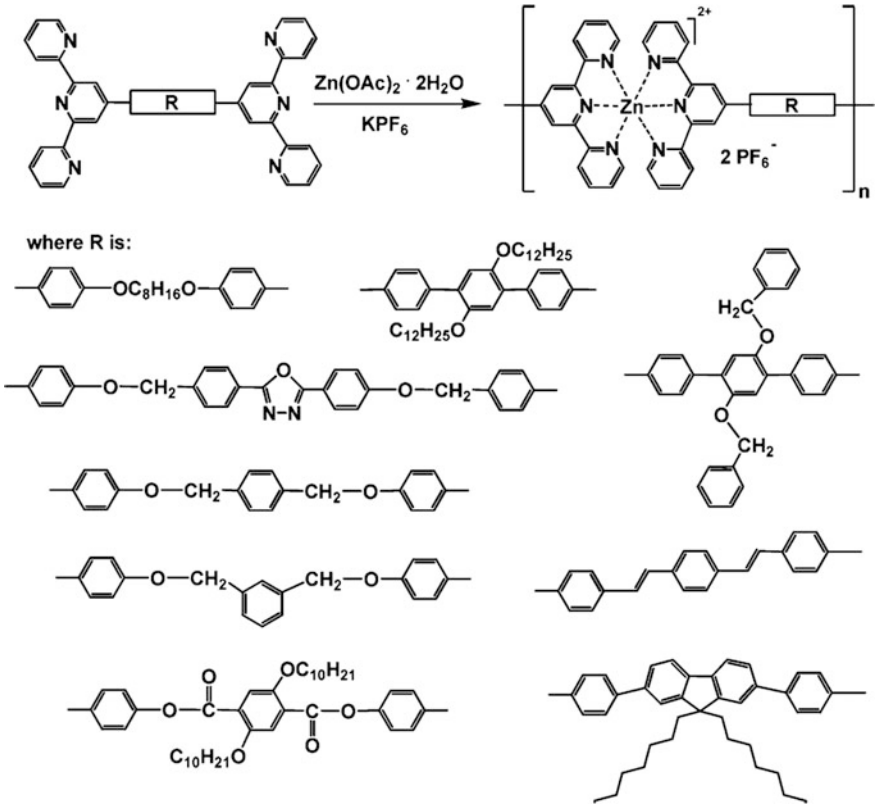

Scheme 7.4 Schematic representation of synthesis of Zn(II) MSP based on bis-tpy ligands [203]

combinatorial approach different important parameters including system of solvents, dot spacing and a substrate temperature, as well as properties of UV-vis absorption and emission were subjected to efficient and reproducible screening in materials. As a result, homogeneous films of thickness 150–200 nm were obtained during printing at 40–50 °C and from the mixture of DMF and acetophenone solvents in the ratio 90/10.

Promising is using labile metal chelates for building chiral forms, since they offer dynamic transformation of chiral molecular form as response to external stimuli (Fig. 7.7) [211].

MSPs are obtained by coordination polycondensation reaction of tpy-functionalized polyhedral silsesquioxane with Co(II) and Cu(II) ions [212]. It occurs that optical and electrochemical properties of MSPs depend on substituent in peripheral pyridine, and MSPs themselves have electrochromism during the oxidation process.

MSPs based on tpy ligands have recently shown their potential to optoelectronic applications based on (i) their excellent properties of charge transfer or

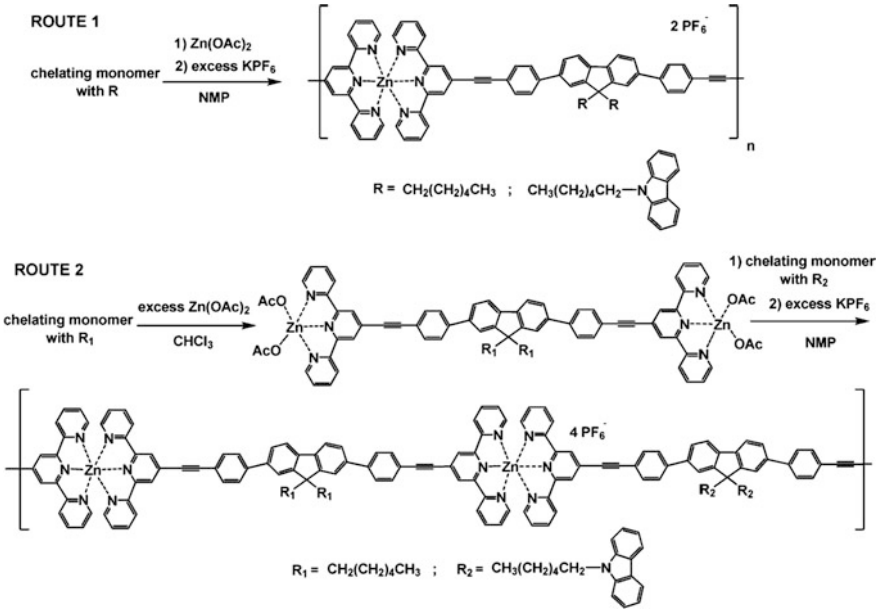

Scheme 7.5 Scheme of synthesis of Zn(II) homopolymers (route 1) and Zn(II)-*alt*-copolymers (route 2) [204]

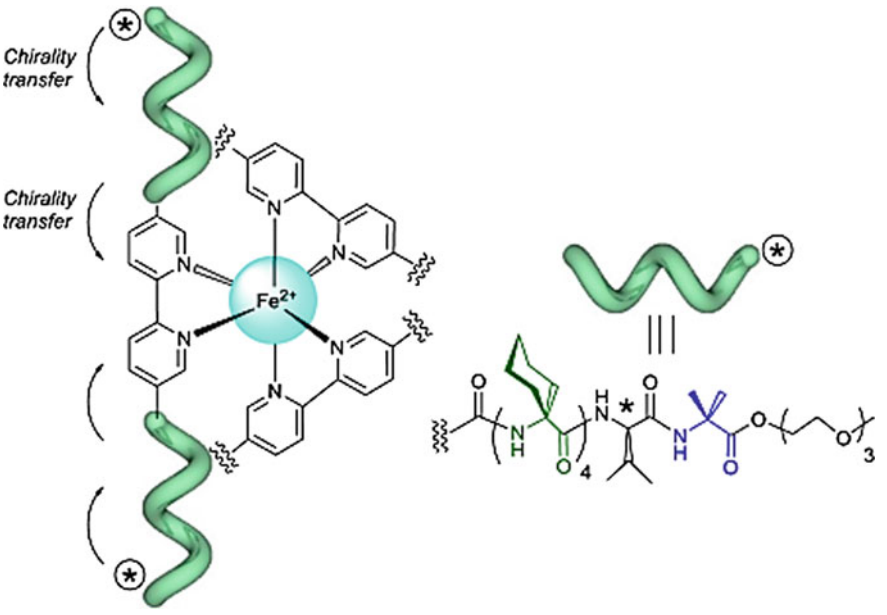

Fig. 7.7 Chirality induction in an octahedral tris-bipyridyl Fe(II) complex induced by (S)-valine via a helical tetrapeptides [211]

(ii) intriguing luminescent properties of the system, depending on their architecture, and the general properties of the luminescence correlate with the polymer structure [213].

Importantly, the architecture of the polymers and types of metal coordinated to tpy-containing MSP, can lead to unique photophysical properties [11, 13, 214]. As a result, quenching or increase in polymer fluorescence can change making it possible to apply MSPs as luminescent sensors for metal ions and in photo elements [13, 75, 215–217]. For example, tpy-containing Ru homo- and copolymers are used for production of polymer solar elements and solar elements sensitized by a dye [217]. These MSPs are obtained on the basis of poly (*p*-phenylene vinylenes) functionalized with terminal tpy residuals, and can quench fluorescence, thus showing that polymers can transfer energy to tpy-containing Ru chelates.

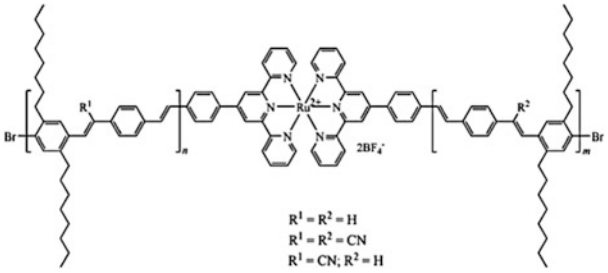

Considerable efforts were taken in recent years for development of new metallosupramolecular architectures of dyes, since they are of keen interest as modeling systems for natural light-harvesting and photosynthetic complexes, and for potential applications in solar energy transformation, photonics, and molecular electronics. Various metallosupramolecular assemblies of dyes are recently built using M–L coordination [218].

Another way to obtain these macromolecular assemblies is integration of fluorescent dye anion (sulforhodamine, SRB) in Fe(II)-based MSP via counter-ion exchange (Fig. 7.8) [219]. Solid state device made using the obtained polymer shows electrochromic properties based on electrochemical redox of Fe(II) ions at voltage ±2.8 V, which displays due to appearance and disappearance of MLCT absorption in MSP.

The Zn and Cd MSPs are produced based on 1,4-diketo-pyrrolo[3,4-*c*] pyrrol derivatives of ditopic tpy-ligands [220]. It occurs that MSPs modified by a phenyl block have shown maximum absorption at about 504 and 506 nm in films, while MSP, in which a thiophene fragment is incorporated, exhibited strong and wide visible absorption at 300–800 nm with a maximum at 601 and 598 nm and shoulder peaks at about 665 and 671 nm, respectively.

The Zn MSP, carrying dibenzo-24-crown-8 arms, is obtained by coordination of Zn(II) ions with conjugated bis-tpy ligand, which shows depending on concentration emissions from blue to white and yellow (Fig. 7.9) [221].

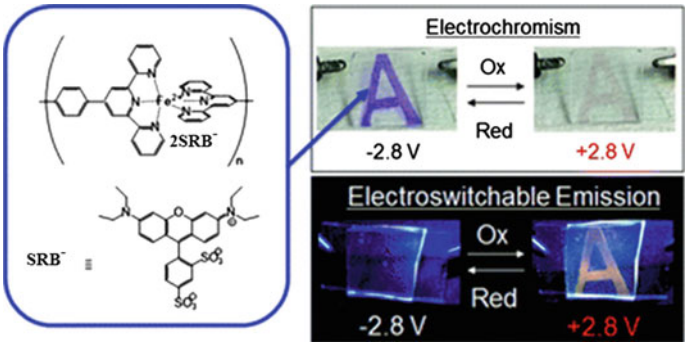

Fig. 7.8 The electrochemically reversible photoluminescence of sulforhodamine B (SRB) anions is demonstrated based on the redox of Fe ions in a MSP [219]

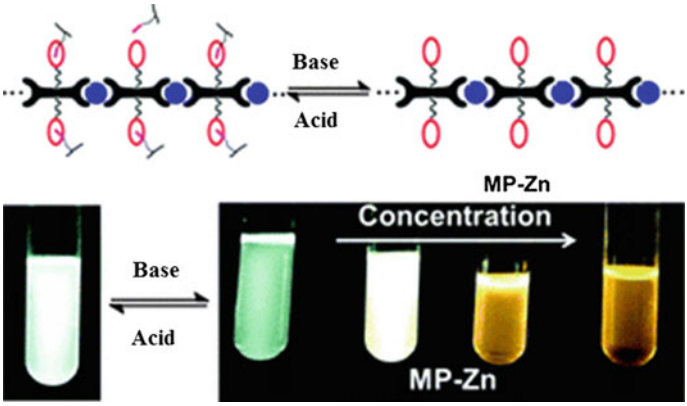

Fig. 7.9 Zn MSP, carrying dibenzo-24-crown-8 arms, which shows depending on acid-base concentration emissions [221]

Tridentate 2,6-bis(1′-methyl-benzimidazolyl)-4-hydroxypyridine (BIP) is a universal ligand for building stimulus-responsive MSP (Scheme 7.6) [196, 222–224].

An interesting class of soluble Eu(III) MSPs is developed [225] on the basis of tridentate ditopic pybox ligand, which shows high metal emission quantum yields up to 73%, and also unique dynamic behavior in solution (Fig. 7.10).

Chelating ligands containing 2,6-bis(1,2,3-triazole-4-yl) pyridine (btp) fragment is one of widespread motifs in chemistry during last decade [226]. This class of ligands formed in one-pot click reaction is studied for different purposes, for example, for generation of supramolecular self-assembling d- and f-metals, and formation of dendritic and polymer networks, etc. For example, Eu(III) and Tb(III)-directed assembly of btp ligands is studied in CH_3CN using monitoring of their different photophysical properties. As a result, stoichiometry and stability constants of different chiral supramolecular assemblies in solution have been found [227].

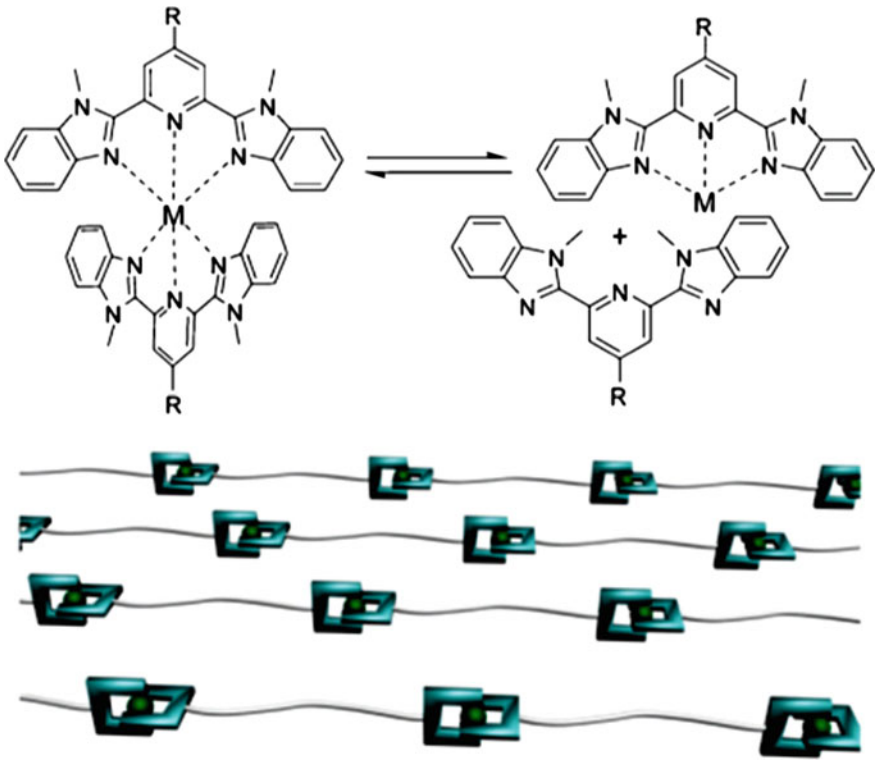

Scheme 7.6 Reversible dimer formation from two BIP molecules driven by M–L coordination and cartoon representation of the formation of MSP based on this dimer formation

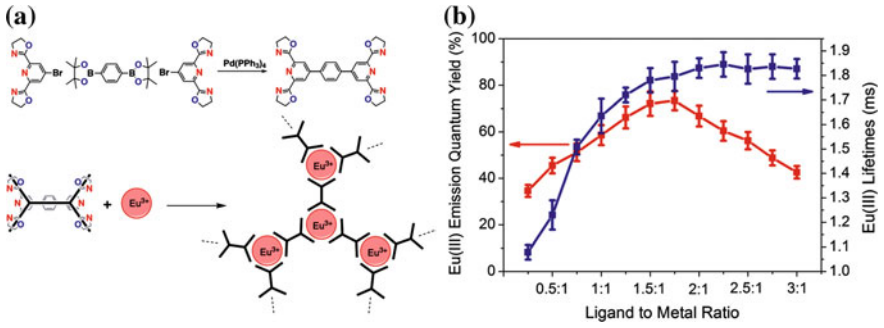

Fig. 7.10 **a** Ligand synthesis and schematic representation of the preparation of soluble dynamic Eu(III) MSPs with pybox-related ditopic ligands. **b** Relative Eu(III) emission quantum yields (left axes) and Eu(III) emission lifetimes (right axes) for different ligand to metal ratios in chloroform/acetonitrile [225]

Ditopic btp ligands containing π-conjugated spacer and solubilizing groups involved in the click reaction are used for synthesis of Ru(II) MSPs, which have intensive absorption of visible light by MLCT. As it turned out, MSPs obtained have high molecular weight and medium hardness. Studies of polymers in solid state have confirmed formation of MSPs, whose macromolecules have rod-like conformation (Fig. 7.11). Besides, polymers form films by coating solutions drop-casting [228].

Another widespread ligand for MSP production is 2,6-bis(1′-methylbenzimidazolyl) pyridine (Mebip). In particular, MSP synthesis based on poly (*p*-phenylene ethynylene) and poly (*p*-xylene) macromonomers with Mebip terminal groups and different metal salts is developed [229, 230]. It is interesting that oppositely to other MSPs, where character of a metal salt and counter-ion plays important role, only insignificant differences in obtained MSP properties were observed depending on a metal ion, for example, Fe(II), Zn(II), La(III), and counter-ion (ClO_4^-, OTf^-, NTf_2^-). Instead of it, properties of the studied MSPs are determined, first of all, by the character of telechelic oligomer.

Another type of tpy back-to-back ligand 1,4-bis(1,2′:6′,1″-bis-pyrazolylpyridin-4′-yl) benzene was developed [231], which was used for production of linear Fe(II) supramolecular oligomer/polymer (Scheme 7.7). Synthesized MSP has shown reversible spin transition above room temperature with wide hysteresis loop (about 10 K).

Neutral linear dynamic MSPs based on acyl hydrazone bound with Co(II), Ni (II), Zn(II) and Cd(II) ions are obtained using metallosupramolecular polymerization [232]. Choice of monomer ligand, as was established, takes place in a mixture of subcomponents (carboxyaldehydes and bisacyl hydrazides) controlled by hexacoordination to a certain metal ion. It is important that MSPs change their constitution by exchanging and reshuffling their components with other MSPs through exchange of ligands at coordination site of a metal in solution and in neat phase (Fig. 7.12). As a result, these MSPs are subjected to considerable changes of their mechanical and optical properties.

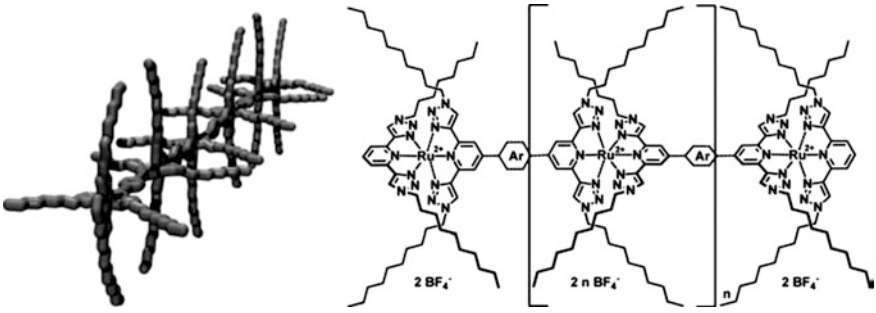

Fig. 7.11 Rod-like conformation in the solid state and structure of Ru MSP based on ditopic btp ligands featuring a π-conjugated spacer and clicked-on solubilizing groups

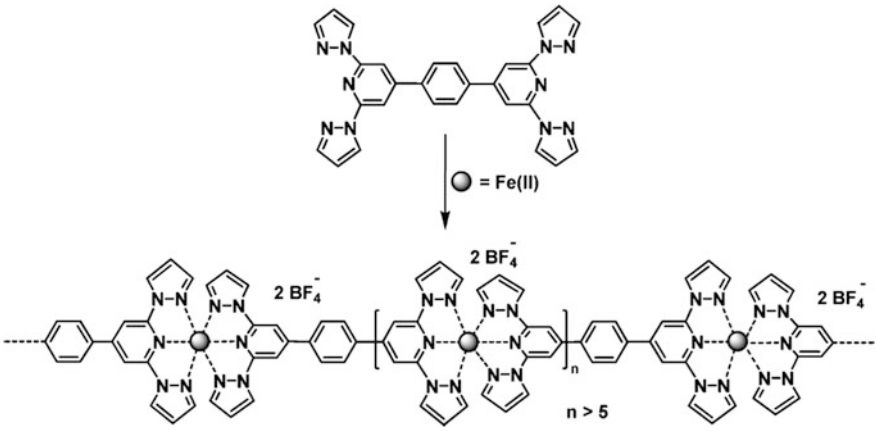

Scheme 7.7 Schematic representation of Fe(II) MSP based on 1,4-bis(1,2′:6′,1″-bis-pyrazolylpyridin-4′-yl) benzene

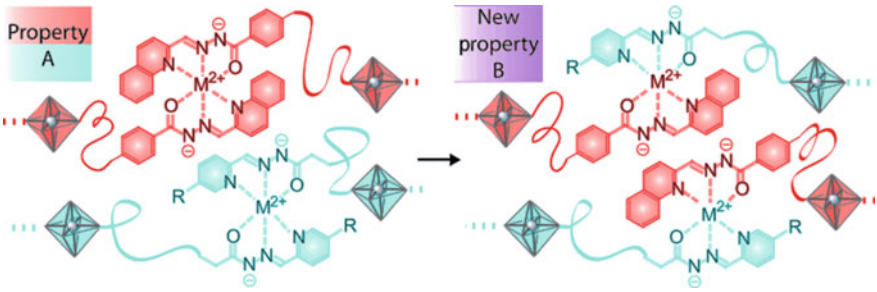

Fig. 7.12 Scheme of the transformation of properties that result from constitutional M–L exchange reactions in dynamic MSPs

Interesting concept for MSP synthesis is application of ionophore ligands, which, as is known, are bound with high affinity to alkali metal ions. Thus, tris (spirotetrahydrofuranyl) ionophores with rigid spacers are constructed from 1,3-butadiyne units, which are selectively linked with Li(I) in 2:1 complex with formation of rigid rod-like MSP, which, however, is limited soluble [233].

Also MSP should be noticed, containing (triethanolamine) Cu(II) fragments linked by pyromellate units, which can be used as a catalyst precursor for peroxidation of cyclohexane into cyclohexanol and cyclohexanene with hydrogen peroxide at room temperature [234, 235].

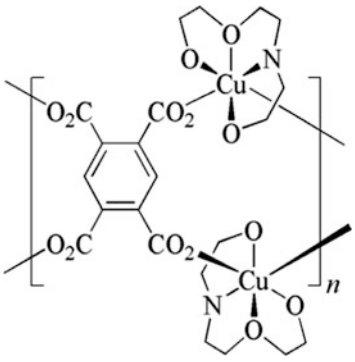

If oligomers or polymers with chelating fragments at a chain ends are used in the process of metallosupramolecular polymerization, various linear metallosupramolecular block-copolymers can be obtained [236]. This brings to systems, which combine typical features of block-copolymers (for example, microphase separation between immiscible constituent blocks), and supramolecular polymers (for example, reversibility and retuning supramolecular bonds strength). In this case M–L coordination can be used for bridging between different blocks of homopolymers or for linking together different block-copolymers.

In this way, for example, di- and tri-block-copolymers (A-[M]-B [237–239], A-[M]-B-[M]-A [240, 241] or A-[M]-B-*b*-C [239, 241] were obtained, where [M] is an M–L center. If A, B, and C blocks are immiscible, then these block-MSPs can behave as amphiphilic block-copolymers with self-assembling character. The only ligand used presently for block-MSP synthesis is tpy [236]. It is important that asymmetrically directed supramolecular interactions should be involved for formation of these complex macromolecular architectures [242]. In other words, the synthesis of block-MSPs requires the formation of heteroleptic complexes, and the formation of homoleptic complexes should not occur. For such selective complexation two-staged procedure of chelation is necessary. Really, first a mono-chelate should is formed, which then is developed into desired bis-chelate under certain conditions [243]. Most extensive studies on the subject were performed for block-MSP Ru, since high stability of bis-tpy-Ru(II) chelates makes it possible to preserve integrity of resulting block-copolymers in different media, such as organic solvents or water, even at extreme pH and salt concentrations [244].

Efficient way of block-MSP synthesis is growth of two polymer blocks from heteroleptic Ru chelate, which acts as double initiator, since chelation will take place between small molecules [243]. The most well-studied system in this aspect is PS-[Ru]-PEO block-copolymer and, in particular, PS_{20}-[Ru]-PEO_{70} composition, in which PEO obtained by NMRP method, and commercially available PS are used, and numbers bottom mean average DP of PEO and PS blocks, respectively [245].

It should be noted that formation of homo- and block-MSPs depends considerably on reaction conditions, such as stoichiometry of reagents, a solvent and a salt type, time, temperature, and concentration.

The amphiphilic block-MSPs allow for purposeful formation of micellar aggregates in water [245–248]. Thus, slow and regular water addition, using a syringe pump, to the PS_{20}-[Ru]-PEO_{70} initial solution of copolymer in DMF brings to strictly defined micellar solution almost without further aggregation of micelles. At that, these micelles have shown single-mode size distribution with average molecular weight 318,000, which corresponds to aggregation number 53 of copolymer chains in a micelle [249].

Interesting observations were made when studying PS_{20}-[Ru]-PEO_{70} copolymer in melt. In particular, when hexafluorophosphate (PF_6^-) was used as a counter-ion, the observed morphology was spherical, not expected laminar, taking into account the copolymer composition [249]. Due to aggregation of tpy-Ru(II) chelates and counter-ions spherical aggregates are formed with radius about 1.5 nm surrounded by a polymer shell with external radius about 2.4 nm. When bulk tetraphenylborate (BPh_4^-) was used as a counter-ion, highly ordered laminated melt was obtained with 11.9 nm periods after annealing at 55 °C for 40 h [250]. These studies of nanometer organization of PS_{20}-[Ru]-PEO_{70} in both selective solvents and in volume have shown considerable effect of bis-tpy Ru chelates on microphase separation between PS and PEO blocks. Similar conclusions were made for investigation in melt of viscous-elastic properties of linear supramolecular assemblies obtained by addition of various amounts of Ni ions to linear entangled PEO building blocks with terminal modified tpy group [251]. In particular, it occurs that elasticity of these supramolecular assemblies is mainly determined by dynamic of entanglement of building blocks, while supramolecular interactions impede or suppress their relaxations. At that, by regulation of a number of metal ions, it is possible to control relaxation time and level of low-frequency plateau of these supramolecular assemblies. It is important that additions of metal ions more than 1:2 metal ion/tpy stoichiometric ratios makes it possible to induce secondary supramolecular interactions, which can bound linear supramolecular assemblies and, thus, bring to gelation of a system.

Since the method of production of block-MSPs depends on combination of two macroligands through simple two-staged synthesis, it is quite easy to create database of block-copolymers. For example, thus obtained 4 × 4 database of PS-[Ru]-PEO block-copolymers and morphology of produced thin films were studied [252]. We shall also notice another 13-member database, which was used for studying behavior of micelle formation of block-MSPs in water [253]. Apart from formation of copolymer databases, one more advantage of block-MSPs is in reversibility of bis-tpy chelates. Really, oxidation of Ru(II) ions to Ru(III) should be accompanied by transformation of initial bis-chelates into mono-chelates. This reversibility can be used predominantly for formation of definite nanoporous structures, which was shown in production of nanoporous thin films of PS_{375}-[Ru]-PEO_{225} copolymer [254].

Apart from PS-[Ru]-PEO metallosupramolecular copolymers, we shall notice amphiphilic poly (ethylene-*co*-butylene)-[Ru]-PEO copolymer, for which quasi-equilibrium state is found between micelles and clusters presumably, due to softness of micellar core. Addition of a great excess of water-soluble competitive ligand brought to decomposition of bis-tpy chelates and appearance of water-dispersed poly (ethylene-*co*-butylene) nanoparticles decorated by charged metal complexes on their surface [237, 238]. Rod-like micelles were obtained [255] from poly (Fc-silane)-[Ru]-PEO copolymer in water and the micelles had a constant diameter, but were rather polydisperse in length. Also synthesis of amphiphilic PS-[Ru]-poly (NIPAM) using RAFT polymerization with tpy-functionalized agent of chain transfer is described [256].

It should be noted amphiphilic diblock-MSPs containing heteroleptic bis-tpy chelates Co(II) and Ni(II) in a block junction of PS and PEO (Fig. 7.13) [257].

Straightforward approach to synthesis of AB_nA block-copolymers through tpy-Ru(II) chelation is described (Scheme 7.8) [258]. The applied approach of combinatorial optimization made it possible to carry out systematic screening of optimal conditions for one-pot polymerization reaction of bis-tpy-hexadecane with $RuCl_3$ under reduction conditions. The established laws were applied for purposeful synthesis of Ru(II)AB_nA supramolecular triblock-copolymer using mono-tpy-PEG as chain stopper during reaction of metallosupramolecular polymerization of bis-tpy-hexadecane.

Individually optimized synthetic approaches were used to study of the formation of AB_nA supramolecular triblock-copolymers based on Ni(II), Fe(II), and Co(II) chelates [240]. For Ni(II) AB_nA supramolecular triblock-copolymers end capper treatment was varied to regulate length of the medium block B. It is important that synthesized triblock-MSPs are self-assembled in aqueous solution due to their amphiphility.

Metallosupramolecular PS-*b*-polyisoprene-[Ni]-PS triblock-copolymer is prepared efficiently using two-stage procedure (Fig. 7.14) [259]. It should be noted that metal chelates are located predominantly in adjacent spherical area and form a core-shell structure, and the obtained multiphase material has different elastomer properties with considerable strength and creep.

Also we should mention triblock-copolymer ABC obtained by chelation of tpy-functionalized PS-*b*-P2VP with tpy-functionalized PEO [241], which is used

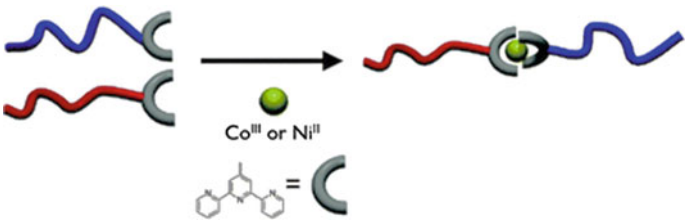

Fig. 7.13 Synthetic scheme towards the formation of PS_{240}-[Co]-PEO_{230} and PS_{240}-[Ni]-PEO_{230} metallosupramolecular block-copolymers [257]

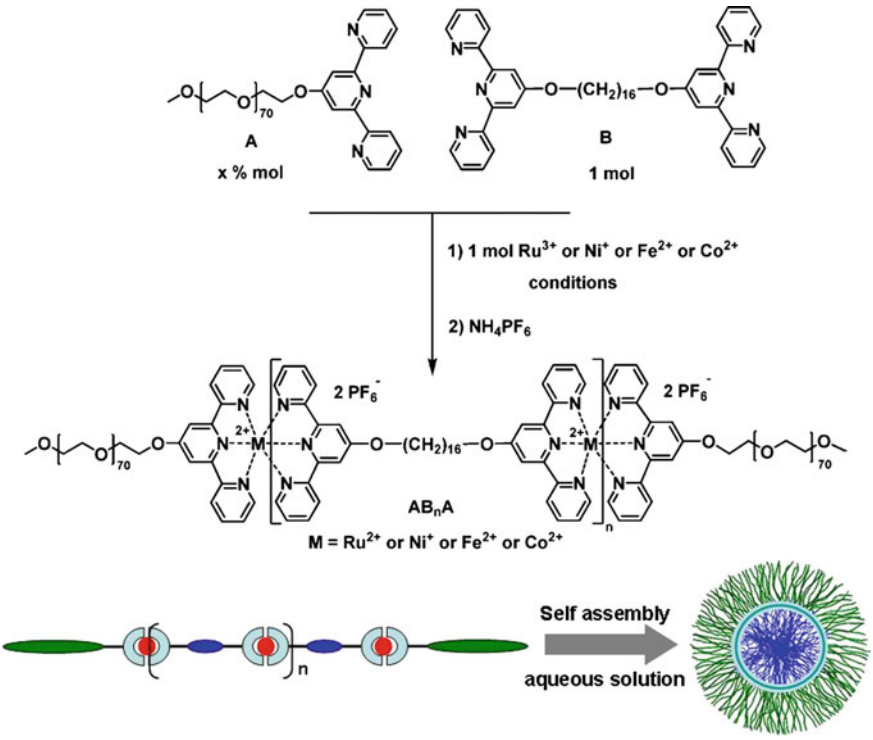

Scheme 7.8 Synthesis of supramolecular M(II)-AB_nA triblock-copolymer and schematic representation of micelle formation [258]

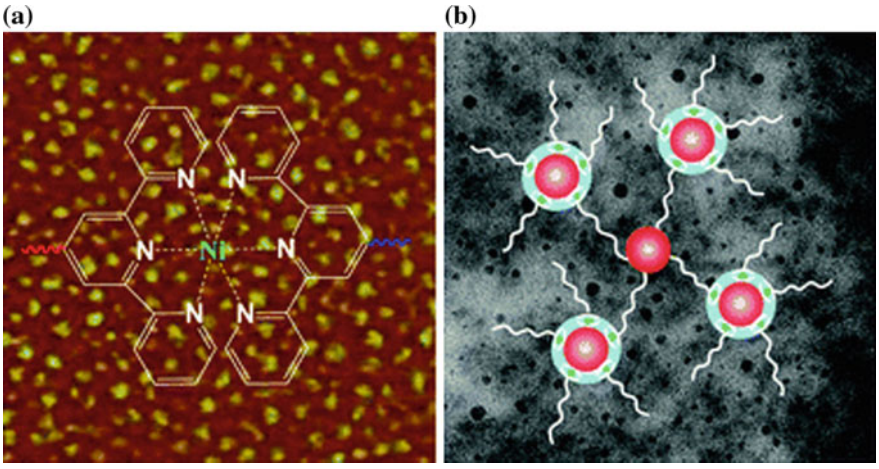

Fig. 7.14 AFM phase image (**a**) and TEM image without staining (**b**) of metallosupramolecular triblock-copolymer

for preparation of core/shell-crown micelles consisting of PS core, P2VP shell, and PEO crown, where P2VP is poly-2-vinylpyridine.

It should be noted that linear MSPs provide control over dynamic helicity at supramolecular level [260]. Strong M–L interactions between individual molecular components in controlled helical nodes, beginning from columnar aggregates to spiral polymers and cholesteric liquid crystals bring to stereo induction from molecular level to the level of supramolecular helical architectures.

7.4 Branched Metallosupramolecular Polymers

Telechelic ligand molecule with three chelating ends can be used to obtain branched MSP (Fig. 7.15a) [140]. Branched MSPs can also be formed in the mixed system of ditopic ligands and f-block of metal ions [77, 129, 261, 262], where f-block metal ions can link three chelating ends, which act as cross-linkers (Fig. 7.15b).

Two constitutional isomers of branched MSPs are self-assembled from tpy-ligands in ternary system [263]. Restrictions of possible outcomes for self-assembling finally provide optimal conditions for isolation of molecular bowtie or its isomer butterfly motif. It is noteworthy that these structural isomers have very different drifts in diversification of ionic mobility corresponding to different sizes and forms at high charge states.

Interesting chelating ligand for branched MSP fabrication is hexathiobenzene carrying six peripheral tpy units (Fig. 7.16), which can excite coupled aggregation-induced emission (AIE) reflected by a core in solid state [264]. Phosphorescence of hexathiobenzene core is involved during chelation of Mg(II) in THF, because M–L coordination impedes intramolecular rotation and the chromophore core motion, thus helping to radiation deactivation of the luminescent excited state. When $[Mg(tpy)_2]^{2+}$ units of a polymer structure are excited, the phosphorescence core sensibilization has efficiency >90%. It is important that a polymer light-harvesting

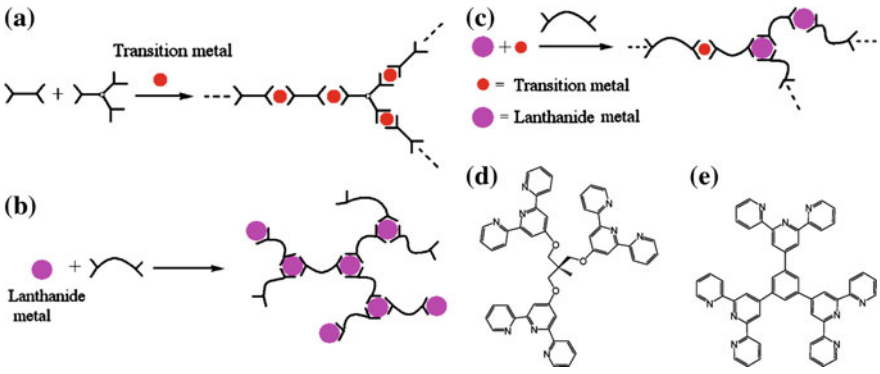

Fig. 7.15 **a–c** Illustration of branched MSP and **d** and **e** examples of branched ligands [140]

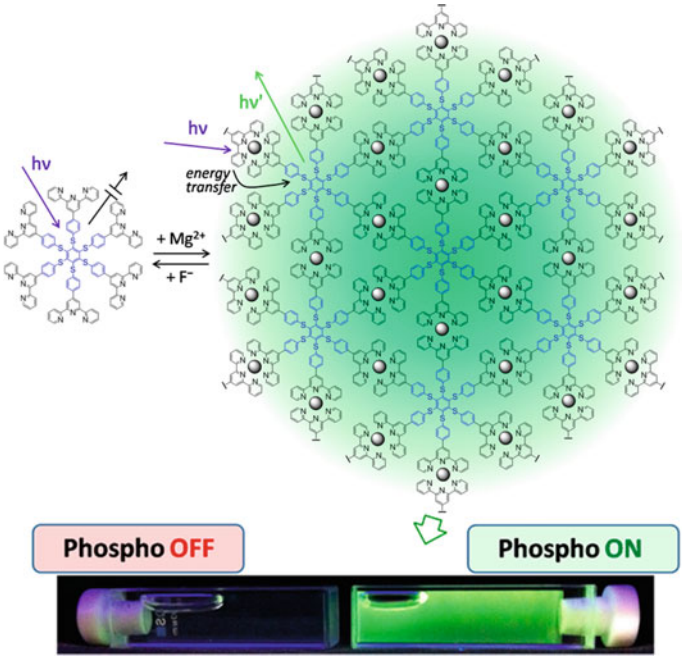

Fig. 7.16 Simplistic 2D representation of the self-assembled structure and aggregation induced phosphorescence of the hexathiobenzene core is turned on upon Mg(II) chelation [264]

antenna can be decomposed with a fluoride ion addition, thus switching off emission and offering a new tool for the fluoride ion probing. In other words, this unique system can be a sensor of cation or anion.

Among branched MSPs, a special place take star-like MSPs [236, 265], obtained using widespread bpy ligand, which forms complexes with a vast variety of metal ions and is ideal candidate for production of multi-armed star-like MSPs, because bpy functionalized in 4- and/or 4′-position can be quite easily synthesized. To produce star-like MSPs, two approaches are made based either on homoleptic chelates, in which metal ion is coordinated with similar chelating ligands, or on heteroleptic chelates, in which different polymer ligands are coordinated around a metal center. An example of the first approach is production of six-armed star-like block-copolymers with $[Fe\{bpy(CH_2Cl)_2\}_3](PF_6)_2$ used as hexafunctional initiator for oxazoline polymerization [266]. The first block was formed from hydrophilic 2-ethyl-2-oxazoline, and the second block is formed from hydrophobic 2-phenyl-2-oxazoline or 2-undecyl-2-oxazoline. Studying morphology of films of six-armed star-like copolymer has shown [267] that 2-ethyl-2-oxazoline block forms cylindrical micro domains in poly (2-undecyl-2-oxazoline) matrix. In another example $[Ru\{bpy(CH_2OH)_2\}_3](PF_6)_2$ is applied as a hexafunctional initiator for production of six-armed star-like copolymer using ROMP and ATRP combination [268]. We shall also notice use of [Fe(II){5,5″-bis(bromomethyl)-tpy}$_2$](PF$_6$)$_2$

complex as a metal supramolecular initiator for living polymerization of 2-ethyl-2-oxazoline bringing to clearly defined hydrophilic polymers with central supramolecular building block and star-like architectures [269]. It is important to emphasize that using metallosupramolecular initiators for living polymerization provides precise control over molecular weight, and also integration of additional (chelating) fragments at the ends of polymer chain [155].

Using approach based on homoleptic complex, also hetero-armed star-like copolymers can be obtained; however, this needs orthogonal synthesis of asymmetric macroligands from a double initiator. The 4-chloromethyl-4′-hydroxymethyl-bpy is used as such a double initiator for consequent polymerization of ε-caprolactone using ROMP and St with ATRP [270]. At the final stage bpy-PS-poly (ε-caprolactone) macroligand is coordinated with Fe(II).

We shall also notice production of hetero-armed star-like copolymers based on heteroleptic complexes. In particular, macroligands carrying one or two PS chains are first ATRP synthesized using 4-(chloromethyl)-bpy and 4,4′-bis-(chloromethyl)-bpy as initiator, respectively [271]. Then bis-bpy Ru complexes are obtained with these macroligands, and at the final stage the second type of a macroligand carrying one or two PMMA chains also produced using ATRP, is linked to bis-complexes giving hetero-armed star-like copolymers with 3 and 6 arms. It should be emphasized that an important factor of adjustment for control over hetero-armed star-like copolymer assembling is polarity of a solvent, which has an effect on conformation of polymer chains.

Six-armed star-like copolymers are obtained via two-staged synthesis: formation of Ru bis-bpy chelate with microligand carrying two PCL chains obtained by ROMP followed by chelation with bpy, carrying either two PS chains (grown using ATRP) or two PEG chains obtained by grafting PEG to 4,4′-bis-(chloromethyl)-bpy using Williamson reaction (Scheme 7.9) [272].

Apart from bpy ligand other chelating ligands were used for synthesis of hetero-armed star-like copolymers. For example, ligands from the family of

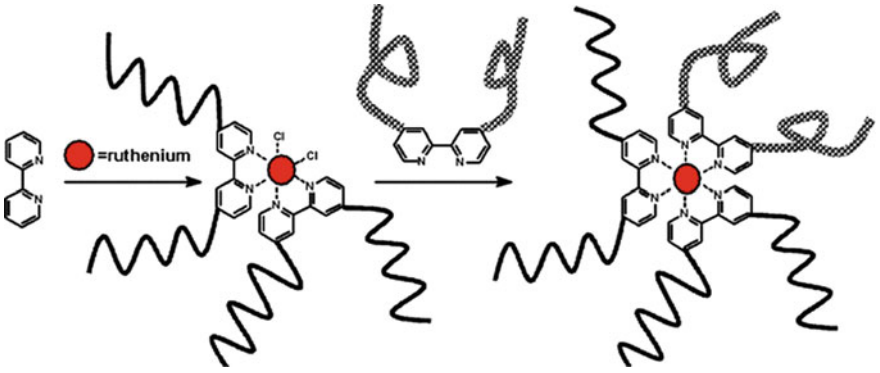

Scheme 7.9 Synthesis of polymeric Ru(II) bis(bpy) dichloride complexes and Ru(II) tris(bpy)-centered heteroarm stars [272]

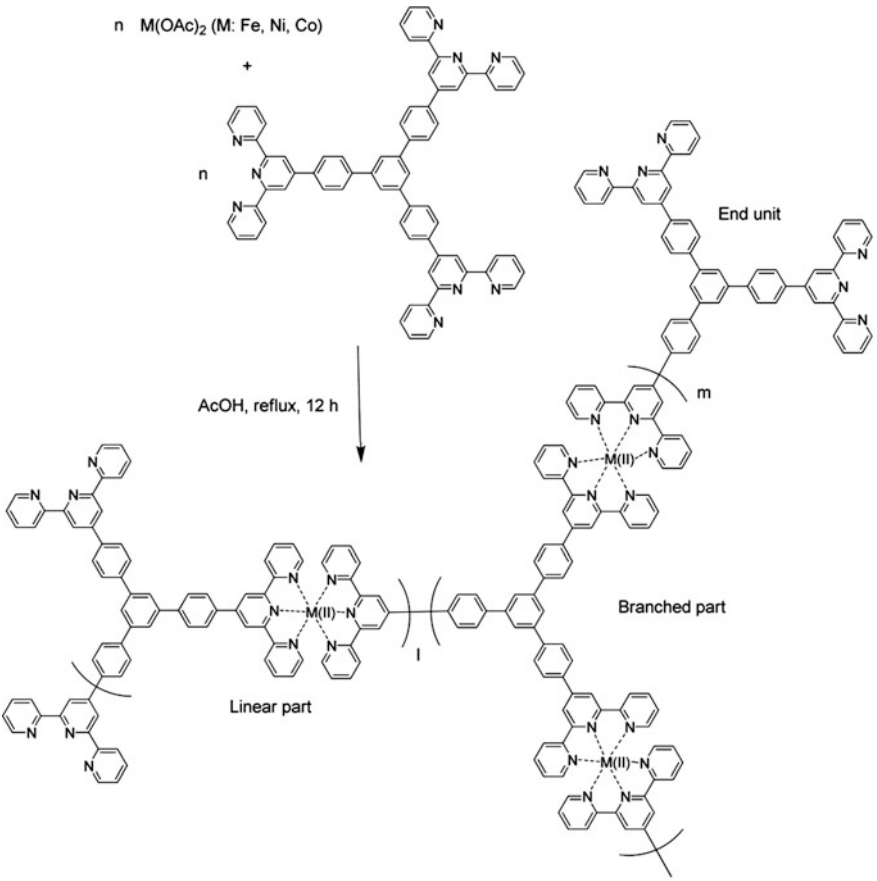

Scheme 7.10 Production of Fe(II)-, Co(II)- and Ni(II)-based MSPs including linear and branched parts [274]

β-diketones in combination with bpy are chosen for building heteroleptic complex with lanthanide ion [273]. First macroligands are obtained by D,L-lactide polymerization using ROMP with dbm functionalized by a hydroxyl group as initiator, and then three macroligands are chelated to Eu(III) to obtain three-armed star. At the final stage, bpy carrying two PCL chains are coordinated to this tris-complex to obtain penta-armed star-like block-copolymer.

There is an interesting application of tris-chelating ligand for production Fe(II)-, Co(II)- and Ni(II)-based MSPs including linear and branched parts in their structure (Scheme 7.10) [274].

It should be especially noted that each part of metallosupramolecular block-copolymers makes its contribution to properties of resulting materials [108]. Besides, self-assembling these copolymers is used in thereafter for development of more advanced architectures, in particular, smart, and stimulus-responsive nanostructures.

7.5 Cross-Linked Metallosupramolecular Polymers

Reversible M–L coordination interactions between monomer units are actively used in synthesis of MSP networks [77, 78, 129, 130, 261, 262, 275, 276]. Multiple MSP networks are synthesized with different mechanical, chemical, and stimulus-responsible properties, which can be easily controlled by fine tuning molecular architecture, and also thermodynamic and kinetic stability choosing respective M–L pairs [75, 76, 277]. It should be emphasized that rational design of MSP networks needs a clear idea on correlation between supramolecular building blocks and properties of resulting material [40, 129, 262, 275, 276].

Thus, self-assembling is done in solution between Eu(III) and rigid ditopic tridentate tpy ligand, which brings to formation of MSP networks (Fig. 7.17) [278]. Depending on M–L ratio used for initial self-assembling process, morphology of these materials can be changed from 1D micron fibers to 3D coordination network. It should be noted that tpy-based ditopic ligand can be efficient sensor for Eu(II) emission, hence, emission lifetimes and energy of a ligand in triplet state of MSP depends considerably on M–L ratio. Therefore, the obtained micron-sized fibers can be efficient optic wave-guide for Eu(II) radiation.

Similar dependence of surface morphology on M–L ratio is established in the series of Fe(II)-based MSPs with 3D structures obtained by staged chelation of Fe(II) salt with different ratios of linear bis-tpy (L1) ligand and branched tris-tpy (L2) ligand (Fig. 7.18) [279]. All 3D polymers had blue color due to MLCT absorption,

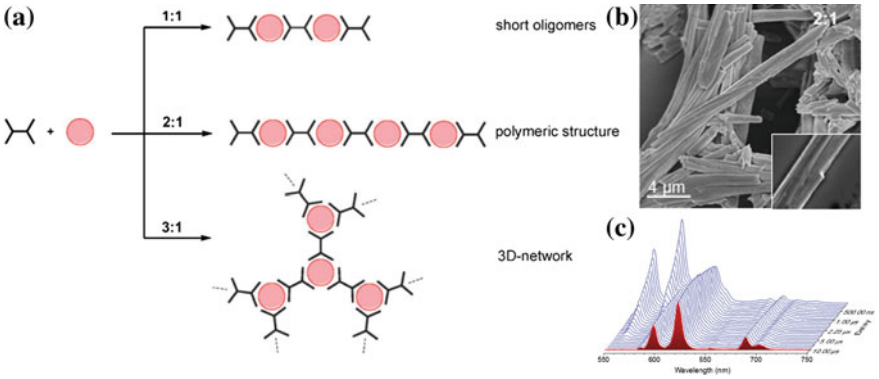

Fig. 7.17 **a** Proposed mechanism for the self-assembly process in solution at different M:L ratios. **b** SEM images of the samples in the solid state: M:L ratio 1:1 (a), 2:1 (b), 3:1 (c). **c** Time-gated emission maps for the $^5D_1$–^7F_J (J = 0–3) and $^5D_0$–^7F_J (J = 0–4) transition recorded between 100 ns and 10 ms (500 ns gate, 2 nm band width) [278]

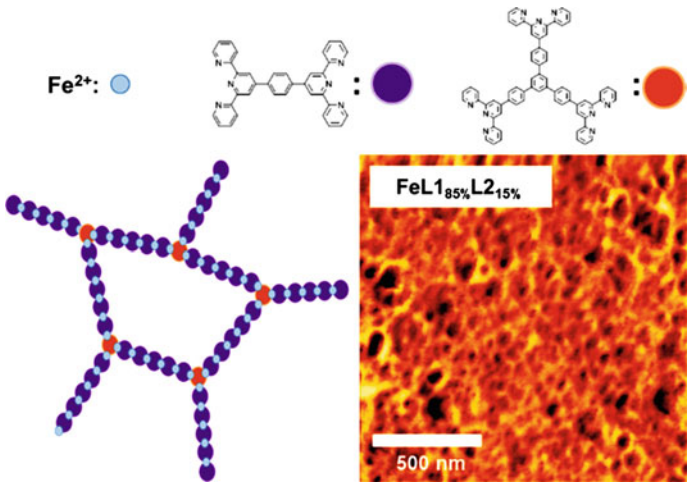

Fig. 7.18 Synthesis and AFM image of the 3D Fe(II)-based MSP with different content of L1 and L2 [279]

and showed excellent electrochromic properties. In particular, the most highly porous 3D structured film has shown the best electrochromic efficiency: as compared with 1D linear polymer, switching times for dying (0.31 → 0.19 s) and for bleaching (0.58 → 0.36 s) are improved by 37.9 and 38.7%, respectively. Besides, the transmission coefficient has increased by 21.8% (41.6 → 50.7%), and efficiency of dying has increased by 45.3% (263.8 → 383.4 $cm^2\ C^{-1}$).

It should also be noted that MSP networks can form via M–L coordination with participation of preliminary formed polymer chelating ligands. In particular, coordinated self-assembling Zn(II) ions and polytopic polyiminofluorene-tpy ligands is used for production of electrochromic films with nanometer thickness (Fig. 7.19). The films can be switched between yellow, red, and blue, and show switching times 500 ms, high contrast and high stability [133].

Another example is chelation of $ZnCl_2$ and $Fe(ClO_4)_2$ with conjugated copolymer based on poly(phenylene-*alt*-fluorene) main chain and Mebip ligand linked to the main chain with flexible spacer groups (Fig. 7.20) [280]. Multiple successive adsorptions of metal salts and polymer bring to coordinated supramolecular assembling cross-linked MSP on a substrate, and thickness is controlled by a number of applied stages of adsorption. Since fluorescence of the polymer main chain is not completely quenched by M–L interaction, the films have bluish luminescence.

For CPL, it is typical to form micellar structures in diluted solutions, which decompose at addition of transition metal ions with formation of cross-linked MSP (Fig. 7.21). It has been shown, for example, in the cases of tpy end-capped by poly (2-dimethylamino) ethyl methacrylate-*b*-poly (NIPAM) diblock-copolymers [281], PS-*b*-poly (*tert*-butyl acrylate) with tpy-end-capped [282], tpy-terminal hydroxy-telechelic materials Pluronics P105 and P123 [283].

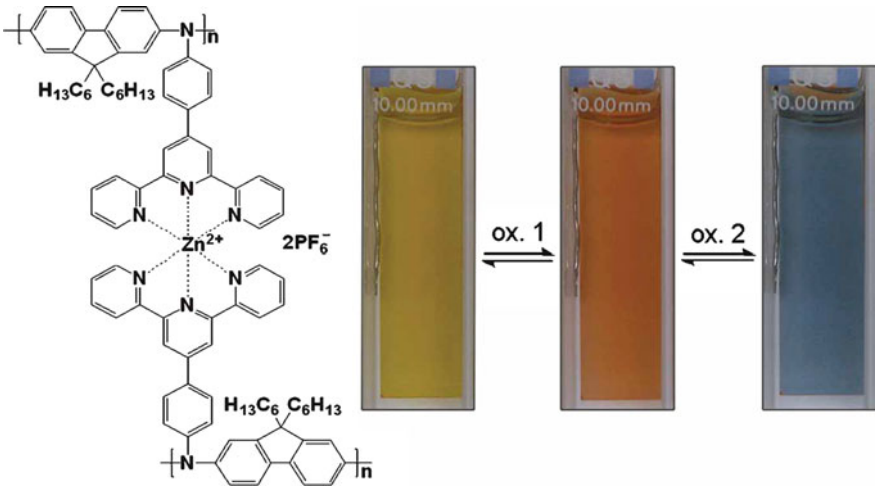

Fig. 7.19 Production of electrochromic films based on Zn(II) ions and polytopic polyiminofluorene-tpy ligands [133]

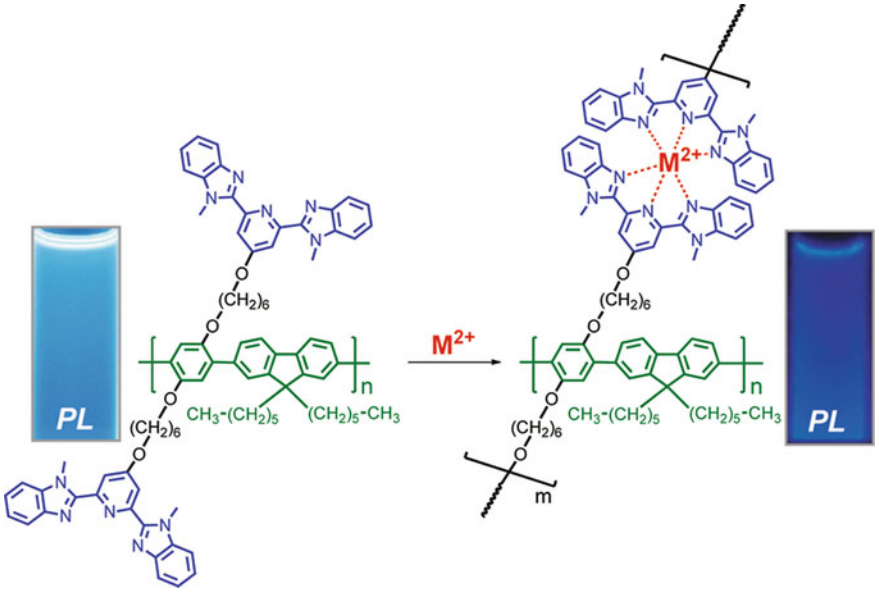

Fig. 7.20 Metal ion coordination of chelating polymer involving cross-linking side chains [280]

The process of formation of metallosupramolecular network based on 3:1 M–L complexes between ditopic oligomers and metal ions proceeds by formation of 1:1 and 1:2 complexes (Fig. 7.22) [284].

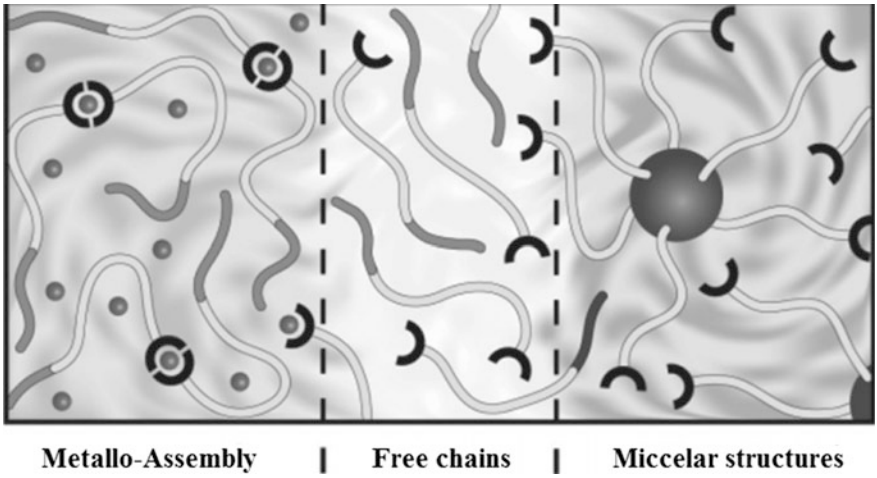

Fig. 7.21 Self-assembly behavior of poly (NIPAM)-*b*-poly [(2-dimethylamino) ethyl methacrylate-tpy] double-hydrophilic diblock-copolymers in aqueous solution in response to heat and transition metal ions [281]

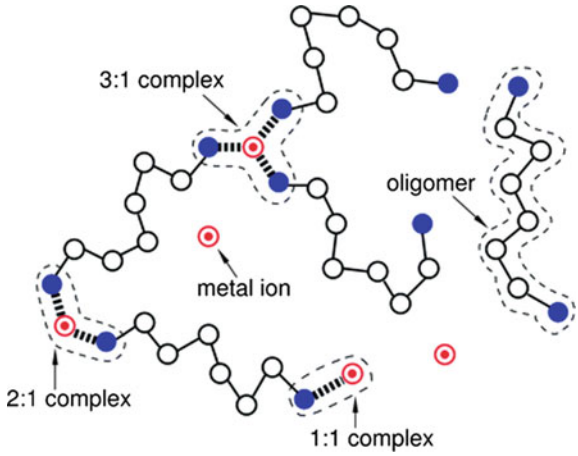

Fig. 7.22 A schematic representation of metallosupramolecular polymers [284]

Monte-Carlo modeling has shown that this process is mostly influenced by concentration of chelating ligand and M–L ratio. At a constant concentration of ligand in the ligand-enriched area 3:1 M–L complexes predominate. Their fraction decreases as a metal content increases, bringing to 2:1 complexes with maximum about M–L ratio 1, and fraction of 1:1 complexes has maximum at M–L ratio 2. It follows from analysis of molecular-weight distribution and decreased average size of metallosupramolecular networks that a network formation takes place in restricted

range of M–L ratios. For example, at low concentration the reversible network begins to form in the range of M–L ratios about 0.75, where there is a considerable fraction of 2:1 as well as 3:1 M–L complexes, and as ligand concentration increases, network formation broadens to wider range of M–L ratios. At ligand concentration slightly over the beginning of a network formation it grows via integration of sol molecules into dangling fragments of the network. At higher concentrations this mechanism of network growth becomes inactive, and fraction of dangling fragments begins to decrease simultaneously with sol fraction. In the M–L range close to stoichiometric composition, the total number of oligomers in sol and dangling fragments are almost constant depending on oligomer concentration and becomes unity at the beginning of network formation.

7.6 Heterometallic Supramolecular Polymers

Strategy of coordination-driven self-assembling is successfully used for structuring such interesting assemblies as heterometallic supramolecular polymers (hetero-MSPs). It is principally important that integration of two different metals gives resulting hetero-MSP properties of individual metals as well as new properties stipulated by synergetic effect of one metal on another. To obtain such systems, different synthetic approaches are developed. In particular, the simplest of them includes stepwise chelation of two different metals, at that first monomer bis-complex of one metal with ditopic ligand is formed, and then metallosupramolecular polymerization with another metal takes place. An example of this approach can be stepwise chelation of Eu(III) and Fe(II) ions with asymmetric ligand based on dicarboxylate-substituted tpy and non-substituted tpy [285]. It should be noted that hetero-MSP has shown unique, reversible «ON-OFF» switching Eu(III) luminescence by electrochemical redox of Fe ions in solid state.

In another interesting example, independent coordination of Fe(II) and Rh(I) ions with one heteroditopic ligand containing two metal-coordinating centers at two ends has brought to formation of linear supramolecular polymers (Scheme 7.11) [286]. In this case different metals are specifically bound by different ligand fragments and take a certain kind of coordination geometry. The obtained hetero-MSP is interesting representatives of self-supported heterogeneous chiral catalysts, which have high activity, enantioselectivity, and for more than 10 times repeated use in heterogeneous asymmetric hydrogenation of different derivatives of functionalized olefins. These hetero-MSPs can be obtained by stepwise or one-pot synthesis, in which rigid tpy unit and soft MonoPhos fragment Feringa is coordinated selectively with Fe(II) and Rh(I) independently. It should be noted that Fe ions play a role of «glue» for self-support function way to link discrete fragments of a catalyst together, while Rh part is used as a catalytic center and as a spacer. It would be very

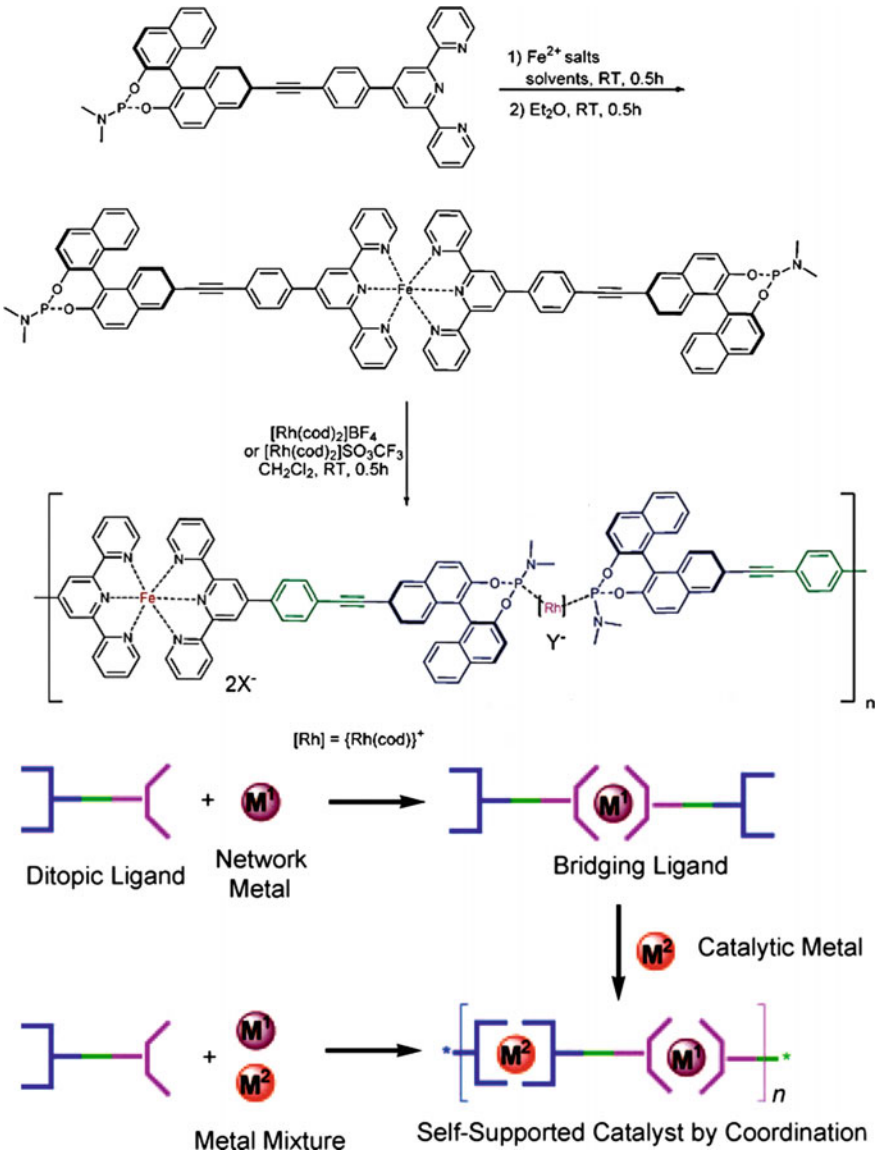

Scheme 7.11 Synthesis of a class of self-supported catalysts through orthogonal coordination of two different metal ions with a single ditopic ligand [286]

difficult to realize the abovementioned functions if only one type of metal ion was applied for self-assembling. In this case the self-sorting comes into effect, i.e. self-assembling some supramolecular assemblies from multicomponent mixtures,

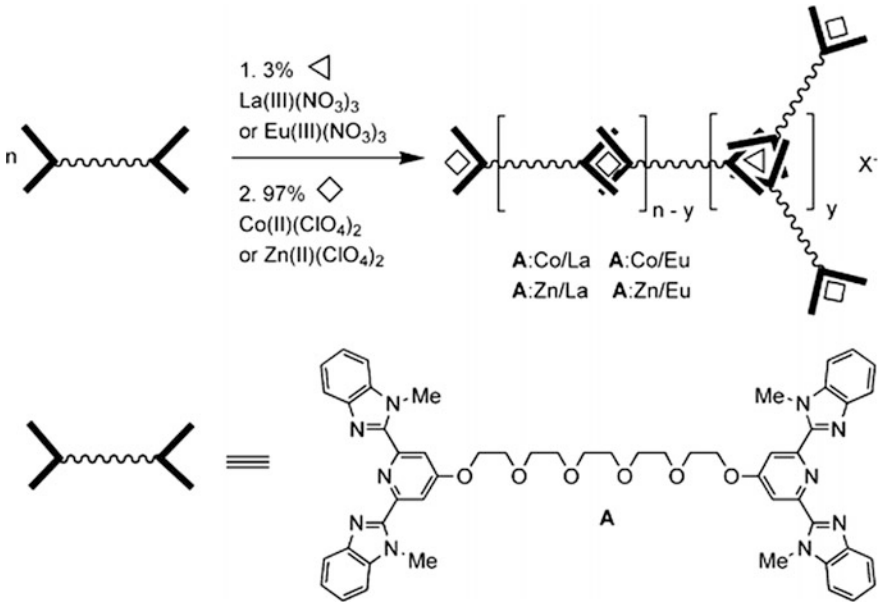

Scheme 7.12 Representative scheme of the formation of MSP by assembling the 2,6-bis (benzimidazolyl)-pyridine ligand, transition metal ions and lanthanides in the appropriate ratio [76]

which is one of important principles in contemporary supramolecular chemistry [287–291]. Strategy of self-sorting is most attractive since it provides approach to very complicated supramolecular architectures. Moreover, metal-driven selection between final MSP types can be quantitatively reached in solution or in crystal state using coupled coordination/packing of interactional algorithms inside dynamic metallosupramolecular databases [292].

Consistent chelation of transition metal ions and lanthanides makes it possible to obtain hetero-MSPs containing linear and branched blocks (Scheme 7.12), which has significantly broaden a range of supramolecular materials with new dynamic properties [76].

Also approaches have been developed when the first metal is used for production of linear MSP, and the second metal is used for cross-linking metallosupramolecular chains (Scheme 7.13). It is interesting that under action of different competitive ligands metallosupramolecular network can be reversibly assembled and disassembled and thus shows dynamic properties [293].

The hetero-MSP formed by a consistent chelation of two different organic building blocks is a kinetic intermediate to final stable hexanuclear metallomacrocycle carrying 4Ru(II) and 2Fe(II) ions obtained through thermodynamic disassembling/repeated assembling route [294].

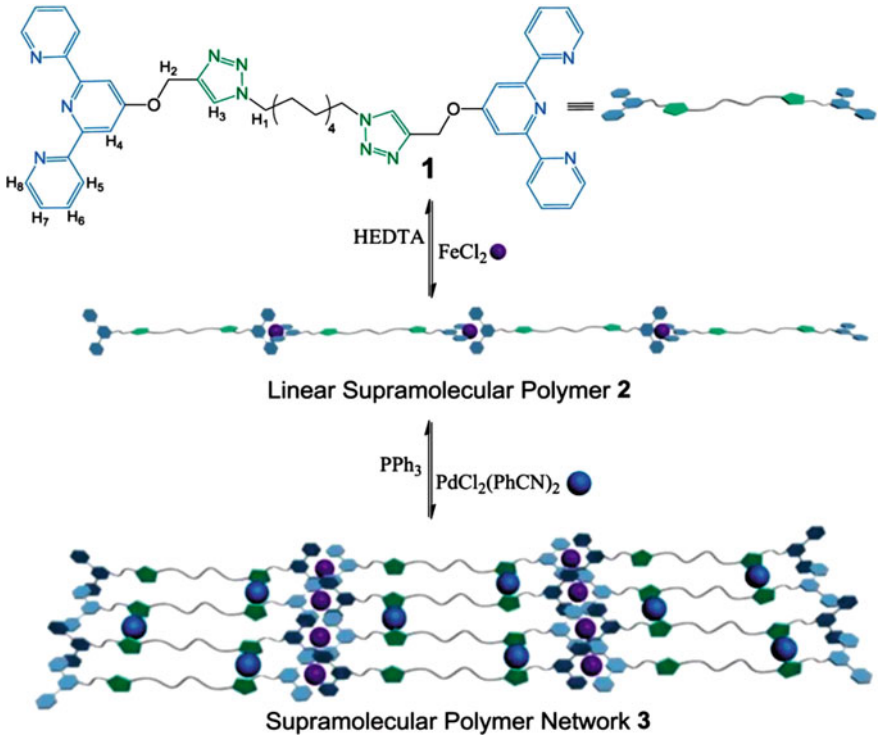

Scheme 7.13 A representation of the self-assembly of the metallosupramolecular network, where (HEDTA) is (2-hydroxyethyl) ethylenediaminetriacetic acid [293]

7.7 Metallosupramolecular Polyelectrolytes

Metallosupramolecular polymerization with neutral polytopic ligands brings to charged MSPs, which are called metallosupramolecular polyelectrolytes (MEPE). In MEPE synthesis bis-tpy are most often used as ditopic ligands, which provide formation of extended rod-like MEPE (Fig. 7.23) [156, 295]. DP of MEPEs in solution depends on concentration of components and on initial M–L ratio and is determined by dynamic equilibrium of association and dissociation. For M:L = 1 chain length grows exponentially with concentration, which means uncontrolled chain length growth. However, if there is excess of one component, growth stops as long as one component is consumed even if total concentration is additionally increased. This means that molecular weight of MEPEs can be controlled by M–L ratio [76]. In the case of Fe(II), Co(II), and Ni(II) a chain is short for M:L less than 1, it is longer for M:L = 1, it is medium for M:L over 1, because the binding constant K_1 associated with initial chelation of metal ion and tpy is lower than K_2, which reflects association of following tpy ligand thus elongating the chain [76]. Using chain monotopic stopper 4′-(phenyl)-tpy, it is possible to predictably control

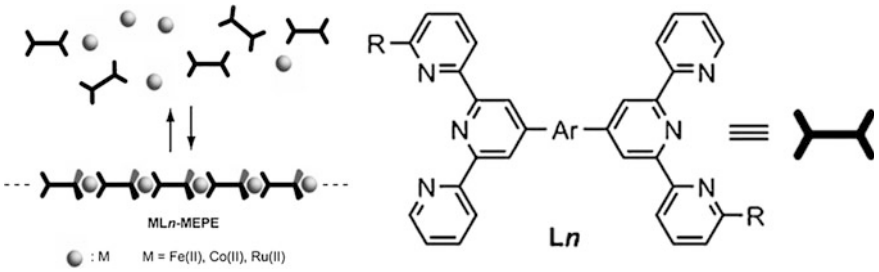

Fig. 7.23 Organic-metallic hybrid polymers (ML_n-MEPE) formed by chelation of bis(tpy)s (L_n) with metal ions such as Fe(II), Co(II), and Ru(II) ions [295]

average molecular weight, chain length, and viscosity of MEPEs (Fig. 7.24) [296]. The resulting linear bis-tpy-based MEPEs have attracted great attention since they are self-assembling in (aqueous) solution with metal ions such as Fe(II), Co(II), Ni (II), Cu(II), and Zn(II) with several hundred nanometers in length [297].

MEPEs' structure depends on ligand construction and preferable coordination geometry of a metal ion, and also on a solvent character and pH. Choice of a

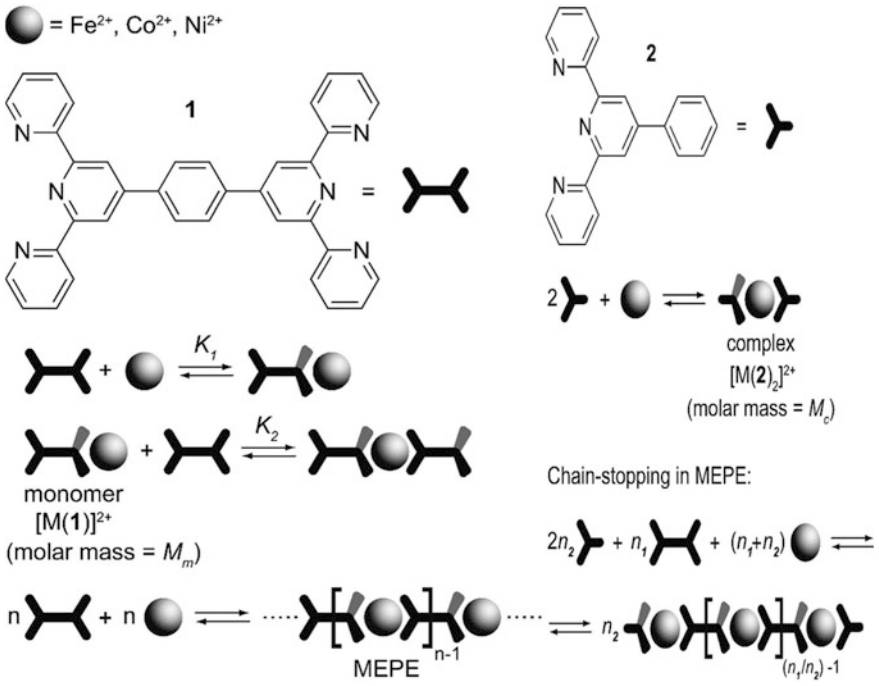

Fig. 7.24 Synthesis of MEPEs with predictably control average molecular weight, chain length, and viscosity using chain forming ligand and chain stopping ligand [296]

counter-ion not only determines solubility of MEPEs in different solvents, but controls microenvironment of metal ions and, thus, has effect on architecture of polyelectrolytes. Modularity of MEPEs self-assembling makes it possible to introduce different metal ions, chelating ligands, and counter-ions, thus generating abundance of materials with wide range of properties [298]. With different metal ions integrated into a polymer chain several interesting functions become available, including magnetic, electrorheological, photophysical, electrochemical, and electrochromic [179]. In this sense important is a fact that attractive optical, electrochemical, and electrochromic properties of MEPEs can be easily studied for their high solubility in different solvents including water. Moreover, conclusions can be made about structure-property correlation of projected structures. Positive charge of a metal ion can be used for integration of MEPEs in different architectures of materials, including liquid crystals, nanostructures and thin films [76, 299].

In most cases, metal-driven self-assembling MEPEs is easily indicated by naked eye due to strong coloring solution at chelation of metal ions. For example, Fe-MEPE shows strong absorption band in visible range about 590 nm relating to MLCT transition, which is responsible for deep blue color. Ligand shows a strong band about 290 nm associated with π-π^* transition. Moreover, small bands are generated at 240–340 nm depending on a certain ligand [87, 300–302]. Furthermore, MEPE formation is accompanied by increase in viscosity of solution, which provides additional indication of MEPEs formation. Since viscosity depends on a chain length, increasing viscosity is associated with growing chains. For example, for Fe-MEPE viscosity reaches maximum at M:L = 1 [303].

Studying MEPEs based on bis-tpy Ru(II) chelates with a spacer varying from oligomers to polymers has shown that a spacer length is an important factor for formation of linear or cyclic types and, therefore, it can have an effect on DP [96, 192, 304, 305]. To suppress polyelectrolyte effect of Ru(II)-MEPEs, it was necessary to add different concentrations of salts for viscosity experiments. It is important that lamellar polymer chains should form.

In the recent years MEPEs have gained wide development as a new area for electrochromic applications [75, 76, 81, 132, 157, 160, 175, 306]. As applied potential is increased, metal centers are oxidized to higher valent state, and MLCT decreases. Optically this brings to decrease in visible optical density caused by switching MEPEs from colored to transparent state [295]. Therefore, choice of metal ions and ligands plays a significant role in electrochromic characteristics in MEPE system and has an effect on efficiency of electrochemical and optical properties [307]. In particular, MEPEs easily form thin films of high optical quality using different methods including LbL deposition or coating with linear and continuous film growth [308]. Moreover, MEPE thin films immobilized on transparent conducting electrodes show desired electrochromic properties with high switching rate and low switching (commutation) potential, since, change of redox state is, as a rule, associated with change in optical properties [308]. Metal chelates show redox transitions based on a metal ion and ligand totally up to five redox stages [309]. In other words, MEPE connect universal and usually reversible electrochemistry of MSP with advantage of recycling polymer materials [310, 311]. These highly

efficient electrochromic properties are demonstrated for example for Fe-MEPE, Co-MEPE, and Ru-MEPE based films, for which loss of absorption about 20% is detected after 4000 redox cycles [157, 312, 313]. The compounds show response times from 0.65 s for OMe-substituted Fe-MEPE to 1 s for respective Ru-MEPE, to 3 min for Co-complexes, respectively. Electron-acceptor functional groups, such as bromine, bring to prolonged response times. Electrochromic memory time, which is a period, during which a thin film remains colorless after removal of applied potential, is elongated by MEPE functionalization. Non-substituted MEPEs return in colored state after about 30 s, while functionalized MEPEs require up to 15 min to reduction [81, 313]. These films can be used for stimulus-responsive layers [314] and for electronic displays and devices such as electronic papers or electrochromic windows (smart-windows) [307, 308, 313–315].

It should be noted that during annealing Fe-MEPE based films at temperatures above 100 °C blue color transits to green, and previously reversible electrochromic properties are lost, even after cooling to room temperature [316]. Study of solid Fe-MEPE in situ during annealing has shown that thermo-induced transition is not accompanied by redox process on Fe(II) center, but is related to structural changes in Fe(II) coordination sphere. In particular, in low-temperature state Fe(II) ion is in quasi-octahedral coordination surrounded by six nitrogen atoms of pyridine rings. In this case length of axial Fe–N bond is 1.94 Å, while lengths of equatorial bonds are up to 1.98 Å. At the same time in high temperature state FeN_6-node shows distortion with axial Fe–N bonds elongated to 2.01 Å (Fig. 7.25).

Substantial interest has heterometallic MEPEs including Fe(II) and Co(II) ions, which combine properties of individual MEPEs and, therefore, show their different states: red-violet, blue, and transparent [317].

Very promising direction is also synthesis of cross-linked MEPEs based on bis-tpy Fe(II) chelates [140]. It occurs that molecular weight of networks reaches high values and depends on cross-linking degree, for example, it is shown that from

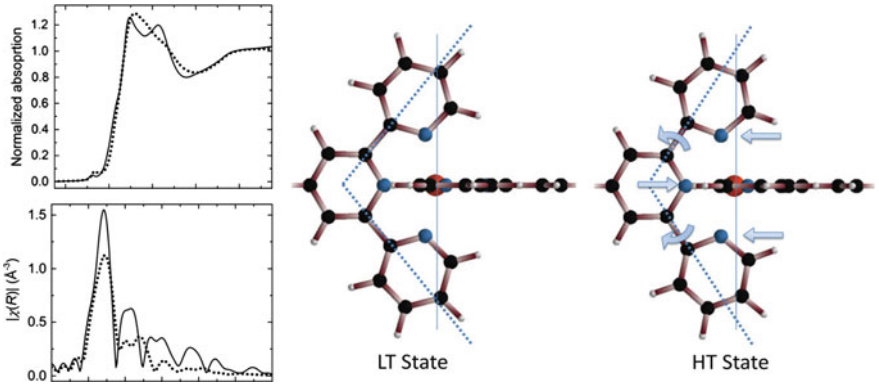

Fig. 7.25 XANES (top) and EXAFS (bottom) spectra of LT (solid line) and HT (dotted line) states of solid Fe-MEPE [316]

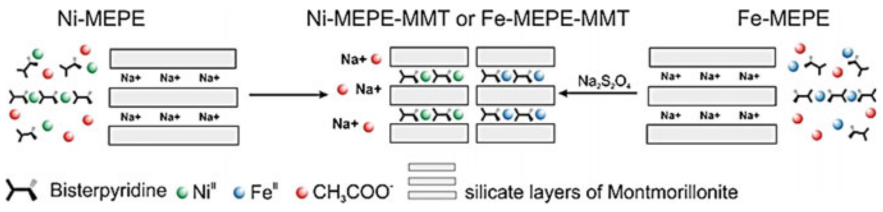

Fig. 7.26 Nanocomposites consisting of montmorillonite glue and Ni(II) or Fe(II) MEPE [321]

1.5 to 9% of cross-linking degree the networks are soluble in aqueous and acetic acid solutions. For higher cross-linking degrees (more than 9%) solutions are heterogeneous with colored deposits precipitated from solution.

We shall notice production of composition materials by incorporation of MEPEs host materials [318, 319]. While most high molecular weight polymers cannot migrate into pores, components of MEPEs can diffuse and collect in a host.

Innovation concept [320] is developed for design of electrorheological liquids based on disperse phase of rigid rod-like MEPE intercalated into mesoporous SBA-15 silica. At electric field applied to this composite dispersed in silicon oil, rheological measurements shows considerable change in elasticity modulus, which points to solidification of fluid medium. Apart from strong electrorheological effect and low current density, five times smaller amount of MEPE is required than in comparable electrorheological liquids based on host-guest systems.

Using water intercalation, nanocomposites are obtained consisting of montmorillonite glue ($Na_{0.6}(Al_{1.64}Mg_{0.36})Si_4O_{10}(OH)_2{\cdot}nH_2O$) and MEPE with Fe(II) and Ni(II) ions (Fig. 7.26) [321]. For both nanocomposites substantial electrorheological effect is established, which depends on intercalated MEPE.

It is shown [322] that for diluted solutions, where small MEPE aggregates prevail, nanometer crystals can be grown on interphase boundary. MEPEs form linear rods, which are arranged into sheets, at that, four sheets intersect a unit cell, while adjacent sheets are rotated by 90° with respect to each other.

7.8 Orthogonal Self-assembling

Oppositely to majority of biological systems, synthetic supramolecular chemistry uses, as a rule, only one type of non-covalent interaction. Therefore, there is an important task of stabilization of clearly defined MSP architectures solved with a combination of several non-covalent interactions [169, 323–330]. Using a combination of a set of non-covalent interactions provides additional possibilities for development of very complicated and multifunctional MSPs. For example, dynamic supramolecular polymers with linear or cross-linked topology are reported [331]. Use of supramolecular interactions to direct of spontaneous assembling molecules is of paramount importance due to their very specific character, controlled affinity,

and reversibility. These specific and rather controlled interactions can be manipulated independently and simultaneously, thus providing orthogonal self-assembling of components with several (more than one) motifs of interaction, which do not influence each other [134, 332, 333]. In other words, use of orthogonal self-assembling guarantees that any change in a system caused by one interaction has no effect on another interaction [334]. The greatest advantage of orthogonal combination of different non-covalent bonds in supramolecular structures is its bringing to materials production with some properties, which are responsive under action of different stimuli. It is important that introduction of different supramolecular functional groups (multifunctionalization) into one synthetic fragment can improve substantially possibilities for applications of these materials, and orthogonal self-assembling provides total control over the self-assembling stage, and, therefore, over material properties.

If only one type of supramolecular recognition is present in the main chain of a polymer, usually statistic mixtures are obtained upon action of two or more functional reagents (Scheme 7.14, top) [169]. In this case, control over reaction of self-

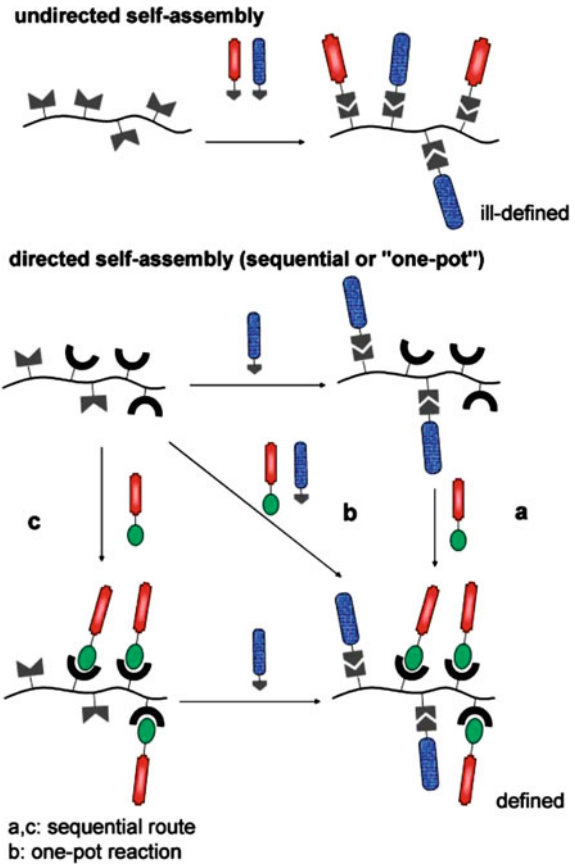

Scheme 7.14 Statistical (top) and defined (bottom) multifunctionalization of a polymer by self-assembly [169]

assembling is limited, and a product is weakly defined. A combination of different (orthogonal) supramolecular linking units, however, makes it possible to control the self-assembling stage (Scheme 7.14, bottom). This well-defined multifunctionalization of polymers can be reached if there is high selectivity of orthogonal recognizing elements to their complementary counterparts. For multiply repeated self-assembling two different synthetic ways are possible. Functionality may be introduced via consistent supramolecular self-assembling, and then another one. However, more promising is one-pot approach to a given mulifunctionalized product, because it reduces one stage of reaction. This strategy of controlled multifunctionalization provides fine tuning polymer architectures, and their properties, which shows ways to new specially developed functional materials.

7.8.1 *Combination of M–L Coordination with H-Bonding Interactions*

Among different non-covalent linking interactions in building supramolecular polymers, M–L coordination and formation of H-bonds are two basic and most studied classes of interactions [11, 169, 335–338]. Therefore, it is not accidentally that particularly these types of supramolecular interactions are widely used in orthogonal self-assembling. In this respect among the most well-known supramolecular motifs there are ureidopyrimidinone as an H-bonding block and tpy as a metal-chelating fragment [169, 261, 339]. In particular, successful dimerization of H-bonding block is shown, as well as metal-tpy chelation with addition of $FeCl_2$ or $Zn(OAc)_2$ in solution. These two linking points at different ends of a spacer provide orthogonal self-assembling in linear polymers through two synthetic routes (Scheme 7.15). It should be noted that using a covalent polymer poly (ε-caprolactone) as a spacer between two linking sites increases solubility of obtained telechelic polymer in non-polar solvents [170]. It is important that MSP shows film-forming properties and transparence at thin thickness of film, which differ considerably from those of opaque and fragile films of original polymers. Besides, MSPs have different physical properties as compared with its initial polymers, just with a few non-covalent linking sites being integrated. Moreover, reversibility of polymer chelation can be controlled by addition of competitive ligand HEEDTA (hydroxyethyl ethylenediaminetriacetic acid) or metal ions opening a way for building new «switching» functional polymers (Scheme 7.16) [340, 341]. These self-assembled polymers can be adjusted using different external stimuli through addressing either quaternary H-bonding block or a tpy-metal supramolecular motif. In particular, formation of H-bonding fragment can be adjusted by temperature or a solvent, while a metal chelate fragment can be modulated using competitive ligands, and electrochemistry.

There is an interesting approach in which tpy fragment is replaced by chiral Feringa MonoPhos ligand for bifunctional monomer synthesis, which can form

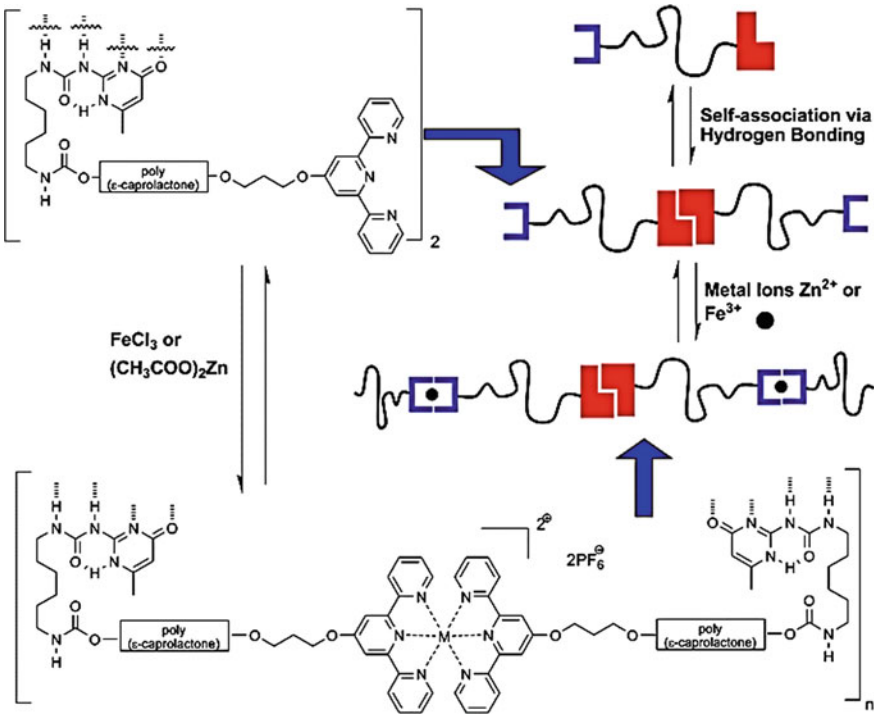

Scheme 7.15 Schematic representation of a supramolecular polymer containing alternating tpy metal chelates and quadruple H-bonds in the main chain [319]

linear self-assembled polymer with alternant orthogonal P–Rh coordination and ureidopyrimidinone dimerization in the main chain by addition of $[Rh(COD)_2]BF_4$ [171]. The obtained MSP is insoluble in non-polar solvents such as toluene, and is highly efficient and enantioselective heterogeneous catalyst of hydrogenation reaction, and can be repeatedly used during many cycles.

We shall notice that supramolecular polymers based on H-bonds are, as a rule, confined to organic solvents, such as chloroform, and are weak in competitive polar solvents such as DMSO. At the same time, switchable MSP obtained on the basis of a small heteroditopic monomer with two orthogonal linking interactions is stable in a strongly polar solvent [324, 337]. This monomer has guanidiniocarbonyl pyrrol carboxylate zwitter-ion motif at one end and tpy block at the other end (Fig. 7.27). High association constants $K > 10^8\ M^{-1}$ of both tpy-block and of a zwitter-ion motif in DMSO are important preliminary condition of linear supramolecular polymer fiber formation with a considerable DP in polar solvents. This supramolecular system provides production of large aggregates in polar solvent and can be adjusted reversibly between polymers and low molecular weight molecules reacting at external stimuli in two different directions, which can be included in design of functional materials.

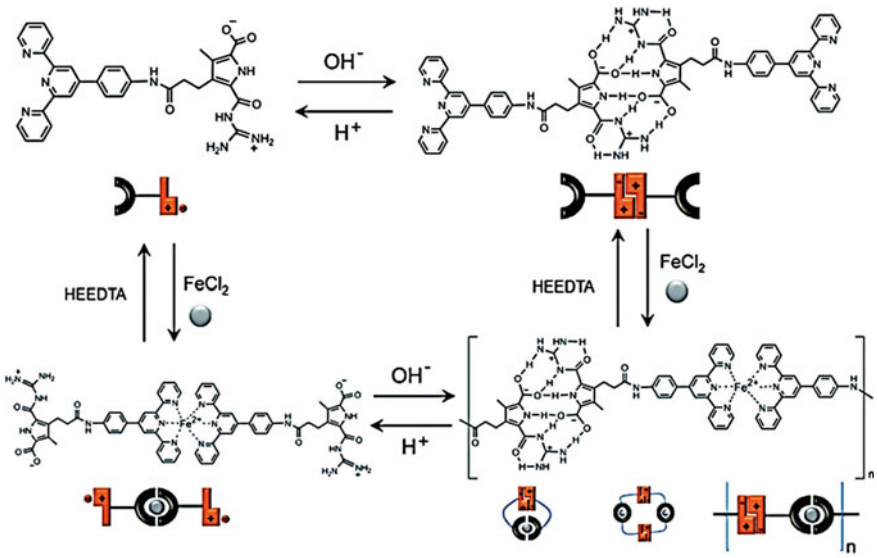

Scheme 7.16 Schematic molecular structure of initial ligand, and the dynamic polymerization of the metal–ligand complex

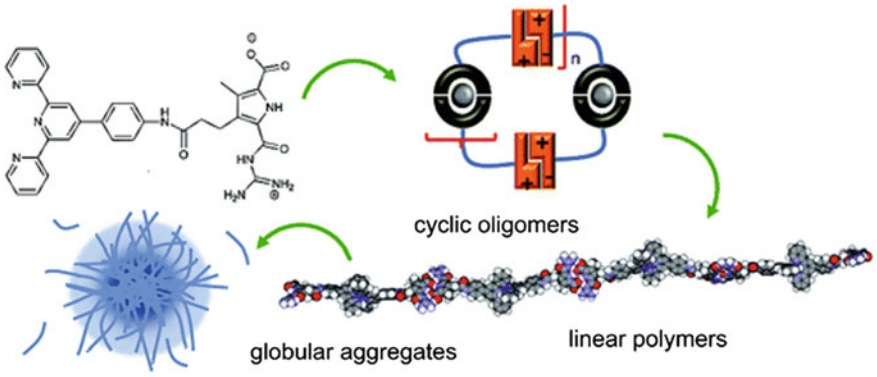

Fig. 7.27 Scheme of the self-assembly of monomer in solution

Very easy and universal approach to these materials is based on traditional polymers carrying different fragments of recognition in a side chain. For example, ROMP is used for synthesis of one type of statistic copolymers based on norbornene carrying Pd-pincer complexes (M–L coordination) and diaminopyridine fragments (H-interactions) as groups of a side chain (Fig. 7.28a) [333]. A copolymer can be functionalized stepwise or by the one-pot method by adding Py and *N*-butyl thymine showing good selectivity and independence from each other within the limits of recognition motif and the main polymer chain. It is important that thermal properties

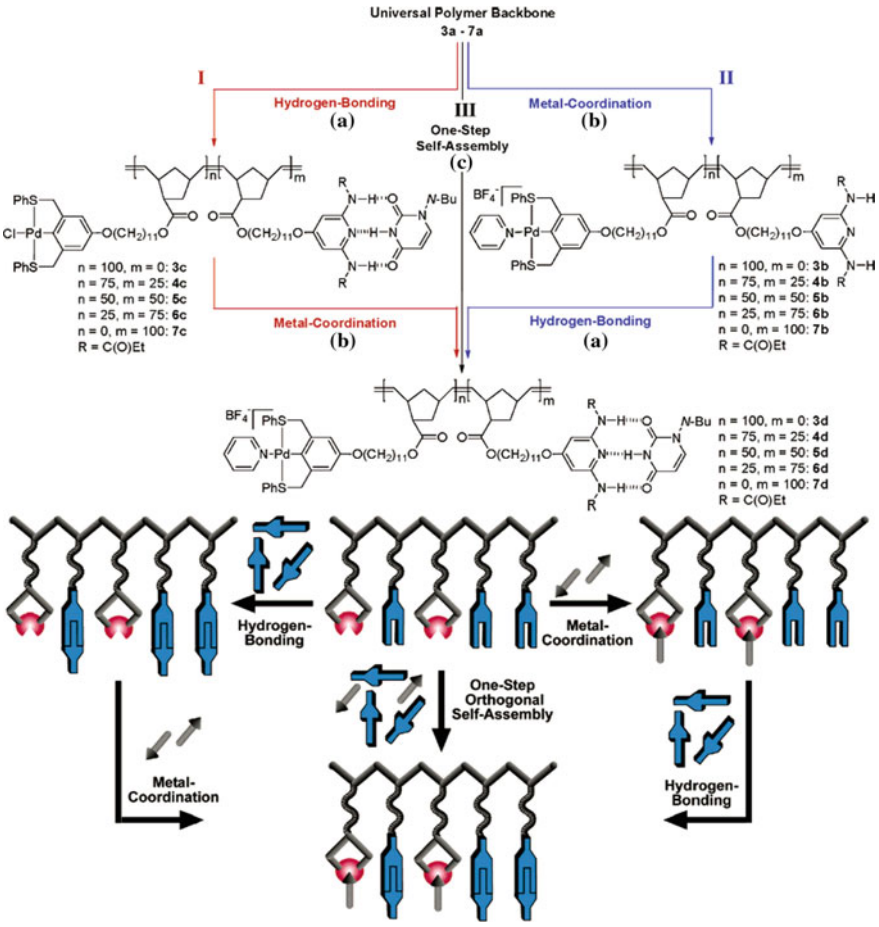

Fig. 7.28 Schematic representation of cross-linking via a palladated pincer (**a**) and H-bonding units (**b**) with bifunctional complementary recognition units [333]

such as T_g and T_d can be modified by such functionalization, which provides easy way of control over functionalization of a copolymer and makes it possible to design functional materials based on a statistic copolymer. There is another way of functionalization using H-bonding fragment for cross-linking by adding telechelics containing two complementary H-bonding groups (Fig. 7.28b). Besides, for this purpose perylene molecule can be used to incorporate fluorescent dye into a supramolecular polymer. In both cases a supramolecular fragment not taking part in cross-linking was functionalized with mono-functionalized recognition blocks [342].

We shall also notice MSPs built from ABC triblock-copolymers based on covalent bond with orthogonal combination of Pd-pincer-pyridine coordination and H-interaction of heterocomplementary Hamilton receptor–cyanuric acid (Fig. 7.29)

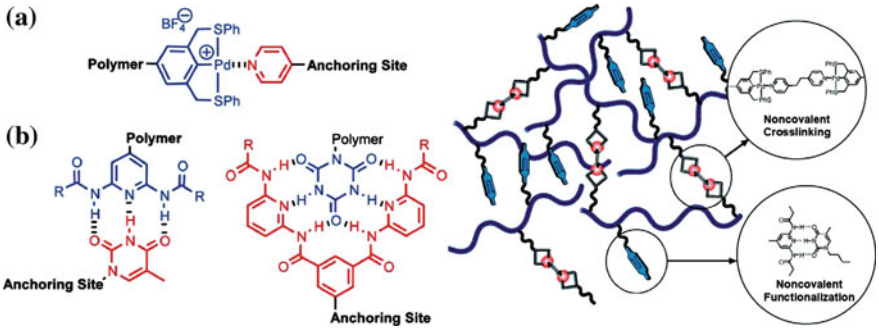

Fig. 7.29 Cartoon representation of the formation of ABC triblock-MSP [342]

[323, 342]. In this synthesis initiator *N*,*N*′-bis[6-(alkanoylamino) pyridin-2-yl] isophthalamide (often called Hamilton receptor or Wedge) and Py-based chain-terminator are used to obtain heterotelechelic poly (norbornene imide) polymer containing two terminal supramolecular motifs. It should be noted that M–L coordination has no effect on H-bonding fragment in telechelic polymers. Targeted triblock-MSPs are then obtained in one-pot reaction by a simple mixing of three components in solution: two telechelic polymers and one heterochelic polymer.

7.8.2 Combination of M–L Coordination with Host-Guest Interaction

Presently MSPs built using orthogonal self-assembling based on M–L and host-guest interactions attract more and more attention due to their interesting properties and potential applications [343]. M–L interactions provide MSP with different coordination geometries, strong, but tunable coordination binding capacities, and also magnetic, redox, photophysical, and electrochromic properties, while host-guest interactions give good selectivity and convenient enviro-responsiveness to these polymers. Therefore, MSP built by orthogonal M–L and host-guest interactions have wide applications in soft matter, fluorescence, probing, heterocatalysis, electronics, gas storage, etc.

β-CD is one of the most well-known types of a host, which is widely used in MSP building [52]. Thus, through double non-covalent interactions in the main chain consisting of low molecular weight monomers polypseudorotaxane is obtained (Fig. 7.30) [325]. In this case one rod-like host monomer contains two azobenzene groups at two ends bound to viologen units as hydrophilic electropositive barriers, which can be encapsulated in β-CD through hydrophobic host-guest interactions. Another monomer is 4,4′-bipy grafted with β-CD, which can be coordinated with Pd(II)-en nitrate, strong and quantitative bidentate acceptor

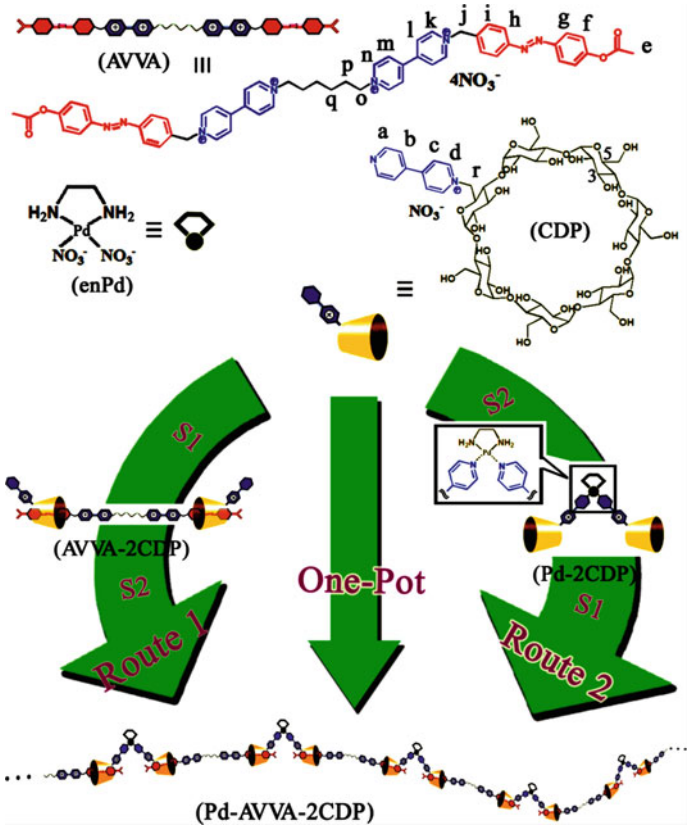

Fig. 7.30 Schematic representation of the construction processes for the functional polypseudorotaxane, based on heteroditopic ligand containing two azobenzene groups on two ends linked with viologen units of 4,4′-bipy grafted with β-CD (AVVA is guest compound containing two azobenzene groups in the two ends linked by viologen units)

for Py derivatives in water. Functional polypseudorotaxane can be obtained by mixing in water three components by spontaneous and orthogonal self-assembling using coordination Pd–N interaction and host-guest azobenzene-β-CD interaction. The desired MSP can also be obtained stepwise through preliminary formation of intermediate complexes based on M–L or host-guest interactions and the second type of interaction involved afterwards. Besides, in this system behavior of assembling/disassembling can be realized with photo isomerization induced by azobenzene in the main chain. Taking into account low cytotoxicity of β-CD in aqueous phase, these sensitive MSP can be of great potential for such applications as biomaterials for drug delivery, gene delivery, tissue engineering, etc.

We shall also notice synthesis of nanometer bis(polypseudorotaxane) based on endowing bridging bis(β-CD) with multiple coordinated metal centers, in which β-CD is a host for amino-terminal polypropylene glycol (PPG) being a guest, and

Ni(II) complexes as template fragments [344]. Two PPG chains were threaded separately in cavities of metal-bridging bis(β-CD) forming two-chained structures, they also played a stabilizing role in the assembling process (Fig. 7.31). It is important that the self-assembling process goes owing to advantageous entropy contributions, which accompany a considerable positive change in enthalpy. Bis (polypseudorotaxane) (∼20 nm in length) was also successfully preorganized to elongated bis(molecular tube) (∼200 nm in length) using intra- and intermolecular addition of ∼10 discrete bis(polypseudorotaxane) units and the following removal of polymer templates [345]. This bis(molecular tube) can efficiently capture C_{60} in holes formed by adjacent metal-bridging bis(β-CD) units, which can be then used for selective recognition of organic/inorganic/biological substrates.

1D metal-containing molecular wire with given properties for molecular electronics materials is obtained through M–L polymerization of Ru(II)-Pp with isolated bridging ligand [346]. It should be noted that this molecular wire combines advantages of organic isolated molecular wires with properties stipulated by presence of transition metal complexes. Quantitative self-inclusion of bis(β-CD) precursor followed by interaction with *p*-iodopyridine through Sonogashira coupling brings to bis(β-CD) containing Py-coordinating sites at both ends (Fig. 7.32). 1D metal-containing isolated wire is formed in situ using UV-irradiation of bis(β-CD) and carbonyl Ru(II)-Pp. As was expected, this wire not only shows hardness, linearity and structural stability, but also high intramolecular mobility of charge. It is important that this MSP can be subjected to reversible monomer-polymer transitions under special conditions, for example, in presence of CO or under UV irradiation. These workabilities obtained from unique reversible character of M–L bond are impossible for ordinary covalent-bound molecular wires.

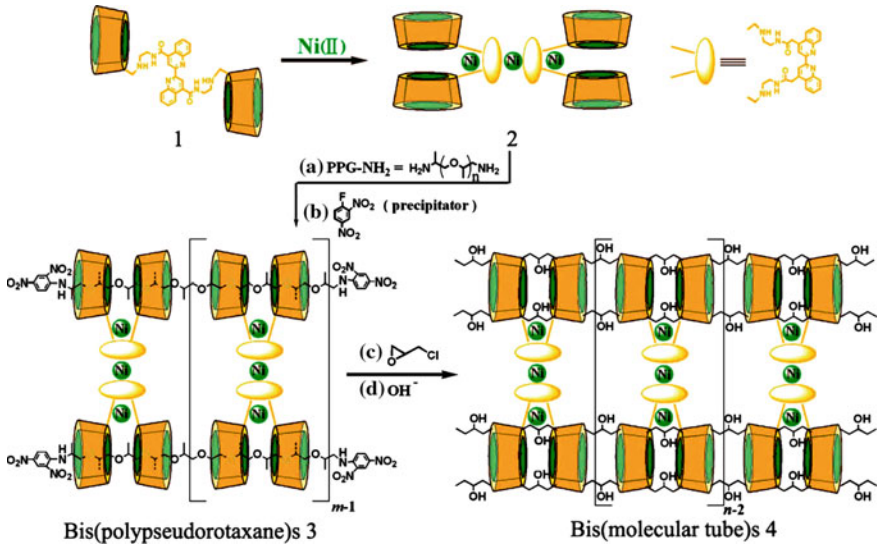

Fig. 7.31 Cartoon representation of the formation of bis(polypseudorotaxanes) by multiple metallo-bridged α-CD

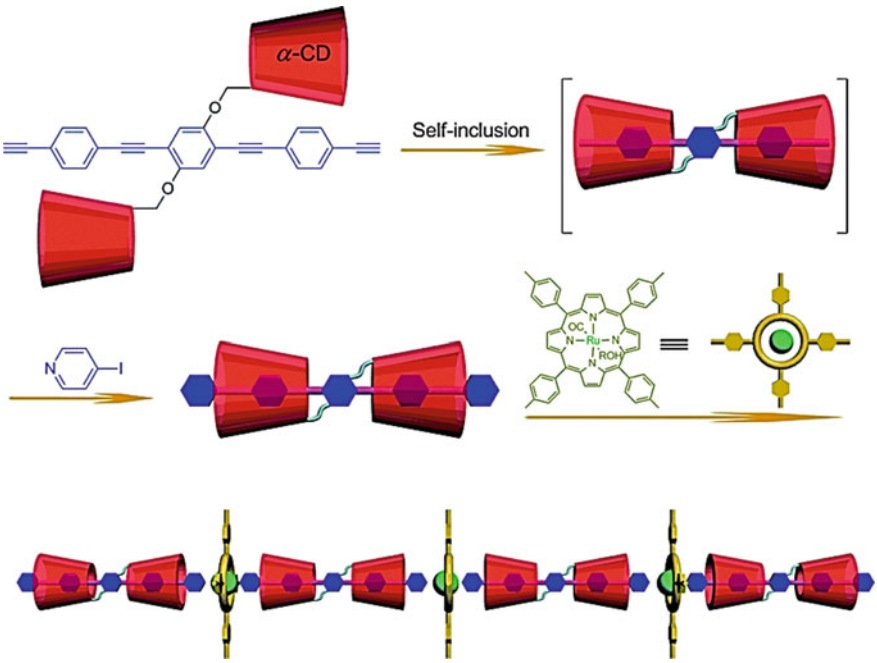

Fig. 7.32 Scheme of the formation of a polymeric insulated molecular wire via orthogonal self-assembly

Another important object in contemporary supramolecular chemistry are cucurbit[*n*]urils (CB[*n*], n = 5–8, 10), which are macrocyclic oligomers consisting of six or more glycoluril units. Hydrophobic cavity and polar carbonyl groups surrounding portals belong to structural features of CB[*n*]. Using carboxylate- and cyano-groups as terminal fragments, and lanthanide metal ions as spacers, which have big ionic radii and higher CNs than transition metal ions, 3D polyrotaxane network is obtained [347]. Besides, using orthogonal approach, double-chained 1D polyrotaxane and zigzag-like 1D polyrotaxane are synthesized from L-like pseudorotaxane and Cd(II) and Co(II) ions, respectively (Fig. 7.33) [348]. It is important that topologically intriguing MSP can be orthogonal assembled from exhaustively developed CB-based host-guest interactions and correctly chosen M–L interactions. CB[8] has an interesting ability of linking two guests simultaneously, which is widely used for building supramolecular assemblies. Combination of this ability with M–L self-assembling will, undoubtedly, advance MSP formation. For example, linear CB[8]-based MSP is obtained in aqueous solution using CB[8]-based host-guest interactions and tpy-Fe coordination as supramolecular motifs [349]. Synthetic route includes production of heteroditopic ligand consisting of naphthalene fragment and tpy-block, which can be bound with Fe(II) ion forming a monomer and two naphthalene residuals at head and tail (Fig. 7.34). The following host-guest CB[8]-naphthalene interaction brings to MSP

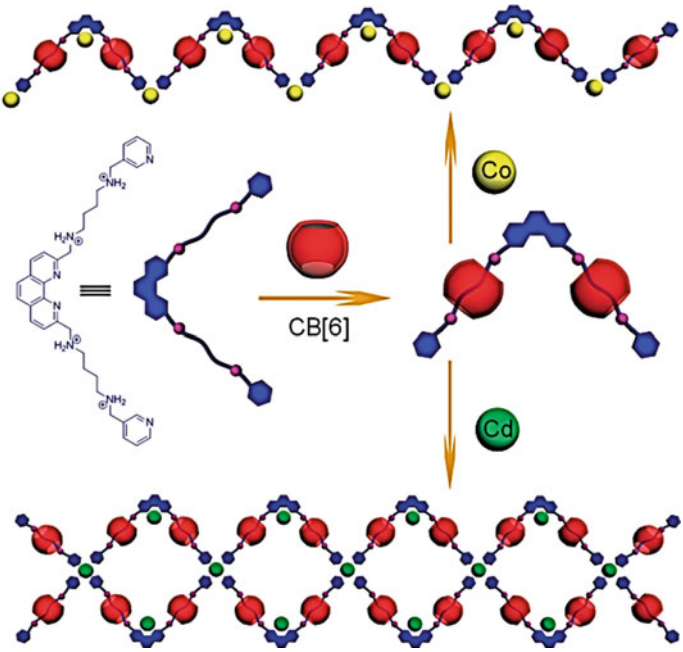

Fig. 7.33 Cartoon representation of the formation of a double-chained 1D polyrotaxane and a zigzag-shaped 1D polyrotaxane

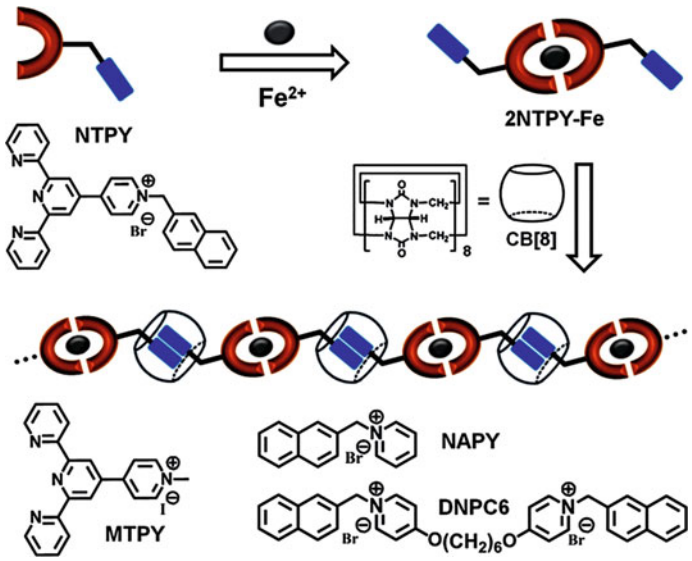

Fig. 7.34 Schematic representation of the orthogonal supramolecular polymerization based on CB[8] and M–L coordination

formation. It is important that introduction of tpy-Fe spacer not only increases solubility of monomers, but suppresses cyclization, thus facilitating efficiency of supramolecular polymerization. Metallosupramolecular polymerization can be controlled by tuning molar ratio of metal-containing monomer and CB[8].

For development of supramolecular chemistry pillar[n]arenes are important, which represent a class of macrocyclic hosts with symmetric pillar architectures and rigid electron-donor cavities [350–353]. Thus, based on amino-modified copillar[5] arene [c2]daisy with tpy stoppers, a solvent-driven muscle-like MSP is prepared [354]. Synthesis included fabrication of double threaded rotaxane dimer in chloroform driven by Van der Waals forces (mainly, dispersion forces) between parts of exo-cavity of long alkyl groups (Fig. 7.35). This monomer can change its length continuously by changing polarity of a solvent similarly to molecular spring based on amino-modified copillar[5]arene [355–357]. The following addition of Fe(II) brings to formation of muscle-like MSP based on individual compression or tension of each sequence of a daisy chain of repeated unit. With daisy units of a chain in broaden geometry at low pH (left) the total length of the polymer l_{ext} is estimated as ~15.9 μm. At higher pH (right) compression by ~1.2 nm of repeated units decreases length of a polymer 1_{cont} to ~9.4 μm, which corresponds to enhancement of nanoscopic motion of more than three orders of magnitude as a result of ~3000 artificial molecular machines working coherently in the same polymer chain. Developed MSP can be considered as a new platform for design of artificial molecular machines for imitation of living systems.

One of the promising directions of application of linear supramolecular polymers using pillar[5]arene-based host-guest interactions is design of fluorescent sensors for detection of different metal ions, for example, Cu(II) [358] and Zn(II) [359]. We shall

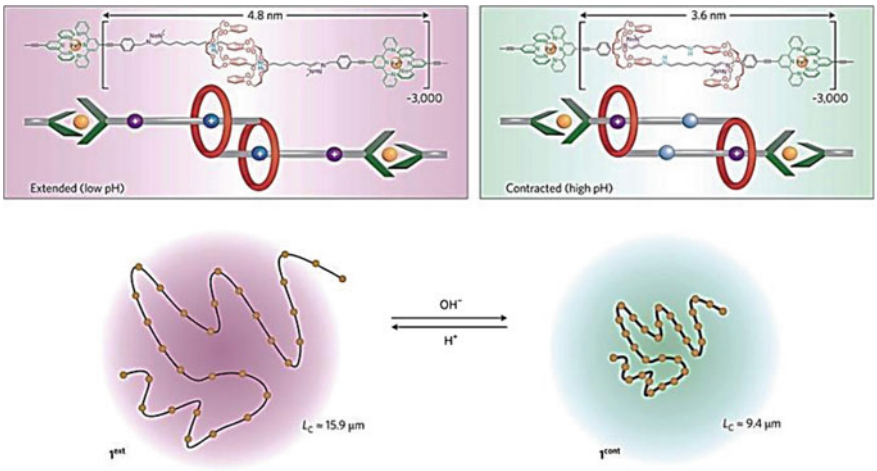

Fig. 7.35 Amplification of muscle-like mechanical actuation within a metallosupramolecular [c2]daisy chain polymer. Dialkylammonium ion (NH_2^+), blue; [24] crown-8, red; neutral amine, light-blue; triazole units, purple; tpy, green [356]

also notice supramolecular polymer networks assembled using combination of orthogonal tpy-Zn(II), carbine-Ag(I) and pillar[10]arene/alkyl chain of recognition motif, which show dynamic properties as response to external stimuli [360].

The most commonly used in supramolecular chemistry are host-guest interactions based on different crown ethers. For example, benzo-21-crown-7 is the smallest benzocrown ether, which can form threaded structures with secondary dialkylammonium salts [361]. Orthogonal self-assembling based on this supramolecular motif and M–L coordination provides efficient way of building highly efficient MSPs [362]. For this, heteroditopic monomer has been developed, which carries secondary ammonium salt fragment and tpy ligand on both sides of a long flexible aliphatic chain. A chelating ligand makes it possible to decrease percent of cyclic oligomers and advances linear expansion, which, finally, brings to relatively low critical concentration of polymerization during supramolecular polymerization. Further on heteroditopic monomer can be complexed with benzo-21-crown-7-based monomer of AA type with formation of [3]pseudorotaxane structure (Fig. 7.36). We shall also notice another heteroditopic monomer which contains benzo-21-crown-7 and tpy blocks on two ends and complementary BB type homoditopic monomer of secondary ammonium salt [363]. Then MSP of the main chain was obtained using one-pot mixing two recognition motifs and metal ions. Since non-covalent interactions used in these systems were the same as the abovementioned ones, the materials have shown analogues dynamic and responsive properties. These two adaptive MSP are attractive objects for further fabrication of intelligent supramolecular materials with given properties.

An MSP is considered obtained through coordination of Zn(II) with a conjugated bis-tpy ligand carrying dibenzo-24-crown-8 arms, which can form stable responsive 1:1 threaded structure with complementary dibenzylammonium salt guest through

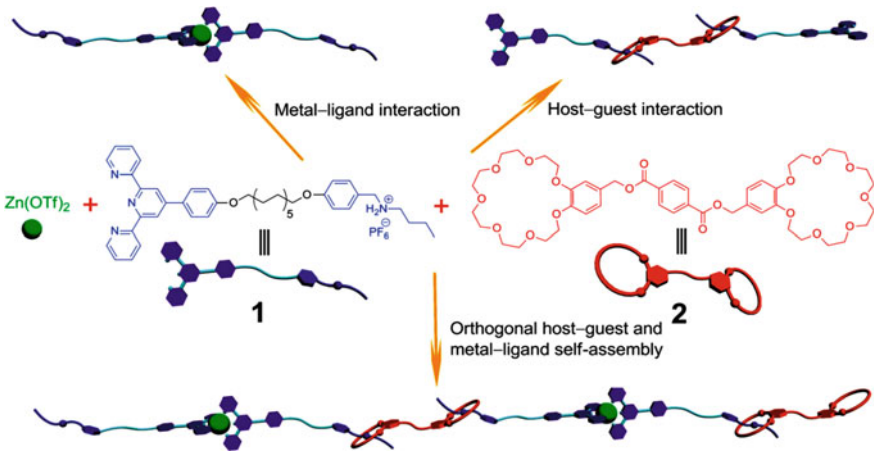

Fig. 7.36 Cartoon representation of the formation of a linear supramolecular polymer and the corresponding intermediates from monomers **1** and **2**

combination of [N^+–H···O] and [C–H···O] H-bonds and π-π-stacking [221, 364]. These long chained polymers are characterized by high DP at high concentration. It is interesting that the MSP has shown concentration dependent emissions from turquoise to white and then to yellow color in the range of concentrations 1.25–125 mM. Following alternative addition of 2.4 equivalent of base (*N-tert*-butyl-*N′*, *N′*,*N″*,*N″*,*N‴*,*N‴*-hexamethyl-phosphorimidic triamide) and 2.8 equivalent of CF_3COOH has brought to dethreading and rethreading of dibenzylammonium salt in host fragments and, therefore, to reversible fluorescent emission. Recently also excellent responsive MSP networks obtained through orthogonal self-assembling dibenzo-24-crown-8/dibenzylammonium salt and metal-tpy motifs are reported [365, 366]. In this case, successive reversible emissions are realized by acid-base controlled recognition of dibenzo-24-crown-8 residuals in MSP-Zn with dialkylammonium ion centers.

Elegant combination of special bistable dibenzo-24-crown-8-based [c2]daisy chain rotaxane and M–L-driven supramolecular polymerization was applied to realize linear amplification of muscle-like translation molecular motions by orders of magnitude [367, 368]. These polymer chains were long and quite well soluble, so that micrometric changes in their contour length could be measured at synchronizing multiple contractions and expansions. Other binding constants of secondary ammonium and triazolium ions with dibenzo-24-crown-8 motif give a possibility of efficient pH-responsive translation motion at molecular level (Fig. 7.37).

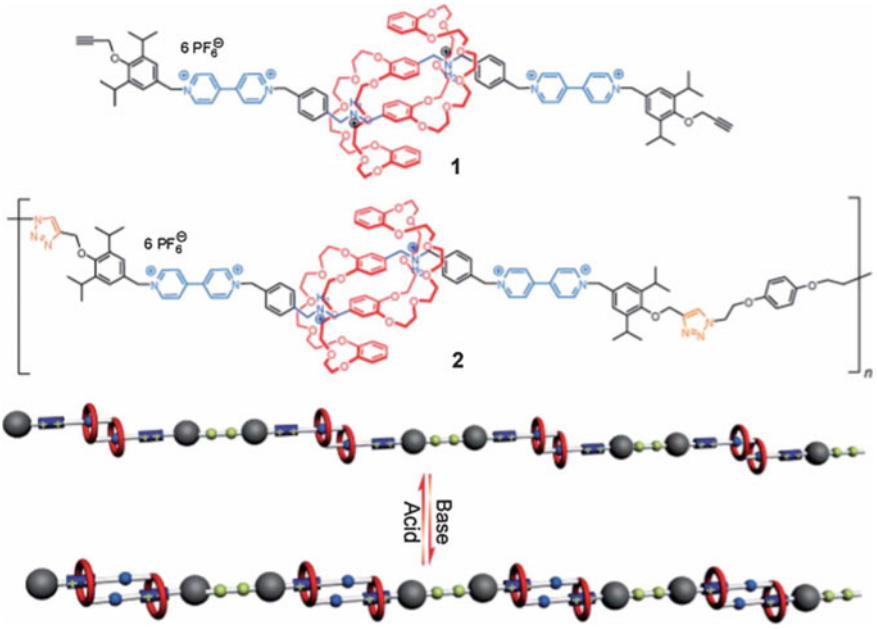

Fig. 7.37 Chemical structure of the difunctional [c2]daisy chain and cartoon representation of the acid-base switching contraction-extension process of the resultant MSP

In particular, M–L driven processes of supramolecular polymerization with Zn $(OTf)_2$ or $FeCl_2$ are confirmed.

We shall also notice fluorescent supramolecular polymer with AIE properties formed by crown ether-based host-guest interactions, which is used as a fluorescent sensor for Pd(II) ions [369].

Recently well-organized supramolecular polymer massifs are successfully built based on «tweezing directed self-assembly» strategy [370]. For this purpose, special heteroditopic monomers were developed and synthesized (Fig. 7.38) [371]. Since two electron-deficient alkynylplatinum(II)-tpy tweezers on molecular unit of a tweezers can specifically encapsulate electron-rich alkynylgold(III) diphenylpyridine, mixing equivalent amounts of heteroditopic monomers gives a dimer complex. Following addition of homotritopic monomer brings to expected A_2B_3 type supramolecular hyperbranched polymers with potassium cation-responsive character. At the same time, the process of supramolecular polymerization can also be realized using one-pot mixing three monomers, which points to highly specific non-covalent recognition of a tweezers-guest motif. This new supramolecular motif broadens host-guest set of tools and represents universal strategy for MSP fabrication.

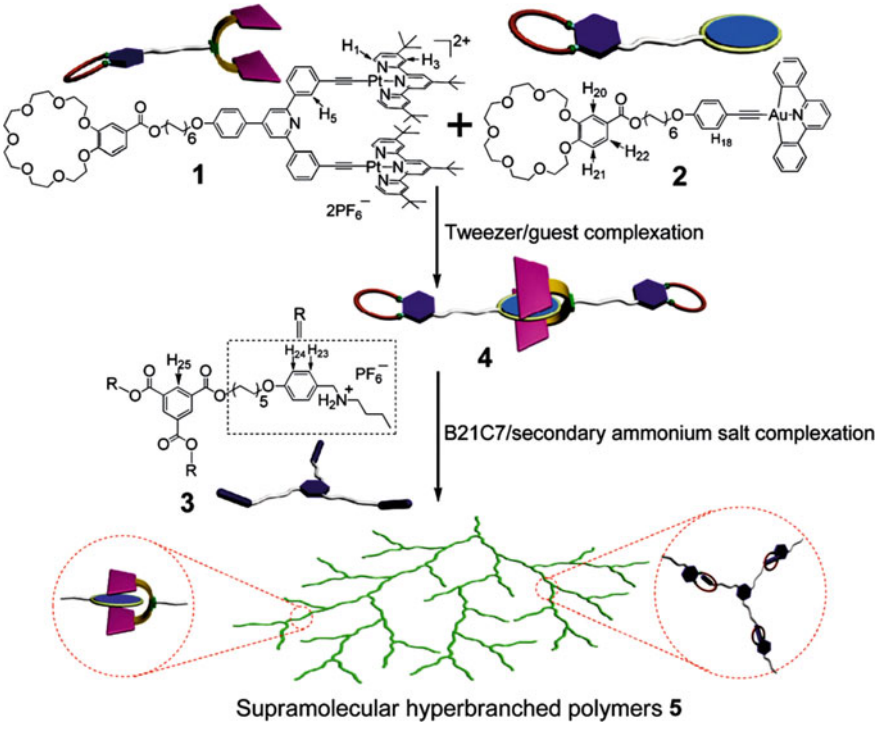

Fig. 7.38 Cartoon representation of the construction of a supramolecular hyperbranched polymer

Substantial attention is given to integration of bioactive types into synthetic supramolecular systems from the point of view of biosensors or «nanoreactors» design. For example, biotin being one of the most known natural non-covalent linking blocks (which forms stable «complexes» with avidin and streptavidin proteins) was linked to tpy fragment. A metal-tpy spacer can be adjusted for regulation of stability and kinetics, and also can be reversibly opened by external stimuli. For these purposes non-polymer and polymer PEG spacers were used [372]. These compounds are the attractive examples of a link between biochemistry and metallosupramolecular chemistry and are convenient building blocks for design of functional (nano)architectures. Another example is functionalization of bpy with biotin and following production of respective Fe(II) complex [373]. This complex is a «redox biotin bridge» for potential applications as a biosensor, since addition of avidin to a complex brings to a change in Fe(II)/Fe(III) redox signal of cyclic voltammetry, thus making it possible to monitor avidin addition. Besides, 3D orientation of biotin fragments provides fixing several avidin units.

Very promising is design of multicomponent supramolecular systems highly complicated due to combination of orthogonal self-assembling and self-sorting approach. For example, driven by orthogonality of M–L coordination and host-guest interactions and directed by several molecular codes during self-sorting, five types of simple components (up to eighteen precursors) were successfully self-assembled into two new tris [2]pseudorotaxanes by one-pot highly selective method (Fig. 7.39) [374].

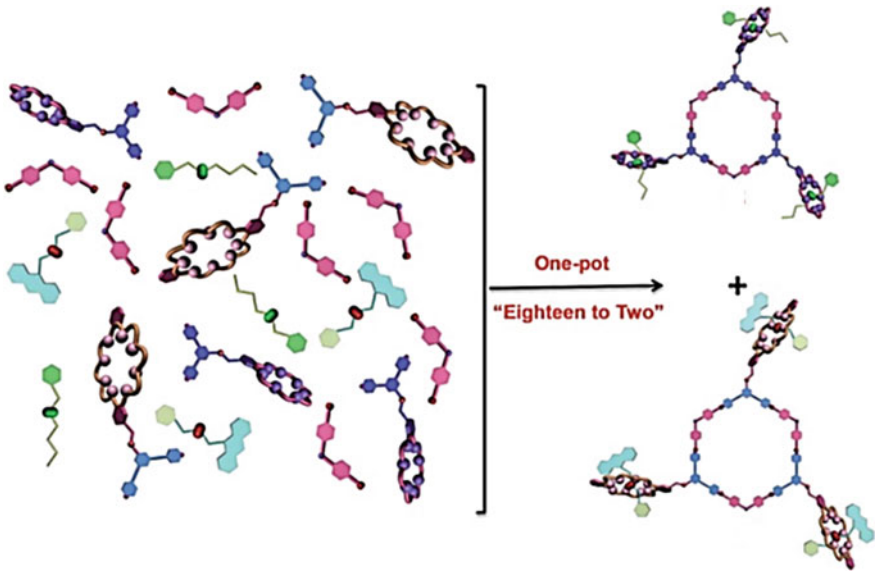

Fig. 7.39 Scheme of combination of orthogonal self-assembling and self-sorting approach

7.9 Hierarchical Self-assembling

Creation of complicated supramolecular architectures has become recently possible due to application of the concept of hierarchical self-assembling, which is determined as multilevel non-covalent self-assembling supramolecules including a range of successive interactions with gradually decreasing strength [133, 345]. It should be noted that hierarchical self-assembling is used at building several systems in nature, such as tobacco mosaic virus and cell cytoskeleton. In this approach supramolecular assemblies are self-organized through coordination of supramolecules between each other or their co-assemblies with other modulus. For example, through electrostatic interaction, M–L-based supramolecules can be integrated in films, liquid crystals, micelles, hydrogels, etc., which have a number of switchabilities and other desirable properties [33]. Besides, hierarchical self-assembling makes it possible to obtain exotic and complicated nanostructures, which are interesting for nanotechnologies and materials science [375, 376].

In recent decades, different strategies have been developed, which bring to hierarchical molecular self-assembling. We shall notice that for greater variety of linear and branched MSP self-assembled from small telechelic ligands and metal ions, it is scarcely possible to form hierarchical structures due to their homopolyelectrolyte character. Nevertheless, MSP based on Zn(II) and ditopic ligand can be organized in spherolites in gels formed by these MSP (Fig. 7.40) [130, 377, 378].

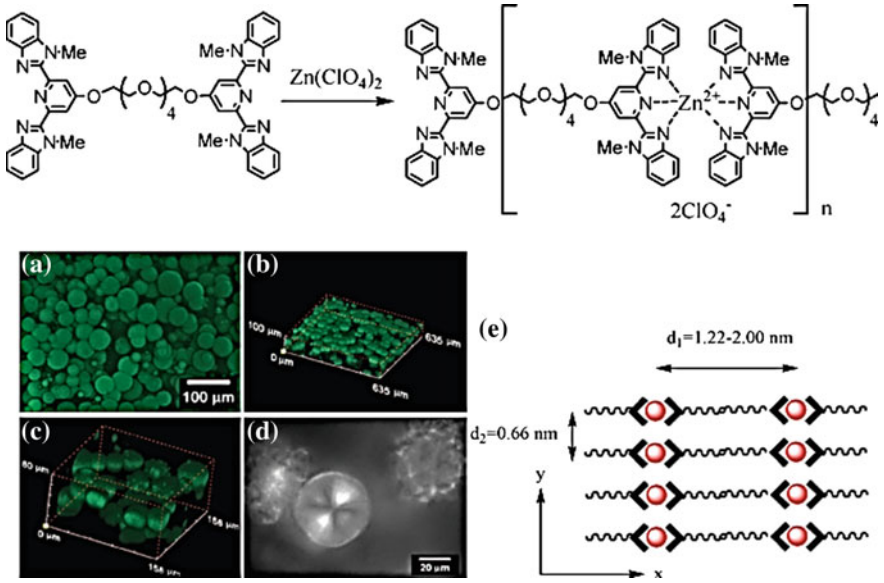

Fig. 7.40 Schematic representation of the formation MSP using ditopic ligand with metal salt, Zn $(ClO_4)_2$, in polar solvents. LSCM images **a** z-projection image, **b** and **c** 3D image of the MSP gel formed in 60/40 (v/v) DMSO/water mixture as shown in (**a**), and **d** polarized images of the MSP gel formed in 70/30 DMSO/water mixture (v/v) showing the coexistence of regular and irregular particles. **e** Illustrates the molecular packing mode in the aggregates

As the results of laser scanning confocal microscopy (LSCM) show, spherolites form through radial lamellar crystallization, and aggregation of these spheres at higher concentrations form a gel skeleton.

Hierarchical self-assembling MSP is easily accessible with block-MSP using if long hydrophobic and hydrophilic polymer blocks coexist in one MSP chain. For example, it is shown that micelles are formed in solution of such block-MSPs as PS_x-[M]-PEO_y [236], poly(ethylene-*co*-butylene)$_{70}$-[M]-PEO_{70} [238], PEO_{70}-[M]-$(CH_2)_{16}$-PEO_{70} [239], PS_{32}-*b*-$P2VP_{13}$-[M]-PEO_{70} [241] and polydimethylsiloxane-[M]-PEO_{70} [379], where [M] indicates position of M–L bond. Addition of HEEDTA to PS_{32}-*b*-$P2VP_{13}$-[M]-PEO_{70} brings to detachment of a PEO block and remains chelating groups on a micelle surface. It is important that PEO block could be restored if detached polymer chains would be mixed with micelles again (Fig. 7.41). This is one of examples of responses on exposure to environmental stimuli of MSP micelles. It is interesting that three-armed star-like block-MSP is self-assembled in vesicles in acetone, while tetra-armed analogue gives micelles again [265].

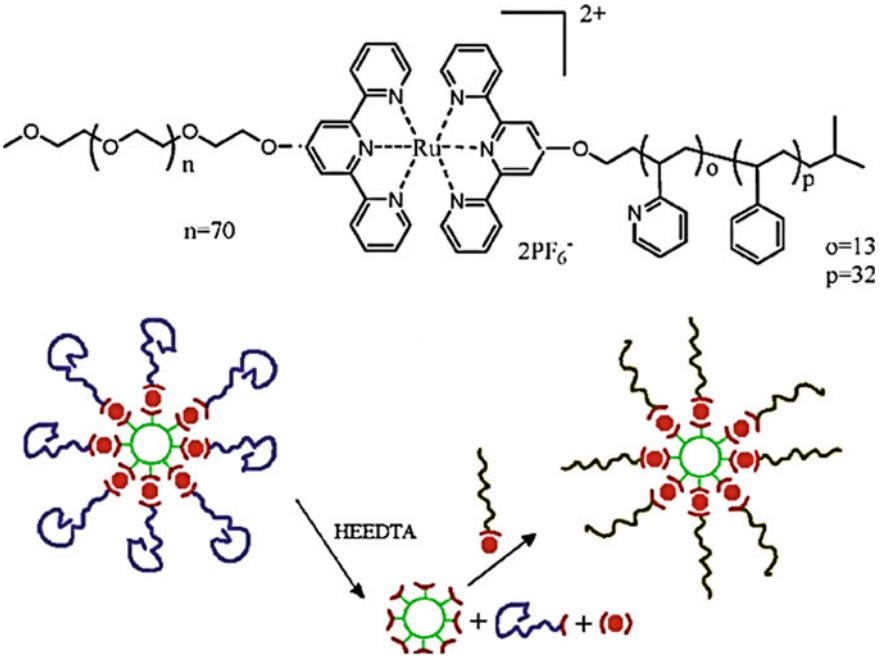

Fig. 7.41 The reversibility of tpy-Ru(II) complexes allow PSM of the micelles. The micellar hydrophobic core (green open circle) is surrounded by tpy (red brackets) Ru (red solid circle) bis-complexes; addition of a strong competing ligand (HEEDTA) allows the release of the coronal chains and the micellar core can be isolated. Reattach the coronal chains to the micellar core can be realized [241]

Multiple studies consider hierarchical self-assembling with MEPE participation, which can interact with such oppositely charged modulus as polymers, colloids or molecules carrying opposite charges [157]. It should be noted that exchange between counter-ions and MEPE brings to respective polyelectrolyte-amphiphilic complexes (PAC) [113, 380]. Whereas MEPEs are easily soluble in aqueous solutions, PACs are neutral and hydrophobic, therefore, soluble in ordinary organic solvents. For example, we shall notice PAC with liquid crystalline properties obtained by self-assembling dihexadecyl phosphate (DHP) with Fe-MEPE and Ni MEPE based on ditopic ligand 6,6′,6″-bis(2-pyridyl)-2,2′:4′,4″:2″,2‴-quaterpyridine (Fig. 7.42, left) [300, 381–385]. In these PACs MEPE rods are incorporated between interdigitated DHP layers with formation of lamellar structures [300]. It is important that the respective Fe-PACs show unusual temperature-induced spin crossover [383–385].

It is well known that crystalline field of a strong ligand around metal ions forces them to stay in LS state [386, 387]. In particular, Fe(II) ion in Fe(II)-MEPE is diamagnetic, since all electrons are coupled. At low temperature PACs are assembled densely in LB films and in crystalline state, which has no effect on strong crystal field around Fe(II) ions. As temperature increases, energy released during phase transition changes the crystal field abruptly, so that a system becomes HS and paramagnetic (Fig. 7.42, right) [384].

We shall notice interesting shape of multi-comb MSP containing benzene sulfonate counter-ions with long alkyl tails (Fig. 7.43) [388]. In this case a polymer supramolecule is based on functionalization of side chain of covalent polymer (P4VP) using Zn(II)-2,6-bis-(octylaminomethyl) pyridine M–L coordination, which

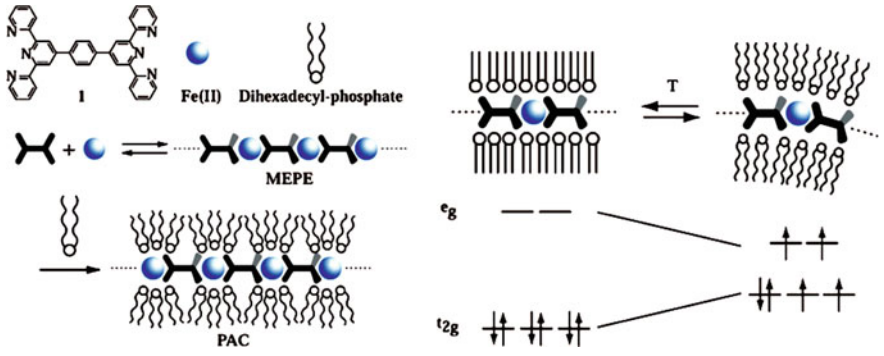

Fig. 7.42 (Left) Self-assembly of ditopic ligand **1** and $Fe(OAc)_2$ results in formation of the linear, rigid-rod-type MEPE. In a consecutive step, MEPE is assembled with DHP, resulting in formation of the corresponding PAC. Spreading PAC at the air-water interface and subsequent transfer of the Langmuir monolayers on a solid support results in a well-defined multilayer, which section is schematically shown in the bottom of the scheme. (Right) Upon heating the multilayer, the alkyl chains of the mesophase melt, resulting in a distortion of the metal ion coordination geometry. The unfavorable coordination of the tpy around the Fe(II) cation results in a lowering of the energy gap between the d-orbital subset, giving rise to a reversible transition from a diamagnetic LS state to a paramagnetic HS state

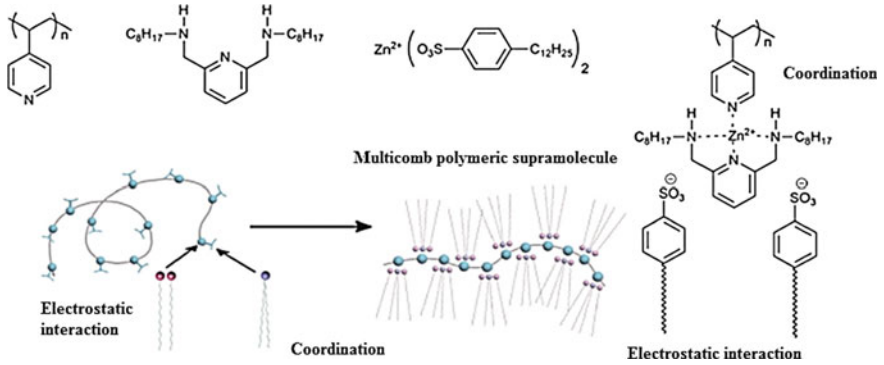

Fig. 7.43 Concept of binding several side chains with respect to one repeating unit of polymer main chain based on coordinated alkylated ligands and alkyl-functionalized counter-ions

then is electrostatically bound with sulfonate counter-ions. It is important that fragments of mutually repulsing overload side chains should reinforce cylindrical organization of the copolymers.

When mixing MSP with oppositely charged diblock-copolymer, neutral micelles can be formed in a solution volume [389]. These micelles belong to the family of the complex of coacervate core micelles (C3Ms) [390] or polyion coacervate (PIC) micelles [391]. It is obvious that MSP acts as homopolyelectrolyte in this micellar system. It should be noted that formation of micelles in supramolecular system includes two synergetic processes: polymerization with M–L coordination and micelle formation. In presence of oppositely charged block-copolymers local concentration of LMC can be increased considerably, so that DP significantly enhanced, in particular, «polymers» come into action.

This long «polymer» corresponds to «chain-matching» criterions to form electrostatic micelles [390]. It is interesting that size of a micellar core can be increased considerably by substitution of a part of diblock polyelectrolyte with homopolyelectrolytes of amphiphilic micellar systems [392]. Thus, the of Zn-L/P2MVP$_{41}$-PEO$_{205}$ core size of micelles is increased with coefficient 10, where P2MVP is poly (2-methylvinylpyridine), and L is 1,11-bis(2,6-dicarboxypyridin-4-yloxy)-3,6,9-trioxaundecane [392]. A number of metal ions in micelles can be controlled, which is very important for such micelles as potential carriers of heavy metal. Like the covalent C3Ms, the micelles formed by M–L coordination are also sensitive to additional salt. For example, for the micellar system Zn-L/P2MVP$_{41}$-PEO$_{205}$ critical concentration of micelle formation depends on salt exponentially [393]. Besides this, micelles show dependence on a character of coordinated metal ion [394]. For example, if transition metals of the first row are used, metal ion excess will have no effect on C3Ms. However, when transition metal ions of the first row are replaced by those from the second or third row, C3Ms can be broken by excess of metal ions. This indicates that metal ions from the first transition row do not extract ligands from a micellar core, while metals from the second and third row do

this, which results in formation of positively charged ends of a coordination chain and C3Ms falling-apart. It is also noticeable that excess of diblock-copolymers brings to formation of worm-like micelles, which remind strings of a spherical micelles, thus showing that there is weak attraction between these micelles [395, 396].

MSP are formed in organic solvents through M–L driven supramolecular self-assembling using 1:1 mixture of $(dppp)M(OTf)_2$ complexes (M = Pd(II) or Pt (II), dppp = bis-(diphenylphosphino)-propane, OTf = triflate) and non-linear bidentate dipyridyl-substituted ligand. In methanol aqueous solutions MSP hollow bubbles form and smaller completely filled nanospheres (Fig. 7.44) [397].

We shall notice universal hierarchical approach to assembling copolymer-metal nanostructures, in which one level of self-assembling guides the next one. For example, at the first stage ultrathin diblock-copolymer films form regular platform of highly anisotropic strip-like domains. At the second stage of assembling, the differential wetting guides diffusing metal atoms to aggregate selectively along the platform making highly-organized metal nanostructures. In this case a metal located on a copolymer matrix provides highly ordered configurations in the case when a system is far from equilibrium. Two different assembling regimes of the metal component of chains can be distinguished, particularly, of separate nanoparticles and of continuous wires; each is characterized by different ordering kinetics and stunningly different current-voltage characteristics [398].

Hydrophilic polymer-linked SCS-pincer Pd(II) complex and Py-functionalized PS form amphiphilic diblock-MSP, which is self-assembled in clearly defined monodisperse non-covalently linked micelles. It is important that hydrophobic domain of a core is easily removed using dialysis at low pH, giving a hollow polymer nanocage with well-defined internal functionality [399].

Spontaneous self-assembling of cationic nanoporous metal-organic coordination cages (nanocages) brings to giant hollow vesicle-like structures in polar solvents. These well-soluble nanocages (macrocations) are separated by hydrophobic areas, and their assembling proceeds not due to hydrophobic interactions, but due to

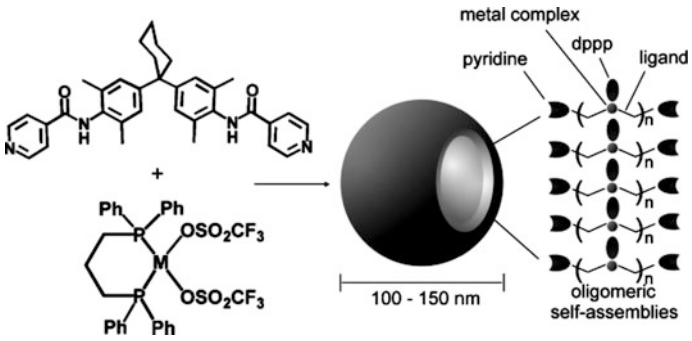

Fig. 7.44 Schematic representation of vesicle formation from self-assembled oligomer coordination compounds [397]

counter-ion driven attractions. As a result, blackberry structure is formed, in which self-assembled nanocages can provide a wide spectrum of functionalities, which cannot be achieved with purely inorganic systems [400].

Higher level of MSP with special functionalities will bring to unexpected surprises in hierarchical self- and/or co-assembling containing MSP. For example, a change in spacer structure of a telechelic ligand of the molecules can cause a considerable effect on function and hierarchical self-assembling properties of MSP and also can have an effect on topological feature of co-assembling with oppositely charged particles. MSP can be fluorescent at incorporation of a fluorescent group into a spacer [158, 401]. Moreover, responsiveness of molecular assemblies containing MSP to stimuli has not being studied thoroughly yet. This will also be very interesting to operate with coordinating force to control hierarchical interaction of molecular assemblies. For example, modified monoligand amphiphil is used to form micelles; these micelles will produce gels initiated by addition of metal ions (Fig. 7.45) [402].

Using a model system of 4-armed PEG hydrogels cross-linked with multiple kinetically distinct dynamic M–L complexes, it is shown that polymer materials with decoupled spatial structure and mechanical characteristics can be developed [403]. This model of hydrogels with kinetically different cross-linkings makes it possible to project time hierarchy of gel networks separately from spatial hierarchy, and thus to show new conceptual frameworks for viscous-elastic materials. In other words, by regulation of relative concentration of two types of M–L cross-linkings, it is possible to control mechanical hierarchy of a material by changing types of cross-linkings, but not by modifying a polymer itself.

The new strategy applied to fine supramolecular nanomaterials is using supracolloidal self-assembling, in which micelles or colloids are used as building blocks [404]. This directed supracolloidal self-assembling is done by dynamic covalent bonds and M–L coordination in water. Conjugation of a ligand precursor to water-soluble block-copolymer through dynamic covalent bonds brings to dehydration and micelle formation of a functionalized polymer. Reversible reaction facilitates penetration of metal ions into core-shell interfaces and, oppositely, M–L coordination advances reaction over interfaces. It should be noted that Cu(II)

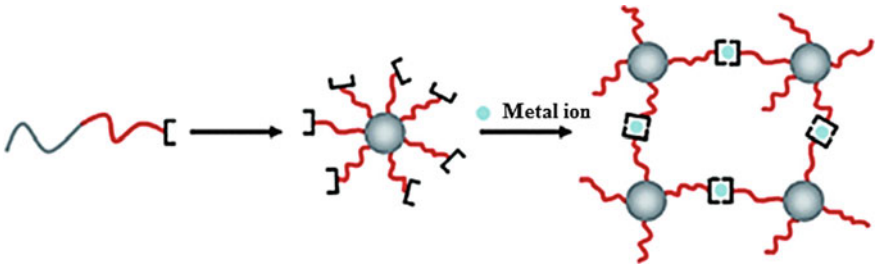

Fig. 7.45 Hierarchical self-assembling PS-*b*-poly (*tert*-butyl acrylate)-copolymer tpy ligand, leading to formation of supramolecular network of micelles [402]

coordination takes place entirely in each isolated micelle. However, Zn(II) coordination induces directed self-assembling, whose nanostructures are developed stepwise from nanorods, nanowires, necklaces, and, finally, to supracolloid networks of increasing scale to several ten microns. Post-reactions of simultaneous dynamic conversion of covalent bond and Zn(II)-coordination over core-shell interfaces provide these supracolloidal networks with vast specific surface for hydrophobic dative metal centers accessible for substrates in water. Therefore, directed supracolloidal self-assembling is a universal platform for creation of metal-hybridized nanomaterials, which are promising as enzyme-inspired water catalysts.

We shall also notice synthesis of supramolecular inorganic/organic hybrid colloids using concurrent and consequent self-assembling [405]. This conception of co-assembling broadens sphere of studying self-assembling block-MSP and provides new routes for design of hybrid colloids. In addition, such self-assembly offers unlimited opportunities for development of inorganic/organic hybrid functional materials.

7.10 Metallosupramolecular Polymer Gels

Gels are formed from a gelator and a liquid-solvent, at that the gelator concentration can be less than 2 wt%. Gels are divided into two categories: organogels and hydrogels, in which gelator molecules immobilize organic solvents and water, respectively.

In the recent years great interest is attracted to metallosupramolecular polymer gels (MSPGs), in which gelators are either MSP or discrete metal chelates self-assembled through other types of non-covalent interactions into supramolecular assemblies [101, 340, 406–415]. Increased attention to MSPGs is caused by their unique properties, ability to change their structure reversibly under action of external physical or chemical forces. It is extremely important that by changing nature and concentration of gelator it is possible to systematically modify and tuning physical properties of a material [166]. The reason for raising interest is in M–L coordination and its variety, which can easily cause or control self-assembling a gel, and therefore, can have an effect on its properties [101, 416–422]. In these special cases presence of metal ions in MSPGs chemical structure generates their fascinating potential applications, which include catalytic activity [423, 424], bioimaging [425, 426], controlled release [427], redox induced gel-sol switching [428], magnetism, color, rheology, adsorption, and photophysical properties [429].

There is extremely diverse range of compounds which can serve as gelators. Low molecular weight gelators are the key area in supramolecular chemistry studies due to spontaneous and controlled self-assembling phenomena [409, 430–453]. Therefore, search for new gelators for MSPGs is important task of contemporary supramolecular chemistry.

Low molecular weight gelators are self-assembled by combination of non-covalent interactions, such as π-π stacking, H-bonds, hydrophobic-hydrophobic interactions and Van der Waals forces, which brings to formation of entangled self-assembled fibrillar networks (SAFINs) [409, 410], which, additionally, form hierarchical 3D networks self-assembled through joint nodes. It is interesting that fine balance and combination of non-covalent interactions can be easily modified with account for these gelators, due to rational choice and design of chelating ligands in metal chelates, which, in turn, can bring to fine tuning gelation and gel morphologies. Molecules of a solvent are then immobilized due to capillary force in such 3D SAFINs, which results in gelation. It is assumed that 1D H-bonding networks advance gelation, while 2D and 3D networks give either weak gels or are not subjected to gelation at all [453]. Probably, anisotropic interactions, such as H-bonding of gelator molecules, which provides one-directional growth, and absence of such interactions in two other directions, prevent side growth thus bringing to 1D fibers advancing SAFIN formation and a resulting gelation [454–458]. Therefore, there is promising design of 1D network forming a supramolecular synthon, which would make it possible to obtain SAFIN and, finally, provides gelation. Gelator molecules generate hierarchical supramolecular structures, which are macroscopically expressed in gelation. Therefore, molecular modification can control nanometer assembling, the process, which finally determines a specific function of a material [457, 458].

Among low molecular weight gelators, the important place has gold chelates [430]. As an example, we shall notice luminescent bis-cyclometalated alkynylgold (III) complexes with long hydrocarbon chains, which can form stable MSPGs in non-polar organic solvents (*n*-hexane and cyclohexane), probably, using strong London dispersion interactions stipulated by long hydrocarbon chains. It is shown that at reasonable choice of coordinating ligands non-covalent interactions such as π-π stacking, and London dispersion forces can be easily corrected for rational MSPGs construction based on the gold(III) system (Fig. 7.46) [431]. Absorption of isobestic point at 408–410 nm supposes complete transformation of supramolecular assemblies into monomer types during sol-gel transition as temperature increases. On the other hand, there is irradiation at 570–620 nm, which is quenched at higher temperatures. This observation is associated with the fact that in gel state hardness of a medium will increase, and this will bring to decrease in molecular vibrations and motions, so that non-radiation deactivation ways will be delayed. At the same time, at higher temperatures non-radiation decay will be increased as a result of emission quenching. It is worth noticing a double functionalized MSP, self-assembled from two cyclometalated Au(III) complexes in acetonitrile [459]. For MSPGs partly aligned nanofibers with diameters and length up to 50 nm and ten micrometers, respectively, are detected (Fig. 7.47), and amino group of guanamine-like fragment of a ligand is involved in H-bonding interactions in the complex self-assembling. A 1D structure of MSPG with alternating H-bonding and π-π stacking interactions between two cations is suggested. It is known that many metal chelates have long living excited triplet states strongly irradiating in visible region, due to which metallogelators are ideal for luminescence-based technologies,

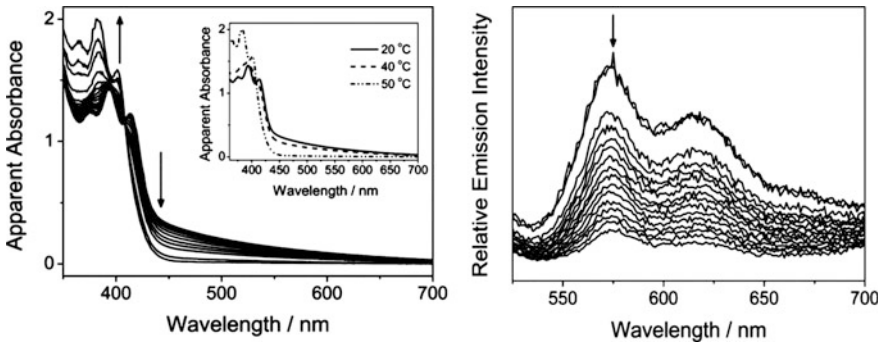

Fig. 7.46 UV-vis absorption spectral traces of the sol-gel phase transition of MSPG in hexane upon an increase in the temperature from 10 to 50 °C. Inset: spectral traces at 20, 40, and 50 °C (left); corrected emission spectra of the hexane gel of MSPG upon an increase in the temperature from 10 to 40 °C (right) [431]

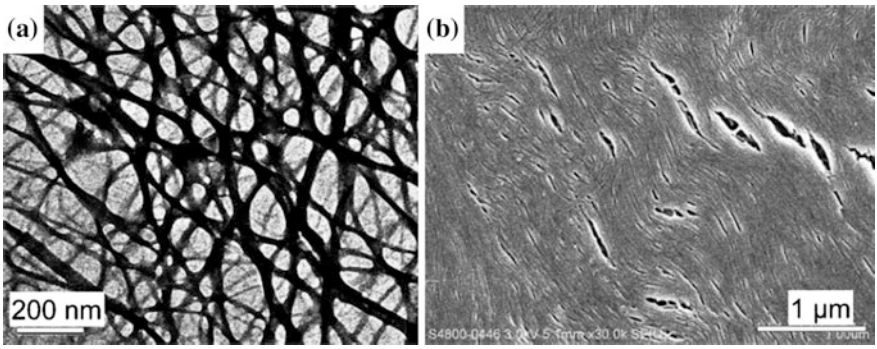

Fig. 7.47 **a** TEM image, **b** SEM image of MSPG. Photographs showing formation of the viscous fluid (supramolecular polymer) of MSP in CH_3CN [459]

photoelectricity and photocatalysis. This principle of design is implemented using trinuclear Au(I) pyrazolate metallocyclic gelator, whose phosphorescence at room temperature can be written in gel phase [418], therefore, these MSPG can be used to obtain safe inks for preparation of rerecording phosphorescent paper.

Among metal chelates of molecular type, the most attention has been attracted to polypyridyl complexes of transition metals. Thus, Cu(I) complex of bis(cholesterol)-functionalized bpy ligand gels PhCN, 1-PrCN and THF-MeCN [428]. It is interesting that greenish-blue gel color formed with Cu(I) chelate in 1-PrCN was absolutely different from reddish-brown sol color (Fig. 7.48). This is, probably, ascribed to distortion of coordination geometry of metal chelate in gel phase induced by molecular packing in gel fibers. Besides, due to presence of redox-active metal center, the sol-gel phase transition can be reversibly induced by addition of oxidants and reducing agents, which also bring to changes in geometry of a metal

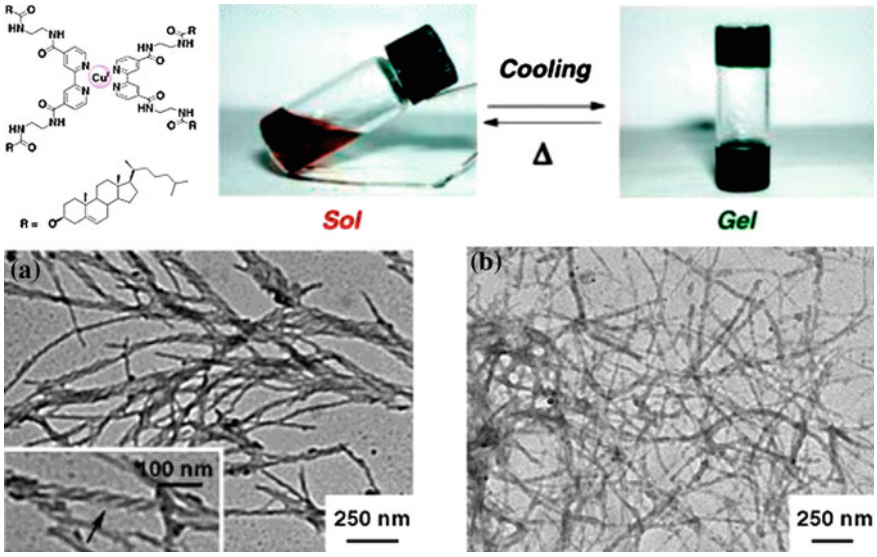

Fig. 7.48 Phase transition and thermochromic behavior of the sol and the gel phases of 1-PrCN gel based on Cu(I) chelate c bpy ligand, and TEM images of 1-PrCN gels prepared from initial ligand and metal chelate [428]

ion coordination as an oxidation degree changes, thus having effect on ability of a complex to π-stacking.

We shall also notice pseudo-planar trinuclear Cu(II) complex with inositol and bpy, which forms hydrogel at pH = 12.4 [460] that gives fiber super-structure. In this case π-π stacking interaction between bpy, presence of axial ligation, and H-bond of hydroxyl promote the formation of hydrophobic cavities, which hold the water molecules to form a hydrogel.

Steroid-phen conjugate is a powerful gelator for MeOH–H_2O even at such low gelator-to-solvent ratios as 0.1 wt% in absence of metal ions [461]. In particular, this gel is solved at storage with the formation of transparent solution of low viscosity, which reversibly forms the gel again at heating up to about 70 °C. Drastic differences between a ligand and metal chelate are ascribed to different spatial location of chelating ligands enforced by complexation of a metal.

Metal complexes with tpy ligands are wide range of metal chelate gelators. Chelating ability of tpy ligands provides metal ion capturing, therefore bringing to stable gels with restructured emission properties [462, 463]. Under ultrasonic conditions a range of hydrogels of tpy derivative carrying a carboxyl group is obtained with one equivalent of $CeCl_3$, $PtCl_2$, $CuCl_2$ or $EuCl_3$. We shall also notice chiral BINOL derivative of tpy [464]. Using ultrasound, suspension of Cu(II) chelate of this ligand in $CHCl_3$ gives a gel, which is potentially useful for visual chiral probing. In particular, the gel stayed stable at addition of (R)-phenylglycinol,

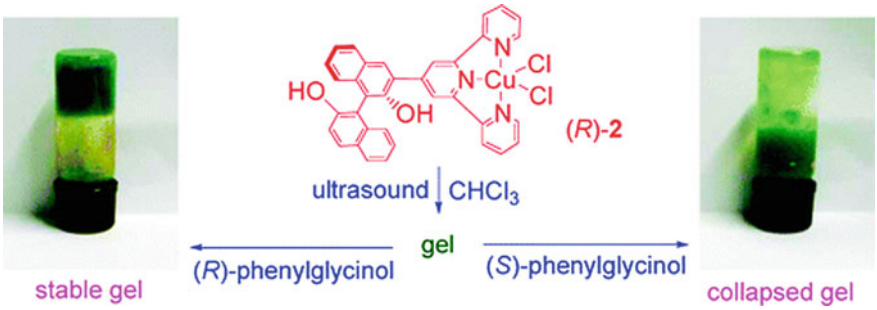

Fig. 7.49 Enantioselective response of the gel of Cu(II) chelate with BINOL derivative tpy in $CHCl_3$ toward (R)-phenylglycinol and (S)-phenylglycinol [464]

while the gel was decomposed under the same conditions at addition of (S)-phenylglycinol (Fig. 7.49).

In the case of ligand based on tpy and benzene-1,3,5-tricarboxamide central core, self-assembling molecules in the helix proceeds through triple H-bonding, and preorganized supramolecular polymers were additionally bound with Eu(III) using coordination between tpy groups and Eu(III) (Fig. 7.50) [83]. In the gel tpy fragments also functionalized as a sensitizing antenna for filling excited state $^5D_0$ Eu (III) and brought to the formation of typical Eu(III)-centered irradiation at 595, 616, 650, and 696 nm.

It is interesting that an iron complex with a tpy ligand carrying long alkyl chains gives stable gel in cyclohexane, while its ruthenium analogue does not form gel [465]. Besides, an initial chelating ligand and its iron complex give liquid crystalline phases in pure melted forms, while again the ruthenium complex does not do so.

We shall also notice metal-pincer complexes, which are efficient gelators. Thus, planar Pt(II) tpy alkynyl complexes blocked by tri(alkoxy)phenyl units carrying long chains of hydrophobic groups are good gelators for dodecane, and Pt···Pt, π-π and hydrophobic interactions take part in gelation [466, 467]. Intermolecular Pt···Pt

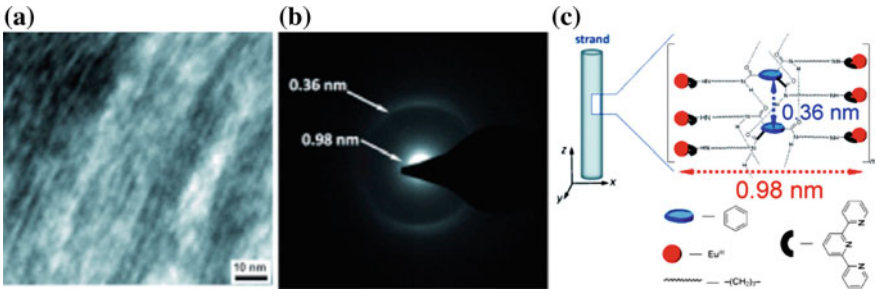

Fig. 7.50 **a** TEM image and **b** electron diffraction pattern of Eu(III) chelate gel, and c self-assembly of ligand based on tpy and benzene-1,3,5-tricarboxamide central core and Eu(III) into gel fibers

interactions and π-π interaction between Pt(II) tpy alkynyl fragments were also a driving force in the case of Pt(II) complexes of other tridentate N-donor ligands [468–471]. It is important that these Pt(II) alkynyl gels have shown sharp spectroscopic and luminescent changes at the sol-gel transition, in particular, Pt···Pt interaction (about 3.6 Å) provides a change in color and NIR emission [470].

CNC-Pd-pincer bis(imidazolylidene) complex with attached two C_{16} alkyl chains form gels in different protonic and aprotic solvents even at such low concentrations as 0.2 wt% [472]. It is interesting that larger fibers are found in xerogels of protonic solvents (for example, methanol, acetic acid), while dense networks of fine fibers are formed in aprotic solvents (for example, DMF, DMSO, DMA, and THF). In this case, π-π stacking of heteroarene fragments, Van der Waals interactions between alkyl chains, and metal-metal interactions are responsible for aggregation. This Pd-pincer bis(carbene) complex is efficient catalyst for double Michael addition of α-cyanoacetate to methyl vinyl ketone, at that DMSO-based gel has shown higher catalytic activity than that DFM-based. Analogous aromatic-linker-steroidal metallogels have unique ability to visual enantioselective separation of (R)- and (S)-BINAP [473]. In particular, after addition of (S)-BINAP, the gels sustained heating and the following cooling, while gels containing (R)-BINAP decomposed. This response can be caused by blocking intermolecular π-π stacking and metal-metal interactions after substitution of chlorine-containing BINAP ligand. It is interesting that Pt-pincer gelators gel not only a wide range of protonic and aprotic organic solvents, but also different types of Ils, such as imidazolium, pyridinium, piperidinium, pyrazolidinium and ammonium salts [474]. Gel networks formed in Ils contain straight and long cotton-like fibers (10–25 mm in length and about 500 nm in width) (Fig. 7.51). Gelation in these materials is determined by non-covalent interactions, such as π-π interaction of widened planar metal-hybrid (hetero)arene fragments, Van der Waals interactions between alkyl chains and Pd···Pd interactions. Gels are more efficient catalysts for double Michael addition of

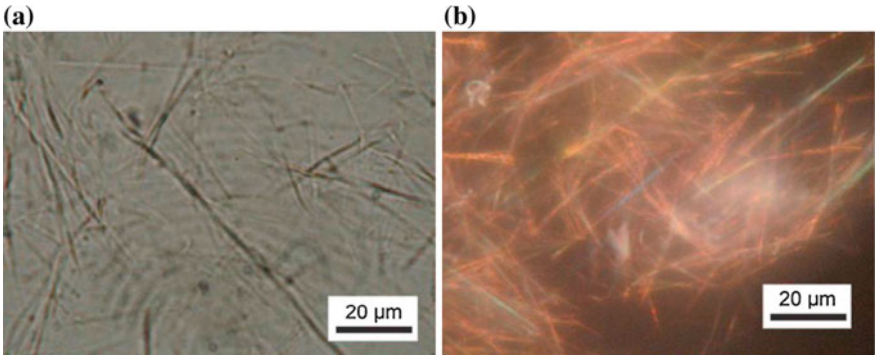

Fig. 7.51 Dark-field optical microscopic images of gels formed by Pd(II) pincer complex (5 mg mL^{-1}) with ionic liquids

α-cyanoacetate to methyl vinyl ketone as compared with respective homogeneous analogues [475].

Among metal chelates of intracomplex type, we shall notice a chiral clothespin-like *trans*-bis(salicylaldiminato) Pd(II) complex, which formed gels with a wide range of solvents without long alkyl chains or H-bond, but only after ultrasonic treatment (Fig. 7.52) [476]. For example, a complex formed by a normal solution in acetone after three second ultrasonic treatment transformed into opaque gel. Other similar complexes either with *syn*-conformation or with longer linking chains formed straightforward solutions, which were not affected by ultrasonic treatment. Ultrasonic irradiation also caused gelation of dipeptidyl Pd(II) complex using H-bonding intermolecular self-assembling [477]. Immediate and precise control over phosphorescent irradiation can be fulfilled using ultrasound-induced gelation of organic liquids with non-emissive solutions of racemic, short-linked dipalladium salicylaldimine complex (n = 5) and optically pure long-linked same chelate (n = 7). In this case increase in emission appears as a result of increase in planarity of chelate nodes in gel fibers. Dimeric homo- and heterometallic chelates first form colloid particles in solution, ultrasonic energy leads to sonocrystals; the following ultrasonic treatment disturbs certain sonocrystal samples to stimulate anisotropic growth of gel fibers (Fig. 7.53) [478]. Irradiation from gels can be controlled by changing the ultrasonic treatment time, a space length, and optical activity of complexes. In other words, structure-dependent homo- and heterochiral aggregations and ultrasonic control of aggregation morphology are key factors for emission enhancement.

We shall also notice integration of chelating HQ and multidentate hydrazinopyridine-IDA motifs in metallogels. Thus, square-planar Pt bis-Q complex functionalized via amide bonds by long chains forms gels with interesting emission behavior [479]. This chelate gels a wide range of solvents at low concentrations with fiber formation of about 50–200 nm in width and several microns in length. The absorption bands are shifted to longer wavelength in the gel (orange) as compared with the sol (yellow) according to π-stacking. A model of packing is

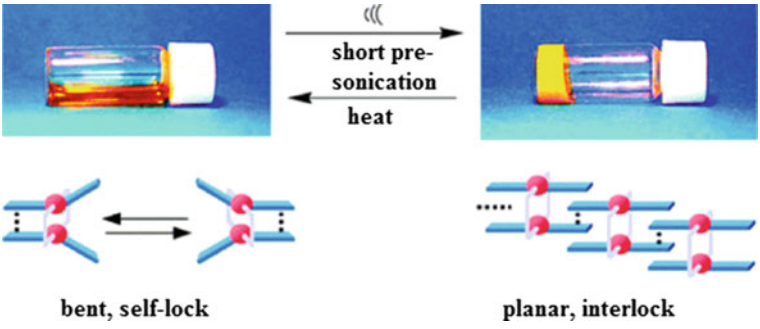

Fig. 7.52 Ultrasound-induced gelation of a chiral clothespin-like *trans*-bis(salicylaldiminato) Pd (II) complex with schematic molecular packing

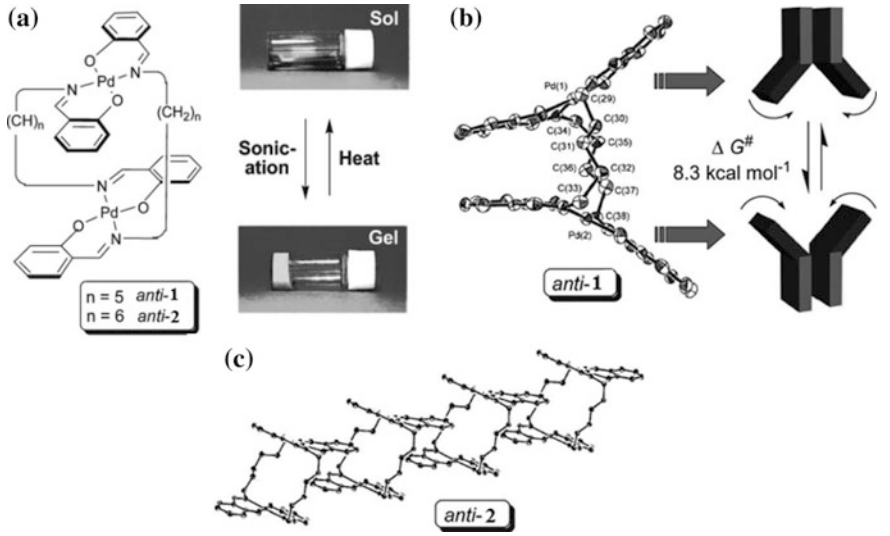

Fig. 7.53 **a** Molecular structures of anti-**1** and anti-**2** (left). Photograph showing mechano-responsive behavior of a solution of anti-**1** (right). **b** X-Ray crystal structure of anti-**1** (left) and schematic representation of the flipping motion in anti-**1** (right). **c** X-Ray solid-state structure of anti-**2**

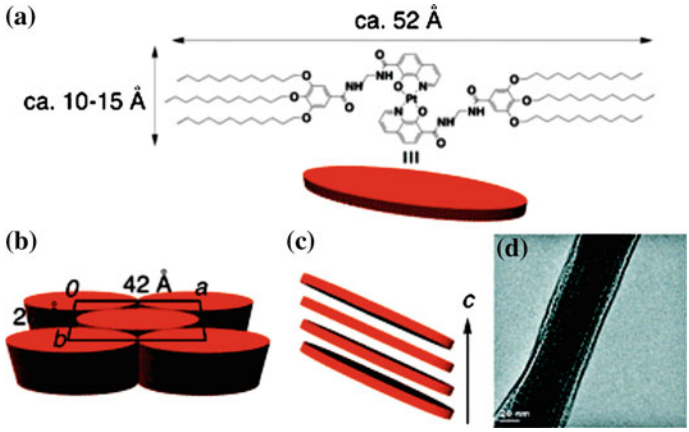

Fig. 7.54 **a** Molecular scales of Pt bis-Q chelate; **b** proposed packing model of chelate in the gel tissues; **c** tilted arrangement of chelate along the *c* axis; and **d** HR-TEM image of the chelate and *p*-xylene gel

proposed based on XRD of the gel phase with intercolumnar spacing 42 Å (Fig. 7.54). Dodecane gel of Eu complex with hydrazinopyridine-IDA nanocoordinated ligand with amide bonds and long chains has shown visible and NIR luminescence [480].

Interesting redox-responsive and enantioselective properties are found in MSPG based on Cu(II) complex of HQ-substituted L-glutamide [481]. In particular, it was shown that MSPG decomposed into sol after reduction and could be reduced after the following oxidation, besides, supramolecular chirality and morphology also changed reversibly with sol-gel transition. It should be noted that MSPG showed enantioselective recognition of chiral aromatic amino acids (Fig. 7.55). Thus, new blue emission band about 393 nm appeared when MSPG encountered with L-aromatic amino acids, while no new blue emission band was observed for respective D-aromatic amino acids. At that, such enantioselectivity was only observed in the gel state and such phenomenon was not observed in solution.

Also planar Cu(II)-β-diketonates functionalized with long chains that gel cyclohexane due to Van der Waals and other non-covalent interactions are interesting as gelators [418, 482]. In particular, there is a considerable decrease in hyperfine coupling at transition from isolated complexes to gel-like state, at that a signal from free complexes is regarded as a shoulder on «aggregated» signal thus showing coexistence of free and aggregated complexes.

Undoubtedly, macrocyclic complexes (M-Pp and M-Pc) are also efficient gelators. One of directions of enhancement of gelating ability of M-Pp is axial coordination of bridging ligands [483, 484]. Thus, for example, Zn-Pp itself does not gel benzene or toluene, however, addition of piperazine as axial ligand actually caused gelation. Triethoxysilyl-functionalized free base Pp could gel some solvents, while its copper analogue gels wider range of solvents at lower concentrations [484, 485]. It is important that in the first case sheet-like structures have formed, while in the second case fiber structures have formed (Fig. 7.56).

In another example, Cu-Pp formed flat ribbons, while free base Pp and Ni-Pp gave helically bent ribbons [486]. It should be noted that it is possible to adjust a helix step by the formation of mixed-Pp ribbons with different Cu/Ni ratios. An interesting observation is made in the case of tri-substituted Zn-Pp, which has three long hydrocarbon chains linked with the Pp core through ester bonds and one group of free acid [487, 488]. Based on combined experimental studies a model of

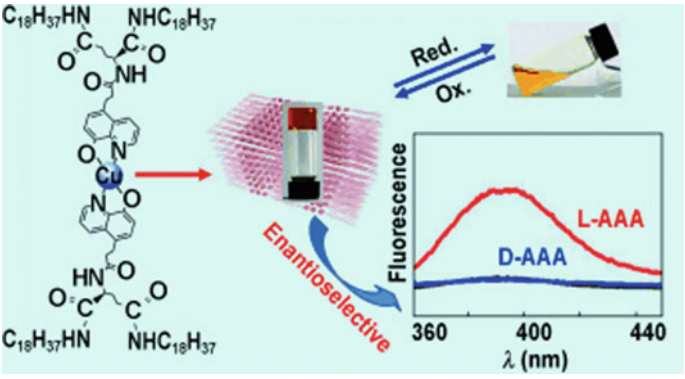

Fig. 7.55 MSPG having enantioselective recognition of chiral aromatic amino acids

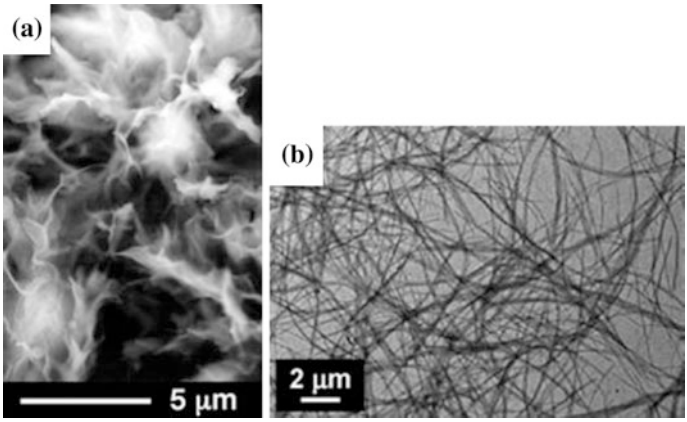

Fig. 7.56 **a** SEM image of the xerogel of self-assembled free base Pp in benzene and **b** TEM image of the xerogel prepared from the anisole gel of Cu-Pp

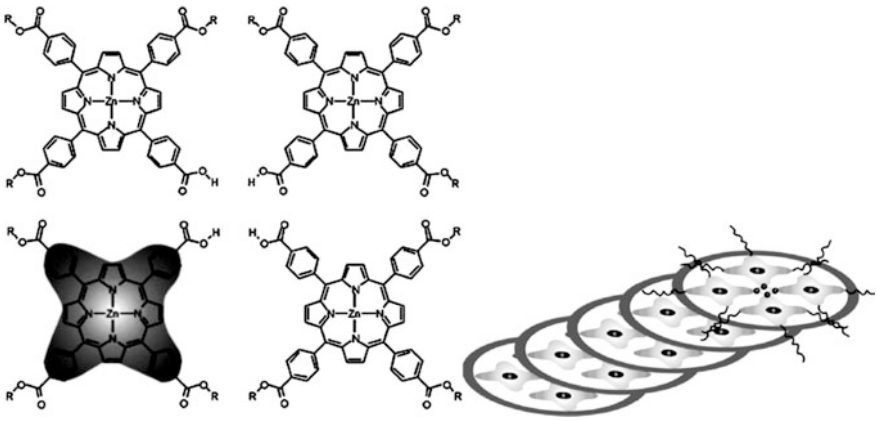

Fig. 7.57 Tetramer association of trimester Zn-Pp and their off-set stacking to produce fibers

packing regime is proposed consisting of planar tetramers with carboxylic acids positioned in centers in the off-set stacking (Fig. 7.57) [488].

Hydrogels are obtained from Fe(III)-tetraphenyl-Pp-functionalized 4-armed PEO films, in which water plays a role of cross-linking agent and swelling agent [489]. It is important that depending on pH, hydrogels present either characteristic of a chemical network or a dynamic transient network, at that intriguing behavior is completely reversible.

Two interesting observations are made during studying some Zn-Pp-cholesterol conjugates [490]. First, only molecules with two or four methylene spacers between Pp and cholesterol groups gave gels, while those with three or five were unable to gel the same solvents. Probably, even spacers give extended molecular conformations

suitable for packing cholesterol groups, while odd spacers give folded conformations. Secondly, addition of C_{60} reinforced the obtained gels; in particular, T_{gel} is abruptly increased (80 °C against 30 °C for initial Zn-Pp) up to Zn-Pp:C_{60} ratio 2:1 corresponding to sandwich-complexes with C_{60}.

We shall also notice M-Pc functionalized by chiral diols, which give fiber assemblies from aqueous solutions [491]. This self-assembling is a result of π-π interaction between Pc rings and H-bonding between diol units. It is important that the rings become closely linked as polarity (water content) of a solvent increases, and fiber aggregates and viscous solutions are observed only for Cu complex, but not for Zn analogue.

The host-guest interactions with participation of LMC are also used for MSPG production. Thus, MSPG is developed, which demonstrates LCST based on back-to-back twin bowls of 3D symmetric tri(spiroborate)-cyclophanes [492]. As compared with standard calix [4] arene (about 12.5–6 Å), cyclophane has wider cavities (about 17–11 Å) on both sides of a symmetry plane, which facilitates its linking with big guest molecules through π-π-stacking and electrostatic interactions. The studies have shown that a host can interactively encapsulate guest molecules $[Ir(tpy)_2](PF_6)_3$, which brings to MSP formation (Fig. 7.58a). It is interesting that thermal reversibility behavior of gelation is noticed at heating of a host solution (10 mM) and a guest solution (10 mmol) in *N*,*N*,*N*′,*N*′,*N*″,*N*″-hexamethylphosphor acid triamide (HMPA) above LCST, as a result phase transition takes place with organogel formation (Fig. 7.58b). Upon cooling to environmental temperature, the gel converted to sol during 15 min.

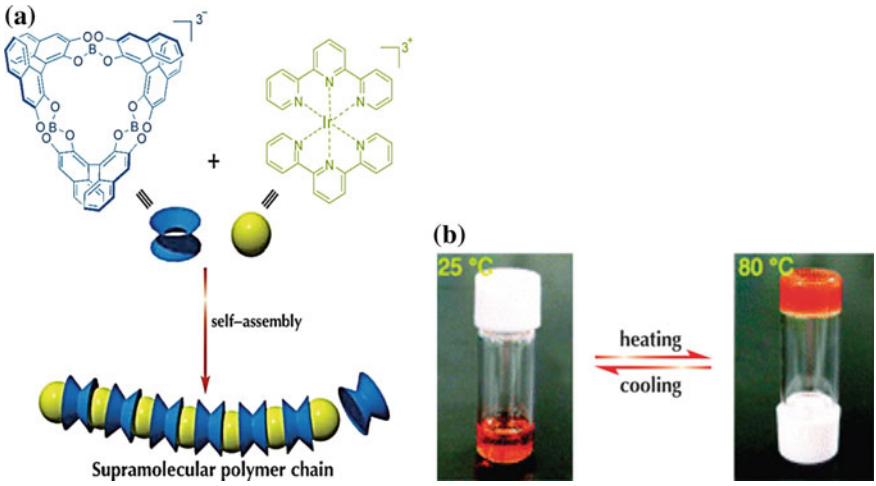

Fig. 7.58 **a** Cartoon representation of the formation of MSPG by iterative clathration of twin-bowl-shaped cyclophane with guest molecule; **b** illustration of the thermal reversibility of the resultant MSPG

However, the great majority of studies of MSPGs consider using M–L coordination as a main driving force. As a structural feature of MSPGs, these M–L bonds should present either in a polymer chain or as a link between covalent-bound units. Usually a MSPG is a combination of a metal ion and bridging organic ligands, which form multidimensional networks through capturing a solvent as a result of non-covalent interactions. As physical properties of these gels are similar to ordinary macromolecular polymer gels, MSPGs are often entirely reversible and can be assembled and disassembled in presence of additional energy (heat, ultrasound, shaking). Besides, as compared with gels obtained from purely organic gelators, metal ions included in fibrillar networks can give MSPGs with additional functions. Using fine tuning a system by choosing a metal ion and ligand, and directed self-assembling with external stimuli, rational synthesis of practically important systems is possible [248].

Thus, reversible coordination networks are obtained by combination of diphenylphosphinite telechelic poly-THF with Rh(I) or Ir(I) ions, which can coordinate four phosphoric ligands [493]. Oppositely to Rh(I)-based gels, in which gelation goes almost instantly, formation of Ir(I) gels needs about 30 min. Two obtained gels show very different mechanical properties, in particular, Ir(I) gels exhibit higher elasticity modulus than Rh(I) gels. This is associated with different linking kinetics of these two metal ions upon transition from the second row of d-block to third, since Ir(I) phosphinite complexes show far lower exchange rates than Rh(I) phosphinite complexes. Sonification has caused gel liquefaction, and when stored, the gel-fraction increased again with the rate determined by kinetics of M–L complexation. It is shown that ultrasonic treatment brings to ligand exchange, leading to decrease in a fraction of metal centers in active cross-linkings, and therefore, to decreased gel-fraction.

Viscous-elastic behavior and responsiveness to sonification of analogues MSPGs from ditopic phosphine-terminal poly-THF oligomers and Pd(II) chloride are studied [494, 495]. In this case collapse of gas bubbles formed during ultrasonic treatment generates shearing forces, which can cause damage in M–L bonds and thus bring to a chain termination and appearance of vacant coordination sites. When tangential stress is removed, MSPGs are reformed.

We shall also notice using bpy-chelating fragments in MSPG synthesis. Thus, polymer linear poly(*p*-dioxanones) carrying bpy units are cross-linked with Fe(II) ions with the formation of a permanent network, while crystallizing *p*-dioxanone segments serve as thermal trigger [496]. Another example is hydrogel formation from polyoxazoline containing pendant bpy blocks with many different transition metal ions [497]. Addition of Co(III), Fe(II), Ni(II) or Ru(II) ions has brought to non-covalent cross-linking and swelling bpy-branched polymers, however, stable hydrogels at room temperature are obtained only by treatment with Fe(II) and Ru (II) salts. Inertness and stability constants of bpy-metal complexes and, respectively, MSPG stability are determined by environmental conditions, such as pH, redox state, temperature and a solvent. Thus, thermal stimulus brings to acceleration of ligand exchange causing thermal cleavage of hydrogels, and swelling degree and stability of gels in water depend on bpy group content in a polymer. Bent-shaped

ligand monomers containing dendritic aliphatic side chains of different lengths form a complex with Ag(I) ions through the self-assembling process, which depends on nature of a side chain and counter-ions [498, 499]. In this case responsiveness is a result of a change in a secondary structure of a coordination chain, for example, of a transition from helical to zigzag-shaped chain, when a change in conformation of hydrophilic side groups is initiated by external stimulus or counter-ion size changes.

Extensive studies are concerned with tpy-chelating ligands for MSPG production. Thus, when transition metal ions are added, concentrated aqueous solutions of side chain of a tpy-functionalized poly (2-(dimethylamino) ethyl methacrylate) transform into MSPGs [500]. The PSM of poly(pentafluoride-St) obtained by selective substitution by tpy-functionalized synthones [501] is presented as universal method for MSPG preparation, which were then transformed into gel with addition of Fe(II) ions due to metallosupramolecular linking.

Apart from linear polymers, multiarmed star-like polymers containing tpy fragments have shown their applicability in preparation of metallosupramolecular networks [194] even in combination with ditopic ligands. Thus, four-armed PEG with tpy ends synthesized by post-modification of commercial PEG is used for preparation of MSPGs with addition of Fe(II) ions [502]. The obtained MSPGs have shown chemo-responsiveness, however, they were destroyed by addition of ammonia as a competitive ligand. MSPs based on 8-armed PEG partly substituted by tpy end groups and transition metal ions Ni(II), Fe(II), Co(II), and Zn(II) form nanoparticles under diluted conditions and gels at higher concentrations [503]. In particular, at polymer concentrations higher than 5 wt% cross-linking with addition of transition metals provides hydrogels, at that elastic hydrogels are formed with Ni (II), Fe(II), and Co(II), while Zn(II) gels are relatively viscous. It is important that only Zn(II) gels show thermos-reversed sol-gel transition at the temperature 25 °C independent on a polymer concentration. It is interesting to notice that this observation correlates with the results of study of MSPGs based on PMMA copolymers with tpy units in the side chains [504].

A simple strategy of incorporation of self-assembling behavior of amphiphilic block-copolymers and metal-tpy complexes in hierarchical levels is developed [402]. The first level of self-assembling was reached due to dissolution of tpy terminal-functionalized PS-*b*-poly (*tert*-butyl acrylate) diblock-copolymers in selective solvent for *tert*-butyl acrylate block. As a result, micelles were obtained consisting of PS core and poly (*tert*-butyl acrylate) coronal chains carrying a tpy ligand on their end. The second level is initiated by addition of metal ions [505]. It is important that intra-micellar chelations bring to exclusively flower-like micelles in diluted solutions [282], while micellar MSPG are formed in concentrated solution. At that, by varying conditions (temperature and a co-solvent presence) rod-shaped or spherical micelles with hard or soft cores are obtained [506]. Studies of such amphiphilic copolymer as poly (triethyleneglycol methyl ether methacrylate)-*b*-PS with tpy groups randomly distributed inside a water-soluble block [507] have shown the same results. Micelles of this copolymer form gels after addition of Ni(II) ions at far lower concentration than that of a respective homopolymer, which points to the effect of hydrophobic PS block on critical concentration of gelation.

We shall notice a tripodal tpy ligand, which forms helical 1D supramolecular polymers/gels in solution mediated through H-bonds and π-π interactions. Additional cross-linking these gels into 3D MSPG with a range of metal ions such as Fe(II), Ni(II), Cu(II), Zn(II), and Ru(III) brings to formation of color or colorless gels. Fiber-like morphology of these gels is found, in which metal ions work as «supramolecular glue» linking stands together in large architectures with higher ordering [508].

MSPGs are obtained using a chelating polymer containing a tridentate btp ligand block and transition metal ions and/or lanthanide ions. It is interesting that gelation and gel properties, for example, swelling, can be adjusted using thorough choice of metal ions and their combinations, solvents, concentrations, etc. [509]. Self-assembling direction with participation of polytopic chelating ligands can be regulated by integration of respective substituents in chelating fragments. Thus, interaction of btp trimethyl ether with Eu(III) has shown formation of luminescent 1:3 complex, which has been studied in solution and solid state, while btp tricarboxylic acid forms deep red luminescent hydrogel [510]. It is established that repeated btp unit takes predominantly *anti-anti* conformation and, therefore, extended heteroaromatic polymer strands take helical conformation (Fig. 7.59). Addition of Fe(II), Zn(II), and Eu(II) metal ions has brought to instant gelation as a result of coordination cross-linking of the polymer chains. In other words, in btp ligand based MSPG the bridging metal complexes serve not only as cross-linking points, but provide different functions potentially useful for design of new magnetic or emitting materials [152, 153].

It should be noted poly (*n*-butyl acrylate-*co*-MMA) copolymers carrying Mebip side groups (varied in the range 3.2–7.6%), which form MSPG using the metal salt, Zn trifluoromethanesulfonate [511]. Development of massif of anion sensors based on MSPGs, which can precisely detect CN^-, SCN^-, S^{2-} and I^- in water is interesting. This massif of sensors is based on new design approach called «competitive coordination control AIE mode» for development of anion-responsive MSPG,

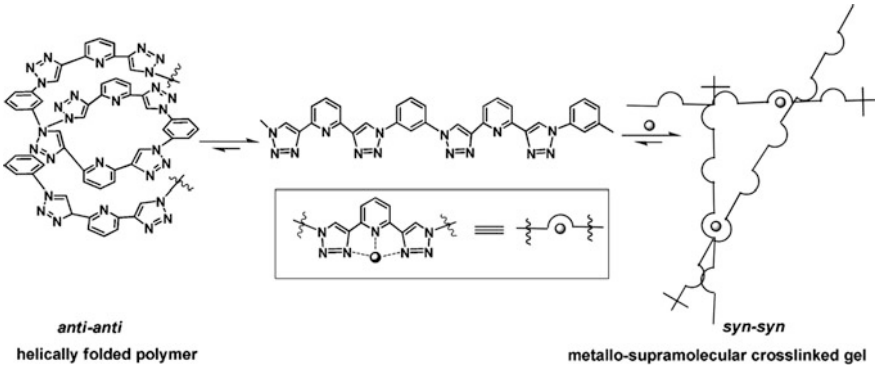

Fig. 7.59 Schematic representation of metal chain-extended polymers based on BPT chelating units

which need only one synthesized gelator [512]. Rational integration of Ca(II) and Fe(III) into supramolecular gel resulted in production of bimetallic MSPG, which can reversibly «switch on» its fluorescence upon detection of $H_2PO_4^-$ with a certain selectiveness through competitive coordination of Ca(II) and Fe(III) with gelators and $H_2PO_4^-$ [513]. Therefore, bimetallic MSPG can work as $H_2PO_4^-$ test-set and can be used in rerecording safe imaging (display) materials.

We shall notice MSPG formation using P4VP and ditopic metal chelate cross-linkings [78, 514]. Thus, MSPG were obtained during addition of bis-Pd(II)-pincer complex with methyl substituents or more thermodynamically and kinetically stable Pt(II) analogues to P4VP in DMSO. Substitution of *N*-methyl substituent with ethyl has no effect on thermodynamics of N–Pd(II) interaction; however, exchange rate of ligand decreases by about two orders of magnitude. Reversible gel-sol transition can be controlled by tuning pH of a system or using competitive additives, such as dimethylaminopyridine or Cl^--ions, which can displace Py in the main polymer chain [275]. Mixing different cross-linkers, i.e. bifunctional Pd(II) or Pt(II)-pincer complexes with P4VP has given systems with strong to weak gel transition, rather than a distinct gel-sol shift [276]. When concentration of each cross-linker was over the critical percolation threshold, kinetically slow cross-linker, i.e. Pt(II)-containing metallopincers determined properties of a gel. When sufficient amount of competitive cross-linker was added to drop concentration of «active» cross-linking unit below their individual percolation thresholds, but still providing the total number of active cross-linkers being above the percolation threshold, a gel is formed, whose properties are controlled by kinetically rapid cross-linker, Pd(II)-containing metallopincer.

The concept is developed [77, 114, 115, 129, 196, 223, 515–517] of MSPGs building based on chelation of a ditopic ligand monomer with combination of lanthanide(III) ions and transition metal ions. Since ionic radii of lanthanide metals are far bigger than those of transition metals, they can form complexes with three tridentate ligands, which brings to formation of 3:1 M–L complexes, and, therefore, can form strong dynamic coordination networks. In this case, gels are formed by mixing telechelic chelating ligand with combination of lanthanide (cross-linker) and transition (chain extender) metal ions, respectively. Taking into account that lanthanides are weaker binding metal ions, as compared to transition metal ions, metal complexes based on lanthanides can be successfully treated as switching branching points, which can give response with temperature or load changing. Addition of lanthanide ions (<5 mol% per ligand) followed by transition metal ions addition (>95 mol% per ligand) to telechelic chelating monomer solution brings to MSPG production. Bis-tpy linking ligand consisting of two O-Mebip ligands with penta (ethylene glycol) pendant core to each end is used as a telechelic chelating ligand. Under respective conditions transition metal ions such as Co(II) or Zn(II) can bind two O-Mebip ligands and, therefore, act as a chain extender for generation of linear polymers. Lanthanide ions, for example, La(III), Eu(III) can link one or three O-Mebip ligands depending on a counter-ion nature, and, therefore, potentially be the chain growth stopper or a trifunctional cross-linker. MSPG formation can be

easily achieved upon addition of transition metal ions and lanthanide ions to ditopic ligand in appropriate solvent. Since lanthanide complexes are less stable, branching points are open when a gel is heated or if mechanical stress is applied with shaking, forcing gel to liquefy. After cooling or removal of mechanical load, gel immobility is reformed. It is important that Eu(III)-based gels show typical red luminescence of complex Eu(III) ion, which is sensitized by energy transfer from ligand to ion. If Eu (III) complex is open under action of heat or mechanical load, luminescence is changed to blue, which is associated with ligand-centered emission.

Luminescent MSP is developed [518], which is surprisingly subjected to sol-gel transition with rise in temperature. In this approach, a linear conjugated polymer material is synthesized into DMSO through condensation of a linear diamine and dialdehyde subcomponents around Cu(I) templates in presence of bulk trioctylphosphine ancillary ligands. This polymer solution undergoes sol-gel transition with increase in temperature, contrary to behavior of most MSPGs, which do so on cooling. Development of cross-linkings by copper chelation was accompanied by formation of sterically overloaded copper-trioctylphosphine complexes in equilibrium with free phosphine ligands. Since these MSPGs undergo sol-gel transition with temperature, due to formation of active cross-linkings between linear polymer chains, emission intensity and color are easily adjusted depending on temperature. It is interesting that luminescence changed color from orange to green when a sample was heated, and turned back to orange when a sample was left to cool to room temperature.

MSPGs based on catechin-modified four-armed star-like PEG and Fe(III) ions were obtained [519]. Since stoichiometry of pyrocatechin-Fe(III) complexes is determined by protonation degree of pyrocatechin hydroxyls, control over intermolecular cross-linking is possible only via pH. Besides, possible dissolution of cross-linked tris-complex gel using treatment by strong chelating EDTA agent is shown.

Interesting innovated MSPG is developed based on tritopic ligand having a bis-tpy cyclam block and divalent metal ions such as Co(II) and Ni(II) (Scheme 7.17) [520–522]. A ligand metalation in DMF with $Co(ClO_4)_2$ in molar ratio 1:1 brings to red solution, which points to formation of $(tpy)_2Co(II)$ derivative, in which cyclam block remains metal-free. Addition of another equivalent $Co(ClO_4)_2$ to the previous solution brings to formation of a cyclam-Co(II) block and, respectively, to MSPG formation. When ligand metalation is carried out in DMF with addition of two molar equivalents of Co(II), MSPG is formed spontaneously at concentrations below 1.0 wt%. In the gels, respective network includes original fibers ($R \approx 35$ Å), bundles of these fibers, and a fraction of limited sized aggregates (rods with the ratio $f \approx 3$–5). It is found that distribution of the latter structural components is sensitive to character of metal ions. These MSPG show a range of original constructing features and easy control over developed structures in gels, tuning their thermodynamic parameters.

Achiral benzo-21-crown-7-substituted bis(carbamide) low molecular weight gelator is hierarchically self-assembled in helical fibrils, which then transform into

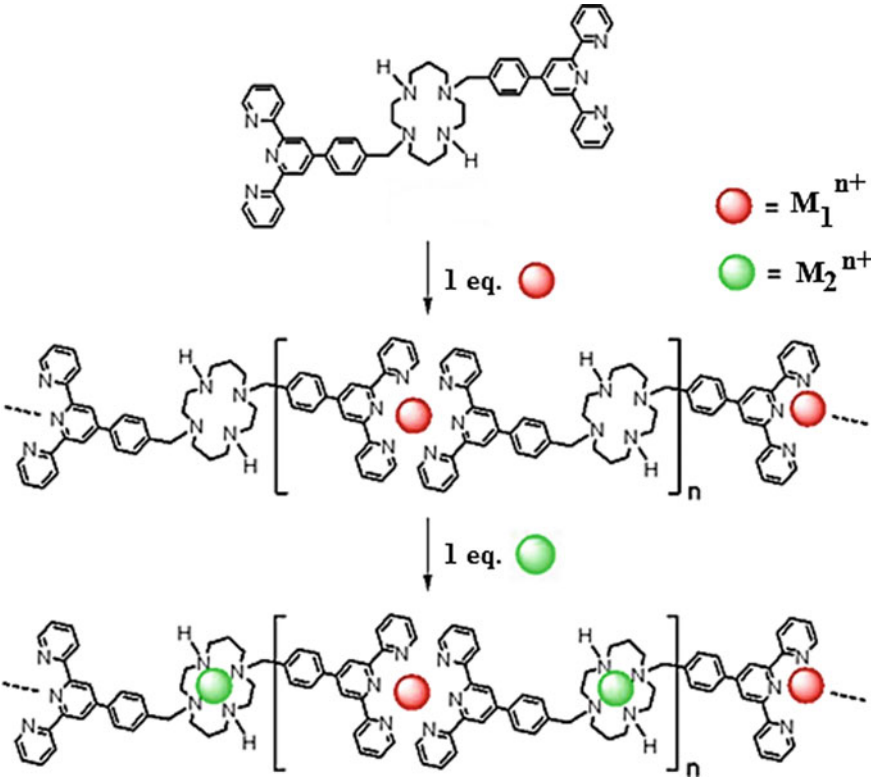

Scheme 7.17 Scheme of the formation of MSP by self-assembly of tritopic ligand, having bis-tpy cyclam unit, and $Co(ClO_4)_2$

bundles and then form stable gel in acetonitrile [523]. K(I) binding to crown ethers causes gel-sol transition, and addition of cryptand, which scavenges K(I) ions, can make this process reversed. Based on this gelator and chemical stimulus, a range of different systems can be developed, which behave how logical gates. Thus, depending on choice of these components OR, AND, XOR, NOT, NOR, XNOR, and INHIBIT elements were realized. In some cases a type of logical element is determined by concentration of input signal, so that even more complicated reaction with gel in direction of two input signals would be achieved.

It is worth noticing using advantage of cationic cobaltocenium as a key building block for switching organogels to hydrogels using highly efficient ion exchange [524]. It is interesting that using unique complexing ability, cobaltocenium fragments provide a robust soft substrate for utilization of antibiotics from water. Besides, a substantial polyelectrolyte nature of MSPG provides to kill bacteria with multiple drug stability.

7.11 Self-assembled Metallosupramolecular Monolayers

Self-assembled monolayers are ordered molecular assemblies spontaneously are formed upon adsorption of adsorbate on a solid surface and organized in more or less large ordered domains [525–529]. SAMs provide a convenient way for formation of surfaces with specific chemical functionalities. The main parameters providing control of molecule positions on surface are stoichiometry of binding, stacking density, binding dynamics, bond strength, order, and reversibility. Covalent immobilization of molecules does not suggest a convenient universality and flexibility for most of these parameters, while supramolecular interactions provide control over these criteria. Really, the self-assembling process of nanometer ordered structures makes it possible to control film composition and thickness with accuracy up to fractions of nanometer. To prepare SAMs, amphiphilic molecules are actively used, which are bound with one functional group to surface, while another functional group is responsible for interaction with other adsorbed molecules. During SAM formation usually a substrate is coated with low-concentrated solution of respective molecules, which through covalent bonds form a self-assembled monolayer, and excess molecules are removed by washing a sample in solvent. Using LbL technique, two or more components are deposited consequently and repeatedly to elongation a monolayer in a controlled way [530–533]. Using M–L interactions in LbL technique provides design and production of new, highly ordered, highly oriented, universal and robust 2D functional multilayered thin films and even 3D nanoarchitectures based on MSP.

Stepwise building multilayered structures using M–L interactions (Fig. 7.60a) has considerable synthetic value, since coordination bonds propose a good balance between hardness and reversibility [534]. Metallosupramolecular structure has an anchor layer consisting of SAM, chemisorbed to surface. Then an anchor ligand follows, which includes chelating fragments. Metal ions play a role of a cross-linking for the following layer of ligands, which has a chelation center of a metal ion. Finally, on the top of this layer alternately deposit the next layer of metal ions and chelating ligands to increase the film thickness. Depending on whether a ligand includes two or three chelating fragments, linear or branched structures can be obtained, respectively. It is important that M–L interactions are subjected to spontaneous and quantitative conjugation between metal sources and ligand molecules, which, in the end, brings to defect-free self-assembled multilayers. The role played by M–L interactions is not confined only to linking of adjusted layers. The resulting M–L supramolecular motifs can give practically important functions to final products, such as redox properties, magnetism, emission, catalytic activity and intermetallic interactions.

To obtain supramolecular SAMs based on M–L interactions the most widely used is the method of solution-based LbL growth. It provides achievement of exactly defined surfaces with different functionalities by pre-functionalization of different substrates (in particular, Au, Si, SiO_2, ITO glass, etc.), for example, with thiol or silicon-organic molecules to start SAM development containing either

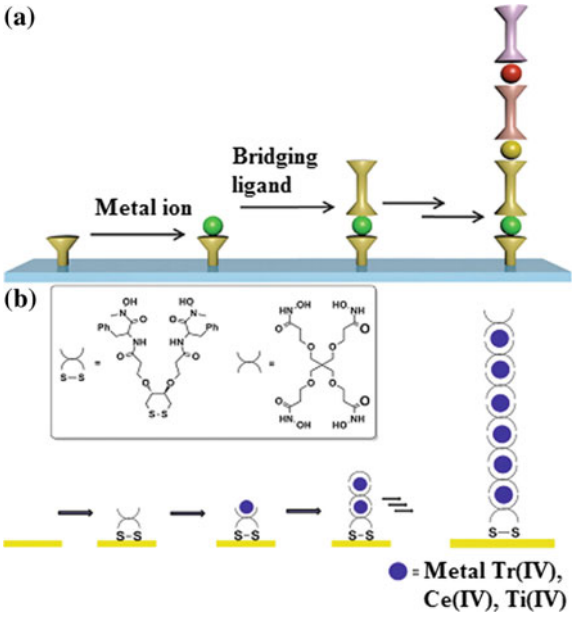

Fig. 7.60 **a** Stepwise coordination process on a substrate surface. **b** Schematic presentation of the molecules used for multilayer construction and an idealized structure of the M–L-based multilayers

monofunctional OH-, COOH- or N-end groups or chelating fragments. Then surfaces are functionalized with these organic spacers, which provide several available functionalities and long-range 2D order, direct orientation, nucleation, structure, stability, and quality of additionally deposited thin films.

As an example, we shall notice directed self-assembling bishydroxamate-based metal chelate multilayers on Au using LbL approach (Fig. 7.60b) [535]. In this case supramolecular M–L interactions bring to higher thickness, increased roughness, higher electric resistance, and better rigidity of surface. In the same way branched metal chelate multilayer films are obtained on Au surface functionalized with SAM bishydroxamate disulfide molecules by alternate deposition of organic ligand having three bis-hydroxamate arms and a metal ion such as Zr(IV), Ce(IV), and Ti (IV) [536, 537]. However, multilayer assembling is usually very slow process, which, depending on a ligand type, metal ions and used solvent, can take a long time, which is inappropriate for practical commercial applications. In this connection more rapid method is developed [538] for assembling metal chelate M–L-based multilayers on functionalized surfaces called accelerated self-assembling procedure (ASAP). In this method rapid binding organic layers of a ligand proceeds for a few minutes: a small volume of an organic ligand solution is spread on a surface modified by a metal-containing layer and is evaporated under conditions of natural convection, as a result a surface is covered by excess of organic ligand. Further extensive rinsing in pure solvents brings to removal of weakly adsorbed molecules from surface leaving only new metal chelate adsorbed layer.

Non-covalent M–L coordination is developed for assembling supramolecular photocurrent-generating systems [539]. In this case, SAMs are built from molecules

consisting of disulfide alkyl group covalently bound with 12-residual helical peptide and capped with alanine residual containing pyrene chromophore. Consequent deposition of three or more components has brought to pyrene-containing multilayer based on Cu(II)-, Co(II)-, and Fe(III)-chelation (Fig. 7.61a–c). These systems on Au surface have shown high stability and high current generation in presence of methyl viologen and triethanolamine for cathode and anode currents, respectively. It occurs that the highest cathode photocurrent is observed in Cu(II) system, and Fe(III) chelate system has shown the highest anode current.

It is interesting to study behavior of a charge trap in heterometallic chelate SAMs (Fig. 7.61d) [540]. In this case a change in sequence of self-assembling layers of two isostructural bpy-based metal chelates brings to materials with electrochemical properties, which depend on assembling order. Thus, Os chelate layer formed on 8-nm thick Ru chelate layer has shown a sharp peak of catalytic oxidation without a visible reduction wave, while a Ru chelate layer has given a reversible redox wave. And on the contrary, a Ru chelate layer based on thick Os chelate layer has shown a sharp reduction peak and strained oxidation wave, whereas a reversible redox pair of Os chelate layer appeared. This series of phenomena can be explained by electron transfer between the upper layer and the electrode through the bottom layer.

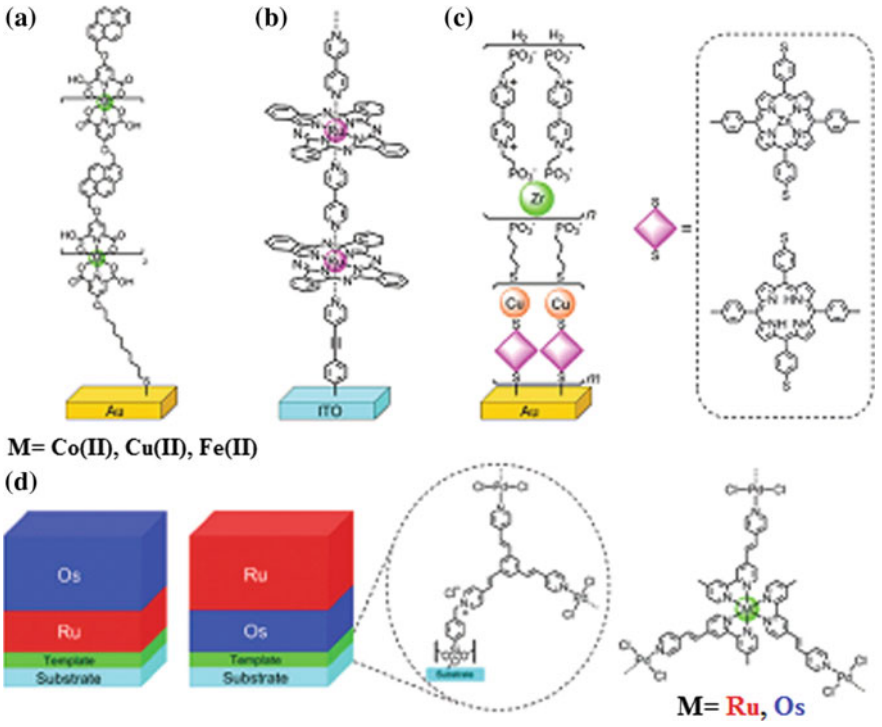

Fig. 7.61 **a–c** Examples of metal complex multilayers for photocurrent generation. **d** Example of a redox film showing charge trapping

SAMs were obtained by alternating the deposition of $PdCl_2$ and iron bpy complexes 1–4 (Fig. 7.62) from solution on a pyridine-terminated monolayer. This monolayer is covalently bound to the surfaces of ITO, quartz, and silicon substrates through a chlorobenzyl-functionalized coupling layer. SAMs are used for production of highly efficient electrochromic assemblies, which display practical combination of low voltage work and efficient electrochromic switching, and also durable thermal and redox stability (1.12×10^5 cycles) [541]. These molecular assemblies can be integrated into solid-state configuration; at that SAM molecular structure correlates with growth and principle of materials action.

Undoubtedly, most studies of SAM are carried out with tpy ligands. Thus, M–L assembling is performed on Au for preparation of redox-active mono- and polymetallic systems with participation of Co, Cr, and Os chelates with thiol-modified tpy ligand 4′-(5-mercaptopentyl)-tpy and tetrapyridylpyrazine (Fig. 7.63) [542]. It occurs that free ligand, as well as tpy-containing metal chelates are strongly adsorbed on surface of Au electrodes, at that in the case of metal chelates they retain their redox-active responses at potentials very close to non-adsorbed analogues in homogeneous solution.

The similar approach is used for building polymetallic complexes by repeated deposition of Fe(II) and/or Co(II/III) ions with azobenzene-bridging bis-tpy ligand on tpy-terminal SAM on Au [543]. It is interesting that purposed formation of desired number of polymer units, for example, 47-dimensional $Co(tpy)_2$ structures and desired sequence of Co-Fe heterometallic structures in a polymer chain, for example, 10-dimensional $Co(tpy)_2$ plus 5-dimensional $Fe(tpy)_2$ is possible.

We shall notice use of click chemistry for covalent binding acetylene-functionalized Fe(II) bis-tpy chelate on azide-terminal SAM [544]. Using decomplexation of formed supramolecular chelate, ligand-modified monolayer can be obtained, which is then used for additional chelation reactions, leading to reversible functionalization of substrates (Scheme 7.18). It is important that right choice of coordinating ions of transition metals provides tuning binding force and physicochemical properties of formed chelates, and therefore, design of surface properties.

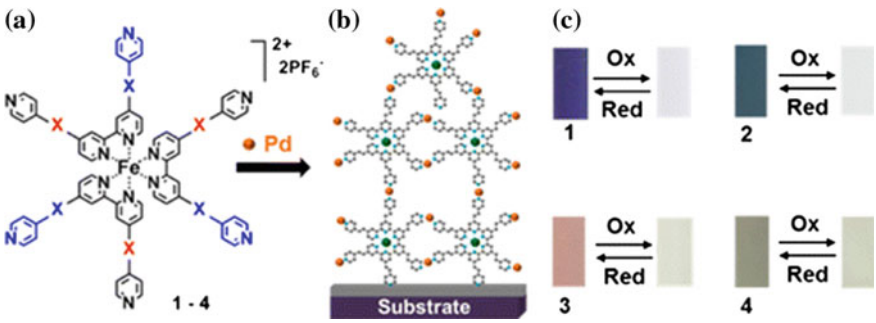

Fig. 7.62 Molecular structures of polypyridyl complexes **1–4** (**a**) and SAMs (**b**). Electrochromic switching of the SAMs (**c**)

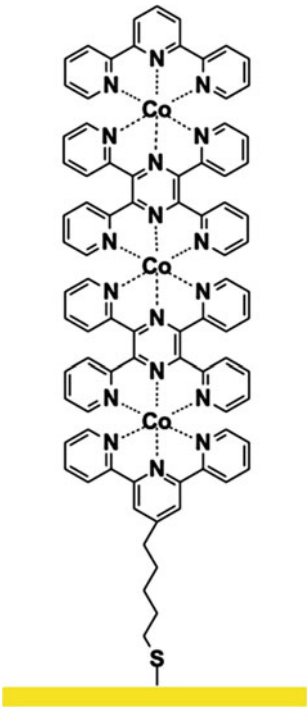

Fig. 7.63 Assembly scheme for the construction of tpy-metal complex layer on Au

Using chelation of Pt(II) ions with asymmetric ligand containing tpy and pyridyl residues, luminescent MSP is synthesized, which has characteristic dipole moment [545]. A polymer was specifically fixed on Au electrodes to obtain two types of films (films 1 and 2), in which polymer chains are positioned with regard to their dipoles in opposite directions (Fig. 7.64). It occurs that the film 1 has higher conductivity in positive field displacement with an average rectification coefficient 20, while the film 2 has higher conductivity in the negative area displacement with an average rectification coefficient factor 18.

1,3-Butadiyne-cross-linked diruthenium chelate is fixed on Au electrode surface in horizontal position for SAMs formation showing multiple irreversible redox behaviors on the electrode surface (Fig. 7.65) [546]. It is interesting to notice that types of diruthenium with different oxidation degrees, in particular, Ru_2(II, III) states, which are non-stable and cannot be isolated from solution, can be detected in situ using IR spectroscopy.

It should be especially noted that linear and branched bis(tpy) metal chelates based SAMs relate to such interesting class of materials as molecular wires [547, 548]. These systems have a clear and distinctive electronic functionalities, intra-wire redox conductivity and excellent long-range electron transfer capacity [532]. It is important that these systems are built with a wide range of tpy-containing chelating ligands. Wires based on bis(tpy) metal chelates consist of four components: surface-linked tpy ligand (A series), metal ions, bridging tpy

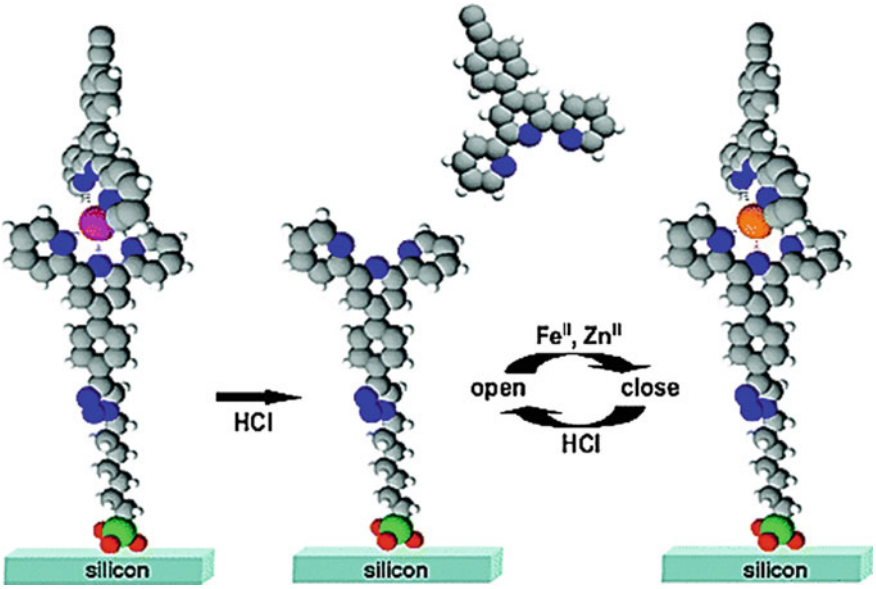

Scheme 7.18 Scheme of reversible functionalization of substrates

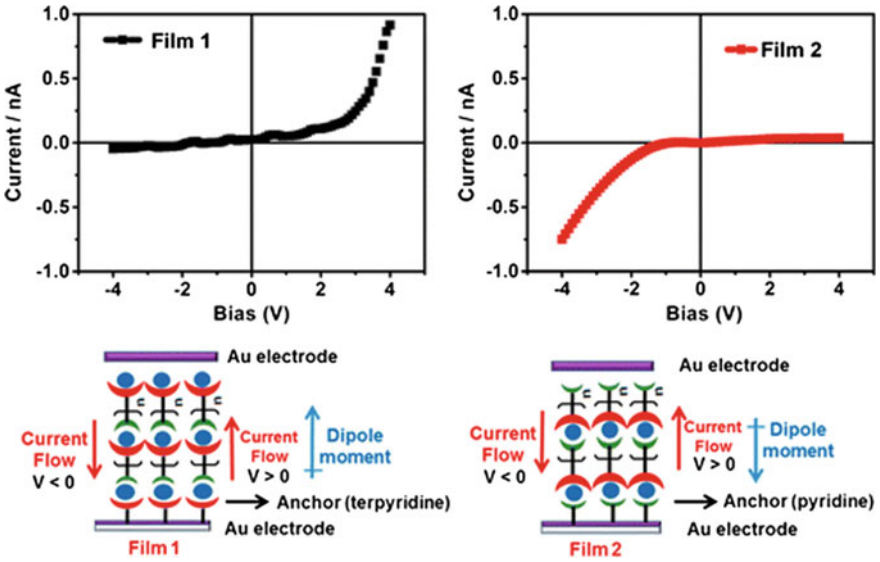

Fig. 7.64 Production of two types of films (films 1 and 2), in which polymer chains are positioned with regard to their dipoles in opposite directions

ligand (series L) and redox-active terminal tpy ligand (series T) (Fig. 7.66). After modification of the electrode surface with, for example, sulfide or hydroxylation

Fig. 7.65 1,3-Butadiyne-cross-linked diruthenium chelate fixed on Au electrode surface

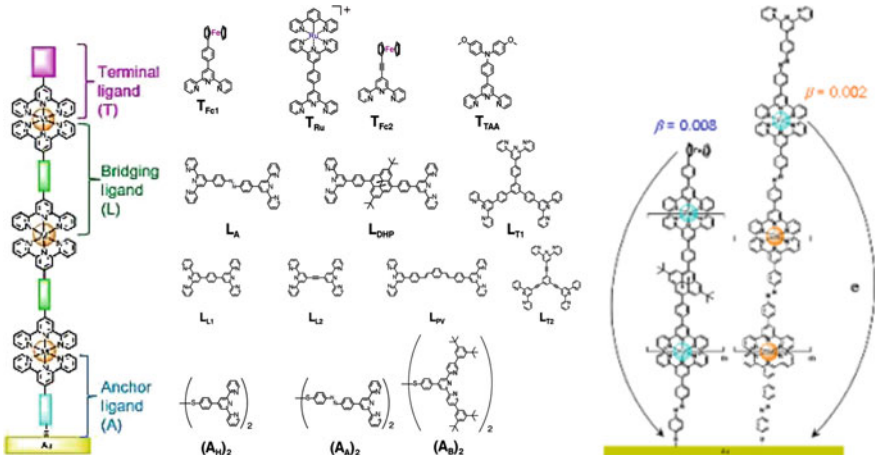

Fig. 7.66 Long-range electron transport ability of $M(tpy)_2$ wires

methods, molecular wires are simply produced by consequent submergence of the electrode in metal ion solution and a bridging ligand. The process is ended by decoration a wire end by redox-active functional groups, such as Fc, triarylamine or cyclometalated Ru(II) complexes. Combination of different components can provide different types of molecular wires.

The obtained wires show a lot of interesting function, including behavior of electron transfer and long-range electron transport capacities from redox part of a terminal to electrode through bis(tpy) metal chelates [549, 550]. The rate constant of electron transfer for 1D molecular wire is quantitatively determined as follows:

$$K = k_0 \exp\left(-\beta^d\right),$$

where k is the rate constant of electron transfer between the redox part and the electrode, d is a distance between the electrode and redox part, k_0 is the constant of

zero distance, β is a distance attenuation factor. Extraordinary capacities of the long-range electron transport is confirmed by low attenuation coefficient $\boldsymbol{\beta}$ (for example, 0.008 and 0.002 $Å^{-1}$ for Fe and Co chelate-based wires, respectively) [551, 552], which are far lower than for alkyl chains (1 $Å^{-1}$), DNA chains (0.1–1.4 $Å^{-1}$) and oligo (phenylene vinylene)-bridging wires (0.01 $Å^{-1}$). It is important that electron transport capacity can be easily adjusted using respective components of molecular wires, at that bridging ligand and metal ions have a substantial effect on β, while anchor and terminal ligand have no effect on β, but change k_0 (Fig. 7.67) [553].

Unusual nanostructures such as chain-of-beads are obtained from drop-casting of acetone solutions of Fe chelates with 2,6-di[pyrazol-1-yl] pyridine on the surface of HOPG [554]. It is important that beads in each chain are identical in size with diameter in the range 2–6 nm and height up to 10 Å, which correlates with content of small molecular cluster (about 10–50 molecules). It is interesting to notice that the beads can be separated into two types depending on conductivity, which correlates with their positions in chains and can correspond with the molecules containing high-spin and low-spin Fe centers. For some beads switching between two forms was observed during few minutes under a constant bias, which was apparently random [555]. This system is one of a few examples of SAMs, which relate to a wide range of spin-crossovers undergoing a transition between electron spin states under action of temperature, pressure or light [556, 557].

Pd(II)-directed chiral metal chelate multilayers are prepared on surface of the substrates through LbL assembling using hydroquinone anthraquinone-1,4-diyl diether of bidentate ligands as spacer [558]. It is important that molecular chirality of ligands remains in metal chelate multilayers. We shall also notice electrochromic behavior of Fe chelates obtained from tetra-2-pyridyl-1,4-pyrazine and hexacyanoferrate species in polyelectrolyte multilayers on ITO substrate [559]. Modified electrodes have shown excellent electrochromic behavior with intense and persistent dying, and chromatic contrast about 70%.

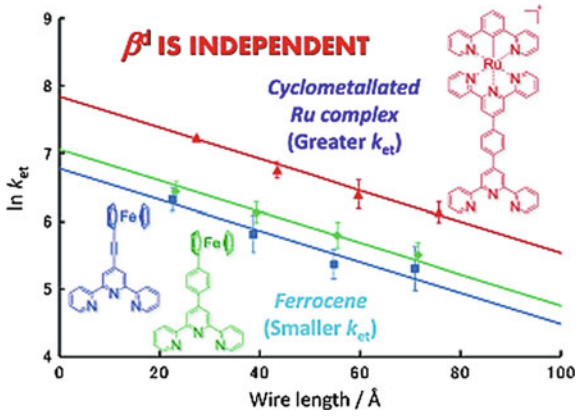

Fig. 7.67 Dependence of the rate constant of electron transfer versus wire length for bridging ligand, metal ions, anchor and terminal ligand

Cavitand-based cages on SAMs are subjected to metal-induced self-assembling, at that, M–L coordination provided direct observation of formation of such assemblies and detection of a single-molecular level [560]. Cavitand functionalized with four alkylthioether groups at the lower rim and four tolylpyridine groups at the upper rim can link with Au surface through thioether groups and form a coordination cage with $[Pd(dppp)(CF_3SO_3)_2]$ via its Py groups [561]. Using complexation of another cavitand, immobilized heterocages can be obtained from solution. It is important that the cages can be reversibly assembled and dissembled on Au surface, and AFM measurements distinguish an individual cavitand and cage molecules 2.5 and 5.8 nm in height, respectively.

M–L interaction is used for studying supramolecular rotors (Scheme 7.19) as potential components of a machine type system, through axial ligation of big π-functional molecules working as rotors, with the surface, which is a stator component [562].

The effect of a number of layers on photocurrent generation with using SAM obtained by coordination of Ru-Pc through 4,4′-bipy bridges (Fig. 7.68) is studied [563–565]. It is found that thicker layers generated lower photocurrents due to internal resistance of molecular wire.

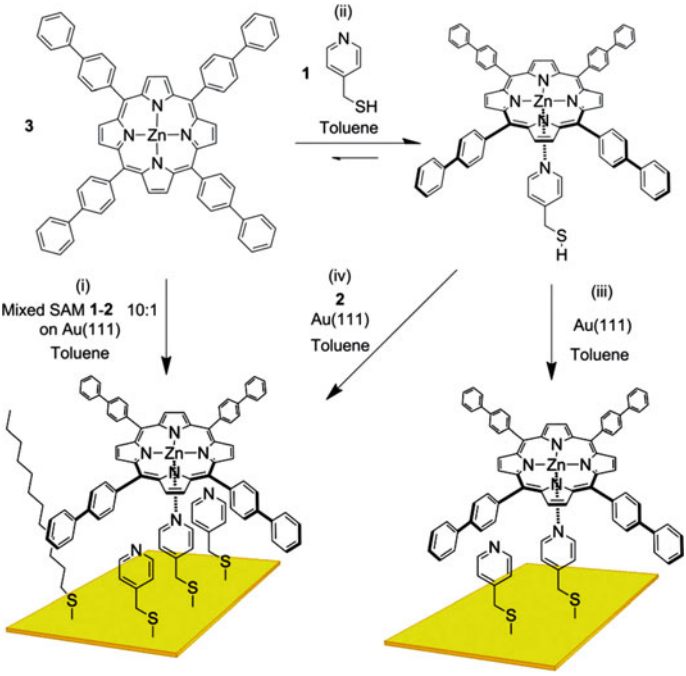

Scheme 7.19 Scheme of supramolecular rotors fabrication through axial ligation of big π-functional molecules working as rotors, with the surface, which is a stator component

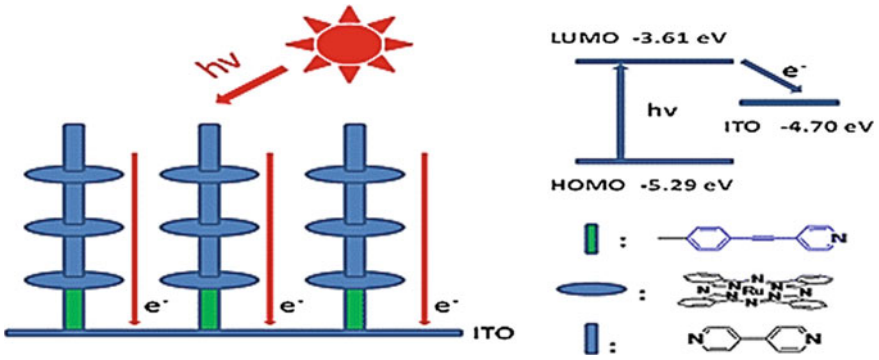

Fig. 7.68 Schematic energy-level diagram for a self-assembled sixbilayer Ru-Pc film on modified ITO electrode

We shall notice multivalent binding of a supramolecular complex on polyvalent host surface by uniting of orthogonal host-guest CD and M-en coordination motifs [566]. In this orthogonal supramolecular system a heterotopic divalent spacer with CD-complexing adamantyl group and chelating en ligand is used. This spacer can link CD in solution and immobilize CD on SAMs (Fig. 7.69). In the similar way vesicles are obtained, which carry host units (CD) by their interaction with guest (adamantyl) functionalized ligands through orthogonal polyvalent host-guest and M–L motifs [567]. Vesicles of amphiphilic CD recognized metal chelates with adamantyl ligands using integration into host caverns on vesicle surfaces. In the case of Cu(II) chelates interaction was predominantly intravesicular, while for Ni(II) chelates interaction was intervesicular, and addition of the guest-metal complex brought to aggregation of vesicles into dense multilayer clusters. Valence of supramolecular recognition on vesicle surface, and balance between intravesicular and intervesicular interactions can be adjusted using M–L coordination of a guest molecule.

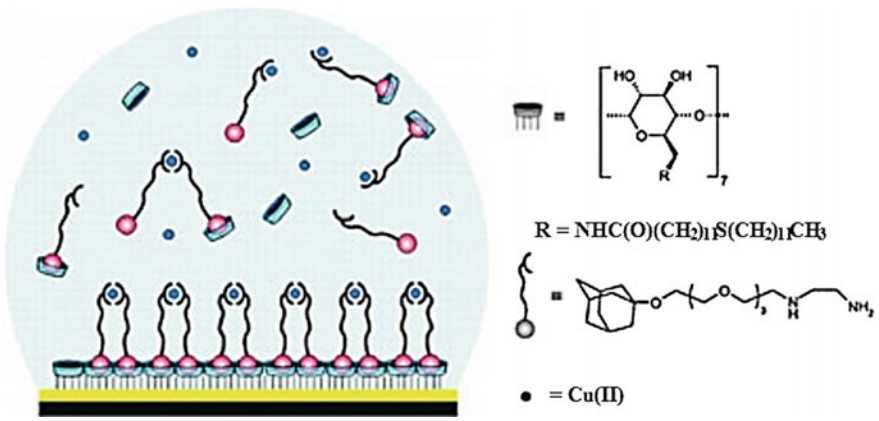

Fig. 7.69 Complexation on CD SAMs by host-guest and M–L coordination

7.12 Supramolecular Metal Chelate Dendrimers

Using dendritic architectures for supramolecular chemistry is focused on unique capability of their branched shell to influence processes of molecular recognition in center, branches and periphery of dendrimers [84, 179, 568–574]. Substantial attention in the recent years has being focused on using of supramolecular dendrimers, since self-assembling of building blocks through non-covalent interactions is a spontaneous process, which brings to the most stable structure and makes it possible to skip most stages of synthesis. Information on a structure programmed in dendritic architecture controls the assembling process and, as a consequence, properties of generated supramolecular structures. Self-assembling provides ideal approach for intensification of branching of small, synthetically available, relatively inexpensive dendritic systems (for example, dendrons) in strongly branched complicated nanometer aggregates. Supramolecular nano-assemblies including dendrimers and such objects as fullerenes, rotaxanes, CB[*n*], CD, MWCNT, etc. are of great interest [575–581]. Supramolecular dendritic polymers, which perfectly combine advantages of dendritic and supramolecular polymers, are a new class of non-covalently bound strongly branched macromolecules with 3D globular topology [582]. Due to their dynamic/irreversible character, unique topology and exclusive physicochemical properties (for example, low viscosity, high solubility, and a great number of functional terminal groups), supramolecular dendritic polymers have attracted high attention last year's [583]. In particular, reversibility of non-covalent interactions provides ability of supramolecular dendritic polymers to experience dynamic switching of a structure, morphology and function in response to different external stimuli such as pH, temperature, light, stress, and redox agents. Such behavior in future provides flexible and reliable platform for design and development of intelligent supramolecular polymer materials and functional supramolecular devices. Supramolecular dendritic polymers can be classified with respect to their topological structures, which contain the following six classes: supramolecular dendrimers, supramolecular dendronized polymers, supramolecular hyperbranched polymers, supramolecular linear-dendritic block-copolymers, supramolecular dendritic-dendritic block-copolymers, and supra molecular dendritic multi-armed copolymers (Fig. 7.70). These types of supramolecular dendritic polymers differ by morphologies, unique architectures, and specific functions, which provide their high potential for application in different fields. An important fact is that supramolecular dendritic polymers can self-assemble in various supramolecular structures, such as micelles, vesicles, fibers, nanorings, tubes, and many hierarchical structures.

Certainly contemporary supramolecular chemistry of dendrimers includes coordination motifs in studies of synthesis of supramolecular metallodendrimers and, in particular, MCD and their properties [84, 179, 584–589]. The most developed method of directed assembling of supramolecular MCD is using of M–L coordination. Different key strategies are proposed, using which metals are applied in self-assembling of several dendritic building blocks. Most often a metal center

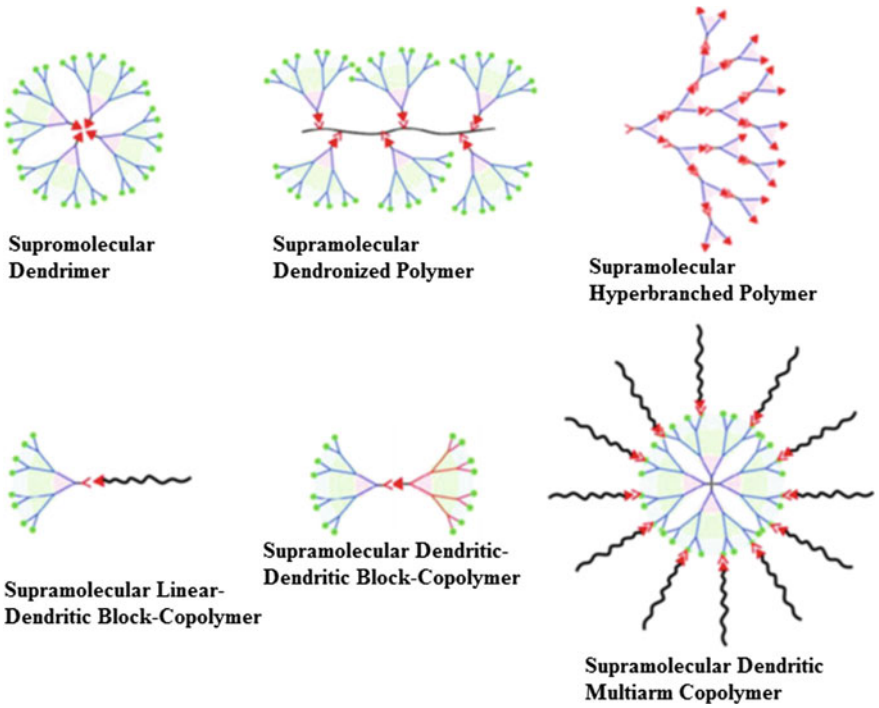

Fig. 7.70 Classes of existing supramolecular dendritic polymers with different topological structures

forms a core of supramolecular MCD with dendrons, which have chelating groups in the focal point coordinated around one central metal ion. Thus, $[Ru(bpy)_3]^{2+}$ core was actively used for this purpose at earlier stage of dendrimer chemistry [590] as a branching point in dendritic architecture, which is subjected to self-assembling with respectively projected ligands for generation of supramolecular MCD in one stage. As an example, supramolecular deca-Ru MCD can be regarded, which includes bpy and 2,3-dipyridyl-pyrazine as a terminal and bridging ligands, respectively (Fig. 7.71) [591–593]. It is interesting that oxidation of six equivalent peripheral Ru(II) centers to Ru(III) generates species containing 26 positive charges. Electrostatic effect of these charges prevents further oxidation of interior Ru(II) centers inside electrochemical window [594, 595]. Similar types of assembling with participation of bridging bis(2,3-pyridyl) pyrazine ligands and additional bpy termini can reach large sizes. For example, the largest dendrimer of this type containing 1090 atoms, 22 from which were metal centers [591], had the assumed size 5 nm and total charge +44 (+2 per a metal center). Apart from 22 metal atoms, this dendrimer consists of 24 terminal ligands and 21 bridging ligands.

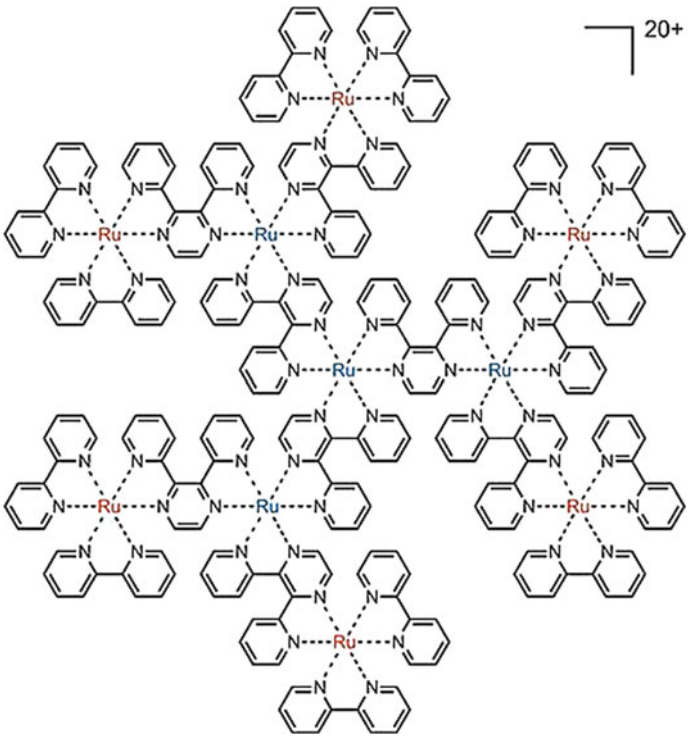

Fig. 7.71 Supramolecular deca-Ru MCD, which includes bpy and 2,3-dipyridyl-pyrazine as a terminal and bridging ligands

It should be noted that multi-tpy chromophores also form 2D networks by M–L complexation, which causes substantial changes in their photophysical properties (Fig. 7.72) [596].

Using interaction of Ru(II) and dendron-functionalized tpy-ligands, dendrimers can be built linked together by tpy-Ru coordination interactions [84, 179]. In order to do this, periphery of spherical dendrimer would be functionalized with several tpy blocks, and the following reaction with Ru(II) focused by a dendron provided location of additional branching layer on dendritic surface using M–L interactions. These structures, as a rule, have several metal ions inside branches holding dendritic structure together. In the same way supramolecular MCD are built, which integrate perylene as a functional core with ⟨tpy-Ru(II)-tpy⟩ termini (Fig. 7.73) [597]. For them, a wide absorption spectrum is typical with enhanced coefficients of molar absorption corresponding to increase in a number of ⟨tpy-Ru(II)-tpy⟩ units.

We shall also notice supramolecular mono-, bis-, and tris-Ru-based MCD, which cover a wide absorption range 250–750 nm with optical band gaps 1.51–1.86 eV [598]. It is important that for these MCD energy levels can be effectively controlled not only by different generations of dendritic thiophene arms, but also by their

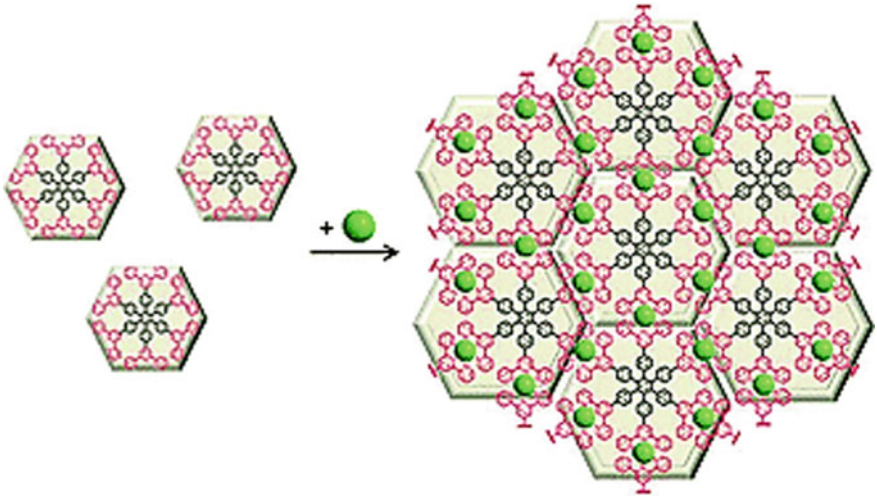

Fig. 7.72 2D networks formed multi-tpy chromophores by M–L complexation

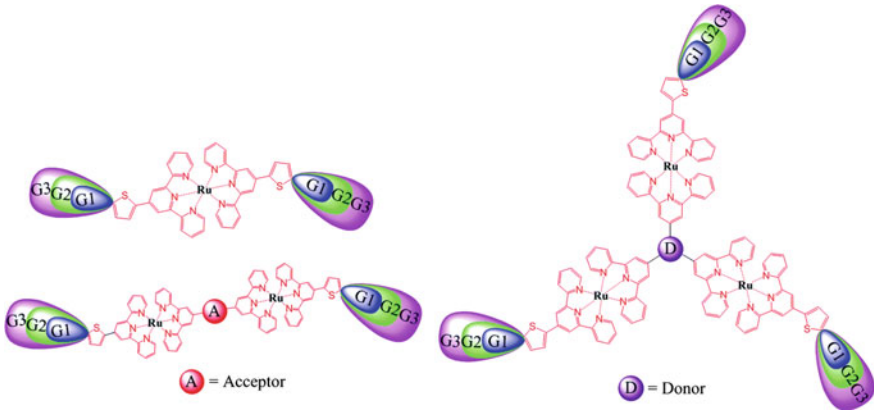

Fig. 7.73 Supramolecular MCD, which integrate perylene as a functional core with ⟨tpy-Ru(II)-tpy⟩ termini

π-conjugated core ligands carrying different electron-donor (triphenylamine) and acceptor (benzothiadiazole) residuals. Among different generations (G1–G3) dendrimers, G3 has the highest value of efficiency of energy transformation in each series of Ru-based dendrimers. There is an interest in shape-resistant supramolecular MCD, in which ⟨tpy-Ru(II)-tpy⟩ or ⟨tpy-Fe(II)-tpy⟩ connectivities are used as branching fragments or nodes (Fig. 7.74) [599]. A considerable increase in drift time of charge state, photophysical properties (molar extinction coefficients), and electrochemical stability of complexes were observed at increasing of generation of these complexes, which agrees with change in molecular size.

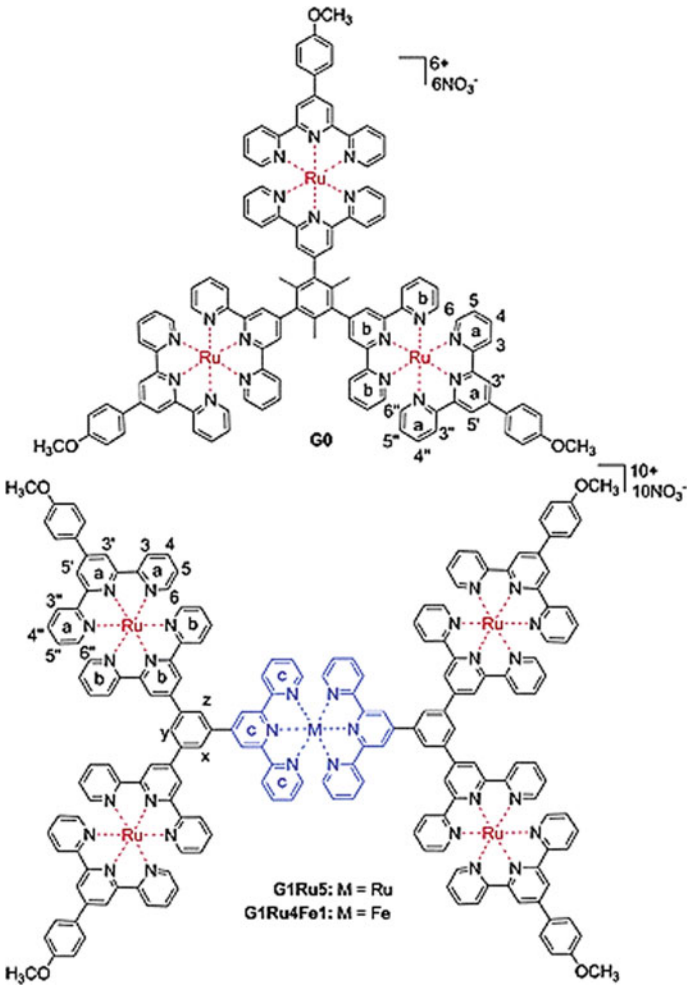

Fig. 7.74 Shape-resistant supramolecular MCD, in which ⟨tpy-Ru(II)-tpy⟩ or ⟨tpy-Fe(II)-tpy⟩ connectivities are used as branching fragments or nodes

Using consistent integration of different metal ions during synthesis with polypyridyl ligands, different supramolecular hetero-MCD structures can be obtained [600]. As an example we shall mention a dendritic-like four-nuclear complex $[Os\{(L_1)Ru(L_2)_2\}_3]^{8+}$ containing $\{Os(L_1)_3\}^{2+}$ chromophor as a core and three $\{(L_1)Ru(L_2)_2\}^{2+}$ polypyridyl building blocks as peripheral subunits, where L_1 = 2,3-bis (2-pyridyl)pyrazine; L_2 = 1′-((bpy-4-yl)methyl)phenothiazine. This MCD can be considered as integrated system with light-harvesting antenna-reaction center, in which Os subunit is efficient antenna unit in combination with well-known electron-donor subunits (phenothiazine fragments) [601]. In this system light absorbed by peripheral Ru(II) chromophores are transferred to the Os(II) core, however,

luminescence of Os(II) core is efficiently quenched through moderately exergonic reduction electron transfer by peripheral phenothiazine donors, despite presence of intermediate Ru(II) centers.

Coordination-driven self-assembling is a simple and very efficient approach for preparation of cavity-core supramolecular MCD, which have cavities with definite shape and size [602–615]. In general case synthesis based on this strategy is simple, and yield is almost quantitative, therefore a need in the following purification disappears. What is more important is that coordination-driven self-assembling is a powerful tool for building of supramolecular polygons and polyhedra with strictly defined and controlled cavities working as cores. As an example self-assembling of molecular squares can be considered based on simple modulus through interaction between four $(dppp)M(OTf)_2$ (M = Pd, Pt) linear components with 4,4′-bipy bidentate angular units, which are substituted in their 3,3′-positions with Frechet-type dendrons from G0 to G3 (Scheme 7.20) [616]. It is important that in obtained MCD squares there are absent a great number of other polygons or open-chained oligomers. They carry nanometer cavities inside a non-polar dendritic shell. Totally eight amide groups decorate rims of the cavity linking dendrons in a square.

There is interest in dendritic bis(tpy) Fe(II) wires with terminal Fc units synthesized on Au(111) surface by stepwise coordination using three-way tpy ligand, Fc-modified tpy-ligand and Fe(II) ions (Fig. 7.75) [617]. For the obtained systems an unusual phenomenon of electron transfer is found. In particular, current-time profile does not follow exponential decay, which is common for linear molecular wires, and non-exponentiality was more noticeable in the forward direction of

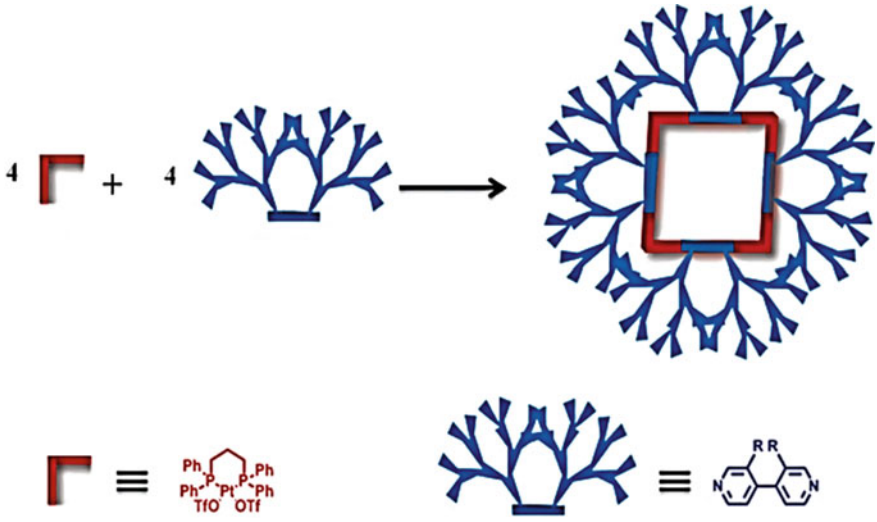

Scheme 7.20 Cartoon representations of the formation of eight-component square MCD from 180° G0–G3 dendritic donors and 90° dendritic acceptor

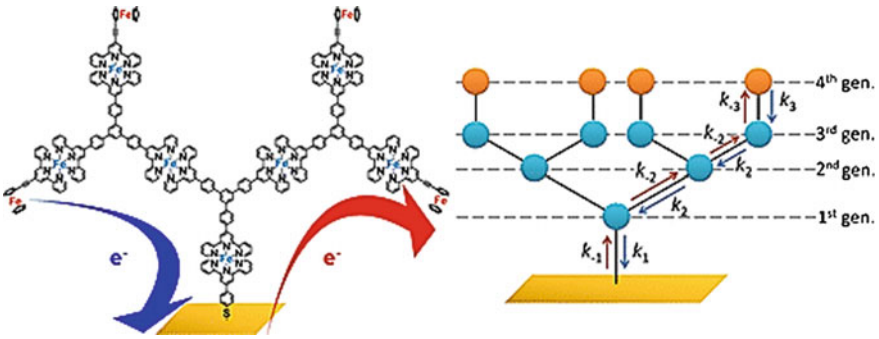

Fig. 7.75 Dendritic bis(tpy) Fe(II) wires with terminal Fc units synthesized on Au(111) surface by stepwise coordination using three-way tpy ligand, Fc-modified tpy-ligand and Fe(II) ions

electron transfer (from terminal Fc to Au electrode, oxidation) than backwards (from Au electrode to terminal Fc, reduction).

We shall also notice examples of using the supramolecular MCD self-assembling concept with participation of orthogonal non-covalent interactions, for example, Hamiltonian receptor-cyanuric acid and $Ru(bpy)_3$ M–L-linking motifs (Scheme 7.21) [618]. It is important that consequent divergent sequence of reactions, as well as one-pot reaction from AB_2 building block, which contains a focal bpy fragment and two units of Hamilton receptors, can be applied for synthesis of such supramolecular MCD. It is important that a terminal analogue of derivatives of cyanuric acid can be tailored with a great variety of functional groups.

Another example is supramolecular MCD assembled by two different orthogonal supramolecular interactions: Pd-pincer coordination and cyanuric acid-melamine H-bonded rosette motifs (Scheme 7.22) [619]. The resulting supramolecular MCDs are as big as 28,000, which make them one of the biggest known MCDs.

M-Pp and M-Pc dendrimers are actively used in synthesis of supramolecular MCD. Thus, supramolecular MCD based on multiporphyrin metallodendrimers consisting of focal free Cu-Pp with eight Zn-Pp wings and multipyridyl Cu-Pp with eight pyridyl groups are obtained through multiple axial ligations of pyridyl groups to Zn-Pp [620]. It is important that apparent association constant between two main fragments (2.91×10^6 M^{-1}) is rather high for fiber assembling to form at micromolar concentrations. The fiber assemblies with correct height (about 2 nm) and regular diameter about 6 nm are formed. It should be noted that by formation of supramolecular MCD intramolecular energy transfer changes to intermolecular energy transfer, from Zn-Pp to Cu-Pp with pyridyl groups.

We shall also notice supramolecular MCD consisting of self-assembled derivatives of zinc chlorophyll [621]. In this case, coordination-driven self-assembling of pyridine-pendant zinc chlorophyll derivatives proceeds through intermolecular axial ligation between a nitrogen atom of the pyridine ring and zinc atom in the chlorine ring (Scheme 7.23).

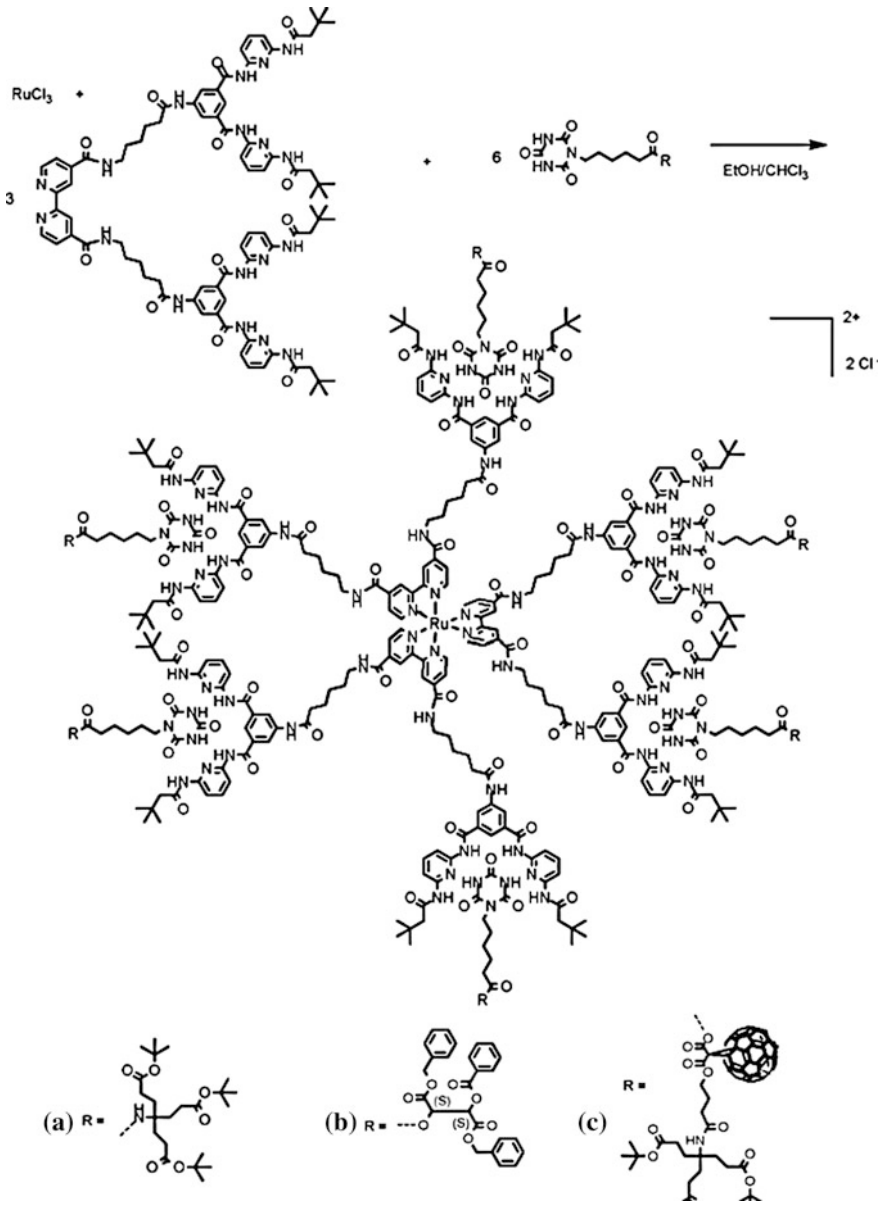

Scheme 7.21 Complete self-assembly of supramolecular structures

The coordination-driven strategy is also used for assembling of fullerene-rich supramolecular MCD [622, 623]. The M-Pp dendrimers form supramolecular complexes with fullerene derivatives through electrostatic interactions, π-π interactions and coordination bonds. For example, fullerene-rich supramolecular dendritic structures

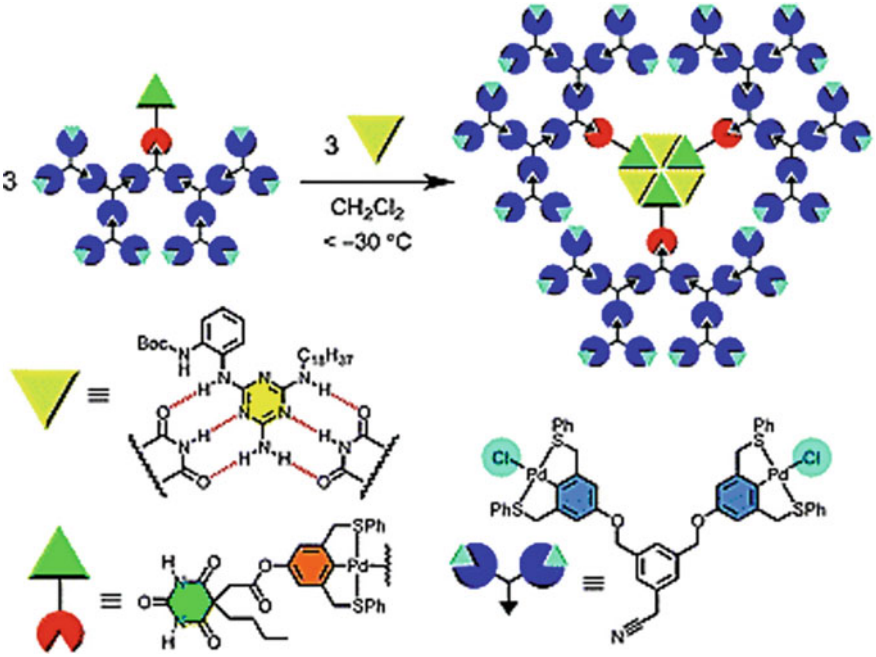

Scheme 7.22 Self-assembled dendrimer featuring orthogonal Pd-pincer coordination and cyanuric acid-melamine H-bonded rosette motifs

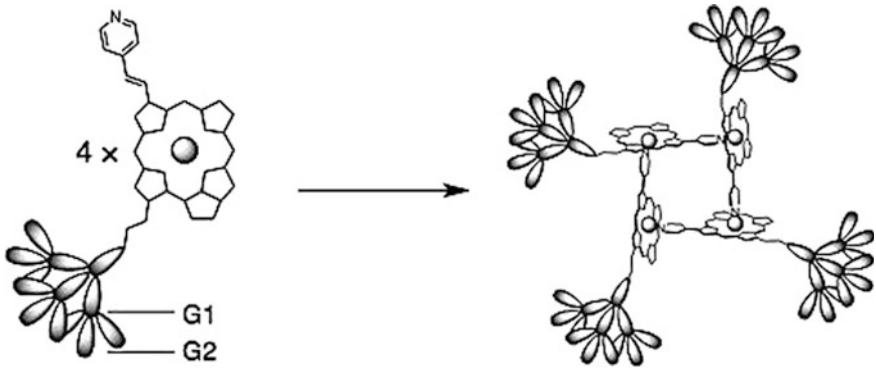

Scheme 7.23 Synthesis of supramolecular MCD by coordination-driven self-assembling pyridine-pendant zinc chlorophyll derivatives

are obtained as a result of apical coordination of C_{60} derivatives carrying pyridyl fragments to dendritic molecules with M-Pp units [624]. It is interesting that clear visualization of the petal-like structure is displayed. Average affinity of binding in assumption 1:1 coordination between separate Zn-Pp blocks and Py is 1.2×10^6 M^{-1}.

This value is more than by 2 orders of magnitude higher than the association constants reported for monodentate coordination between Zn-Pp and Py derivatives, which can be ascribed to simultaneous coordination of two Zn centers by two Py-containing fragments.

In another example, terminal amines of G1–G3 PAMAM dendrimers were modified through grafting of M-Pp derivatives with activated ester [623]. M-Pp dendrimers were then used for formation of supramolecular assemblies with C_{60} using acetonitrile/toluene mixed solvent bringing to clustering of nanometer assemblies (Fig. 7.76).

For efficient delivery of photosensitizers, ionic M-Pp dendrimer is used to form PIC of micelles (Fig. 7.77) [625–630]. We shall notice that M-Pp-including PIC micelles have high stability and high photo cytotoxicity. Moreover, great hydrodynamic volume of micelles brings to quite precisely localized drug delivery to a tumor tissue. In the same way ionic dendrimer Pc with absorption of long-wave light was developed for efficient light delivery at PDT and also formed PIC micelles containing *cis*-dichlorodiammineplatinum (II), anti-cancer drug with PEG-*b*-poly (L-aspartic acid) (molecular weight of a PEG segment is 12,000, DP of a segment of aspartic acid is 68 or 96) [628]. These supramolecular MCD can be efficient nano-devices for anti-cancer drug carriers with sustained release drug and PDT.

We shall also notice supramolecular chiral assemblies obtained by π-π interactions between aromatic rings of M-Pp dendrimers. Thus, dendritic Zn-Pp with two carboxylic groups can form J-aggregates in $CHCl_3$ through π-π interactions of Pp

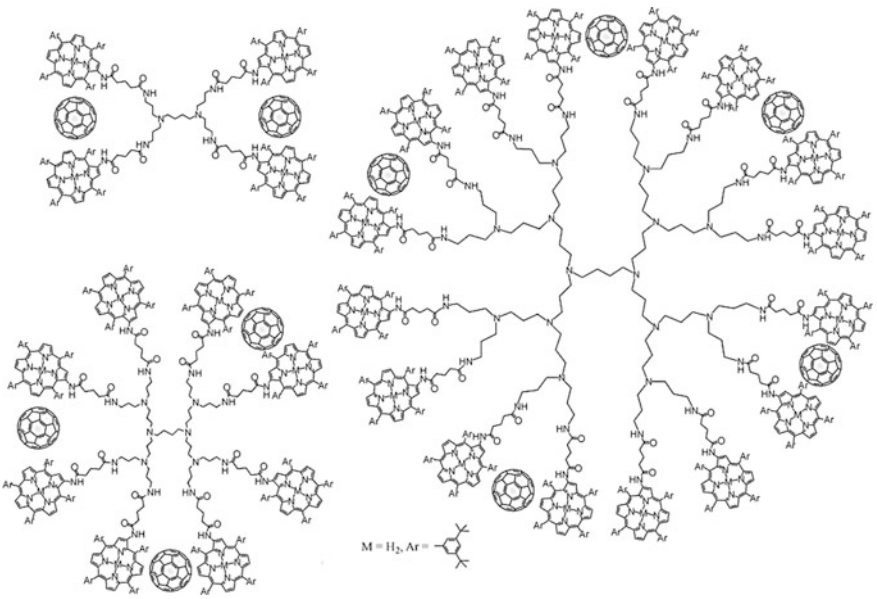

Fig. 7.76 Non-covalent assemblies of C_{60} with G1 to G3 POPAM dendrimers decorated at the surface by multiple Pp macrocycles

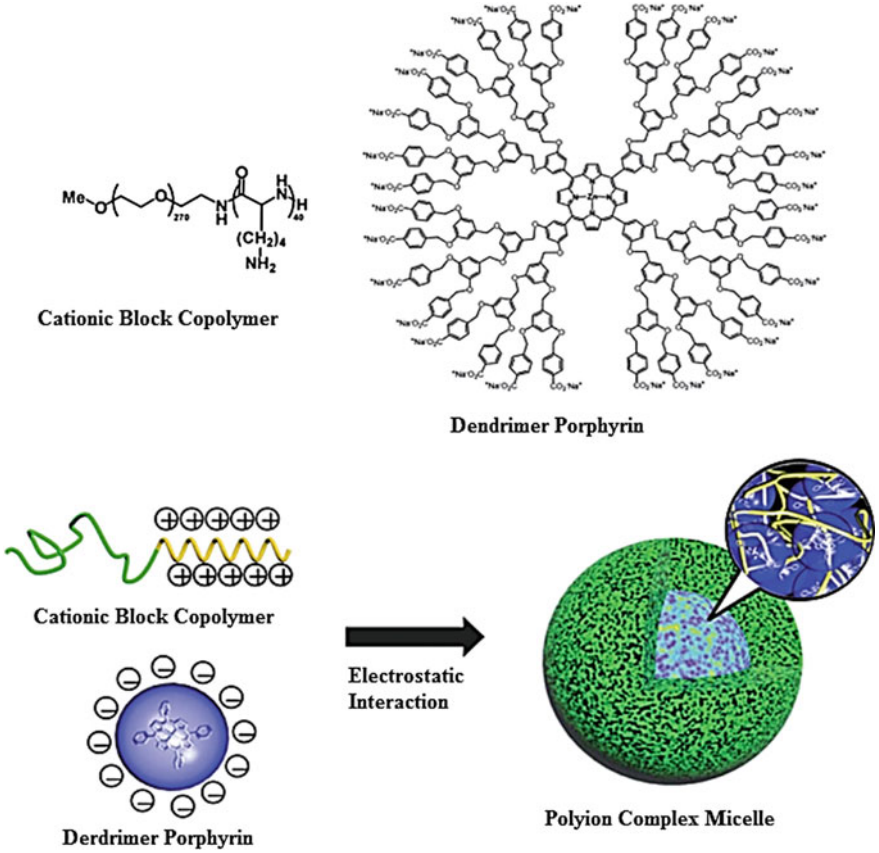

Fig. 7.77 Structures of cationic block copolymer and dendrimer Pp, and formation of its PIC micelle

rings and also aromatic rings of their dendritic substituents (Fig. 7.78) [631]. Besides, H-bonding between carboxylic groups can also be very important driving force for formation of J-aggregates. It is important that centrifugation of J-aggregates solutions would give optically active films, whose chirality can be chosen by spinning direction. Apart from centrifugation mixing of benzene solutions of achiral dendritic Zn-Pp with two carboxylic groups can also produce supramolecular chirality. It is interesting to notice that when direction of mixing is changed from clockwise to anticlockwise, opposite CD signals are detected. For this system nanofibers formed by M-Pp assembling through J-aggregation play very important roles, in particular, some of observed chiroptical activities can also grow from macroscopic chiral alignment of nanofibers [632].

Another direction of the studies of supramolecular MCD is fixing of LMC on preliminary formed supramolecular polymers. In this view very promising is use of such interesting supramolecular polymers as dendrimerosomes [573, 574, 633–636].

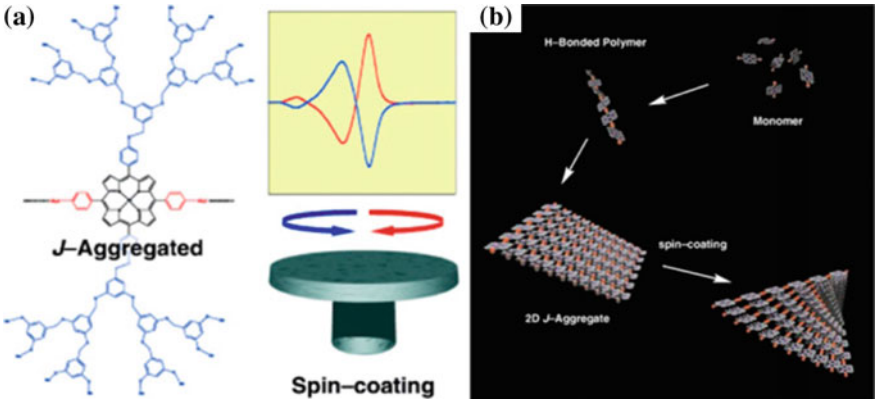

Fig. 7.78 **a** J aggregation of achiral dendritic Zn-Pp and macroscopic chirality from spinning. **b** Mechanism for the formation of chiral assemblies

These nanostructures are obtained from amphiphilic «Janus dendrimers» one part of which is hydrophilic and another one hydrophobic. A simple injection of amphiphilic Janus dendrimer solution with a definite primary structure into water or a buffer gives uniform submicron onion-like vesicles called dendrimersomes. Size and number of alternating internal closed bilayers is predicted by initial concentration of a Janus dendrimer. The transverse dimension of a dendrimersome shows that this supramolecular structure looks like a double membrane forming a cell wall (Fig. 7.79). A great variety of nanostructures formed spontaneously at placing Janus dendrimers in water has been discovered and studied, at that a family of supramolecular systems is formed, including vesicles, tubes, discs, and other shaped systems. Dendrimerosomes are stable for a long time, they are uniform by size, changing self-organization conditions they can be tailored into a necessary shape and, moreover, they can be quite easily functionalized. Their size, stability, and membrane structures are defined by chemical structure of a Janus dendrimer and the self-assembling method. A simple method of injection for production is available without special equipment, making uniform vesicles, and thus forming promising means for fundamental studies and technological applications in nanomedicine and other areas.

Dendrimerosomes are efficient and universal nanoplatform for fixing LMC, in particular, hydrophilic or amphiphilic MR chelates [637, 638]. Thus, for example, amphiphilic Gd(DOTA)-like complex functionalized by two octadecyl chains, is synthesized and incorporated into bilayer of dendrimerosomes [637]. In other example dendrimerosomes were loaded by clinically proved MRI probe Gadoteroidol (Fig. 7.80) and compared with respective nanoparticles taken from more branched dendrimers [639]. It is important to notice that the lifetime of these systems in blood is comparable with lifetimes of liposomes, which points to a possibility of their using for different biomedical applications.

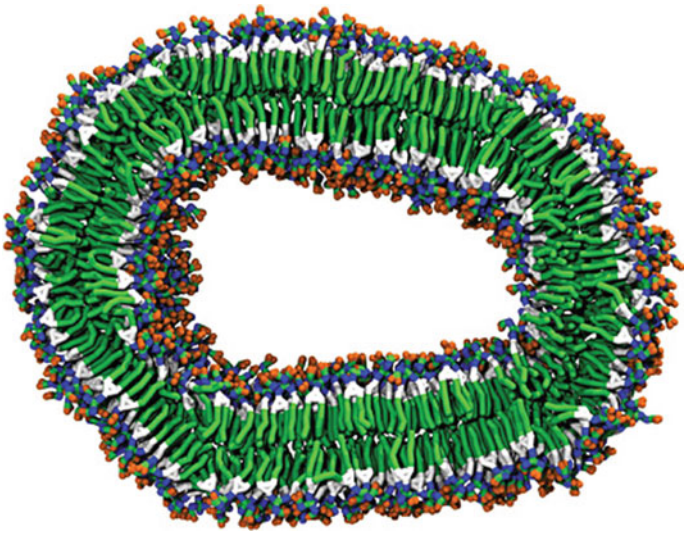

Fig. 7.79 The cross section of dendrimerosomes showing its double layer, similar to the cell membrane

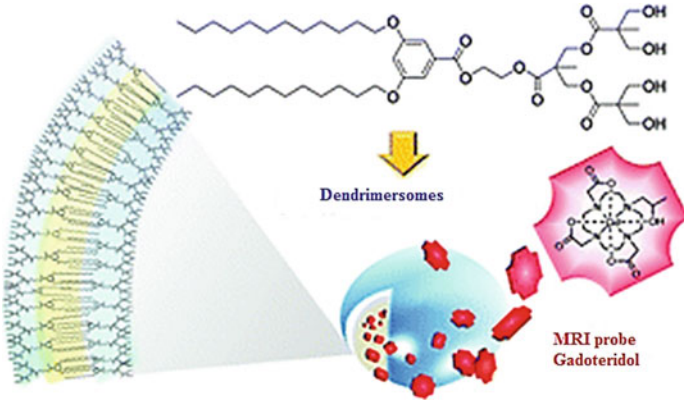

Fig. 7.80 Production of dendrimerosomes loading by clinically proved MRI probe Gadoteroidol

7.13 Stimuli-Responsive Metallosupramolecular Polymers

Stimulus-responsive materials have attracted great interest during recent years, since these materials can show abrupt change in properties as a response to a stimulus application such as light, temperature, mechanical action, pH, ionic force, polarity of a solvent, electric fields, chemical substances, etc. [49, 99, 640–643]. In accordance with a type of a stimulus, to which they respond, these materials are

classified as photo-, chemo-, electro-, or mechano-active substances. Application of a stimulus brings to change in properties of a material, such as fluorescence, mechanical stress, change in color, etc. Such stimulus-responses can be displayed by different materials, from inorganic to organic, from molecular to macroscopic level, and from natural to synthetic materials. A programmed assembling of molecules into supramolecular polymers has a great interest for development of stimulus-responsive «smart» materials. Control over morphology, dynamics, and responsiveness of MSP is of high value for future applications [340, 341]. Due to dynamic and reversible character of non-covalent interactions, MSP can be adapted to environment and have a wide range of intriguing properties, such as degradation, of shape memory and self-healing, which makes them unique candidates for supramolecular materials [644, 645].

Thermo-responsiveness is one of fundamental and most available properties of supramolecular polymer materials, because weak non-covalent interactions are by their character subjected to thermal stimulus. Therefore thermo-responsive supramolecular materials have attracted a wide range of interests. The main advantage of supramolecular polymers is a strong dependence of their melt viscosity on temperature, which makes them easily treated and applied. As an example we can consider Fe(II) and Zn(II) MSP based on PCL of telechelic polymers containing two functional units at their ends: a tpy ligand and ureidopyrimidinone quaternary H-binding motif [170]. Double logarithmic dependence of specific viscosity of Fe (II) MSP solution on concentration has shown two-phase linear dependence pointing to the ring-chain equilibrium. Bulk rheological properties of PCL-Fe(II) MSP are characterized by two abrupt changes in viscosity with temperature. The first change at lower temperature is ascribed to melting of poly (ε-caprolactone) main chain, while the second change is due to weakening of M–L bonds within the supramolecular chain. Oppositely to this, Zn(II)-containing MSP have shown only one change in viscosity at lower temperature. Probably, thermodynamic stability of M–L bonds plays important role in observed rheological behavior of these MSP.

Using ability of tridentate BIP ligand to bind cations of transition metals Zn(II) and Co(II) in the ratio 2:1, and big cations of La(III) and Eu(III) lanthanides in the ratio 3:1 [77], MSP are obtained, in which Zn(II) and Co(II) (95%) are used for linear growth, and La(III) and Eu(III) ions (5%) for cross-linking (Fig. 7.81a) [130]. Gel-like materials based on four combinations of metal cations Co/La, Co/Eu, Zn/La, and Zn/Eu have shown reversible thermo-responsiveness (Fig. 7.81b) and interesting thixotropic behavior (Fig. 7.81c) as a result of gel-sol transition induced by mechanical force (shaking). The mechanism of mechano-responsive behavior involves formation of «loose dangling chain ends» in L:Zn/La system, when it is subjected to mechanical loading [129]. Restoring of the system includes reorganization of «broken ends» and reforming of the initial structure. L:Zn/Eu-containing MSP is, in addition, also chemo-responsive. In particular, adding of formic acid brought to immediate gel-sol transition and quenching of Eu(III) emission, since aromatic BIP ligands, which coordinate Eu(III) cation, are substituted by formate-anions. The process is made reversible by thorough drying of the material followed by repeated swelling in respective organic solvent.

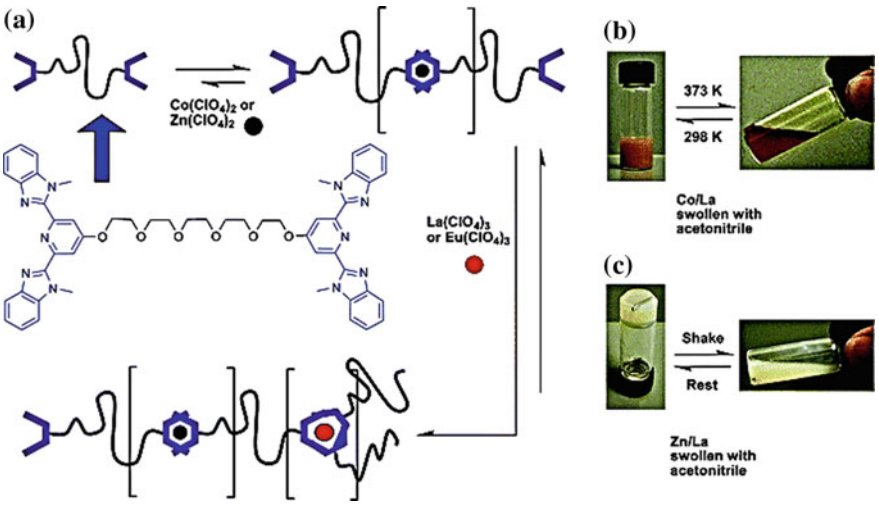

Fig. 7.81 **a** Schematic representation of the formation of a MSP from bifunctional ligand and lanthanide/transition metal cations. Photographs showing **b** the thermo-responsive nature of the L:Co/La system and **c** the thixotropic nature of the L:Zn/La system

There is also interest in thermo-responsive MSP which use thermally induced interconversion between *cis*- and *trans*-isomers on a cyclam block [646]. In the *cis*-isomer substituents are on one side of the cyclam plane, while in the *trans*-isomer subunits are above and below the cyclam plane. In MSP, formed by bis-tpy-cyclam ligand and Ni(II) ions temperature-initiated *cis-trans* transitions on the cyclam block bring to macroscopic phase sol-gel transition. Initially kinetically preferable *cis*-isomers, which form coil-like aggregates, present in the solution. During heating the *cis*-form transits into the *trans*-form and coils broaden to rod-coils, which brings to aggregates consisting of rigid and flexible segments and to gelation (Fig. 7.82).

Light, as remote stimulus, has a special meaning and is attractive regarding its wide use in molecular devices and smart materials, since it provides a wide range of controlled parameters, such as a wavelength, duration, and intensity. Reversible control over self-assembling of non-covalent building blocks by photo-irradiation is a key process for controlling photo-responsive MSP. Thus, MSP based on rod-like guest compound, containing two azobenzene units, β-CD macrocycle or its derivative, and en Pd(II) nitrate [325] can react to light irradiation due to photoisomerization of the main chain containing azobenzene fragments.

Supramolecular materials are dynamic non-covalent bond-based materials, therefore any chemical substrate, which can weaken or break non-covalent bonds, will make the materials give a response to it. It is important that integrated chemical agent will change initial chemical environment, and then will have more or less effect on properties of materials. Chemo-responsiveness is an astounding property, which can provide available important applications of MSP.

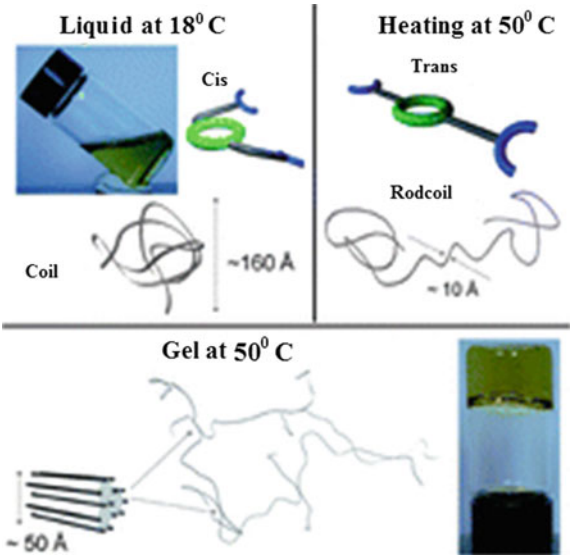

Fig. 7.82 Schematic representation of coil-rodcoil transition and gelation during heating

In this view, we shall notice MSP based on polyhedral oligomer silsesquioxane and Co(II) or Cu(II) tpy complexes [212] or amino-phen Sn(II) complex [190], which has shown properties of gelation at high concentrations of metal ions, at that gelation is reversible after addition of competitive metal-chelating agent, such as EDTA. In another interesting example MWCNT functionalized with tpy form MSPs in presence of Co(II) or Ni(II) ions, which can also be de-chelated by EDTA addition, which can be seen by change in color [647]. A pH-induced transformation between mononuclear neutral complexes and MSP in the system consisting of cyclam and bis-tpy fragments is shown (Scheme 7.24) [648]. This ligand at interaction with Cu(II) in molar ratio 1:1 gives green MSP solution, however, in presence of a base, red-pink solution is obtained, which corresponds to square-planar mononuclear Cu(II) complex. It is interesting that both these types become interconvertible with addition of base or acid. Besides, it turned out that addition of second equivalent of a transition metal ion such as Fe(II), Ni(II), Co(II) or Cu(II) to the square-planar mononuclear Cu(II) complex brings to MSP formation consisting of homo- or heterometallic complexes [649]. It is important to notice that addition of acid to homometallic Cu(II) MSP brings to polymer dissociation into binuclear complexes, in which Cu ions are coordinated with tpy fragments.

Using redox reactions for modulation of MSP properties gains substantial attention, since a change in redox conditions can bring to macroscopic changes in their properties. Obviously, MSP are exclusive candidates for creation of electro-responsive supramolecular materials, because metal ions can be subjected to oxidation and reduction with external electrochemical stimulus. Moreover, integration of metal ions also can change aggregation regimes and give approach to a wide

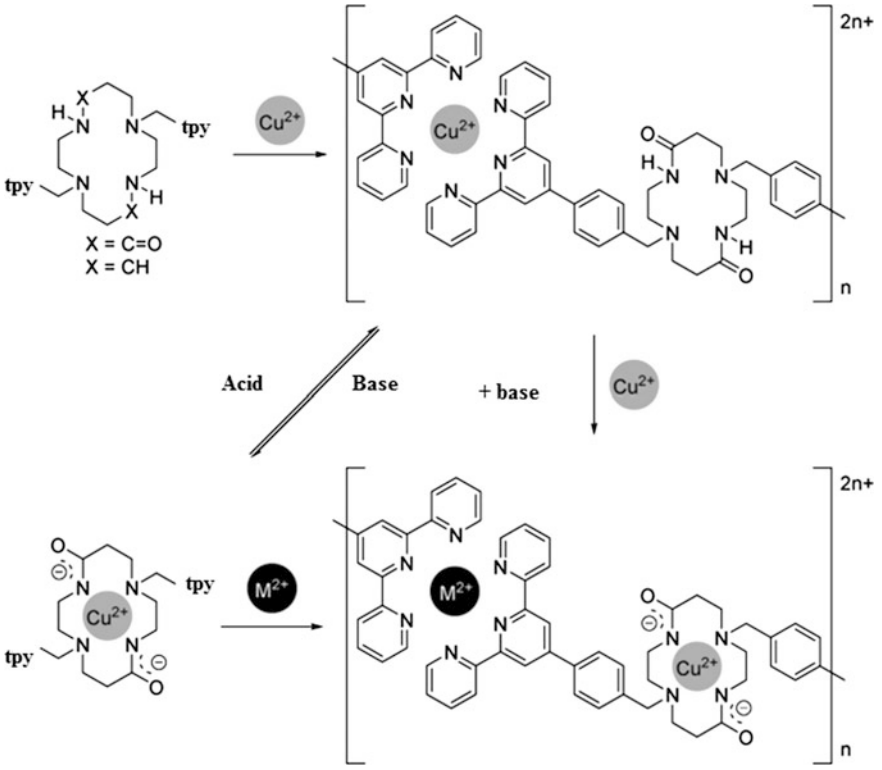

Scheme 7.24 Chelation routes of Cu(II) by ligand in the absence and presence of a base, the subsequent acid-base driven interconversion, and formation of homo- or hetero-MSPs

spectrum of interesting properties. For example, in order to obtain MSP which show a redox-responsive gel-sol transition and electrochromic properties [521, 522], metal ions and polytopic ligand containing two chelating tpy terminal units bound through complexing cyclam macrocycle, are used. It is interesting that these MSP have shown properties of gelation as a function of a solvent composition and of counter-ion nature, and can be controlled by M:L stoichiometry, concentration and temperature. Moreover, the self-assembling process is sensitive to external stimuli, such as electric input (redox-responsiveness) or a counter-ion type (chemo-responsiveness). During electrochemical oxidation of Co(II) to Co(III) gel easily undergoes transformation into solution, at that the gel can be reformed by reduction of Co(III) to Co(II). Incorporation of additional positive charges into polymer chains during oxidation has effect on solubility of the system and destabilizes gel, thus making the gel-sol transition. Variety of colors and reversible gelation of MSP is accumulated by a simple redox stimulus, thus demonstrating advantages of metal ion incorporation into supramolecular systems.

We shall notice redox-responsive MSPs consisting of a ditopic ligand end-capped by a poly-THF macromonomer, self-assembled with Cu ions, in which DP of MSP and, consequently, viscosity of its solutions depends on oxidation degree of copper ion. A combination of methods is used to show that Mebip ligands at the ends of poly-THF link Cu(II) with the ratio 2:1 and Cu(I) with the ratio 2:2 in solution. Therefore, at the fixed 1:1 or 1:2 stoichiometry of a macromonomer to Cu ions, viscosity of their solutions shows dramatic changes due to addition of chemical oxidant (nitroso tetrafluoroborate) or reducing agent (aqueous ascorbic acid) (Fig. 7.83) [650].

An interesting example is MSP containing a tpy-end three-armed PEG, which has shown sol-gel transition during aerobic oxidation [651]. Aerobic oxidation of Co(II) to Co(III) is accompanied by sol-gel transition, at that; the material can be molded in hydrogels of different shapes. Addition of a reducing agent has brought to reversible gel-sol transition and solution under action of air is then re-gelled due to aerobic oxidation of the reducing agent.

While mechanic load on polymer materials is inevitable, mechano-responsive materials act as especially attractive class of intelligent materials. As a rule, mechanical responses of polymer materials are derivatives of chemical and physical structure of polymer chains; therefore, dynamic, reversible non-covalent bonds are attractive candidates for building of mechano-responsive materials via incorporating them into polymer main chains. Thus, it is found [476] that binuclear Pd(II) *anti*-complex is self-assembled into long-chained assemblies in solution forming gel under ultrasonic irradiation. The gel can be easily transformed back into sol upon heating (T_{gel}), at that the sol-gel transition can repeat infinitely without a noticeable degradation of a system. For gelation racemic mixture of *anti*-complex is required as one of two enantiomers ((+)- or (−)-*anti*-complex) or even only *syn*-

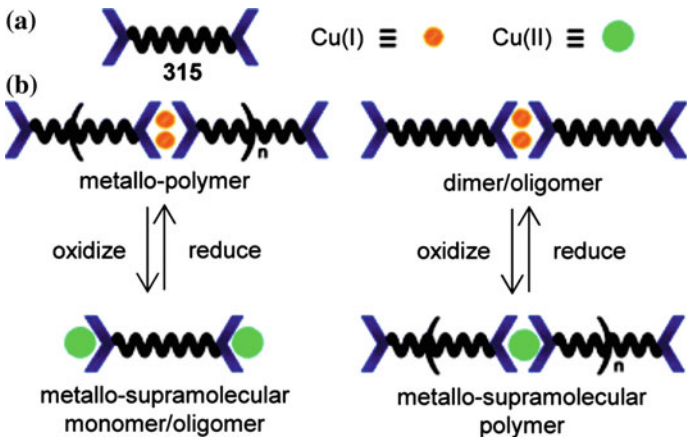

Fig. 7.83 Cartoon representation of **a** ligand and **b** redox regulation DP with Cu:L ratios 1:2 (left) and 1:1 (right)

compex giving a homogeneous solution without any change in properties of a current solution. An assumption is taken that the clothes-PEG-like conformation of *anti*-complex prevents oligomerization because of absence of preliminary organization. However, external stimulus (ultrasound) can have an effect on conformation distribution, which provides formation of a «regular» conformer or insignificant amount of short oligomers with lifetimes, which allow their further extension into the observed aggregates.

There is a great interest in intelligent materials integrated with independent multi-responsiveness, which are reached due to masterly integration between structures of materials and responsiveness of non-covalent interactions. Thus, multi-responsive MSPG [76, 113, 128, 129] are obtained by addition of Zn(II) or Co(II) perchlorate (97 mol% with respect to ligand) to the solution of bis-terdentate bridging ligand, which have shown thermo-, chemo-, and mechano-induced gel-sol behavior phase transition. During heating, and then cooling reversible gel-sol transition was observed. It has been shown that this transition takes place, mostly, due to labile ligand-lanthanide ion interactions, which are different from ligand-transition metal ion interactions. In the same way a gel collapse took place upon addition of 0.85 wt% formic acid to the system due to stronger linking of lanthanide ions to carboxylic acids. One of the most interesting properties of MSPG is mechano-responsivity, which shows thixotropic (shear-thinning) behavior. Free-flowing sol is obtained by shaking of gel, which has reformed opaque gel again after storage. The observations have shown that gelation takes place through flocculation of semi-crystalline colloid particles, whose size can be reduced or even particles disappear under action of mechanical stress. Since nitrate-ion is a coordinating one by nature, branching can increase in presence of non-coordinating perchlorate-ion instead of nitrate-ion, which results in increase in mechano-responsiveness of gels. These gels showed reversible thermo-, chemo-, and mechano-responsive properties. It is obvious that MSPG open possibilities for projecting of multi-responsive organo-inorganic hybrid materials, whose properties can be easily adjusted by changes in combinations of metal ions.

The concept of photo-active mechano-responsive MSP based on using bis-tpy linked ligand, namely, HO-BIP, is developed. An interesting aspect of this concept is that the studied ligands can form 2:1 metal complexes with transition metal ions and 3:1 complexes with lanthanide ions. Therefore, it is possible to create gels by mixing telechelic chelating ligand with combination of lanthanide (cross-linker) and transition (chain extender) metal ions, respectively. These gels show responses to thermo-, chemo- (with formic acid) and mechanical stimuli. Mechano-responsive character of MSP based on Zn/La gel has shown thixotropic (shear-thinning) behavior. It has been found that lanthanide gels have shown very strong luminescent properties based on energy transfer from ligand to metal ion, for example, Eu(III). This photophysical property can be interrupted by heating or mechanical loading, and, consequently, luminescence color changes from red to blue, and emission then respected to the ligand center.

We shall notice a series of stimulus-responsive MSP-based films consisting of Mebip ditopic end-capped poly-THF at different ratios of Zn(II) and Eu(II) [222]. Combination of optical properties of Eu(III) complex with its more labile nature brings to formation of highly stimulus-responsive materials. Films of Eu(III)-containing MSP show expressed optical response to increase in temperature (Fig. 7.84a, b) or under action of chemical substances (Fig. 7.84c, d), such as triethyl phosphate, which was used as imitator for organophosphorus pesticides and nerve gases.

MSP based on btp ligand and Zn(II) and Eu(III) ions have shown different mechanical properties and thermal stability depending on gel composition [652]. For example, photoluminescence properties of the gels can be well adjusted depending on the ratio between Zn(II) and Eu(II) and a solvent used for gelation. Besides, the gels can be converted into sol by heating, which is also accompanied by emission quenching, and its reversibility is detected during cooling. In the similar way these gels have shown mechano-, photo-, and chemo-responsive properties.

Upon linking a tpy motif to linear polymers carrying short hydrophobic segments, primary hydrophobic interactions bring to formation of micellar nanostructures in water [653, 654]. Metallosupramolecular micellar hydrogels, which show thermo-mechanical responsivity, are obtained through hierarchical assembling of hetero-chelate associating polymer. At the first stage the associating polymer is solved in

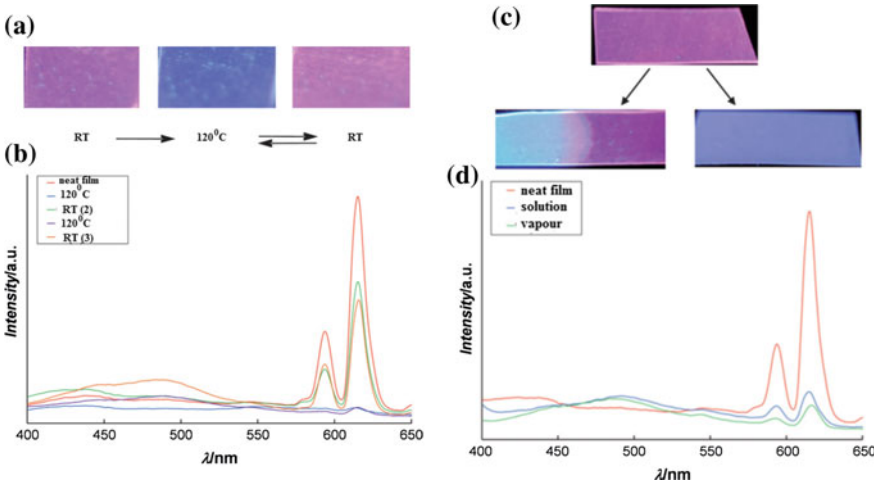

Fig. 7.84 **a** Temperature sensing: sample heated to 120 °C resulting in quenching of the Eu(III) fluorescence and subsequent return upon cooling back to room temperature (Zn(II):Eu(III) 70:30); **b** photoluminescence spectra (excited at 377 nm) of the above films showing the reversible disappearance of the Eu(III) metal-based emission at 590 and 615 nm upon heating and subsequent return with cooling. **c** Picture of a film fluorescing under UV light (λ = 365 nm) before and after dipping into a 10 mM solution of triethyl phosphate in hexane for 1 min (left) and exposure to triethyl phosphate vapor (24 h., rt) (right); **d** photoluminescence spectra (excited at 377 nm) of the above films. Both films show a decrease in the characteristic Eu(III) emission peaks at 590 and 615 nm

aqueous solution with formation of micellar nanostructures carrying chelating fragments at the end of coronal chains. At the second stage supramolecular assemblies are formed at addition of transition metal ions to micellar solutions, which results in almost instant gelation. These gels have shown reversible gel-sol transitions under mechanic stress and temperature-induced self-healing properties.

Linear MSPs based on Zn(II) and heteroditopic monomer carrying secondary ammonium salt of guest and tpy moiety have shown multistimuli-responsiveness, trigged by heat, pH or competitive ligand, such as cyclen [362]. In particular, specific viscosity of MSP decreases considerably above 50 °C, which points to decomposition of supramolecular polymers at elevated temperature. Besides, addition of 1.5 equivalents of Et_3N deprotonates fragments of secondary ammonium salt, which also results in MSP decomposition. Therefore, obviously MSP are highly adaptive materials capable of undergoing reversible transitions under action of different external stimuli.

Multistimulus-responsive behavior of metal-containing system was reported being achieved by using photoisomerization of dithienylethene fragment (Fig. 7.85) [655]. Mixing dithienylethene derivative of dicarboxylic acid with Al(III) has given a transparent solution, from which a metal-containing gel was obtained during heating. The gelation process depends on anion addition: their coordination with Al (III) or formation of H-bonds with ligands disturbs the gelation process. The obtained gels have shown reversible photochromic behavior: yellow solution of the open (O) form transforms into yellow gel of O-form during heating and can be transformed into red gel of the closed (C) form under UV irradiation. The red C-gel transforms into red C-solution during storage at room temperature in dark place and then returns to initial yellow O-solution under action of visible light.

Highly dynamic and adaptive non-covalent interactions forming supramolecular materials can be destructed in presence of competitive reagents (analytes) [656]. A change in physical properties of MSP by pollution, for example, adsorption and emission can be output signals for registration of quantity and quality of analytes, which is a basic principle for supramolecular sensors. It should be noted that some non-covalent interactions such as guest-host interactions [657] are highly specific and this can provide production of and selective sensors for special analyte. Thus, a special amphiphilic receptor TbL^+ complex is developed, which is self-assembled in water and forms stable vesicles [658]. The L^{2-} ligand consisted of bis(pyridine) anionic arms and long alkyl chain (Scheme 7.25). Upon addition of different nucleotides there is sigmoidal increase in luminescence intensity, which is ascribed to drift of coordinated water molecules by phosphate groups. Linking of TbL^+ complexes to each phosphate block bound by phosphoanhydride bonds goes cooperative, probably, by adaptive change of their molecular orientation in bilayer. Dynamic non-covalent interactions of alkyl chains have brought to adaptive and highly synergetic assembling between highly organized receptors (TbL^+ complex) on a membrane surface.

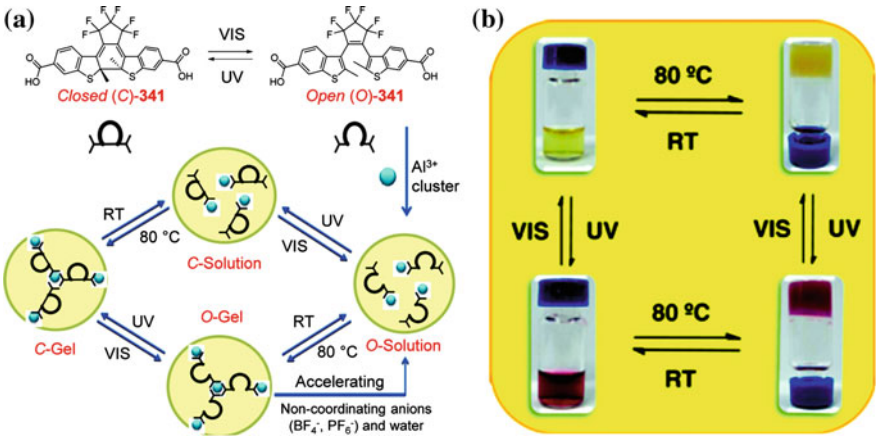

Fig. 7.85 **a** Reversible photoisomerization between the open- and closed-ring forms of the photochromic dicarboxylic acid ligand, and schematic representation of multiple transformations among gels and solutions in both open and closed forms (denoted as O-gel, O-solution, C-gel, and C-solution) after coordination. **b** Reversible gel-gel and gel-solution transformations of system upon heating/cooling, and UV-vis irradiation, and the multiple responsive behaviors toward color, fluorescence, water, and anions

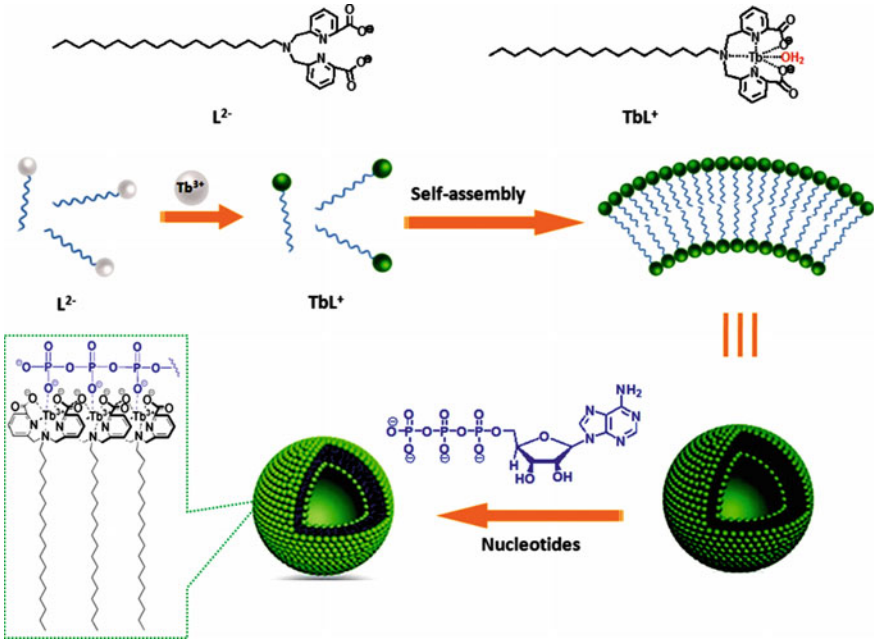

Scheme 7.25 Molecular structures of the ligand L^{2-} and TbL^{+} amphiphilic complex and schematic representation for self-assembly of TbL^{+} in water for the detection of ATP molecules

7.14 Self-healing and Shape-Memory Metallosupramolecular Polymers

Contemporary materials with inherent ability to repair damage at molecular level can be useful in a wide range of applications. The majority of so far developed healed polymer-based materials require heating a damaged zone above their glass transition temperature, and then pressure application in order to promote a contact, wetting, diffusion and repeated entangling of polymer chains [659–661]. Nevertheless, the healing process is, as a rule, slow and not efficient and hardly applied in practice. More promising in this view is MSP using [662]. Thus, optically healed supramolecular polymers are developed consisting of ditopic Mebip fragment and poly (ethylene-*co*-butylene) motif as a spacer for bridging of metal-binding fragments (Fig. 7.86a) [663, 664]. Under action of UV irradiation M–L motifs are excited, and absorbed energy is transformed into heat, thus bringing materials to depolymerization, dilution, and healing of defects. In this case re-forming of supramolecular polymer comes after a light source removal, which results in healing of a material (Fig. 7.86b). This property of self-healing proceeds through making cuts in 350 to 400-μm thick polymer films, at that, these samples under following irradiation by 320 to 390-nm UV light have shown healing during 30 s (Fig. 7.86c). It is interesting that under light irradiation the cuts were filled, and then appeared.

This work is broaden using MSP consisting of poly (butyl acrylate-*co*-MMA) functionalized by Mebip side chains, which is cross-linked by zinc trifluoromethanesulfonate salt [511]. In particular, this MSP has shown triple shape memory, as a result, it can reversibly gain shape «V», «S» or original rectangular sheet during heating or cooling. Shape reforming and healing is reached upon applying of thermal of light stimulus due to specific M–L interactions, which serve not only as «inert» cross-linkings of a network at low temperature to reform a shape, but also dissociate at high temperature for healing. The healing rate is high and efficiency of healing is close to $\sim$90% (Fig. 7.87).

There is interest in MSP-based self-healing coatings produced by integration of Fe bis-tpy complexes in polymer network based on methacrylates [665]. We shall also notice supramolecular materials, which can be simultaneously and reversibly self-healed without external stimuli based on metallosupramolecular interactions [666]. In particular, 3D transition supramolecular networks are formed from a macromolecule containing tridentate btp ligand fragments coordinated with transition and/or lanthanide metals. As compared with initial macromolecule, the obtained supramolecular films have improved mechanical properties, such as Young modulus, strength and impact toughness, which can be easily adjusted by the stoichiometric ratio of Zn(II) to Eu(III) and Tb(III). Metallosupramolecular films, as well as gels, show fast and efficient properties of self-healing due to kinetically labile character of M–L interactions. We shall notice thermally-responsive gels, which use thermally induced interconversion between *cis*- and *trans*-isomers on cyclam blocks, displaying self-healing property [667].

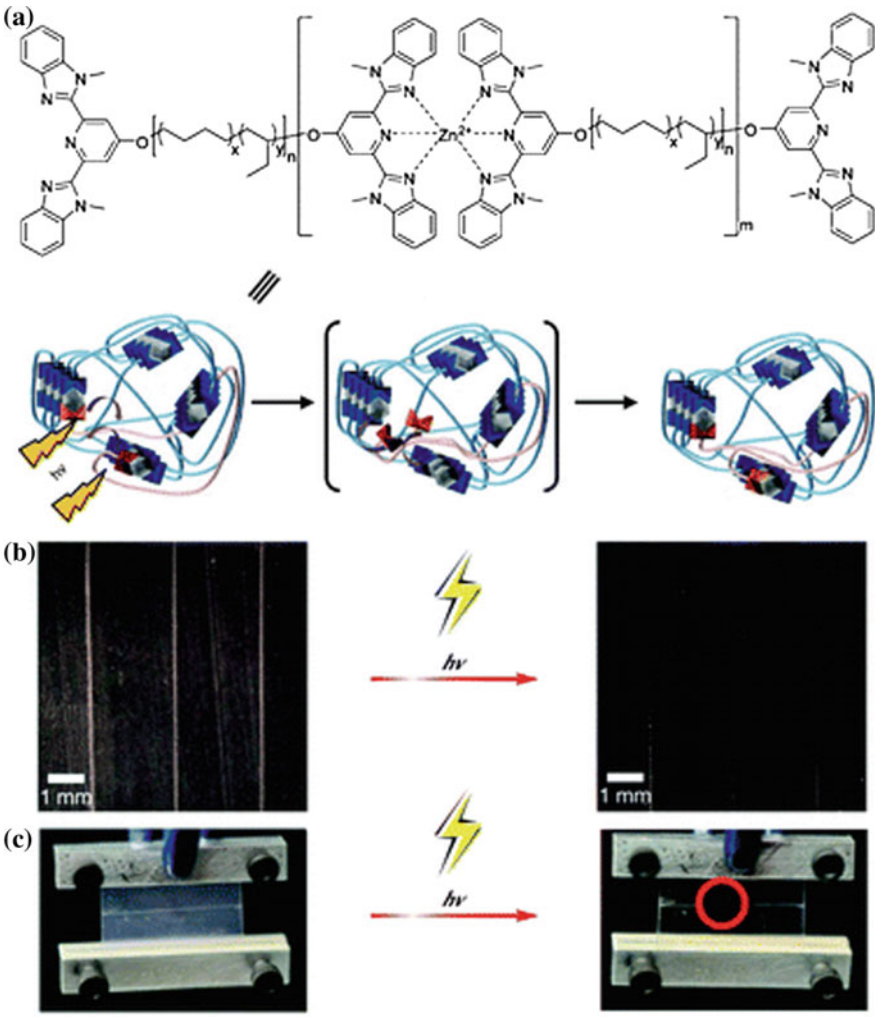

Fig. 7.86 **a** Chemical structure of the MSP and schematic representation of its self-healing process; **b** optical healing of MSP on exposure to light; **c** optical healing of MSP while under a load

The self-healing process is studied in detail using the MSP example including Fe (II)-tpy complexes and different copolymers [668]. In particular, the best results of self-healing were observed at 100 °C for organogel based on lauryl-methacrylate copolymer, while MMA-based gel does not absolutely show self-healing because of lower T_g and, respectively, lower flexibility of a co-monomer. During heating a degree of cross-linking is constant thus showing that self-healing mechanism is not based on decomplexation of tpy complex. Using thermal-induced self-healing mechanism of MSP based on bis-tpy complexes of Fe(II) sulfate and Cd(II)

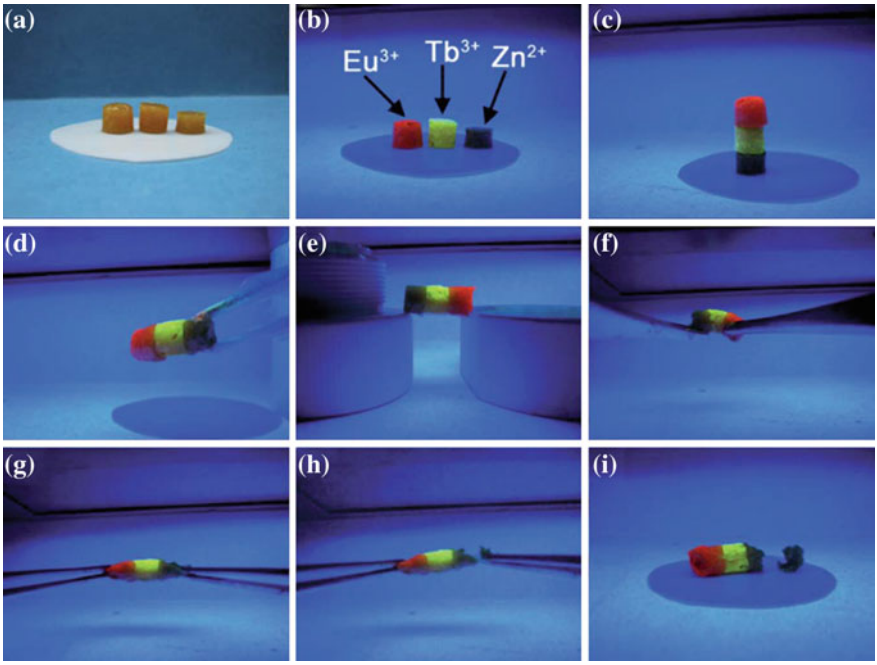

Fig. 7.87 Self-healing the MSPG. **a** Gels containing different metal ions (from left to right are 0:100:0, 0:0:100 and 100:0:0) swollen in toluene; **b** fluorescent image of the three gels under UV light (254 nm); **c** gels were stacked up before self-healing; **d** and **e** the stacked gels were subjected to self-healing under a saturated toluene atmosphere for 1 h; **f–i** the healed gel was then subjected to bending and stretching until fracture

bromide, two possible healing schemes are considered, one of which takes into account decomplexation of cross-linking complexes, and another one is based on dissociation of ionic clusters [669]. It occurs that self-healing mechanisms based on partial decomplexation of cross-linking complexes, are determinative. Apart from nature of a metal, self-healing properties are strongly affected by nature of an anion [670].

We shall also notice using of histidine-metal interactions as reinforcing cross-linkings in self-healing MSP [671]. In particular, a cross-linking of histidine-containing polymers based on butyl methacrylate and lauryl methacrylate with Zn ions brings to MSP networks showing self-healing behavior, which was tunable depending on a certain used Zn salt.

Though polymers with shape memory have been widely developed during the last decade [672], the examples, which use non-covalent interactions in order to fix temporary shape-memory of polymers, are still rare, especially for shape memory of supramolecular polymers [673–676]. The shape memory polymers (SMP) can be deformed to stable temporary shape and reformed to their initial shape using stimuli. These networks are based on presence of two types of pure points to establish their

constant and temporary shapes. Classical strategies for stabilization of temporary shapes are based on cooling below T_g/T_m, where macromolecules are pinned in stressed state. Healing of SMP usually includes heating to temperature above the transition temperature, where a constant shape is remembered. Using of reversible cross-linking groups in SMPs appeared as alternative strategy for stabilization of temporary shapes and providing recyclability to a constant shape.

Ternary (thermo-, photo-, and chemo-) responsive effects with shape memory from photo-cross-linked MSP can be noted as an example [674]. These MSP are obtained by elegant combination of a core of polybutadiene oligomer with capping OMebip ligands and metal ions, in which M–L complexes form a solid phase, which physically cross-links a soft domain of polybutadiene. It is important that any stimulus, which can disturb a solid phase, can be used for fixation of temporary shape and cause its self-healing back into a constant shape, which can be reached by photo-cross-linking of polybutadiene core with tetra-functional thiol through photo-initiated thiol-ene reaction (Fig. 7.88). It has been found that M–L complexes

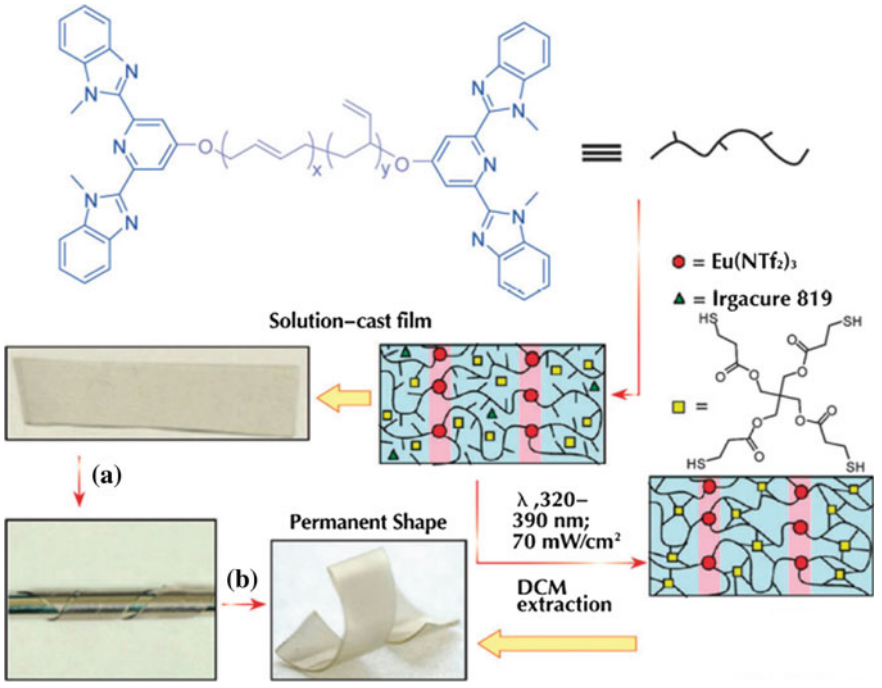

Fig. 7.88 Chelating ligand with terminal groups of polybutadiene macromonomer films, which contain different amounts of tetrathiol cross-linker and photoinitiator (Irgacure 819). Films are solution cast, and the dried films are photo-cross-linked with a targeted 3, 8, and 14 cross-links/chain. The solution-cast uncross-linked films can be fixed into a variety of permanent shapes: **a** a strip of uncross-linked film is wrapped around a cylinder to give a spiral shape, and **b** irradiation with low intensity UV light initiates photo-crosslinking to yield a film with a permanent spiral shape

can absorb light and transfer a part of this energy for heating localization. Therefore, the observed photo-responsive shape memory behavior of MSP film is a result of photothermal transformation process. Besides, chemical substances can also have effect on thermal stability of solid phase of materials through plasticization or decomplexation of M–L chelate. Moreover, a soft phase with different densities of cross-linkings has different shape memory properties with initial restrain of fixation value more than 80% and strain-recovery above 95%.

Such concept of design is used for production of MSPs [677], which react to different stimuli, including influence of heat, UV irradiation, and different solvents. Other SMP are obtained by addition of bistriflimide europium salt [$Eu(NTF_2)_3$] to low molecular weight polybutadiene telechelics carrying Mebip ligands bringing to reversible network. In this case a constant SMP shape is obtained by formation of supramolecular elastomer in a necessary shape with the following photo-cross-linking through thiolene reaction between 1,2-vinyl groups of butadiene core and tetrafunctional thiol. Shape memory can be thermally caused with R_f about 90% and fixing ratio (R_f) above 90% (more typically 97%). Good fixations and strain recoveries are reached, and it is shown that a change in metal ion from Eu(III) to Zn(II) (preserving the same counter-ion) has brought to some decrease in fixation immediately after load removal, and a considerable increase in creep of the temporary shape. It is also important that different solvents, including methanol, acetone, and less triethylamine, can be used to cause shape recovery.

Macromolecular linear poly (*p*-dioxanone) polymers carrying bpy units are cross-linked with Fe(II) ions with formation of a permanent network, while crystallizing segments of *p*-dioxane serve as a thermal trigger for SMP (Scheme 7.26) [496]. Good shape memory characteristics were observed for these SMP, in particular, the R_f approaches 100%, and the extraction coefficient is beyond 93%.

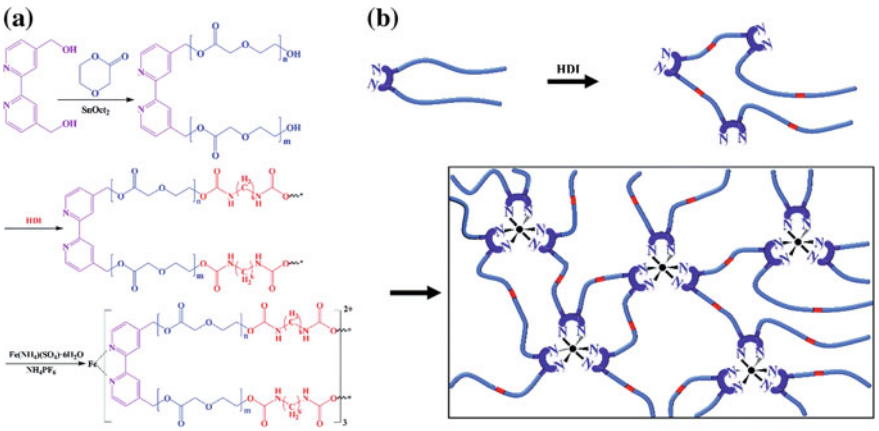

Scheme 7.26 Preparation of metallosupramolecular bpy-poly (p-dioxanone)-Fe. **a** Synthetic route; **b** schematic illustration

The shape memory assisted self-healing (SMASH) polymers include those that combine the shape memory effect with self-healing. Healing of SMASH polymers proceeds in two stages: at the first stage the shape memory effect provides autonomous crack-healing and force applying; at the second stage self-healing of fractured surface takes place. In this view two-component SMASH polymer systems should be noted, in which covalently cross-linked matrices provide the shape memory effect, and healing goes due to diffusion of linear segments of initial polymer ligands at a crack interface [678, 679]. More promising is using of dynamic M–L bond for preparation of SMASH polymers (Fig. 7.89) [511]. Thermal analysis has shown three transitions, which appeared due to Mebip concentration: (a) low T_g of acrylate network (24 °C $\leq T_{g,1} \leq$ 46.8 °C), (b) a glass transition associated with acrylate chains in M–L rich phase divided by domains (68.4 °C $\leq T_{g,2} \leq$ 83.0 °C), (c) a region with high melting point associated with M–L complex decomplexation (95 °C $\leq T_d \leq$ 160 °C). Presence of these two glass transitions and non-covalent network points, ddetermining the permanent shape of SMP, stipulate thermally-induced behavior of the ternary shape memory, and presence of reversible metallosupramolecular bond gives the self-healing capacity. In particular, this was demonstrated by heating of cut and bent samples up to 140 °C, where expected SMASH consequence of shape recovery was observed, crack healing, and self-healing with curable efficiency in the range from 65 to 98%. It is interesting that UV light assisted SMASH has healing efficiencies approaching 100% due to higher temperatures achieved during UV irradiation.

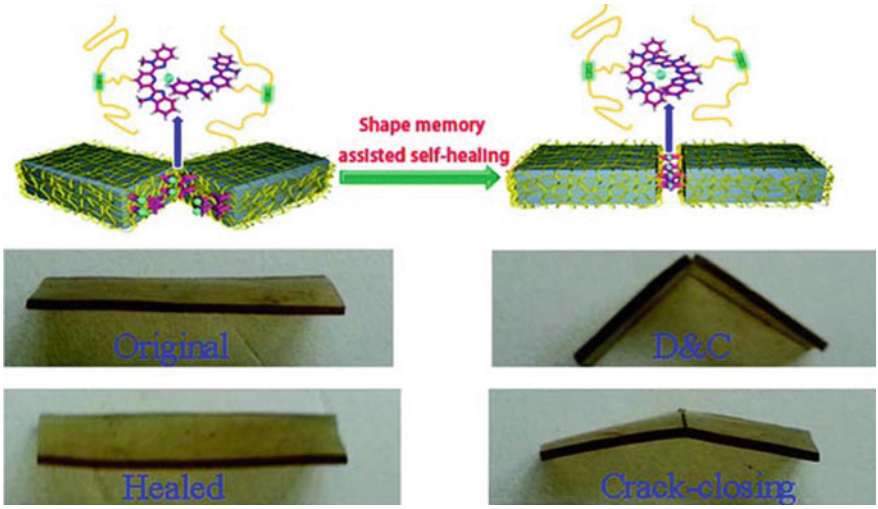

Fig. 7.89 Illustrating the thermal-induced SMASH of supramolecular networks based on poly (*n*-butyl acrylate-*co*-MMA) copolymers bearing Mebip side groups cross-linked by the metal salt zinc trifluoromethanesulfonate. Self-healing experiments conducted as follows: deformation and cracking performed at room temperature; healing performed at 140 °C/25 min

References

1. J.M. Lehn, *Supramolecular Chemistry—Concepts and Perspectives* (Wiley, VCH, Weinheim, 1995)
2. V.G. Machado, P.N.W. Baxter, J.-M. Lehn, J. Braz. Chem. Soc. **12**(4) (2001)
3. J.W. Steed, J.L. Atwood, *Supramolecular Chemistry* (Wiley, Weinheim, 2005)
4. H. Dodziuk, *Introduction to Supramolecular Chemistry* (Kluwer, NY, Boston, Dordrecht, London, Moscow, 2002)
5. J.W. Steed, J.L. Atwood (eds.), *Encyclopedia of Supramolecular Chemistry* (Marcel Dekker, NY, 2004)
6. P.J. Cragg, *Practical Supramolecular Chemistry* (Wiley, Chichester, UK, 2006)
7. K. Ariga, T. Kunitake, *Supramolecular Chemistry—Fundamentals and Applications* (Springer, Heidelberg, 2006)
8. J.W. Steed, D.R. Turner, K.J. Wallace, *Core Concepts in Supramolecular Chemistry and Nanochemistry* (Wiley, Chichester, 2007)
9. R.M. Izatt (ed.), *Macrocyclic and Supramolecular Chemistry: How Izatt-Christensen Award Winners Shaped and Field* (Wiley, Chichester, 2016)
10. G.R. Desiraju, Nature **412**, 397 (2001)
11. A. Wild, A. Winter, F. Schlütter, U.S. Schubert, Chem. Soc. Rev. **40**, 1459 (2011)
12. M. Albrecht, Naturwissenschaften **94**, 951 (2007)
13. W.-S. Tang, X.-X. Lu, K.M.-C. Wong, V.W.-W. Yam, J. Mat. Chem. **15**, 2714 (2005)
14. J.M. Lehn, Proc. Natl. Acad. Sci. U.S.A. **99**, 4769 (2002)
15. O.V. Grineva, Zh Struct, Khim. **47**, 185 (2006)
16. S.Z. Vatsadze, *Comprehensive Problems of Chemistry of Coordination Polymers. Success in the Synthesis of exo-Dentate Tectones* (LAP Lambert Academic Publishing, 2011) (in Russian)
17. M. Simard, D. Su, J.D. Wuest, J. Am. Chem. Soc. **113**, 4696 (1991)
18. E.J. Corey, Pure Appl. Chem. **14**, 19 (1967)
19. K. Ariga, K. Minami, M. Ebara, J. Nakanishi, Polym. J. **48**, 371 (2016)
20. K. Ariga, J. Li, J. Fei, Q. Ji, J.P. Hill, Adv. Mater. **28**, 1251 (2016)
21. G.R. Desiraju, Angew. Chem. Int. Ed. **34**, 2311 (1995)
22. G.R. Desiraju, Angew. Chem. Int. Ed. **46**, 8342 (2007)
23. G.R. Desiraju, J. Mol. Struct. **656**, 5 (2003)
24. C.B. Aakerçy, B.M.T. Scott, M.M. Smith, J.F. Urbina, J. Desper, Inorg. Chem. **48**, 4052 (2009)
25. P.M. Bhatt, Y. Azim, T.S. Thakur, G.R. Desiraju, Cryst. Growth Des. **9**, 951 (2009)
26. R. Banerjee, B.K. Saha, G.R. Desiraju, CrystEngComm **8**, 680 (2006)
27. L.S. Reddy, N.J. Babu, A. Nangia, Chem. Commun. 1369 (2006)
28. C.B. Aakerçy, J. Desper, J.F. Urbina, Chem. Commun. 2820 (2005)
29. D.R. Turner, B. Smith, A.E. Goeta, I.R. Evans, D.A. Tocher, J.A.K. Howard, J.W. Steed, CrystEngComm **6**, 633 (2004)
30. D.K. Kumar, A. Das, P. Dastidar, Cryst. Growth Des. **6**, 216 (2006)
31. S. Kohmoto, Y. Kuroda, Y. Someya, K. Kishikawa, H. Masu, K. Yamaguchi, I. Azumaya, Cryst. Growth Des. **9**, 3437 (2009)
32. H.-J. Schneider, A.K. Yatsimirsky, *Principles and Methods in Supramolecular Chemistry* (Wiley, Chichester, England, 2000)
33. C. Rest, R. Kandanelli, G. Fernández, Chem. Soc. Rev. **44**, 2543 (2015)
34. A. Ciferri, *Supramolecular Polymers*, 2nd edn. (CRC Press, Boca Raton, FL, 2005)
35. U.S. Schubert, C. Eschbaumer, Angew. Chem. Int. Ed. **41**, 2892 (2002)
36. J.M. Lehn, Polym. Int. **51**, 825 (2002)
37. E. Krieg, M.M.C. Bastings, P. Besenius, B. Rybtchinski, Chem. Rev. **116**, 2414 (2016)
38. S. Burattini, B.W. Greenland, D.H. Merino, W. Weng, J. Seppala, H.M. Colquhoun, W. Hayes, M.E. Mackay, I.W. Hamley, S.J. Rowan, J. Am. Chem. Soc. **132**, 12051 (2010)

39. A. Harada (ed.), *Supramolecular Polymer Chemistry* (Wiley-VCH Verlag GmbH & Co. KGaA, Weinheim, 2012)
40. L. Yang, X. Tan, Z. Wang, X. Zhang, Chem. Rev. **115**, 7196 (2015)
41. G.R. Newkome, E.F. He, C.N. Moorefiled, Chem. Rev. **99**, 1689 (1999)
42. G.J. McManus, Z. Wang, M.J. Zaworotko, Cryst. Growth Des. **4**, 11 (2004)
43. T.F.A. De Greef, M.M.J. Smulders, M. Wolffs, A.P.H.J. Schenning, R.P. Sijbesma, E.W. Meijer, Chem. Rev. **109**, 5687 (2009)
44. D. Zhao, J.S. Moore, Org. Biomol. Chem. **1**, 3471 (2003)
45. Z. Chen, A. Lohr, C.R. Saha-Möller, F. Würthner, Chem. Soc. Rev. **38**, 564 (2009)
46. M.M.J. Smulders, M.M.L. Nieuwenhuizen, T.F.A. de Greef, P. van der Schoot, A.P.H. J. Schenning, E.W. Meijer, Chem. Eur. J. **16**, 362 (2010)
47. S.P. Khor, R.J. Varley, S.Z. Shen, Q. Yuan, J. Appl. Polym. Sci. **128**, 3743 (2013)
48. Y. Liu, Z. Wang, X. Zhang, Chem. Soc. Rev. **41**, 5922 (2012)
49. X. Yan, F. Wang, B. Zheng, F. Huang, Chem. Soc. Rev. **41**, 6042 (2012)
50. J.D. Fox, S.J. Rowan, Macromolecules **42**, 6823 (2009)
51. A. Harada, R. Kobayashi, Y. Takashima, A. Hashidzume, H. Yamaguchi, Nat. Chem. **3**, 34 (2011)
52. A. Harada, Y. Takashima, H. Yamaguchi, Chem. Soc. Rev. **38**, 875 (2009)
53. R.J. Wojtecki, M.A. Meador, S.J. Rowan, Nat. Mater. **10**, 14 (2011)
54. T.F.A. de Greef, E.W. Meijer, Nature **453**, 171 (2008)
55. W. Zhang, W. Jin, T. Fukushima, A. Saeki, T. Aida, Science **334**, 340 (2011)
56. E. Krieg, H. Weissman, E. Shirman, E. Shimoni, B. Rybtchinski, Nat. Nanotechnol. **6**, 141 (2011)
57. M.A.C. Stuart, W.T.S. Huck, J. Genzer, M. Müller, C. Ober, M. Stamm, G.B. Sukhorukov, I. Szleifer, V.V. Tsukruk, M. Urban, F. Winnik, S. Zauscher, I. Luzinov, S. Minko, Nat. Mater. **9**, 101 (2010)
58. R.J. Wojtecki, M.A. Meador, S.J. Rowan, Nat. Mater. **10**, 14 (2011)
59. S.K. Yang, A.V. Ambade, M. Weck, Chem. Soc. Rev. **40**, 129 (2011)
60. B. Zheng, F. Wang, S. Dong, F. Huang, Chem. Soc. Rev. **41**, 1621 (2012)
61. T. Aida, E.W. Meijer, S.I. Stupp, Science **335**, 813 (2012)
62. M. Fathalla, C.M. Lawrence, N. Zhang, J.L. Sessler, J. Jayawickramarajah, Chem. Soc. Rev. **38**, 1608 (2009)
63. H.H. Dam, F. Caruso, Adv. Mater. **23**, 3026 (2011)
64. J. Luo, T. Lei, L. Wang, Y. Ma, Y. Cao, J. Wang, J. Pei, J. Am. Chem. Soc. **131**, 2076 (2009)
65. D. Gonzalez-Rodrıgue, A.P.H.J. Schenning, Chem. Mater. **23**, 310 (2011)
66. B.J.B. Folmer, R.P. Sijbesma, R.M. Versteegen, J.A.J. van der Rijt, E.W. Meijer, Adv. Mater. **12**, 874 (2000)
67. L. Sánchez, M.T. Rispens, J.C. Hummelen, Angew. Chem. Int. Ed. **41**, 838 (2002)
68. T. Suzuki, S. Shinkai, K. Sada, Adv. Mater. **18**, 1043 (2006)
69. K.P. Nair, V. Breedveld, M. Weck, Macromolecules **41**, 3429 (2008)
70. L. Brunsveld, B.J.B. Folmer, E.W. Meijer, R.P. Sijbesma, Chem. Rev. **101**, 4071 (2001)
71. E. Kolomiets, E. Buhler, S.J. Candau, J.-M. Lehn, Macromolecules **39**, 1173 (2006)
72. F.J.M. Hoeben, P. Jonkheijm, E.W. Meijer, A.P.H.J. Schenning, Chem. Rev. **105**, 1194 (2005)
73. V.A. Friese, D.G. Kurth, Coord. Chem. Rev. **252**, 199 (2008)
74. D.M.P. Mingos, *Supramolecular Assembly via Hydrogen Bonds* (Springer, Berlin, 2004)
75. R. Dobrawa, F. Würthner, J. Polym. Sci. Part A Polym. Chem. **43**, 4981 (2005)
76. D.G. Kurth, M. Higuchi, Soft Matter **2**, 915 (2006)
77. J.B. Beck, S.J. Rowan, J. Am. Chem. Soc. **125**, 13922 (2003)
78. W.C. Yount, D.M. Loveless, S.L. Craig, J. Am. Chem. Soc. **127**, 14488 (2005)
79. S. Sivakova, D.A. Bohnsack, M.E. Mackay, P. Suwanmala, S.J. Rowan, J. Am. Chem. Soc. **127**, 18202 (2005)
80. J. Adisoejoso, Y. Li, J. Liu, P.N. Liu, N. Lin, J. Am. Chem. Soc. **134**, 18526 (2012)

81. F.S. Han, M. Higuchi, D.G. Kurth, Adv. Mater. **19**, 3928 (2007)
82. F. Peng, G. Li, X. Liu, S. Wu, Z. Tong, J. Am. Chem. Soc. **130**, 16166 (2008)
83. O. Kotova, R. Daly, C.M.G. dos Santos, M. Boese, P.E. Kruger, J.J. Boland, T. Gunnlaugsson, Angew. Chem. Int. Ed. **51**, 7208 (2012)
84. U.S. Schubert, H. Hofmeier, G.R. Newkome, *Modern Terpyridine Chemistry* (Wiley-VCH, Weinheim, 2006)
85. P.R. Andres, U.S. Schubert, Adv. Mater. **16**, 1043 (2004)
86. A.S. Abd-El-Aziz, P.O. Shipman, B.N. Boden, W.S. NcNeil, Prog. Polym. Sci. **35**, 714 (2010)
87. V.A. Friese, D.G. Kurth, Curr. Opin. Colloid Interface Sci. **14**, 81 (2009)
88. Q. Wang, J.L. Mynar, M. Yoshida, E. Lee, M. Lee, K. Okuro, K. Kinbara, T. Aida, Nature **463**, 339 (2010)
89. J.N. Hunt, K.E. Feldman, N.A. Lynd, J. Deek, L.M. Campos, J.M. Spruell, B.M. Hernandez, E.J. Kramer, Adv. Mater. **23**, 2327 (2011)
90. T. Ogoshi, Y. Ichihara, T.A. Yamagishi, Y. Nakamoto, Chem. Commun. **46**, 6087 (2010)
91. J. Fox, J.J. Wie, B.W. Greenland, S. Burattini, W. Hayes, H.M. Colquhoun, M.E. Mackay, S.J. Rowan, J. Am. Chem. Soc. **134**, 5362 (2012)
92. L. Brunsveld, B.J.B. Folmer, E.W. Meijer, MRS Bull. **25**, 49 (2000)
93. A. Cifferi, Macromol. Rapid Commun. **23**, 511 (2002)
94. X. Zhang, C. Wang, Chem. Soc. Rev. **40**, 94 (2011)
95. R. Shunmugam, G.J. Gabriel, K.A. Aamer, G.N. Tew, Macromol. Rapid Commun. **31**, 784 (2010)
96. M. Chiper, R. Hoogenboom, U.S. Schubert, Macromol. Rapid Commun. **30**, 565 (2009)
97. B.M. McKenzie, S.J. Rowan, Metallosupramolecular polymers, networks, and gels, in *Molecular Recognition and Polymers: Control of Polymer Structure and Self-Assembly*, ed. by V. Rotello, S. Thayumanavan (Wiley, Hoboken, 2008)
98. B.M. McKenzie, S.J. Rowan. Metallo-Supramolecular Polymers, in *Encyclopedia of Supramolecular Chemistry*, ed. by J.L. Atwood, J.W. Steed (CRC Press, Boca Raton, 2007)
99. M. Higuchi, J. Mater. Chem. C **2**, 9331 (2014)
100. M. Burnworth, D. Knapton, S.J. Rowan, C. Weder, J. Inorg. Organomet. Polym. **17**, 91 (2007)
101. A.Y.-Y. Tam, V.W.-W. Yam, Chem. Soc. Rev. **42**, 1540 (2013)
102. A.S. Abd-El-Aziz, I. Manners (eds.), *Frontiers in Transition Metal-Containing Polymers* (Wiley, Hoboken, New Jersey, 2006)
103. X.-Y. Hu, T. Xiao, C. Lin, F. Huang, L. Wang, Acc. Chem. Res. **47**, 2041 (2014)
104. Z. Qi, C.A. Schalley, Acc. Chem. Res. **47**, 2222 (2014)
105. K.M.-C. Wong, M.M.-Y. Chan, V.W.-W. Yam, Adv. Mater. **26**, 5558 (2014)
106. J. Zhou, G.R. Whittell, I. Manners, Macromolecules **47**, 3529 (2014)
107. J. Brassinne, C.-A. Fustin, J.-F. Gohy, J. Inorg. Organomet. Polym. **23**, 24 (2013)
108. A.O. Moughton, R.K. O'Reilly, Macromol. Rapid Commun. **31**, 37 (2010)
109. X. Su, I. Aprahamian, Chem. Soc. Rev. **43**, 1963 (2014)
110. G. Lawrance, *Introduction to Coordination Chemistry* (Wiley, Chichester, 2009)
111. L. Cronin, Annu. Rep. Prog. Chem. Sect. A Inorg. Chem. **101**, 348 (2005)
112. O. Costisor, W. Linert, Rev. Inorg. Chem. **23**, 289 (2003)
113. Y. Yan, J.B. Huang, Coord. Chem. Rev. **254**, 1072 (2010)
114. S.J. Rowan, J.B. Beck, Faraday Discuss. **128**, 43 (2005)
115. J.B. Beck, J.M. Ineman, S.J. Rowan, Macromolecules **38**, 5060 (2005)
116. AYu. Tsivadze, Uspehi Khim. **73**, 6 (2004)
117. AYu. Tsivadze, G.V. Ionova, V.K. Mihalko, YuN Kostrubov, Uspehi Khim. **76**, 237 (2007)
118. G.M. Mamardashvili, NZh Mamardashvili, O.I. Koifman, Uspehi Khim. **74**, 839 (2005)
119. G.M. Mamardashvili, NZh Mamardashvili, O.I. Koifman, Uspehi Khim. **77**, 60 (2008)
120. A.N. Khlobystov, A.J. Blake, N.R. Champness, D.A. Lemenovskii, A.G. Majouga, N.V. Zyk, M. Schroder, Coord. Chem. Rev. **222**, 155 (2001)
121. S. Leininger, B. Olenyuk, P.J. Stang, Chem. Rev. **100**, 853 (2000)

122. G.F. Swiegers, T.J. Malefeste, Chem. Rev. **100**, 3483 (2000)
123. YuE Alexeev, B.I. Kharisov, T.C. Hernandez Garcia, A.D. Garnovskii, Coord. Chem. Rev. **254**, 794 (2010)
124. U.S. Schubert, O. Hien, C. Eschbaumer, Macromol. Rapid Commun. **21**, 1156 (2000)
125. S. Schmatloch, M.F. Gonzalez, U.S. Schubert, Macromol. Rapid Commun. **23**, 957 (2002)
126. M.A.R. Meier, B.G.G. Lohmeijer, U.S. Schubert, Macromol. Rapid Commun. **24**, 852 (2003)
127. C.-C. Chen, E. Dormidontova, J. Am. Chem. Soc. **126**, 14972 (2004)
128. B.H. Northrop, Y.-R. Zheng, K.-W. Chi, P.J. Stang, Acc. Chem. Res. **42**, 1554 (2009)
129. Y.Q. Zhao, J.B. Beck, S.J. Rowan, A.M. Jamieson, Macromolecules **37**, 3529 (2004)
130. W.G. Weng, J.B. Beck, A.M. Jamieson, S.J. Rowan, J. Am. Chem. Soc. **128**, 11663 (2006)
131. G. Schwarz, I. Haßlauer, D.G. Kurth, Adv. Colloid Interface Sci. **207**, 107 (2014)
132. Y. Yan, J. Huang, Coord. Chem. Rev. **254**, 1072 (2010)
133. A. Maier, A.R. Rabindranath, B. Tieke, Adv. Mater. **21**, 959 (2009)
134. J.M. Pollino, M. Weck, Chem. Soc. Rev. **34**, 193 (2005)
135. K.A. Aamer, G.N. Tew, Macromolecules **40**, 2737 (2007)
136. M.R. Hammond, A.K. Andreopoulou, E. Pefkianakis, J.K. Kallitsis, R. Mezzenga, Chem. Mater. **21**, 2169 (2009)
137. R. Shunmugam, G. Tew, Macromol. Rapid Commun. **29**, 1355 (2008)
138. K. Calzia, G. Tew, Macromolecules **35**, 6090 (2002)
139. R. Shunmugam, G. Tew, Polym. Adv. Technol. **19**, 596 (2008)
140. T.K. Sievers, A. Vergin, H. Möhwald, D.G. Kurth, Langmuir **23**, 12179 (2007)
141. R. Johnson, C. Fraser, Macromolecules **37**, 2718 (2004)
142. R. Pal, M. Higuchi, D. Kurth, Org. Lett. **11**, 3562 (2009)
143. E. Zangrando, M. Casanova, E. Alessio, Chem. Rev. **108**, 4979 (2008)
144. E.C. Constable, K. Harris, C.E. Housecroft, M. Neuburger, Dalton Trans. **40**, 1524 (2011)
145. P. Wang, C. Moorefield, G. Newkome, Angew. Chem. Int. Ed. **44**, 1679 (2005)
146. B. Zhao, H. Li, Q. Shen, Y. Zhang, Y. Yao, C. Lu, Organometallics **25**, 1824 (2006)
147. R.W. Troff, R. Hovorka, T. Weilandt, A. Lutzen, M. Cetina, M. Nieger, D. Lentz, K. Rissanen, C.A. Schalley, Dalton Trans. **41**, 8410 (2012)
148. P.R. Andres, U.S. Schubert, Synthesis 1229 (2004)
149. G. Seeber, B. Kariuki, L. Cronin, Chem. Commun. 2912 (2002)
150. Z. Ni, J. Tao, W. Wernsdorfer, A. Cui, H. Kou, Dalton Trans. 2788 (2009)
151. C. Smith, E. Constable, C. Housecroft, B. Kariuki, Chem. Commun. 2068 (2002)
152. R.M. Meudtner, S. Hecht, Macromol. Rapid Commun. **29**, 347 (2008)
153. R.M. Meudtner, M. Ostermeier, R. Goddard, C. Limberg, S. Hecht, Chem. Eur. J. **13**, 9834 (2007)
154. D. Astruc, E. Boisselier, C. Ornelas, Chem. Rev. **110**, 1857 (2010)
155. R. Hoogenboom, U.S. Schubert, Chem. Soc. Rev. **35**, 622 (2006)
156. S.J. Payne, G.L. Fiore, C.L. Fraser, J.N. Demas, Anal. Chem. **82**, 917 (2010)
157. F.S. Han, M. Higuchi, D.G. Kurth, J. Am. Chem. Soc. **130**, 2073 (2008)
158. R. Dobrawa, M. Lysetska, P. Ballester, M. Grüne, F. Würthner, Macromolecules **38**, 1315 (2005)
159. V. Marin, E. Holder, R. Hoogenboom, U.S. Schubert, Chem. Rev. Soc. **36**, 618 (2007)
160. F.S. Han, M. Higuchi, Y. Akasaka, Y. Otsuka, D.G. Kurth, Thin Solid Films **516**, 2469 (2008)
161. C.-F. Chow, S. Fujii, J.-M. Lehn, Angew. Chem. Int. Ed. **46**, 5007 (2007)
162. H.J. Yoon, J. Kuwabara, J.-H. Kim, C.A. Mirkin, Science **330**, 66 (2010)
163. N. Masciocchi, S. Galli, A. Sironi, E. Cariati, M.A. Galindo, E. Barea, M.A. Romero, J.M. Salas, J.A.R. Navarro, F. Santoyo-Gonzalez, Inorg. Chem. **45**, 7612 (2006)
164. L.N. Dawe, J. Miglioi, L. Turnbow, M.L. Taliaferro, W.W. Shum, J.D. Bagnato, L.N. Zakharov, A.L. Rheingold, A.M. Arif, M. Fourmigue, J.S. Miller, Inorg. Chem. **44**, 7530 (2005)

165. G.-W. Zhou, Y.-Z. Lan, F.K. Zheng, X. Zhang, M.-H. Lin, G.-C. Guo, J.-S. Huang, Chem. Phys. Lett. **426**, 341 (2006)
166. S. Bidault, L. Viau, O. Maury, S. Brasselet, J. Zyss, E. Ishow, K. Nakatani, H.L. Bozec, Adv. Funct. Mater. **16**, 2252 (2006)
167. N. Gunnlaugsson, J.P. Leonard, Chem. Commun. 3114 (2005)
168. H. Li, L. Wu, Soft Matter **10**, 9038 (2014)
169. H. Hofmeier, U.S. Schubert, Chem. Commun. 2423 (2005)
170. H. Hofmeier, R. Hoogenboom, M.E.L. Wouters, U.S. Schubert, J. Am. Chem. Soc. **127**, 2913 (2005)
171. L. Shi, X.W. Wang, C.A. Sandoval, M.X. Li, Q.Y. Qi, Z.T. Li, K.L. Ding, Angew. Chem. Int. Ed. **45**, 4108 (2006)
172. V. Marin, E. Holder, R. Hoogenboom, E. Tekin, U.S. Schubert, Dalton Trans. 1636 (2006)
173. J.-M. Lehn, Chem. Soc. Rev. **36**, 151 (2007)
174. J.-M. Lehn, Rep. Prog. Phys. **67**, 249 (2004)
175. G.R. Whittell, M.D. Hager, U.S. Schubert, I. Manners, Nat. Mater. **10**, 176 (2011)
176. J.-C. Eloi, L. Chabanne, G.R. Whittell, I. Manners, Mater. Today **11**, 28 (2008)
177. J.-M. Lehn, Constitutional dynamic chemistry: bridge from supramolecular chemistry to adaptive chemistry, in *Constitutional Dynamic Chemistry*, ed. by M. Barboiu (Springer, Heidelberg, Dordrecht, London, NY, 2012)
178. S. Schmatloch, A.M.J. van den Berg, M.W.M. Fijten, U.S. Schubert, PMSE Prepr. **90**, 645 (2004)
179. U.S. Schubert, A. Winter, G.R. Newkome, *Terpyridine-based Materials: For Catalytic, Optoelectronic and Life Science Applications* (Wiley-VCH, Weinheim, 2012)
180. S.V. Vinogradova, V.A. Vasnev, M.L. Keshtov, Polym. Sci. Ser. B **49**, 267 (2007)
181. S. Kelch, M. Rehahn, Macromolecules **32**, 5818 (1999)
182. C.D. Eisenbach, U.S. Schubert, Macromolecules **26**, 7372 (1993)
183. B. Lahn, M. Rehahn, Macromol. Symp. **163**, 157 (2001)
184. U. Velten, M. Rehahn, Macromol. Chem. Phys. **199**, 127 (1998)
185. U. Velten, M. Rehahn, M., Chem. Commun. 2639 (1996)
186. U. Velten, B. Lahn, M. Rehahn, Macromol. Chem. Phys. **198**, 2789 (1997)
187. M.D. Hossain, M. Higuchi, Synthesis **45**, 753 (2013)
188. D. Hossain, T. Sato, M. Higuchi, Chem. Asian J. **8**, 76 (2013)
189. R.K. Pandey, D. Hossain, S. Moriyama, M. Higuchi, J. Mater. Chem. A **1**, 9016 (2013)
190. M.H. Demirel, S. Köytepe, A. Gültek, T. Seçkin, J. Polym. Res. **21**, 345 (2014)
191. M. Demirel, S. Köytepe, A. Gültek, T. Seçkin, J. Polym. Res. **21**, 1 (2014)
192. H. Hofmeier, S. Schmatloch, D. Wouters, U.S. Schubert, Macromol. Chem. Phys. **204**, 2197 (2003)
193. S. Schmatloch, A.M.J. van den Berg, A.S. Alexeev, H. Hofmeier, U.S. Schubert, Macromolecules **36**, 9943 (2003)
194. S. Schmatloch, U.S. Schubert, Macromol. Symp. **199**, 483 (2003)
195. S. Schmatloch, A.M.J. Van den Berg, H. Hofmeier, U.S. Schubert, Des. Monom. Polym. **7**, 191 (2004)
196. P.K. Iyer, J.B. Beck, C. Weder, S.J. Rowan, Chem. Commun. 319 (2005)
197. T. Vermonden, J. van der Gucht, P. de Waard, A.T.M. Marcelis, N.A.M. Besseling, E.J.R. Sudholter, G.J. Fleer, M.A. Cohen, Stuart. Macromolecules **36**, 7035 (2003)
198. A. Wild, A. Winter, M.D. Hager, H. Görls, U.S. Schubert, Macromol. Rapid Commun. **33**, 517 (2012)
199. H. Padhy, M. Ramesh, D. Patra, R. Satapathy, M.K. Pola, H.-C. Chu, C.-W. Chu, K.-H. Wei, H.-C. Lin, Macromol. Rapid Commun. **33**, 528 (2012)
200. T. Sato, R.K. Pandey, M. Higuchi, Dalton Trans. **42**, 16036 (2013)
201. R. Dobrawa, P. Ballester, F. Würthner, Thermodynamics of 2,2′:6′,2″-terpyridine-metal ion complexation, in *Metal-containing and Metallosupramolecular Polymers and Materials,* ed. by U.S. Schubert, G.R. Newkome, I. Manners, ACS Symposium Series, vol. 928 (Washington D.C., 2006)

202. F. Würthner, Chem. Commun. 1564 (2004)
203. S.C. Yu, C.C. Kwok, W.K. Chan, C.M. Che, Adv. Mater. **15**, 1643 (2003)
204. Y.-Y. Chen, Y.-T. Tao, H.C. Lin, Macromolecules **39**, 8559 (2006)
205. Y.-Y. Chen, H.-C. Lin, J. Polym. Sci. Part A Polym. Chem. **45**, 3243 (2007)
206. M. Chiper, M.A.R. Meier, J.M. Kranenburg, U.S. Schubert, Macromol. Chem. Phys. **208**, 679 (2007)
207. U. Mansfeld, A. Winter, M.D. Hager, R. Hoogenboom, W. Günther, U.S. Schubert, Polym. Chem. **4**, 113 (2013)
208. S. Schmatloch, A.M.J. van den Berg, M.W.M. Fijten, U.S. Schubert, Macromol. Rapid Commun. **25**, 321 (2004)
209. J.-H. Li, M. Higuchi, J. Inorg. Organomet. Polym. **20**, 10 (2010)
210. C. Friebe, A. Wild, J. Perelaer, U.S. Schubert, Macromol. Rapid Commun. **33**, 503 (2012)
211. H. Miyake, Symmetry **6**, 880 (2014)
212. S. Köytepe, M.H. Demirel, A. Gültek, T. Seçkin, Polym. Int. **63**, 778 (2014)
213. R. Siebert, A. Winter, M. Schmitt, J. Popp, U.S. Schubert, B. Dietzek, Macromol. Rapid Commun. **33**, 481 (2012)
214. H. Hofmeier, U.S. Schubert, Chem. Soc. Rev. **33**, 373 (2004)
215. V. Balzani, S. Campagna (eds.), *Photochemistry and Photophysics of Coordination Compounds* (Springer, Berlin, 2007)
216. V. Duprez, M. Biancardo, H. Spanggaard, F.C. Krebs, Macromolecules **38**, 10436 (2005)
217. P. Song, S.-G. Sun, P.-W. Zhou, J.-Y. Liu, Y.-Q. Xu, X.-J. Peng, China. J. Chem. Phys. **23**, 558 (2010)
218. C.-C. You, R. Dobrawa, C.R. Saha-Möller, F. Würthner, Metallosupramolecular dye assemblies, in *Supermolecular Dye Chemistry*, ed. by F. Würthner. Top. Curr. Chem. **258**, 39 (2005)
219. T. Suzuki, T. Sato, J. Zhang, M. Kanao, M. Higuchi, H. Maki, J. Mater. Chem. C **4**, 1594 (2016)
220. X. Chen, K. Guo, F. Li, L. Zhou, H. Qiao, RSC Adv. **4**, 58027 (2014)
221. L. He, J. Liang, Y. Cong, X. Chen, W. Bu, Chem. Commun. **50**, 10841 (2014)
222. J.R. Kumpfer, J. Jin, S.J. Rowan, J. Mater. Chem. **20**, 145 (2010)
223. D. Knapton, M. Burnworth, S.J. Rowan, C. Weder, Angew. Chem. Int. Ed. **45**, 5825 (2006)
224. B.M. Mckenzie, R.J. Wojtecki, K.A. Burke, C. Zhang, A. Jakli, P.T. Mather, S.J. Rowan, Chem. Mater. **23**, 3525 (2011)
225. A. Duerrbeck, S. Gorelik, J. Hobley, J. Wu, A. Hor, N. Long, Chem. Commun. **51**, 8656 (2015)
226. J.P. Byrne, J.A. Kitchen, T. Gunnlaugsson, Chem. Soc. Rev. **43**, 5302 (2014)
227. J.P. Byrne, M. Martínez-Calvo, R.D. Peacock, T. Gunnlaugsson, Chem. – Eur. J. **22**, 486 (2016)
228. B. Schulze, C. Friebe, S. Hoeppener, G.M. Pavlov, A. Winter, M.D. Hager, U.S. Schubert, Macromol. Rapid Commun. **33**, 597 (2012)
229. M. Burnworth, D. Knapton, S.J. Rowan, C. Weder, J. Inorg. Organomet. Polym. **17**, 91 (2007)
230. M. Burnworth, S.J. Rowan, C. Weder, Macromolecules **45**, 126 (2012)
231. C. Rajadurai, O. Fuhr, R. Kruk, M. Ghafari, H. Hahn, M. Ruben, Chem. Commun. 2636 (2007)
232. C.-F. Chow, S. Fujii, J.-M. Lehn, Chem. Asian J. **3**, 1324 (2008)
233. L.A. Paquette, J. Tae, J. Am. Chem. Soc. **123**, 4974 (2001)
234. Y.Y. Karabach, A.N. Kirillov, M.F.C. Guedes da Silva, M.N. Kopylovich, A.J.L. Pombeiro, Cryst. Growth Des. **6**, 2200 (2006)
235. Y.Y. Karabach, A.M. Kirillov, M. Haukka, M.N. Kopylovich, A.J.L. Pombeiro, J. Inorg. Biochem. **102**, 1190 (2008)
236. C.A. Fustin, P. Guillet, U.S. Schubert, J.-F. Gohy, Adv. Mater. **19**, 1665 (2007)
237. J.-F. Gohy, B.G.G. Lohmeijer, U.S. Schubert, Macromol. Rapid Commun. **23**, 555 (2002)
238. J.-F. Gohy, B.G.G. Lohmeijer, U.S. Schubert, Chem. Eur. J. **9**, 3472 (2003)

239. M. Chiper, A. Winter, R. Hoogenboom, D.A.M. Egbe, D. Wouters, S. Hoeppener, C.-A. Fustin, J.-F. Gohy, U.S. Schubert, Macromolecules **41**, 8823 (2008)
240. M. Chiper, M.A.R. Meier, D. Wouters, S. Hoeppener, C.-A. Fustin, J.-F. Gohy, U.S. Schubert, Macromolecules **41**, 2771 (2008)
241. J.-F. Gohy, B.G.L. Lohmeijer, S.K. Varshney, B. Decamps, E. Leroy, S. Boileau, U.S. Schubert, Macromolecules **35**, 9748 (2002)
242. R. Hoogenboom, D. Fournier, U.S. Schubert, Chem. Commun. 155 (2008)
243. B.G.G. Lohmeijer, U.S. Schubert, Angew. Chem. Int. Ed. **41**, 3825 (2002)
244. J.F. Gohy, B.G.G. Lohmeijer, S.K. Varshney, U.S. Schubert, Macromolecules **35**, 7427 (2002)
245. C. Ott, D. Wouters, H.M.L. Thijs, U.S. Schubert, J. Inorg. Organomet. Polym. **17**, 241 (2007)
246. J.F. Gohy, B.G.G. Lohmeijer, U.S. Schubert, Macromolecules **35**, 4560 (2002)
247. O. Regev, J.F. Gohy, B.G.G. Lohmeijer, S.K. Varshney, D.H.W. Hubert, P.M. Frederik, U.S. Schubert, Colloid Polym. Sci. **282**, 407 (2004)
248. G. Mayer, V. Vogel, B.G.G. Lohmeijer, J.F. Gohy, G.A. van den Broek, W. Haase, U.S. Schubert, D. Schubert, J. Polym. Sci. Part A Polym. Chem. **42**, 4458 (2004)
249. M. Al-Hussein, B.G.G. Lohmeijer, U.S. Schubert, W.H. De Jeu, Macromolecules **36**, 9281 (2003)
250. M. Al-Hussein, W.H. De Jeu, B.G.G. Lohmeijer, U.S. Schubert, Macromolecules **38**, 2832 (2005)
251. H. Goldansaz, Q. Voleppe, S. Piogé, C.A. Fustin, J.F. Gohy, J. Brassinne, D. Auhl, E. van Ruymbeke, Soft Matter **11**, 762 (2015)
252. B.G.G. Lohmeijer, D. Wouters, Z. Yin, U.S. Schubert, Chem. Commun. 2886 (2004)
253. P. Guillet, C.A. Fustin, B.G.G. Lohmeijer, U.S. Schubert, J.F. Gohy, Macromolecules **39**, 5484 (2006)
254. C.A. Fustin, B.G.G. Lohmeijer, A.S. Duwez, A.M. Jonas, U.S. Schubert, J.F. Gohy, Adv. Mater. **17**, 1162 (2005)
255. J.F. Gohy, B.G.G. Lohmeijer, A. Alexeev, X.S. Wang, I. Manners, M.A. Winnik, U.S. Schubert, Chem. Eur. J. **10**, 4315 (2004)
256. G. Zhou, I.I. Harruna, Macromolecules **38**, 4114 (2005)
257. C. Mugemana, P. Guillet, S. Hoeppener, U.S. Schubert, C.-A. Fustin, Chem. Commun. 1296 (2010)
258. M.A.R. Meier, D. Wouters, C. Ott, P. Guillet, C.-A. Fustin, J.-F. Gohy, U.S. Schubert, Macromolecules **39**, 1569 (2006)
259. H. Li, W. Wei, H. Xiong, Soft Matter **12**, 1411 (2016)
260. D. Pijper, B.L. Feringa, Soft Matter **4**, 1349 (2008)
261. T. Vermonden, W.M. de Vos, A.T.M. Marcelis, E.J.R. Sudholter, Eur. J. Inorg. Chem. **2004**, 2847 (2004)
262. T. Vermonden, M.J. van Steenbergen, N.A.M. Besseling, A.T.M. Marcelis, W.E. Hennink, E.J.R. Sudholter, M.A. Cohen, Stuart. J. Am. Chem. Soc. **126**, 15802 (2004)
263. A. Schultz, X. Li, B. Barkakaty, C.N. Moorefield, C. Wesdemiotis, G.R. Newkome, J. Am. Chem. Soc. **134**, 7672 (2012)
264. A. Fermi, G. Bergamini, M. Roy, M. Gingras, P. Ceroni, J. Am. Chem. Soc. **136**, 6395 (2014)
265. J.-F. Gohy, M. Chiper, P. Guillet, C.-A. Fustin, S. Hoeppener, A. Winter, R. Hoogenboom, U.S. Schubert, Soft Matter **5**, 2954 (2009)
266. J.E. McAlvin, C.L. Fraser, Macromolecules **32**, 1341 (1999)
267. C. Park, J.E. McAlvin, C.L. Fraser, E.L. Thomas, Chem. Mater. **14**, 1225 (2002)
268. R.M. Johnson, C.L. Fraser, Biomacromol **5**, 580 (2004)
269. U.S. Schubert, C. Eschbaumer, O. Nuyken, G. Hochwimmer, J. Inclusion Phenomena and Macrocyclic Chem. **35**, 23 (1999)
270. A.P. Smith, C.L. Fraser, Macromolecules **35**, 594 (2002)
271. C.L. Fraser, A.P. Smith, X. Wu, J. Am. Chem. Soc. **122**, 9026 (2000)

272. A.P. Smith, C.L. Fraser, Macromolecules **36**, 5520 (2003)
273. J.L. Bender, P.S. Corbin, C.L. Fraser, D.H. Metcalf, F.S. Richardson, E.L. Thomas, A.M. Urbas, J. Am. Chem. Soc. **124**, 8526 (2002)
274. R.K. Pandey, D. Hossain, T. Sato, U. Rana, S. Moriyama, M. Higuchi, RSC Adv. **5**, 49224 (2015)
275. D.M. Loveless, S.L. Jeon, S.L. Craig, Macromolecules **38**, 10171 (2005)
276. D.M. Loveless, S.L. Jeon, S.L. Craig, J. Mater. Chem. **17**, 56 (2007)
277. X. Chu, P. Xing, S. Li, M. Ma, J. Hao, A. Hao, RSC Adv. **5**, 1969 (2015)
278. A. Duerrbeck, S. Gorelik, J. Hobley, A.M. Yong, G.S. Subramanian, A. Hor, N. Long, J. Mater. Chem. C **3**, 8992 (2015)
279. C.-W. Hu, T. Sato, J. Zhang, S. Moriyama, M. Higuchi, A.C.S. Appl, Mater. Interfaces **6**, 9118 (2014)
280. I. Welterlich, B. Tieke, Macromolecules **44**, 4194 (2011)
281. J. Brassinne, E. Poggi, C.-A. Fustin, J.-F. Gohy, Macromol. Rapid Commun. **36**, 610 (2015)
282. P. Guillet, C.-A. Fustin, C. Mugemana, C. Ott, U.S. Schubert, J.-F. Gohy, Soft Matter **4**, 2278 (2008)
283. M. Chiper, S. Hoeppener, U. Schubert, C.-A. Fustin, J.-F. Gohy, Macromol. Chem. Phys. **211**, 2323 (2010)
284. S. Wang, C.-C. Chen, E.E. Dormidontova, Soft Matter **4**, 2039 (2008)
285. T. Sato, M. Higuchi, Chem. Commun. **49**, 5256 (2013)
286. L. Yu, Z. Wang, J. Wu, S. Tu, K. Ding, Angew. Chem. Int. Ed. **49**, 3627 (2010)
287. S. Gosh, L. Isaacs, Complex self-sorting systems, in *Dynamic Combinatorial Chemistry*, ed. by B.L. Miller (Wiley-VCH, Weinheim, 2010)
288. K. Osowska, O.Š. Miljanić, Synlett 1643 (2011)
289. M.M. Safont-Sempere, G. Fernández, F. Würthner, Chem. Rev. **111**, 5784 (2011)
290. M.L. Saha, M. Schmittel, Org. Biomol. Chem. **10**, 4651 (2012)
291. Z. He, W. Jiang, C.A. Schalley, Chem. Soc. Rev. **44**, 779 (2015)
292. I. Kocsis, D. Dumitrescu, Y.-M. Legrand, A. van der Lee, I. Grosu, M. Barboiu, Chem. Commun. **50**, 2621 (2014)
293. Y.-K. Tian, L. Chen, Y.-J. Tian, X.-Y. Wang, F. Wang, Polym. Chem. **4**, 453 (2013)
294. Y. Li, Z. Jiang, J. Yuan, D. Liu, T. Wu, C.N. Moorefield, G.R. Newkome, P. Wang, Chem. Commun. **51**, 5766 (2015)
295. M. Higuchi, Polym. J. **41**, 511 (2009)
296. S.M. Munzert, G. Schwarz, D.G. Kurth, RSC Adv. **6**, 15441 (2016)
297. G. Schwarz, T.K. Sievers, Y. Bodenthin, I. Hasslauer, T. Geue, J. Koetz, D.G. Kurth, J. Mater. Chem. **20**, 4142 (2010)
298. D.G. Kurth, M. Schütte, J. Wen, Colloids Surf.: A: Physicochem. Eng. Asp. **198–200**, 633 (2002)
299. M. Schütte, C. Stolle, D.G. Kurth, Supramol. Chem. **15**, 549 (2003)
300. Y. Bodenthin, G. Schwarz, Z. Tomkowicz, T. Geue, W. Haase, U. Pietsch, D.G. Kurth, J. Am. Chem. Soc. **131**, 2934 (2009)
301. C. Kaes, A. Katz, M.W. Hosseini, Chem. Rev. **100**, 3553 (2000)
302. R.J. Mortimer, Annu. Rev. Mater. Res. **41**, 241 (2011)
303. G. Schwarz, Y. Bodenthin, T. Geue, J. Koetz, D.G. Kurth, Macromolecules **43**, 494 (2010)
304. M.A.R. Meier, H. Hofmeier, C.H. Abeln, C. Tziatzios, M. Rasa, D. Schubert, U.S. Schubert, e-polymers **16**, 1 (2006)
305. M. Rasa, B.G.G. Lohmeijer, H. Hofmeier, H.M.L. Thijs, D. Schubert, U.S. Schubert, C. Tziatzios, Macromol. Chem. Phys. **207**, 2029 (2006)
306. W.-H. Chen, T.-H. Chang, C.-W. Hu, K.-M. Ting, Y.-C. Liao, K.-C. Ho, Solar energy mater. Solar Cells **126**, 219 (2014)
307. S. Bernhard, J.I. Goldsmith, K. Takada, H.D. Abruna, Inorg. Chem. **42**, 4389 (2003)
308. M. Schott, H. Lorrmann, M. Beck, D.G. Kurth, Solar energy mater. Solar Cells **126**, 68 (2014)

309. J. England, C.C. Scarborough, T. Weyhermüller, S. Sproules, K. Wieghardt, Eur. J. Inorg. Chem. **2012**, 4605 (2012)
310. P.M. Beaujuge, J.R. Reynolds, Chem. Rev. **110**, 268 (2010)
311. C.M. Amb, L.D. Aubrey, J.R. Reynolds, Chem. Mater. **23**, 397 (2011)
312. M. Higuchi, Y. Otsuka, R. Shomura, D.G. Kurth, Thin Solid Films **516**, 2416 (2008)
313. M. Higuchi, Y. Akasaka, T. Ikeda, A. Hayashi, D.G. Kurth, J. Inorg. Organomet. Polym. **19**, 74 (2009)
314. H. Krass, G. Papastavrou, D.G. Kurth, Chem. Mater. **15**, 196 (2002)
315. D.G. Kurth, J. Pitarch Lopez, W.-F. Dong, Chem. Commun. 2119 (2005)
316. W. Szczerba, M. Schott, H. Riesemeier, A.F. Thünemann, D.G. Kurth, Phys. Chem. Chem. Phys. **16**, 19694 (2014)
317. M. Higuchi, D.G. Kurth, Chem. Rec. **7**, 203 (2007)
318. D. Akcakayiran, D. Mauder, C. Hess, T.K. Sievers, D.G. Kurth, I. Shenderovich, H.-H. Limbach, G.H. Findenegg, J. Phys. Chem. B **112**, 14637 (2008)
319. D. Akcakayiran, D.G. Kurth, S. Rohrs, G. Rupprechter, G.H. Findenegg, Langmuir **21**, 7501 (2005)
320. G. Schwarz, S. Maisch, S. Ullrich, J. Wagenhöfer, D.G. Kurth, A.C.S. Appl, Mater. Interfaces **5**, 4031 (2013)
321. M.F. Geist, C.S. Peyratout, D.G. Kurth, ChemNanoMat **1**, 489 (2015)
322. U. Kolb, K. Büscher, C.A. Helm, A. Lindner, A.F. Thünemann, M. Menzel, M. Higuchi, D.G. Kurth, Proc. Natl. Acad. Sci. **103**, 10202 (2006)
323. A.V. Ambade, S.K. Yang, M. Weck, Angew. Chem. Int. Ed. **48**, 2894 (2009)
324. G. Gröger, W. Meyer-Zaika, C. Böttcher, F. Gröhn, C. Ruthard, C. Schmuck, J. Am. Chem. Soc. **133**, 8961 (2011)
325. L. Zhu, M. Lu, Q. Zhang, D. Qu, H. Tian, Macromolecules **44**, 4092 (2011)
326. S.K. Yang, A.V. Ambade, M. Weck, J. Am. Chem. Soc. **132**, 1637 (2010)
327. S.-L. Li, T. Xiao, Y. Wu, J. Jiang, L. Wang, Chem. Commun. **47**, 6903 (2011)
328. S.-L. Li, T. Xiao, B. Hu, Y. Zhang, F. Zhao, Y. Ji, Y. Yu, C. Lin, L. Wang, Chem. Commun. **47**, 10755 (2011)
329. S.-G. Chen, Y. Yu, X. Zhao, Y. Ma, X.-K. Jiang, Z.-T. Li, J. Am. Chem. Soc. **133**, 11124 (2011)
330. Z. Niu, F. Huang, H.W. Gibson, J. Am. Chem. Soc. **133**, 2836 (2011)
331. F. Wang, J. Zhang, X. Ding, S. Dong, M. Liu, B. Zheng, S. Li, L. Wu, Y. Yu, H.W. Gibson, F. Huang, Angew. Chem. Int. Ed. **49**, 1090 (2010)
332. E. Elacqua, D.S. Lye, M. Weck, Acc. Chem. Res. **47**, 2405 (2014)
333. J.M. Pollino, L.P. Stubbs, M. Weck, J. Am. Chem. Soc. **126**, 563 (2004)
334. M.L. Saha, S. De, S. Pramanik, M. Schmittel, Chem. Soc. Rev. **42**, 6860 (2013)
335. S.-L. Li, T. Xiao, C. Lin, L. Wang, Chem. Soc. Rev. **41**, 5950 (2012)
336. U. Mansfeld, M.D. Hager, R. Hoogenboom, C. Ott, A. Winter, U.S. Schubert, Chem. Commun. 3386 (2009)
337. G. Gröger, V. Stepanenko, F. Würthner, C. Schmuck, Chem. Commun. 698 (2009)
338. J.A.A.W. Elemans, A.E. Rowan, R.J.M. Nolte, J. Mater. Chem. **13**, 2661 (2003)
339. H. Hofmeier, A. El-ghayoury, A.P.H.J. Schenning, U.S. Schubert, Chem. Commun. 318 (2004)
340. S. Rieth, C. Baddeley, J.D. Badjić, Soft Matter **3**, 137 (2007)
341. W. Li, Y. Kim, J. Lia, M. Lee, Soft Matter **10**, 5231 (2014)
342. J.M. Pollino, K.P. Nair, L.P. Stubbs, J. Adams, M. Weck, Tetrahedron **60**, 7205 (2004)
343. P. Wei, X. Yan, F. Huang, Chem. Soc. Rev. **44**, 815 (2015)
344. Y. Liu, Y. Song, H. Wang, H.-Y. Zhang, X.-Q. Li, Macromolecules **37**, 6370 (2004)
345. Y. Liu, Z.-X. Yang, Y. Chen, Y. Song, N. Shao, ACS Nano **2**, 554 (2008)
346. H. Masai, J. Terao, S. Seki, S. Nakashima, M. Kiguchi, K. Okoshi, T. Fujihara, Y. Tsuji, J. Am. Chem. Soc. **136**, 1742 (2014)
347. E. Lee, J. Heo, K. Kim, Angew. Chem. Int. Ed. **39**, 2699 (2000)
348. K.-M. Park, E. Lee, S.-G. Roh, J. Kim, K. Kim, Bull. Korean Chem. Soc. **25**, 1711 (2004)

349. Y. Liu, Z. Huang, X. Tan, Z. Wang, X. Zhang, Chem. Commun. **49**, 5766 (2013)
350. J.-F. Xu, Y.-Z. Chen, L.-Z. Wu, C.-H. Tung, Q.-Z. Yang, Org. Lett. **15**, 6148 (2013)
351. H. Li, D.-X. Chen, Y.-L. Sun, Y.B. Zheng, L.-L. Tan, P.S. Weiss, Y.-W. Yang, J. Am. Chem. Soc. **135**, 1570 (2013)
352. X. Shu, S. Chen, J. Li, Z. Chen, L. Weng, X. Jia, C. Li, Chem. Commun. **48**, 2967 (2012)
353. M. Xue, Y. Yang, X. Chi, Z. Zhang, F. Huang, Acc. Chem. Res. **45**, 1294 (2012)
354. L. Gao, Z. Zhang, B. Zheng, F. Huang, Polym. Chem. **5**, 5734 (2014)
355. Z. Zhang, C. Han, G. Yu, F. Huang, Chem. Sci. **3**, 3026 (2012)
356. C.J. Bruns, J.F. Stoddart, Nat. Nanotechnol. **8**, 9 (2013)
357. C.J. Bruns, J.F. Stoddart, Acc. Chem. Res. **47**, 2186 (2014)
358. P. Wang, H. Xing, D. Xia, X. Ji, Chem. Commun. **51**, 17431 (2015)
359. B. Shi, K. Jie, Y. Zhou, D. Xia, Y. Yao, Chem. Commun. **51**, 4503 (2015)
360. L. Wu, C. Han, X. Wu, L. Wang, Y. Caochen, X. Jing, Dalton Trans. **44**, 20334 (2015)
361. C. Zhang, S. Li, J. Zhang, K. Zhu, N. Li, F. Huang, Org. Lett. **9**, 5553 (2007)
362. Y. Ding, P. Wang, Y.-K. Tian, Y.-J. Tian, F. Wang, Chem. Commun. **49**, 5951 (2013)
363. Y.-K. Tian, F. Wang, Macromol. Rapid Commun. **35**, 337 (2014)
364. S. Dong, Y. Luo, X. Yan, B. Zheng, X. Ding, Y. Yu, Z. Ma, Q. Zhao, F. Huang, Angew. Chem. Int. Ed. **50**, 1905 (2011)
365. J. Yuan, Q. Li, Q. Hu, Q. Wu, C. Li, H. Qiu, M. Zhang, S. Yin, Chem. Commun. **50**, 722 (2014)
366. J. Zhan, M. Zhang, M. Zhou, B. Liu, D. Chen, Y. Liu, Q. Chen, H. Qiu, S. Yin, Macromol. Rapid Commun. **35**, 1424 (2014)
367. G. Du, E. Moulin, N. Jouault, E. Buhler, N. Giuseppone, Angew. Chem. Int. Ed. **51**, 12504 (2012)
368. X. Yan, B. Zheng, F. Huang, Polym. Chem. **4**, 2395 (2013)
369. D. Chen, J. Zhan, M. Zhang, J. Zhang, J. Tao, D. Tang, A. Shen, H. Qiu, S. Yin, Polym. Chem. **6**, 25 (2015)
370. Y.-K. Tian, Y.-G. Shi, Z.-S. Yang, F. Wang, Angew. Chem. Int. Ed. **53**, 6090 (2014)
371. Y.-K. Tian, Z.-S. Yang, X.-Q. Lv, R.-S. Yao, F. Wang, Chem. Commun. **50**, 9477 (2014)
372. H. Hofmeier, J. Pahnke, C.H. Weidl, U.S. Schubert, Biomacromol **5**, 2055 (2004)
373. N. Haddour, C. Gondran, S. Cosnier, Chem. Commun. 324 (2004)
374. W. Wang, Y. Zhang, B. Sun, L.-J. Chen, X.-D. Xu, M. Wang, X. Li, Y. Yu, W. Jiang, H.-B. Yang, Chem. Sci. **5**, 4554 (2014)
375. A. Wang, J. Huang, Y. Yan, Soft Matter **10**, 3362 (2014)
376. Y. Yan, A. de Keizer, M.A.C. Stuart, N.A.M. Besseling, Adv. Polym. Sci. **242**, 91 (2010)
377. W.G. Weng, A.M. Jamieson, S.J. Rowan, Tetrahedron **63**, 7419 (2007)
378. W.G. Weng, Z. Li, A.M. Jamieson, S.J. Rowan, Macromolecules **42**, 236 (2009)
379. S. Landsmann, A. Winter, M. Chiper, C.-A. Fustin, S. Hoeppener, D. Wouters, J.-F. Gohy, U.S. Schubert, Macromol. Chem. Phys. **209**, 1666 (2008)
380. H. Krass, E.A. Plummer, J.M. Haider, P.R. Barker, N.W. Alcock, Z. Pikramenou, M. J. Hannon, D.G. Kurth, Angew. Chem. Int. Ed. **40**, 3862 (2001)
381. P. Lehmann, C. Symietz, G. Brezesinski, H. Krass, D.G. Kurth, Langmuir **21**, 5901 (2005)
382. Y. Bodenthin, U. Pietsch, J. Grenzer, T. Geue, H. Möhwald, D.G. Kurth, J. Phys. Chem. B **109**, 12795 (2005)
383. B. Arezki, G. Schwarz, Y. Bodenthin, D. Lutzenkirchen-Hecht, C. Markert, R. Wagner, R. Frahm, D.G. Kurth, U. Pietsch, ChemPhysChem **12**, 405 (2011)
384. Y. Bodenthin, U. Pietsch, H. Möhwald, D.G. Kurth, J. Am. Chem. Soc. **127**, 3110 (2005)
385. Y. Bodenthin, G. Schwarz, Z. Tomkowicz, M. Lommel, T. Geue, W. Haase, H. Moehwald, U. Pietsch, D.G. Kurth, Coord. Chem. Rev. **253**, 2414 (2009)
386. Y. Bodenthin, D.G. Kurth, G. Schwarz, Chem. Unserer. Zeeit. **42**, 256 (2008)
387. A.B. Gaspar, M. Seredyuk, Coord. Chem. Rev. **268**, 41 (2014)
388. S. Valkama, O. Lehtonen, K. Lappalainen, H. Kosonen, P. Castro, T. Repo, M. Torkkeli, R. Serimaa, G. ten Brinke, M. Leskelä, O. Ikkala, Macromol. Rapid Commun. **24**, 556 (2003)

389. Y. Yan, N.A.M. Besseling, A. de Keizer, A.T.M. Marcelis, M. Drechsler, M.A. Cohen, Stuart. Angew. Chem. Int. Ed. **46**, 1807 (2007)
390. S. Van der Burgh, A. de Keizer, M.A. Cohen, Stuart. Langmuir **20**, 1073 (2004)
391. A. Harada, K. Kataoka, Macromolecules **31**, 288 (1998)
392. Y. Yan, A. de Keizer, M.A. Cohen Stuart, N.A.M. Besseling, Soft Matter **5**, 790 (2009)
393. Y. Yan, A. de Keizer, M.A. Cohen Stuart, M. Drechsler, N.A.M. Besseling, J. Phys. Chem. B **112**, 10908 (2008)
394. Y. Yan, N.A.M. Besseling, A. de Keizer, M.A. Cohen, Stuart. J. Phys. Chem. B **111**, 5811 (2007)
395. Y. Yan, N.A.M. Besseling, A. de Keizer, M.A. Cohen Stuart, M. Drechsler, J. Phys. Chem. B **111**, 11662 (2007)
396. Y. Yan, L. Harnau, N.A.M. Besseling, A. de Keizer, M. Ballauff, S. Rosenfeldt, M.A. Cohen, Stuart. Soft Matter **4**, 2207 (2008)
397. H.T. Baytekin, B. Baytekin, A. Schulz, C.A. Schalley, Small **5**, 194 (2009)
398. W.A. Lopes, H.M. Jaeger, Nature **414**, 735 (2001)
399. A.O. Moughton, R.K. O'Reilly, J. Am. Chem. Soc. **130**, 8714 (2008)
400. D. Li, J. Zhang, K. Landskron, T. Liu, J. Am. Chem. Soc. **130**, 4226 (2008)
401. R. Dobrawa, F. Wurthner, Chem. Commun. 1878 (2002)
402. P. Guillet, C. Mugemana, F.J. Stadler, U.S. Schubert, C.-A. Fustin, C. Bailly, J.-F. Gohy, Soft Matter **5**, 3409 (2009)
403. S.C. Grindy, R. Learsch, D. Mozhdehi, J. Cheng, D.G. Barrett, Z. Guan, P.B. Messersmith, N. Holten-Andersen, Nat. Mater. **14**, 1210 (2015)
404. N. Xu, J. Han, Z. Zhu, B. Song, X. Lu, Y. Cai, Soft Matter **11**, 5546 (2015)
405. Y. Liu, X. Wang, Polym. Chem. **2**, 2741 (2011)
406. J.W. Steed, Chem. Commun. **47**, 1379 (2011)
407. J.H. Jung, J.H. Lee, J.R. Silverman, G. John, Chem. Soc. Rev. **42**, 924 (2013)
408. J. Zhang, C.-Y. Su, Coord. Chem. Rev. **257**, 1373 (2013)
409. N.M. Sangeetha, U. Maitra, Chem. Soc. Rev. **34**, 821 (2005)
410. R.G. Weiss, P. Terech (eds.), *Molecular Gels. Materials with Self-Assembled Fibrillar Networks* (Springer, Dordrecht, 2006)
411. B. Escuder, J.F. Miravet (eds.), *Functional Molecular Gels* (RSC, Cambridge, 2014)
412. F. Fages (ed.), *Low Molecular Weight Gelators* (Springer, Berlin-Heidelberg, 2005)
413. S. Seiffert (ed.), *Supramolecular Polymer Networks and Gels* (Springer, Heidelberg, NY, Dordrecht, London, 2015)
414. M.J. Mayoral, G. Fernández, Chem. Sci. **3**, 1395 (2012)
415. C. Rest, M.J. Mayoral, K. Fucke, J. Schellheimer, V. Stepanenko, G. Fernández, Angew. Chem. Int. Ed. **53**, 700 (2014)
416. N. Lanigan, X. Wang, Chem. Commun. **49**, 8133 (2013)
417. C.A. Strassert, C.-H. Chien, M.D. Galvez Lopez, D. Kourkoulos, D. Hertel, K. Meerholz, L. de Cola, Angew. Chem. Int. Ed. **50**, 946 (2011)
418. A. Kishimura, T. Yamashita, T. Aida, J. Am. Chem. Soc. **127**, 179 (2005)
419. R. Gavara, J. Llorca, J.C. Lima, L. Rodríguez, Chem. Comm. **49**, 72 (2013)
420. E. Aguiló, R. Gavara, J.C. Lima, J. Llorca, L. Rodríguez, J. Mat. Chem. C **1**, 5538 (2013)
421. A.J. Moro, B. Rome, E. Aguiló, J. Arcau, R. Puttreddy, K. Rissanen, J.C. Lima, L. Rodríguez, Org. Biomol. Chem. **13**, 2026 (2015)
422. J.C. Lima, L. Rodríguez, Chem. Soc. Rev. **40**, 5442 (2011)
423. G. Buhler, M.C. Feiters, R.J.M. Nolte, K.H. Dotz, Angew. Chem. Int. Ed. **42**, 2494 (2003)
424. D.D. Díaz, D. Kühbeck, R.J. Koopmans, Chem. Soc. Rev. **40**, 427 (2011)
425. S.R. Bull, M.O. Guler, R.E. Bras, T.J. Meade, S.I. Stupp, Nano Lett. **5**, 1 (2005)
426. M. Mauro, A. Aliprandi, D. Septiadi, N.S. Kehra, L. de Cola, Chem. Soc. Rev. **43**, 4144 (2014)
427. S. Saha, J. Bachl, T. Kundu, D. Díaz, Chem. Commun. **50**, 7032 (2014)
428. S. Kawano, N. Fujita, S. Shinkai, J. Am. Chem. Soc. **126**, 8592 (2004)
429. T. Vermonden, R. Censi, W.E. Hennink, Chem. Rev. **112**, 2853 (2012)

430. J.C. Lima, L. Rodríguez, Inorganics **3**, 1 (2015)
431. V.K.-M. Au, N. Zhu, V.W.-W. Yam, Inorg. Chem. **52**, 558 (2013)
432. M.-O.M. Piepenbrock, G.O. Lloyd, N. Clarke, J.W. Steed, Chem. Rev. **110**, 1960 (2010)
433. P. Dastidar, Chem. Soc. Rev. **37**, 2699 (2008)
434. M. George, R.G. Weiss, Acc. Chem. Res. **39**, 489 (2006)
435. B.G. Bag, G.C. Maity, S.K. Dinda, Org. Lett. **8**, 5457 (2006)
436. A. Pal, B.S. Chhikara, A. Govindaraj, S. Bhattacharya, C.N.R. Rao, J. Mater. Chem. **18**, 2593 (2008)
437. A. Pal, B. Hajra, S. Sen, V.K. Aswal, S. Bhattacharya, J. Mater. Chem. **19**, 4325 (2009)
438. P. Terech, S. Dourdain, U. Maitra, S. Bhat, J. Phys. Chem. B **113**, 4619 (2009)
439. G. Palui, A. Banerjee, J. Phys. Chem. B **112**, 10107 (2008)
440. C. Vijayakumar, V.K. Praveen, A. Ajayaghosh, Adv. Mater. **21**, 2059 (2009)
441. S. Dutta, A. Shome, S. Debnath, P.K. Das, Soft Matter **5**, 1607 (2009)
442. R. Ghosh, A. Chakraborty, D.K. Maiti, V.G. Puranik, Org. Lett. **8**, 1061 (2006)
443. D.D. Daz, J.J. Cid, P. Vzquez, T. Torres, Chem. Eur. J. **14**, 9261 (2008)
444. A. Dawn, N. Fujita, S. Haraguchi, K. Sada, S. Shinkai, Chem. Commun. 2100 (2009)
445. M. Suzuki, K. Hanabusa, Chem. Soc. Rev. **38**, 967 (2009)
446. M.-O.M. Piepenbrock, G.O. Lloyd, N. Clarke, J.W. Steed, Chem. Commun. 2644 (2008)
447. A.R. Hirst, J.E. Miravet, B. Escuder, L. Noirez, V. Castelletto, I.W. Hamley, D.K. Smith, Chem. Eur. J. **15**, 372 (2009)
448. H. Hopf, H. Greiving, H. Bouas-Laurent, J.P. Desvergne, Eur. J. Org. Chem. 1868 (2009)
449. W. Deng, H. Yamaguchi, Y. Takashima, A. Harada, Chem. Asian J. **3**, 687 (2008)
450. N. Sreenivasachary, J.-M. Lehn, Chem. Asian J. **3**, 134 (2008)
451. A. Ajayaghosh, V.K. Praveen, Acc. Chem. Res. **40**, 644 (2007)
452. A. Ajayaghosh, V.K. Praveen, C. Vijayakumar, Chem. Soc. Rev. **37**, 109 (2008)
453. R. Luboradzki, O. Gronwald, M. Ikeda, S. Shinkai, D.N. Reinhoudt, Tetrahedron **56**, 9595 (2000)
454. A. Ballabh, D.R. Trivedi, P. Dastidar, Chem. Mater. **15**, 2136 (2003)
455. D.R. Trivedi, A. Ballabh, P. Dastidar, Chem. Mater. **15**, 3971 (2003)
456. D.R. Trivedi, A. Ballabh, P. Dastidar, B. Ganguly, Chem. Eur. J. **10**, 5311 (2004)
457. A.R. Hirst, B. Escuder, J.F. Miravet, D.K. Smith, Angew. Chem. Int. Ed. **47**, 8002 (2008)
458. T. Nakanishi, *Supramolecular Soft Matter: Applications in Materials and Organic Electronics* (Wiley, Chichester, 2011)
459. J.-J. Zhang, W. Lu, R.W.-Y. Sun, C.-M. Che, Angew. Chem. Int. Ed. **51**, 4882 (2012)
460. S.A. Joshi, N.D. Kulkarni, Chem. Commun. 2341 (2009)
461. M. Dukh, D. Saman, J. Kroulik, I. Cerny, V. Pouzar, V. Kral, P. Drasar, Tetrahedron **59**, 4069 (2003)
462. K. Hanabusa, T. Hirata, D. Inoue, M. Kimura, H. Shirai, Colloid. Surf. A **169**, 307 (2000)
463. L. Sambri, F. Cucinotta, G. De Paoli, S. Stagnic, L. De Cola, New J. Chem. **34**, 2093 (2010)
464. X. Chen, Z. Huang, S.-Y. Chen, K. Li, X.-Q. Yu, L. Pu, J. Am. Chem. Soc. **132**, 7297 (2010)
465. F. Camerel, R. Ziessel, B. Donnio, D. Guillon, New J. Chem. **30**, 135 (2006)
466. A.Y.-Y. Tam, K.M.-C. Wong, G. Wang, V.W.-W. Yam, Chem. Commun. 2028 (2007)
467. A.Y.-Y. Tam, K.M.-C. Wong, V.W.-W. Yam, Chem. Eur. J. **15**, 4775 (2009)
468. A.Y.-Y. Tam, K.M.-C. Wong, V.W.-W. Yam, J. Am. Chem. Soc. **131**, 6253 (2009)
469. W. Lu, Y.-C. Law, J. Han, S.S.-Y. Chui, D.-L. Ma, N. Zhu, C.-M. Che, Chem. Asian J. **3**, 59 (2008)
470. F. Camerel, R. Ziessel, B. Donnio, C. Bourgogne, D. Guillon, M. Schmutz, C. Iacovita, J.-P. Bucher, Angew. Chem. Int. Ed. **46**, 2659 (2007)
471. A.Y.-Y. Tam, K.M.-C. Wong, N. Zhu, G. Wang, V.W.-W. Yam, Langmuir **25**, 8695 (2009)
472. T. Tu, W. Assenmacher, H. Peterlik, R. Weisbarth, M. Nieger, K.H. Dotz, Angew. Chem. Int. Ed. **46**, 6368 (2007)
473. T. Tu, W. Fang, X. Bao, X. Li, K.H. Dotz, Angew. Chem. Int. Ed. **50**, 6601 (2011)

474. T. Tu, X. Bao, W. Assenmacher, H. Peterlik, J. Daniels, K.H. Dotz, Chem. Eur. J. **15**, 1853 (2009)
475. T. Cardolaccia, Y. Li, K.S. Schanze, J. Am. Chem. Soc. **130**, 2535 (2008)
476. T. Naota, H. Koori, J. Am. Chem. Soc. **127**, 9324 (2005)
477. K. Isozaki, H. Takaya, T. Naota, Angew. Chem. Int. Ed. **46**, 2855 (2007)
478. N. Komiya, T. Muraoka, M. Iida, M. Miyanaga, K. Takahashi, T. Naota, J. Am. Chem. Soc. **133**, 16054 (2011)
479. M. Shirakawa, N. Fujita, T. Tani, K. Kaneko, S. Shinkai, Chem. Commun. 4149 (2005)
480. P. Kadjane, M. Starck, F. Camerel, D. Hill, N. Hildebrandt, R. Ziessel, L.J. Charbonniere, Inorg. Chem. **48**, 4601 (2009)
481. W. Miao, L. Zhang, X. Wang, H. Cao, Q. Jin, M. Liu, Chem. Eur. J. 19, 3029 (2013)
482. A. Kishimura, T. Yamashita, K. Yamaguchi, T. Aida, Nat. Mater. **4**, 546 (2005)
483. T. Kishida, N. Fujita, O. Hirata, S. Shinkai, Org. Biomol. Chem. **4**, 1902 (2006)
484. T. Kishida, N. Fujita, K. Sada, S. Shinkai, Langmuir **21**, 9432 (2005)
485. T. Kishida, N. Fujita, K. Sada, S. Shinkai, J. Am. Chem. Soc. **127**, 7298 (2005)
486. M. Takeuchi, S. Tanaka, S. Shinkai, Chem. Commun. 5539 (2005)
487. T. Zhang, Z. Wen, Y. Hui, M. Yang, K. Yang, Q. Zhou, Y. Wang, Polym. Chem. **6**, 4177 (2015)
488. P. Terech, C. Scherer, P. Lindner, R. Ramasseul, Langmuir **19**, 10648 (2003)
489. P. Terech, C. Scherer, B. Deme, R. Ramasseul, Langmuir **19**, 10641 (2003)
490. M. Schappacher, A. Deffieux, J.-F. Le Meins, Polym. Chem. **4**, 458 (2013)
491. T. Ishi-I, R. Iguchi, E. Snip, M. Ikeda, S. Shinkai, Langmuir **17**, 5825 (2001)
492. H. Danjo, K. Hirata, S. Yoshigai, I. Azumaya, K. Yamaguchi, J. Am. Chem. Soc. **131**, 1638 (2009)
493. J.M.J. Paulusse, D.J.M. van Beek, R.P. Sijbesma, J. Am. Chem. Soc. **129**, 2392 (2007)
494. J. Paulusse, J. Huijbers, R. Sijbesma, Chem. Eur. J. **12**, 4928 (2006)
495. J. Paulusse, R. Sijbesma, Angew. Chem. Int. Ed. **43**, 4460 (2004)
496. T. Zhang, Z. Wen, Y. Hui, M. Yang, K. Yang, Q. Zhou, Y. Wang, Polym. Chem. **6**, 4177 (2015)
497. A. Kokil, I. Shiyanovskaya, K. Singer, C. Weder, J. Am. Chem. Soc. **124**, 9978 (2002)
498. H.J. Kim, J.H. Lee, M. Lee, Angew. Chem. Int. Ed. **44**, 5810 (2005)
499. H.J. Kim, W.C. Zin, M. Lee, J. Am. Chem. Soc. **126**, 7009 (2004)
500. J. Brassinne, F.D. Jochum, C.-A. Fustin, J.-F. Gohy, Int. J. Mol. Sci. **16**, 990 (2015)
501. C. Ott, C. Ulbricht, R. Hoogenboom, U.S. Schubert, Macromol. Rapid Commun. **33**, 556 (2012)
502. M. Kimura, Y. Nakagawa, N. Adachi, Y. Tatewaki, T. Fukawa, H. Shirai, Chem. Lett. **38**, 382 (2009)
503. R. Wang, M. Geven, P.J. Dijkstra, P. Martens, M. Karperien, Soft Matter **10**, 7328 (2014)
504. H. Hofmeier, U.S. Schubert, Macromol. Chem. Phys. **204**, 1391 (2003)
505. C. Mugemana, A. Joset, P. Guillet, M.-S. Appavou, N. De Souza, C.-A. Fustin, B. Leyh, J.-F. Gohy, Macromol. Chem. Phys. **214**, 1699 (2013)
506. J. Brassinne, C. Mugemana, P. Guillet, O. Bertrand, D. Auhl, C. Bailly, C.A. Fustin, J.F. Gohy, Soft Matter **8**, 4599 (2012)
507. F.D. Jochum, J. Brassinne, C.-A. Fustin, J.-F. Gohy, Soft Matter **9**, 2314 (2013)
508. O. Kotova, R. Daly, C.M.G. dos Santos, P.E. Kruger, J.J. Boland, T. Gunnlaugsson, Inorg. Chem. **54**, 7735 (2015)
509. J. Yuan, X. Fang, L. Zhang, G. Hong, Y. Lin, Q. Zheng, Y. Xu, Y. Ruan, W. Weng, H. Xia, G. Chen, J. Mater. Chem. **22**, 11515 (2012)
510. E.P. McCarney, J.P. Byrne, B. Twamley, M. Martínez-Calvo, G. Ryan, M.E. Möbius, T. Gunnlaugsson, Chem. Commun. **51**, 14123 (2015)
511. Z. Wang, W. Fan, R. Tong, X. Lu, H. Xia, RSC Adv. **4**, 25486 (2014)
512. Q. Lin, T.-T. Lu, X. Zhu, B. Sun, Q.-P. Yang, T.-B. Wei, Y.-M. Zhang, Chem. Commun. **51**, 1635 (2015)

513. Q. Lin, B. Sun, Q.-P. Yang, Y.-P. Fu, X. Zhu, Y.-M. Zhang, T.-B. Wei, Chem. Commun. **50**, 10669 (2014)
514. W.C. Yount, D.M. Loveless, S.L. Craig, Angew. Chem. Int. Ed. **44**, 2746 (2005)
515. D. Knapton, P.K. Iyer, S.J. Rowan, C. Weder, Macromolecules **39**, 4069 (2006)
516. D. Knapton, S.J. Rowan, C. Weder, Macromolecules **39**, 651 (2006)
517. M. Burnworth, J.D. Mendez, M. Schroeter, S.J. Rowan, C. Weder, Macromolecules **41**, 2157 (2008)
518. X. de Hatten, N. Bell, N. Yufa, G. Christmann, J.R. Nitschke, J. Am. Chem. Soc. **133**, 3158 (2011)
519. N. Holten-Andersen, M. Harrington, H. Birkedal, B. Lee, P. Messersmith, K. Lee, J. Waite, Proc. Natl. Acad. Sci. U.S.A. **108**, 2651 (2011)
520. L. Qu, J. Fan, Y. Ren, K. Xiong, M. Yan, X. Tuo, P. Terech, G. Royal, Mater. Chem. Phys. **153**, 54 (2015)
521. A. Gasnier, G. Royal, P. Terech, Langmuir **25**, 8751 (2009)
522. A. Gasnier, C. Bucher, J.-C. Moutet, G. Royal, E. Saint-Aman, P. Terech, Macromol. Symp. **304**, 87 (2011)
523. Z. Qi, P. Malo de Molina, W. Jiang, Q. Wang, K. Nowosinski, A. Schulz, M. Gradzielski, C.A. Schalley, Chem. Sci. **3**, 2073 (2012)
524. J. Zhang, J. Yan, P. Pageni, Y. Yan, A. Wirth, Y.P. Chen, Y. Qiao, Q. Wang, A.W. Decho, C. Tang, Sci. Rep. **5**, 11914 (2015)
525. J.G. Vos, R.J. Forster, T.E. Keyes, *Interfacial Supramolecular Assemblies* (Wiley, Chichester, 2003)
526. J.A.A.W. Elemans, S. Lei, S. De Feyter, Angew. Chem. Int. Ed. **48**, 7298 (2009)
527. S. Yu. Zaitsev, *Supramolecular Nano-sized Systems at the Interface. Concepts and Perspectives for Bionanotechnologies* (Lenand, Moscow, 2010) (in Russian)
528. N. Miyashita, D.G. Kurth, J. Mater. Chem. **18**, 2636 (2008)
529. M. Deniz Yilmaz, J. Huskens, Soft Matter **8**, 11768 (2012)
530. W. Tong, X. Song, C. Gao, Chem. Soc. Rev. **41**, 6103 (2012)
531. J. Borges, J.F. Mano, Chem. Rev. **114**, 8883 (2014)
532. Y. Li, X. Wang, J. Sun, Chem. Soc. Rev. **41**, 5998 (2012)
533. Y. Xiang, S. Lua, S.P. Jiang, Chem. Soc. Rev. **41**, 7291 (2012)
534. R. Sakamoto, K.-H. Wu, R. Matsuoka, H. Maeda, H. Nishihara, Chem. Soc. Rev. **44**, 7698 (2015)
535. I. Doron-Mor, H. Cohen, S.R. Cohen, R. Popovitz-Biro, A. Shanzer, A. Vaskevich, I. Rubinstein, Langmuir **20**, 10727 (2004)
536. M. Wanunu, A. Vaskevich, S.R. Cohen, H. Cohen, R. AradYellin, A. Shanzer, I. Rubinstein, J. Am. Chem. Soc. **127**, 17877 (2005)
537. M. Wanunu, A. Vaskevich, A. Shanzer, I. Rubinstein, J. Am. Chem. Soc. **128**, 8341 (2006)
538. M. Greenstein, R.B. Ishay, B.M. Maoz, H. Leader, A. Vaskevich, I. Rubinstein, Langmuir **26**, 7277 (2010)
539. E. Soto, J.C. MacDonald, C.G.F. Cooper, W.G. McGimpsey, J. Am. Chem. Soc. **125**, 2838 (2003)
540. G. de Ruiter, M. Lahav, H. Keisar, M.E. van der Boom, Angew. Chem. Int. Ed. **52**, 704 (2013)
541. S. Shankar, M. Lahav, M.E. van der Boom, J. Am. Chem. Soc. **137**, 4050 (2015)
542. M. Maskus, H.D. Abruna, Langmuir **12**, 4455 (1996)
543. K. Kanaizuka, M. Murata, Y. Nishimori, I. Mori, K. Nishio, H. Masuda, H. Nishihara, Chem. Lett. **34**, 534 (2005)
544. C. Haensch, M. Chiper, C. Ulbricht, A. Winter, S. Hoeppener, U.S. Schubert, Langmuir **24**, 12981 (2008)
545. C. Chakraborty, R.K. Pandey, Md Delwar Hossain, Z. Futera, S. Moriyama, M. Higuchi, ACS Appl. Mater. Interfaces. **7**, 19034 (2015)
546. L.-Y. Zhang, H.-X. Zhang, S. Ye, H.-M. Wen, Z.-N. Chen, M. Osawa, K. Uosaki, Y. Sasaki, Chem. Commun. **47**, 923 (2011)

547. L.D.A. Siebbeles, F.C. Grozema (eds.), *Charge and Exciton Transport through Molecular Wires* (Wiley, Chichester, 2011)
548. L. de Cola (ed.), *Molecular Wires: From Design to Properties*, vol. 257 (Springer-Verlag, Berlin, Heldelberg, 2005) (Topp. Curr. Chem.)
549. H. Maeda, R. Sakamoto, H. Nishihara, Polymer **54**, 4383 (2013)
550. H. Maeda, R. Sakamoto, H. Nishihara, J. Phys. Chem. Lett. **6**, 3821 (2015)
551. A. Bajpayee, H. Maeda, S. Katagiri, R. Sakamoto, H. Nishihara, Chem. Lett. **44**, 1211 (2015)
552. Y. Yamanoi, J. Sendo, T. Kobayashi, H. Maeda, Y. Yabusaki, M. Miyachi, R. Sakamoto, H. Nishihara, J. Am. Chem. Soc. **134**, 20433 (2012)
553. S. Katagiri, R. Sakamoto, H. Maeda, Y. Nishimori, T. Kurita, H. Nishihara, Chem. Eur. J. **19**, 5088 (2013)
554. L. Pukenas, F. Benn, E. Lovell, A. Santoro, L.J. Kershaw Cook, M.A. Halcrow, S.D. Evans, J. Mater. Chem. C **3**, 7890 (2015)
555. A. Grohmann, M. Haryono, K. Student, P. Müller, M. Stocker, Eur. J. Inorg. Chem. 662 (2013)
556. P. Gütlich, H.A. Goodwin (eds.), *Spin Crossover in Transition Metal Compounds I–III*, vol. 234 (Springer, Berlin, Heidelberg, NY, 2004) (Top. Curr. Chem.)
557. M.A. Halcrow (ed.), *Spin-Crossover Materials—Properties and Applications* (Wiley, Chichester, 2013)
558. Y. Tang, M. Chen, D.-J. Qian, L. Zhang, M. Liu, Colloids and Surfaces A: Physicochem. Eng. Asp. **457**, 41 (2014)
559. C.A. da Silva, M. Vidotti, P.A. Fiorito, S.I. Córdoba de Torresi, R.M. Torresi, W.A. Alves, Langmuir **28**, 3332 (2012)
560. S.A. Levi, P. Guatteri, F.C.J.M. van Veggel, G.J. Vancso, E. Dalcanale, D.N. Reinhoudt, Angew. Chem. Int. Ed. **40**, 1892 (2001)
561. E. Menozzi, R. Pinalli, E.A. Speets, B.J. Ravoo, E. Dalcanale, D.N. Reinhoudt, Chem. Eur. J. **10**, 2199 (2004)
562. J. Puigmartı-Luis, W.J. Saletra, A. Gonzalez, D.B. Amabilino, L. Perez-Garcıa, Chem. Commun. **50**, 82 (2014)
563. W. Zhao, B. Tong, Y. Pan, J. Shen, J. Zhi, J. Shi, Y. Dong, Langmuir **25**, 11796 (2009)
564. W. Zhao, B. Tong, J. Shi, Y. Pan, J. Shen, J. Zhi, W.K. Chan, Y. Dong, Langmuir **26**, 16084 (2010)
565. Y. Tong, B. Pan, J. Shi, W. Zhao, J. Shen, J. Zhi, Y. Dong, J. Phys. Chem. C **114**, 8040 (2010)
566. B. Tong, H. Yang, W. Xiong, F. Xie, J. Shi, J. Zhi, W.K. Chan, Y. Dong, J. Phys. Chem. B **117**, 5338 (2013)
567. O. Crespo-Biel, C.W. Lim, B.J. Ravoo, D.N. Reinhoudt, J. Huskens, J. Am. Chem. Soc. **128**, 17024 (2006)
568. C.W. Lim, O. Crespo-Biel, M.C.A. Stuart, D.N. Reinhoudt, J. Huskens, B.J. Ravoo, Proc. Natl. Acad. Sci. U.S.A. **104**, 6986 (2007)
569. C.N. Moorefield, S. Perera, G.R. Newkome, Dendrimer chemistry: supramolecular perspectives and applications, in *Dendrimer-Based Drug Delivery Systems: From Theory to Practice*, ed. by Y. Cheng (Wiley, Chichester, 2012)
570. D.K. Smith, F. Diederich, Supramolecular dendrimer chemistry: a journey through the branched architecture, in *Dendrimers II*, *Architecture, Nanostructure and Supramolecular Chemistry*, vol. 210 (Springer, Berlin, Heidelberg, NY, 2000) (Top. Curr. Chem.)
571. D.K. Smith, A.R. Hirst, C.S. Love, J.G. Hardy, S.V. Brignell, B. Huang, Prog. Polym. Sci. **30**, 220 (2005)
572. D.K. Smith, Chem. Commun. 34 (2006)
573. M. Selin, L. Peltonen, J. Hirvonen, L.M. Bimbo, J. Drug Deliv. Sci. Technol. **34**, 10 (2016)
574. B.N.S. Thota, L.H. Urner, R. Haag, Chem. Rev. **116**, 2079 (2016)
575. H.-J. Sun, S. Zhang, V. Percec, Chem. Soc. Rev. **44**, 3900 (2015)
576. U. Hahn, F. Cardinali, J.-F. Nierengarten, New J. Chem. **31**, 1128 (2007)

577. K.C.-F. Leung, K.-N. Lau, Polym. Chem. **1**, 988 (2010)
578. W. Wang, A.E. Kaifer, Adv. Polym. Sci. **222**, 1 (2009)
579. A.-M. Caminade, R. Laurent, A. Ouali, J.-P. Majoral, Inorg. Chim. Acta **409**, 68 (2014)
580. A.-M. Caminade, A. Ouali, R. Laurent, C.-O. Turrin, J.-P. Majoral, Chem. Soc. Rev. **44**, 3890 (2015)
581. A.-M. Caminade, J.-P. Majoral, Chem. Soc. Rev. **39**, 2034 (2010)
582. K. Ladomenou, V. Nikolaou, G. Charalambidis, A.G. Coutsolelos, Coord. Chem. Rev. **306**, 1 (2016)
583. R. Dong, Y. Zhou, X. Zhu, Acc. Chem. Res. **47**, 2006 (2014)
584. B.M. Rosen, C.J. Wilson, D.A. Wilson, M. Peterca, M.R. Imam, V. Percec, Chem. Rev. **109**, 6275 (2009)
585. M.E. Gallina, G. Bergamini, S. Di Motta, J. Sakamoto, F. Negri, P. Ceroni, Photochem. Photobiol. Sci. **13**, 997 (2014)
586. A.S. Abd-El-Aziz, I. Manners, *Frontiers in Transition-Metal Containing Polymers* (Wiley, NY, 2007)
587. S. Campagna, P. Ceroni, F. Puntoriero (eds.), *Designing Dendrimers* (Wiley, Hoboken, 2012)
588. L.H. Gade (ed.), *Dendrimer Catalysis* (Springer, Berlin, Heidelberg, NY, 2006)
589. Y. Cheng (ed.), *Dendrimer-Based Drug Delivery Systems: From Theory to Practice* (Wiley, Chichester, 2012)
590. D.A. Tomalia, J.B. Christensen, U. Boas, *Dendrimers, Dendrons, and Dendritic Polymers: Discovery, Applications, and the Future* (Cambridge University Press, Cambridge, 2012)
591. F. Vögtle, G. Richardt, N. Werner, *Dendrimer Chemistry: Concepts, Syntheses, Properties, Applications* (Wiley, Weinheim, 2009)
592. P. Ceroni, G. Bergamini, V. Balzani, Angew. Chem. Int. Ed. **48**, 8516 (2009)
593. V. Balzani, P. Ceroni, A. Juris, M. Venturi, S. Campagna, F. Puntoriero, S. Serroni, Coord. Chem. Rev. **219–221**, 545 (2001)
594. V. Balzani, G. Bergamini, P. Ceroni, F. Vogtle, Coord. Chem. Rev. **251**, 525 (2007)
595. V. Balzani, G. Bergamini, P. Ceroni, Adv. Inorg. Chem. **63**, 105 (2011)
596. G.R. Newkome, C. Shreiner, Chem. Rev. **110**, 6338 (2010)
597. F. Puntoriero, A. Sartorel, M. Orlandi, G. La Ganga, S. Serroni, M. Bonchio, F. Scandola, S. Campagna, Coord. Chem. Rev. **255**(21), 2594 (2011)
598. H. El-Batal, K. Guo, X. Li, C. Wesdemiotis, C.N. Moorefield, G.R. Newkome, Eur. J. Inorg. Chem. **2013**, 3640 (2013)
599. R. Satapathy, M. Ramesh, H. Padhy, I.-H. Chiang, C.-W. Chu, K.-H. Wei, H.-C. Lin, Polym. Chem. **5**, 5423 (2014)
600. J.-L. Wang, X. Li, C.D. Shreiner, X. Lu, C.N. Moorefield, S.R. Tummalapalli, F.R. Fronczek, C. Wesdemiotis, G.R. Newkome, New J. Chem. **36**, 484 (2012)
601. I. Angurell, O. Rossell, M. Seco, Inorg. Chim. Acta **409**, 2 (2014)
602. F. Puntoriero, F. Nastasi, M. Cavazzini, S. Quici, S. Campagna, Coord. Chem. Rev. **251**, 536 (2007)
603. L. Xu, L.-J. Chen, H.-B. Yang, Chem. Commun. **50**, 5156 (2014)
604. G.-Z. Zhao, Q.-J. Li, L.-J. Chen, H. Tan, C.-H. Wang, D.A. Lehman, D.C. Muddiman, H.-B. Yang, Organometallics **30**, 3637 (2011)
605. L.-J. Chen, Q.-J. Li, J. He, H. Tan, Z. Abliz, H.-B. Yang, J. Org. Chem. **77**, 1148 (2012)
606. S. Chen, L.-J. Chen, H.-B. Yang, H. Tian, W. Zhu, J. Am. Chem. Soc. **134**, 13596 (2012)
607. J.-K. Ou-Yang, L.-J. Chen, L. Xu, C.-H. Wang, H.-B. Yang, Chin. Chem. Lett. **24**, 471 (2013)
608. N.-W. Wu, J. Zhang, D. Ciren, Q. Han, L.-J. Chen, L. Xu, H.-B. Yang, Organometallics **32**, 2536 (2013)
609. J.B. Pollock, T.R. Cook, P.J. Stang, J. Am. Chem. Soc. **134**, 10607 (2012)
610. S. Shanmugaraju, A.K. Bar, K.-W. Chi, P.S. Mukherjee, Organometallics **29**, 2971 (2010)
611. N.-W. Wu, Q.-J. Li, J. Zhang, J. He, J.-K. Ou-Yang, H. Tan, Z. Abliz, H.-B. Yang, Tetrahedron **69**, 5981 (2013)

612. M. He, Q. Han, J. He, Q. Li, Z. Abliz, H. Tan, L. Xu, H. Yang, Chin. J. Chem. **31**, 663 (2013)
613. L.-J. Chen, G.-Z. Zhao, B. Jiang, B. Sun, M. Wang, L. Xu, J. He, Z. Abliz, H. Tan, X. Li, H.-B Yang. J. Am. Chem. Soc. **136**, 5993 (2014)
614. Q. Han, L.-L. Wang, Q.-J. Li, G.-Z. Zhao, J. He, B. Hu, H. Tan, Z. Abliz, Y. Yu, H.-B. Yang, J. Org. Chem. **77**, 3426 (2012)
615. Y.-R. Zheng, K. Ghosh, H.-B. Yang, P.J. Stang, Inorg. Chem. **49**, 4747 (2010)
616. Q.-J. Li, G.-Z. Zhao, L.-J. Chen, H. Tan, C.-H. Wang, D.-X. Wang, D.A. Lehman, D.C. Muddiman, H.-B. Yang, Organometallics **31**, 7241 (2012)
617. H.T. Baytekin, M. Sahre, A. Rang, M. Engeser, A. Schulz, C.A. Schalley, Small **4**, 1823 (2008)
618. R. Sakamoto, S. Katagiri, H. Maeda, Y. Nishimori, S. Miyashita, H. Nishihara, J. Am. Chem. Soc. **137**, 734 (2015)
619. F. Grimm, K. Hartnagel, F. Wessendorf, A. Hirsch, Chem. Commun. **45**, 1331 (2009)
620. C.-H. Wong, S.C. Zimmerman, Chem. Commun. **49**, 1679 (2013)
621. H. Lee, Y.-H. Jeong, J.-H. Kim, I. Kim, E. Lee, W.-D. Jang, J. Am. Chem. Soc. **137**, 12394 (2015)
622. Y. Shinozaki, T. Tsubomura, K. Sugawa, J. Otsuki, Tetrahedron Lett. **57**, 48 (2016)
623. U. Hahn, F. Vögtle, J.-F. Nierengarten, Polymers **4**, 501 (2012)
624. W.-S. Li, K.S. Kim, D.-L. Jiang, H. Tanaka, T. Kawai, J.H. Kwon, D. Kim, T. Aida, J. Am. Chem. Soc. **128**, 10527 (2006)
625. W.-D. Jang, W.-G. Koh, Dendrimer porphyrin (phthalocyanine), in *Encyclopedia of Biomedical Polymers and Polymeric Biomaterials*, ed. by M. Mishra (Taylor & Francis, Boca Raton, 2015)
626. H.-J. Yoon, W.-D. Jang, J. Mater. Chem. **20**, 211 (2010)
627. F. Figueiraa, P.M.R. Pereiraa, S. Silvaa, J.A.S. Cavaleiroa, J.P.C. Tome, Curr. Org. Synthesis **11**, 110 (2014)
628. J. Kim, H.-J. Yoon, S. Kim, K. Wang, T. Ishii, Y.-R. Kim, W.-D. Jang, J. Mater. Chem. **19**, 4627 (2009)
629. W.-D. Jang, Y. Nakagishi, N. Nishiyama, S. Kawauchi, Y. Morimoto, M. Kikuchi, K. Kataoka, J. Control. Rel. **113**, 73 (2006)
630. W.-D. Jang, N. Nishiyama, K. Kataoka, Supramol. Chem. **19**, 309 (2007)
631. T. Yamaguchi, T. Kimura, H. Matsuda, T. Aida, Angew. Chem. Int. Ed. **43**, 6350 (2004)
632. A. Tsuda, M.A. Alam, T. Harada, T. Yamaguchi, N. Ishii, T. Aida, Angew. Chem. Int. Ed. **46**, 8198 (2007)
633. S. Zhang, H.-J. Sun, A.D. Hughes, B. Draghici, J. Lejnieks, P. Leowanawat, A. Bertin, L.O. De Leon, O.V. Kulikov, Y. Chen, D.J. Pochan, P.A. Heiney, V. Percec, ACS Nano **8**, 1554 (2014)
634. S. Zhang, H.-J. Sun, A.D. Hughes, R.-O. Moussodia, A. Bertin, Y. Chen, D.J. Pochan, P.A. Heiney, M.L. Klein, V. Percec, Proc. Natl. Acad. Sci. U.S.A. **111**, 9058 (2014)
635. M. Peterca, V. Percec, P. Leowanawat, A. Bertin, J. Am. Chem. Soc. **133**, 20507 (2011)
636. V. Percec, D.A. Wilson, P. Leowanawat, C.J. Wilson, A.D. Hughes, M.S. Kaucher, D.A. Hammer, D.H. Levine, A.J. Kim, F.S. Bates, K.P. Davis, T.P. Lodge, M.L. Klein, R.H. DeVane, E. Aqad, B.M. Rosen, A.O. Argintaru, M.J. Sienkowska, K. Rissanen, S. Nummelin, J. Ropponen, Science **328**, 1009 (2010)
637. M. Filippi, D. Remotti, M. Botta, E. Terreno, L. Tei, Chem. Commun. **51**, 17455 (2015)
638. M. Filippi, J. Martinelli, G. Mulas, M. Ferraretto, E. Teirlinck, M. Botta, L. Tei, E. Terreno, Chem. Commun. **50**, 3453 (2014)
639. M. Filippi, D. Patrucco, J. Martinelli, M. Botta, P. Castro-Hartmann, L. Tei, E. Terreno, Nanoscale **7**, 12943 (2015)
640. J. Hardy, F. Schacher (eds.), *Functional Metallosupramolecular Materials* (RSC, Cambridge, 2015)
641. M.W. Urban (ed.), *Handbook of Stimuli-Responsive Materials* (Wiley-VCH Verlag GmbH & Co. KGaA, Weinheim, 2011)
642. M.J.M. Muñoz, G. Fernández, Chem. Sci. **3**, 1395 (2012)
643. A.J. McConnell, C.S. Wood, P.P. Neelakandan, J.R. Nitschke, Chem. Rev. **115**, 7729 (2015)

644. R. Yerushalmi, A. Scherz, M.E. van der Boom, H.-B. Kraatz, J. Mater. Chem. **15**, 4480 (2005)
645. X. Ma, H. Tian, Acc. Chem. Res. **47**, 1971 (2014)
646. M. Yan, S.K.P. Velu, M. Marechal, G. Royal, J. Galvez, P. Terech, Soft Matter **9**, 4428 (2013)
647. S. Köytepe, M.H. Demirel, T. Seçkin, J. Inorg. Organomet. Polym. **23**, 1104 (2013)
648. A. Gasnier, J.-M. Barbe, C. Bucher, F. Denat, J.-C. Moutet, E. Saint-Aman, P. Terech, G. Royal, Inorg. Chem. **47**, 1862 (2008)
649. A. Gasnier, J.-M. Barbe, C. Bucher, C. Duboc, J.-C. Moutet, E. Saint-Aman, P. Terech, G. Royal, Inorg. Chem. **49**, 2592 (2010)
650. A.K. Miller, Z. Li, K.A. Streletzky, A.M. Jamieson, S.J. Rowan, Polym. Chem. **3**, 3132 (2012)
651. T.-A. Asoh, H. Yoshitake, Y. Takano, A. Kikuchi, Macromol. Chem. Phys. **214**, 2534 (2013)
652. J. Yuan, H. Zhang, G. Hong, Y. Chen, G. Chen, Y. Xu, W. Weng, J. Mater. Chem. B **1**, 4809 (2013)
653. J. Brassinne, J.-P. Bourgeois, C.-A. Fustin, J.-F. Gohy, Soft Matter **10**, 3086 (2014)
654. J. Brassinne, A.M. Stevens, E. Van Ruymbeke, J.-F. Gohy, C.-A. Fustin, Macromolecules **46**, 9134 (2013)
655. S.-C. Wei, M. Pan, K. Li, S. Wang, J. Zhang, C.-Y. Su, Adv. Mater. **26**, 2072 (2014)
656. K. Liu, Y. Kang, Z. Wang, X. Zhang, Adv. Mater. **25**, 5530 (2013)
657. A. Hennig, H. Bakirci, W.M. Nau, Nat. Meth. **4**, 629 (2007)
658. J. Liu, M.-A. Morikawa, N. Kimizuka, J. Am. Chem. Soc. **133**, 17370 (2011)
659. S.K. Ghosh, *Self-healing Materials: Fundamental, Design Strategies, and Applications* (Wiley-VCH, Weinheim, 2009)
660. D. Habault, H. Zhang, Y. Zhao, Chem. Soc. Rev. **42**, 7244 (2013)
661. B. Sandmann, S. Bode, M.D. Hager, U.S. Schubert, Adv. Polym. Sci. **262**, 239 (2013)
662. S. Bode, D. Sandmann, M.D. Hager, U.S. Schubert, Metal-complex-based self-healing polymers, in *Self-Healing Polymers: From Principles to Applications*, ed. by W.H. Binder (Wiley, Chichester, 2013)
663. M. Burnworth, L. Tang, J.R. Kumpfer, A.J. Duncan, F.L. Beyer, G.L. Fiore, S.J. Rowan, C. Weder, Nature **472**, 334 (2011)
664. G.L. Fiore, S.J. Rowan, C. Weder, Chem. Soc. Rev. **42**, 7278 (2013)
665. S. Bode, L. Zedler, F.H. Schacher, B. Dietzek, M. Schmitt, J. Popp, M.D. Hager, U.S. Schubert, Adv. Mater. **20**, 1634 (2013)
666. B. Yang, H. Zhang, H. Peng, Y. Xu, B. Wu, W. Weng, L. Li, Polym. Chem. **5**, 1945 (2014)
667. P. Terech, M. Yan, M. Marechal, G. Royal, J. Galvez, S.K.P. Velu, Phys. Chem. Chem. Phys. **15**, 7334 (2013)
668. A. El-ghayoury, H. Hofmeier, B. de Ruiter, U.S. Schubert, Macromolecules **36**, 3955 (2003)
669. S. Kupfer, L. Zedler, J. Guthmuller, S. Bode, M.D. Hager, U.S. Schubert, J. Popp, S. Gräfe, B. Dietzek, Phys. Chem. Chem. Phys. **16**, 12422 (2014)
670. S. Bode, M. Enke, R.K. Bose, F.H. Schacher, S.J. Garcia, S. van der Zwaag, M.D. Hager, U.S. Schubert, J. Mater. Chem. A **3**, 22145 (2015)
671. M. Enke, S. Bode, J. Vitz, F.H. Schacher, M.J. Harrington, M.D. Hager, U.S. Schubert, Polymer **69**, 274 (2015)
672. M. Behl, M.Y. Razzaq, A. Lendlein, Adv. Mater. **22**, 3388 (2010)
673. J. Li, J.A. Viveros, M.H. Wrue, M. Anthamatten, Adv. Mater. **19**, 2851 (2007)
674. J. Li, C.L. Lewis, D.L. Chen, M. Anthamatten, Macromolecules **44**, 5336 (2011)
675. K. Sada, M. Takeuchi, N. Fujita, M. Numata, S. Shinkai, Chem. Soc. Rev. **36**, 415 (2007)
676. C.L. Lewis, E.M. Dell, Inc. J. Polym. Sci. Part B: Polym. Phys. **54**, 1340 (2016)
677. J.R. Kumpfer, J.R. Rowan, J. Am. Chem. Soc. **133**, 12866 (2011)
678. X. Luo, P.T. Mather, ACS Macro Lett. **2**, 152 (2013)
679. E.D. Rodriguez, X. Luo, P.T. Mather, A.C.S. Appl, Mater. Interfaces **3**, 152 (2011)